EOS Data Products Handbook

Volume 1

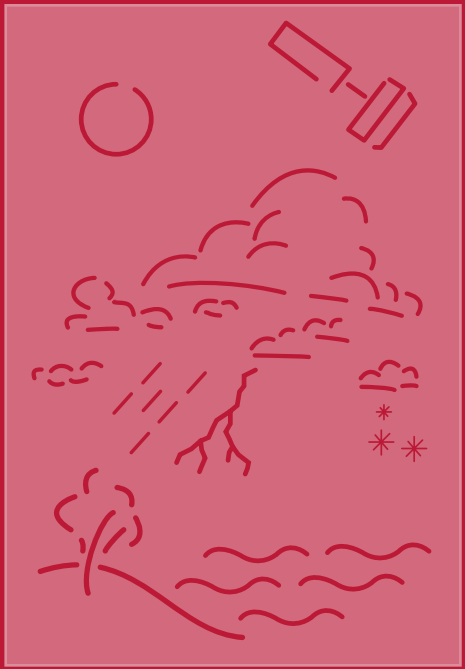

TRMM • Terra

Data Assimilation System

EOS Data Products Handbook

Volume 1

TRMM
CERES
LIS
PR
TMI
VIRS

Terra
ASTER
CERES
MISR
MODIS
MOPITT

Data Assimilation System

EOS Data Products Handbook

Volume 1
Revised 2004

Editors

Michael D. King
NASA Goddard Space Flight Center

Jim Closs
Sterling Spangler
Renny Greenstone
SSAI

Stephen Wharton
NASA Goddard Space Flight Center

Monica Myers
Decision Systems Tech, Inc.

Claire Parkinson
NASA Goddard Space Flight Center

Design and Production

Sterling Spangler

For Additional Copies:

EOS Project Science Office
Code 900
NASA/Goddard Space Flight Center
Greenbelt, MD 20771
eos.nasa.gov

Phone: (301) 867-2037
Internet: leon_middleton@ssaihq.com

NASA Goddard Space Flight Center
Greenbelt, Maryland

Printed April 2003

Acknowledgments

Special thanks are extended to the many individuals who provided information necessary for the completion of this revised first volume of the EOS Data Products Handbook. These include most prominently Stephen W. Wharton and Monica Faeth Myers, whose tremendous efforts brought about the original version of Volume 1, and the members of the science teams for each of the instruments covered in this volume.

Support for production of this document, provided by Tim Suttles, William Bandeen, and Steve Graham is also gratefully acknowledged.

Abstract

The *EOS Data Products Handbook* provides brief descriptions of the data products that will be produced from a range of missions of the Earth Observing System (EOS) and associated projects. This publication is an update of Volume 1, originally published in 1997, which covers the Tropical Rainfall Measuring Mission (TRMM), the Terra mission (formerly named EOS AM-1), and the Data Assimilation System. Volume 2, published in 2000, covers the Active Cavity Radiometer Irradiance Monitor Satellite (ACRIMSAT), Aqua, Jason-1, Landsat 7, Meteor 3M/Stratospheric Aerosol and Gas Experiment III (SAGE III), the Quick Scatterometer (QuikScat), and the Vegetation Canopy Lidar (VCL) missions. Volume 1 provides a list of products and an introduction and overview descriptions of the instruments and data processing, all introductory to the core of the book, which presents the individual data product descriptions, organized into topical chapters. The product descriptions are followed by five appendices, which provide contact information for the EOS data centers that are archiving and distributing the data sets, contact information for the science points of contact for the data products, references, acronyms and abbreviations, and a data products index.

Table of Contents

Abstract I

Foreword IV

List of Data Products *(Organized by Mission Name)* 1

Chapter 1 Introduction 11

Chapter 2 Background 15

Chapter 3 Instrument Descriptions and Data Processing Overviews 21

Chapter 4 Radiance and Imagery Products 47

Chapter 5 Precipitation and Atmospheric Humidity 75

Chapter 6 Cloud and Aerosol Properties and Radiative Energy Fluxes 101

Chapter 7 Lightning 137

Chapter 8 Atmospheric Chemistry 143

Chapter 9 Surface Temperatures of Land and Oceans, Fire Occurrence, and Volcanic Effects 149

Chapter 10 Vegetation Dynamics, Land Cover, and Land Cover Dynamics 159

Chapter 11 Ocean Primary Productivity, Phytoplankton and Organic Matter 177

Chapter 12 Snow and Ice Cover 193

Chapter 13 Data Assimilation System 201

Appendix A: EOS Distributed Active Archive Centers (DAACs) Contact Information 219

Appendix B: Points of Contact 220

Appendix C: References 227

Appendix D: Acronyms and Abbreviations 253

Appendix E: Data Products Index *(Organized by Instrument Name)* 259

Foreword

This is a revised version of the *MTPE/EOS Data Products Handbook, Volume 1, TRMM & AM-1,* published in 1997. The document, *EOS Data Products Handbook, Volume 1, TRMM and Terra*, has been updated to provide you with current information on the Terra and TRMM products available through the EOS Data and Information System.

This document provides high-level descriptions of the science and instrument data sets being produced from the Tropical Rainfall Measuring Mission (TRMM), the Earth Observing System (EOS) satellite, Terra, and the Data Assimilation System (DAS). These data sets are providing essential information for science and policy research in the areas of global change and Earth system science.

The document is broken into 14 chapters. Corresponding data products are grouped within each of chapters 4 through 14. Each data products chapter provides a framework for understanding the science objectives as well as providing a thumbnail sketch of what the product is designed to do.

A list of all products by ID and Data Set Name begins in the following section. That list also contains the page number where you will find the corresponding Product Description and other information.

Additional information on these missions can be found in the *1999 EOS Reference Handbook: A Guide to NASA's Earth Science Enterprise and the Earth Observing System (*King, M. D., and R. Greenstone, 1999), and on the EOS Project Science Office web site at eos.nasa.gov, where you will also find many of our documents in PDF.

Michael D. King
EOS Senior Project Scientist

List of Data Products

(Organized by Mission Name)

TRMM
- CERES
- LIS
- PR
- TMI
- VIRS

Terra
- ASTER
- CERES
- MISR
- MODIS
- MOPITT

Data Assimilation System

Mission	Instrument	Data Set	Proc. Level	Prod. ID	Chapter	Page #
TRMM	*LIS*	Background Product	1A	LIS01	Radiance and Imagery Products	*50*
	LIS	Image Attributes	1B	LIS02	Lightning	*140*
	LIS	Events Statistics	1B	LIS03	Lightning	*140*
	LIS	Group Statistics	1B	LIS04	Lightning	*140*
	LIS	Flash Statistics	2	LIS05	Lightning	*140*
	LIS	Area Statistics	2	LIS06	Lightning	*140*
	LIS	Flash Density	2	LIS07	Lightning	*140*
	LIS	2.5° × 2.5° Equal Angle Monthly Grid	2	LIS08	Lightning	*140*
	LIS	500 km × 500 km Equal Area Monthly Grid	2	LIS09	Lightning	*140*
	LIS	Orbit Attributes	3	LIS10	Lightning	*140*
	LIS	Threshold Attributes	3	LIS11	Lightning	*140*
	LIS	Browse Area	3	LIS12	Lightning	*140*
TRMM	*LIS*	Vector Statistics	3	LIS13	Lightning	*140*
	LIS	Metadata Description	3	LIS14	Lightning	*140*
	LIS	Summary Data	3	LIS15	Lightning	*140*
	LIS	Flash Rate Data	3	LIS16	Lightning	*140*
	LIS	Ephemeris Data	3	LIS17	Lightning	*140*
	LIS	Event Rate Sets	3	LIS18	Lightning	*140*
TRMM	*PR*	Radar Total Power, Noise, and Reflectivity	1B	PR 1B-21 PR 1C-21	Radiance and Imagery Products	*51*
	PR	Rain Occurrence and Rain Type and Bright Band Height	2	PR 2A-23	Precipitation, Atmospheric Humidity and Atmospheric Temperatures	*80*
	PR	Surface Cross-Section as Function of Scan Angle	2	PR 2A-21	Precipitation, Atmospheric Humidity and Atmospheric Temperatures	*79*
	PR	Range Profiles of Rain and Water Content	2	PR 2A-25	Precipitation, Atmospheric Humidity and Atmospheric Temperatures	*81*

Mission	Instrument	Data Set	Proc. Level	Prod. ID	Chapter	Page #
TRMM	***PR***	Monthly Accumulated Rainfall & Vertical Structure, Monthly Combined Accumulated Surface Rainfall	3	PR 3A-25 PR 3A-26	Precipitation, Atmospheric Humidity and Atmospheric Temperatures	*82*
	TMI	Calibrated Brightness Temperatures	1B	TMI 1B-11	Radiance and Imagery Products	*51*
	TMI	Surface Rainfall and Vertical Structure	2	TMI 2A-12	Precipitation, Atmospheric Humidity and Atmospheric Temperatures	*83*
	TMI	Monthly Surface Rainfall	3	TMI 3A-11	Precipitation, Atmospheric Humidity and Atmospheric Temperatures	*84*
TRMM	***TRMM***	Instantaneous Radar Site Rain Map	2A	TRMM 2A-53	Precipitation, Atmospheric Humidity and Atmospheric Temperatures	*89*
	TRMM	Instantaneous Radar Site Convective/Stratiform Map	2A	TRMM 2A-54	Precipitation, Atmospheric Humidity and Atmospheric Temperatures	*90*
	TRMM	Instantaneous Radar Site 3-D Reflectivities	2A	TRMM 2A-55	Precipitation, Atmospheric Humidity and Atmospheric Temperatures	*91*
	TRMM	Combined Surface Rainfall Rate and Vertical Structure	2	TRMM 2B-31	Precipitation, Atmospheric Humidity and Atmospheric Temperatures	*85*
	TRMM	Monthly Combined Accumulated Rainfall and Vertical Structure	3	TRMM 3B-31	Precipitation, Atmospheric Humidity and Atmospheric Temperatures	*86*
	TRMM	1° Daily Combined Rainfall and Monthly Combined Instrument Rainfall	4	TRMM 3B-42 3B-43	Precipitation, Atmospheric Humidity and Atmospheric Temperatures	*88*
TRMM	***TRMM***	5-Day Site Rain Map	3	TRMM 3A-53	Precipitation, Atmospheric Humidity and Atmospheric Temperatures	*92*

Mission	Instrument	Data Set	Proc. Level	Prod. ID	Chapter	Page #
TRMM	TRMM	30-Day Site Rain Map	3	TRMM 3A-54	Precipitation, Atmospheric Humidity and Atmospheric Temperatures	93
	TRMM	Monthly 3-D Structure	3	TRMM 3A-55	Precipitation, Atmospheric Humidity and Atmospheric Temperatures	93
	VIRS	Calibrated Radiances	1B	VIRS 1B-01	Radiance and Imagery Products	52
TRMM & Terra	CERES	Bi-Directional Scans Product	0,1	CER/BDS	Radiance and Imagery Products	61
	CERES	ERBE-like Instantaneous TOA Estimates	2	CER/ES-8	Cloud and Aerosol Properties and Radiative Energy Fluxes	106
	CERES	ERBE-like Monthly Regional Averages (ES-9) and ERBE-like Monthly Geographical Averages (ES-4)	3	CER/ES-4, CER/ES-9	Cloud and Aerosol Properties and Radiative Energy Fluxes	107
	CERES	Single Scanner TOA/ Surface Fluxes and Clouds	2	CER/SSF	Cloud and Aerosol Properties and Radiative Energy Fluxes	109
	CERES	Clouds and Radiative Swath	2	CER/CRS	Cloud and Aerosol Properties and Radiative Energy Fluxes	111
	CERES	Monthly Gridded Radiative Fluxes and Clouds	3	CER/FSW	Cloud and Aerosol Properties and Radiative Energy Fluxes	112
	CERES	Synoptic Radiative Fluxes and Clouds	3	CER/SYN	Cloud and Aerosol Properties and Radiative Energy Fluxes	114
TRMM & Terra	CERES	Monthly Regional Radiative Fluxes and Clouds (AVG) and Monthly Zonal and Global Radiative Fluxes and Clouds (ZAVG)	3	CER/AVG, CER/ZAVG	Cloud and Aerosol Properties and Radiative Energy Fluxes	115

Mission	Instrument	Data Set	Proc. Level	Prod. ID	Chapter	Page #
Terra	***CERES***	Monthly Gridded TOA/ Surface Fluxes and Clouds	3	CER/SFC	Cloud and Aerosol Properties and Radiative Energy Fluxes	*116*
	CERES	Monthly TOA/Surface Averages	3	CER/ SRBAVG	Cloud and Aerosol Properties and Radiative Energy Fluxes	*118*
Terra	***ASTER***	Reconstructed, Unprocessed Instrument Data	1A	AST01	Radiance and Imagery Products	*54*
	ASTER	Registered Radiance at Sensor	1B	AST03	Radiance and Imagery Products	*55*
	ASTER	Brightness Temperature at Sensor	2	AST04	Radiance and Imagery Products	*55*
	ASTER	Browse Data-Decorrelation Stretch Product	2	AST06	Radiance and Imagery Products	*56*
	ASTER	Surface Reflectance and Surface Radiance	2	AST07 AST09	Radiance and Imagery Products	*57*
	ASTER	Digital Elevation Models (DEMs)	3	AST14	Radiance and Imagery Products	*59*
	ASTER	Polar Surface and Cloud Classification Product	4	AST13	Cloud and Aerosol Properties and Radiative Energy Fluxes	*105*
	ASTER	Surface Emissivity and Surface Kinetic Temperature	2	AST05 AST08	Surface Temperatures of Land and Oceans, Fire Occurrence, and Volcanic Effects	*152*
Terra	***MISR***	Reformatted Annotated Product	1A	MIS01	Radiance and Imagery Products	*63*
	MISR	Radiometric Product	1B1	MIS02	Radiance and Imagery Products	*64*
	MISR	Geo-rectified Radiance Product	1B2	MIS03	Radiance and Imagery Products	*65*
	MISR	Ancillary Geographic Product	1B2 & 2	MIS10	Radiance and Imagery Products	*66*
	MISR	Ancillary Radiometric Product	1B1 & 2	MIS11	Radiance and Imagery Products	*66*

Mission	Instrument	Data Set	Proc. Level	Prod. ID	Chapter	Page #
Terra	***MISR***	Top-of-Atmosphere (TOA)/ Cloud Product	2 & 3	MIS04 MIS06 MIS07	Cloud and Aerosol Properties and Radiative Energy Fluxes	*120*
	MISR	Aerosol and Surface Product	2 & 3	MIS05 MIS08 MIS09	Cloud and Aerosol Properties and Radiative Energy Fluxes	*122*
	MISR	Aerosol Climatology Product	2 & 3	MIS12	Cloud and Aerosol Properties and Radiative Energy Fluxes	*123*
Terra	***MODIS***	Level 1A Radiance Counts	1A	MOD01	Radiance and Imagery Products	*67*
	MODIS	Level 1B Calibrated, Geolocated Radiances	1B	MOD02	Radince and Imagery Products	*67*
	MODIS	Geolocation Data Set	1B	MOD03	Radiance and Imagery Products	*68*
	MODIS	Aerosol Product	2	MOD04	Cloud and Aerosol Properties and Radiative Energy Fluxes	*124*
	MODIS	Total Precipitable Water	2	MOD05	Precipitation, Atmospheric Humidity and Atmospheric Temperatures	*95*
	MODIS	Cloud Product	2	MOD06	Cloud and Aerosol Properties and Radiative Energy Fluxes	*127*
	MODIS	Atmospheric Profiles	2	MOD07	Precipitation, Atmospheric Humidity and Atmospheric Temperatures	*98*
	MODIS	Level 3 Atmosphere Products	3	MOD08	Cloud and Aerosol Properties and Radiative Energy Fluxes	*128*
Terra	***MODIS***	Surface Reflectance; Atmospheric Correction Algorithm Products	2	MOD09	Vegetation Dynamics, Land Cover, and Land Cover Dynamics	*162*
	MODIS	Snow Cover	2,3	MOD10	Snow and Ice Cover	*196*
	MODIS	Land Surface Temperature (LST) and Emissivity	2,3	MOD11	Surface Temperatures of Land and Oceans, Fire Occurrence, and Volcanic Effects	*154*

Mission	Instrument	Data Set	Proc. Level	Prod. ID	Chapter	Page #
Terra	***MODIS***	Land Cover Type	3	MOD12	Vegetation Dynamics, Land Cover, and Land Cover Dynamics	*164*
Terra	***MODIS***	Vegetation Indices	3	MOD13	Vegetation Dynamics, Land Cover, and Land Cover Dynamics	*166*
Terra	***MODIS***	Thermal Anomalies – Fires	2,3	MOD14	Surface Temperatures of Land and Oceans, Fire Occurrence, and Volcanic Effects	*156*
Terra	***MODIS***	Leaf Area Index and Fraction of Photosynthetically Active Radiation – Moderate Resolution	4	MOD15	Vegetation Dynamics, Land Cover, and Land Cover Dynamics	*167*
Terra	***MODIS***	Evapotranspiration	4	MOD16	Vegetation Dynamics, Land Cover, and Land Cover Dynamics	*169*
Terra	***MODIS***	Vegetation Production and Net Primary Production	4	MOD17	Vegetation Dynamics, Land Cover, and Land Cover Dynamics	*171*
Terra	***MODIS***	Normalized Water-Leaving Radiance	2,3	MOD18	Radiance and Imagery Products	*69*
Terra	***MODIS***	Pigment Concentration	2,3	MOD19	Ocean Primary Productivity, Phytoplankton and Organic Matter	*180*
Terra	***MODIS***	Chlorophyll Fluorescence	2,3	MOD20	Ocean Primary Productivity, Phytoplankton and Organic Matter	*182*
Terra	***MODIS***	Chlorophyll *a* Pigment Concentration	2,3	MOD21	Ocean Primary Productivity, Phytoplankton and Organic Matter	*184*
Terra	***MODIS***	Photosynthetically Active Radiation (PAR)	2,3	MOD22	Radiance and Imagery Products	*70*
Terra	***MODIS***	Suspended Solids Concentration	2,3	MOD23	Ocean Primary Productivity, Phytoplankton and Organic Matter	*180*
Terra	***MODIS***	Organic Matter Concentration	2,3	MOD24	Ocean Primary Productivity, Phytoplankton and Organic Matter	*184*

Mission	Instrument	Data Set	Proc. Level	Prod. ID	Chapter	Page #
Terra	***MODIS***	Coccolith Concentration	2,3	MOD25	Ocean Primary Productivity, Phytoplankton and Organic Matter	*187*
	MODIS	Ocean Water Attenuation Coefficient	2,3	MOD26	Ocean Primary Productivity, Phytoplankton and Organic Matter	*180*
	MODIS	Ocean Primary Productivity	4	MOD27	Ocean Primary Productivity, Phytoplankton and Organic Matter	*189*
	MODIS	Sea Surface Temperature	2,3	MOD28	Surface Temperatures of Land and Oceans, Fire Occurrence, and Volcanic Effects	*157*
	MODIS	Sea Ice Cover and Ice Surface Temperature	2,3	MOD29	Snow and Ice Cover	*198*
	MODIS	Phycoerythrin Concentration	2,3	MOD31	Ocean Primary Productivity, Phytoplankton and Organic Matter	*190*
Terra	***MODIS***	Processing Framework and Match-up Database	2	MOD32	Radiance and Imagery Products	*72*
	MODIS	Cloud Mask	2	MOD35	Cloud and Aerosol Properties and Radiative Energy Fluxes	*134*
	MODIS	Absorption Coefficients	2,3	MOD36	Ocean Primary Productivity, Phytoplankton and Organic Matter	*184*
	MODIS	Aerosol Optical Depth	2,3	MOD37	Radiance and Imagery Products	*69*
	MODIS	Clear-Water Epsilon	2,3	MOD39	Radiance and Imagery Products	*73*
Terra	***MODIS***	Burn Scars	4	MOD40	Surface Temperatures of Land and Oceans, Fire Occurrence, and Volcanic Effects	*156*

Mission	Instrument	Data Set	Proc. Level	Prod. ID	Chapter	Page #
Terra	***MODIS***	Surface Reflectance BRDF/ Albedo Parameter	3	MOD43	Vegetation Dynamics, Land Cover, and Land Cover Dynamics	*172*
	MODIS	Vegetative Cover Conversion and Vegetation Continuous Fields	4	MOD44A MOD44B	Vegetation Dynamics, Land Cover, and Land Cover Dynamics	*174*
	MOPITT	Geolocated Radiances	1B	MOP 01	Radiance and Imagery Products	*74*
	MOPITT	CO Profile, CO Column, and CH_4 Column Data	2	MOP 02	Atmospheric Chemistry	*146*
DAS	***DAS***	Time-Averaged Single Level Cloud Quantities	4	D4FAXCLD, D4LAXCLD	Data Assimilation System	*205*
	DAS	Time-Averaged Near Surface and Vertically-Integrated Quantities	4	D4FAXENG, D4LAXENG	Data Assimilation System	*206*
	DAS	Time-Averaged 2-Dimensional Surface Data	4	D4FAXLSM, D4LAXLSM	Data Assimilation System	*207*
	DAS	Time-Averaged Surface and Top-of-the-Atmosphere Stresses	4	D4FAXSTR, D4LAXSTR	Data Assimilation System	*208*
	DAS	Time-Averaged Surface 3-Dimensional Cloud Quantities	4	D4LAPCLD	Data Assimilation System	*209*
	DAS	Time-Averaged 3-Dimensional Wind Tendency Fields	4	D4LAPMOM	Data Assimilation System	*210*
	DAS	Time-Averaged 3-Dimensional Moisture Tendency Fields	4	D4LAPMST	Data Assimilation System	*211*
	DAS	Total Column Ozone	4	D4FAXCHM D4LAXCHM	Data Assimilation System	*212*
	DAS	Instantaneous Near Surface and Vertically-Integrated State Variables	4	D4FAXMIS D4LAXMIS	Data Assimilation System	*213*
	DAS	Ozone Mixing Ratio	4	D4FAPCHM D4LAPCHM	Data Assimilation System	*215*

Mission	Instrument	Data Set	Proc. Level	Prod. ID	Chapter	Page #
DAS	***DAS***	Instantaneous 3-Dimensional State Variables	4	D4FAPMIS D4LAPMIS	Data Assimilation System	*216*
	DAS	Time-Averaged 3-Dimensional Temperature Tendency Fields	4	D4LAPTMP	Data Assimilation System	*217*
	DAS	Time-Averaged 3-Dimensional Eddy-Diffusivity and Cloud Mass Flux Fields	4	D4LAPTRP	Data Assimilation System	*218*

Chapter 1

Introduction

TRMM
CERES
LIS
PR
TMI
VIRS

Terra
ASTER
CERES
MISR
MODIS
MOPITT

Data Assimilation System

Introduction

Overview

Volume 1 of the EOS Data Products Handbook (DPH) provides a brief description of the science data products that are available from the Earth Observing System Data and Information System (EOSDIS). The objective of the DPH is to promote a broader understanding of how the EOS data products contribute to science research in the understanding, analysis, and monitoring of global climate change. This volume describes data products that are produced from instruments onboard the Tropical Rainfall Measuring Mission (TRMM) satellite, the Earth Observing System (EOS) Terra satellite (formerly AM-1), as well as products developed by the Data Assimilation Office.

The information in this document was compiled from many sources: principally, the Algorithm Theoretical Basis Documents (ATBDs), which were written by the science teams; abstracts and information from the product generation engineering effort known as the Ad Hoc Working Group on Production (AHWGP); and preliminary information compiled by the Science Processing Support Office (SPSO) of the Earth Science Data and Information System (ESDIS) Project. The data descriptions in this reference have been reviewed by the science team contacts for accuracy. Readers should be aware that this reference is only the "tip of the iceberg" of information available on the EOS data products.

Volume 1 Organization

Chapter 1 provides a roadmap through the document itself. Chapter 2 provides additional background on Earth Science Enterprise (ESE) mission objectives, a table of key characteristics for the TRMM and Terra instruments, and information on the EOSDIS and the EOS Distributed Active Archive Centers (DAACs). Chapter 3 provides an overview (for each instrument) of the process by which the data products are derived from the instrument observations.

Chapters 4 through 12 contain the data set descriptions. Chapter 4 covers imagery and raw instrument data sets, as well as a few instrument ancillary data sets that are the basis for numerous other data sets with broad application to Earth science research. Chapters 5 through 12 emphasize the 24 science themes that have been identified as critical measurements of the EOS program. Chapter 13 contains information about the Data Assimilation Office (DAO), which develops research-quality 4-dimensional atmosphere-ocean-land data assimilation products for EOS.

The purpose of this document's grouping is to provide a first-order indication of the kinds of science research that the data products can be used to support. The science themes are intended both to focus upon the mission objectives during the early EOS time frame and to represent a subset of the overall Earth Science Enterprise science objectives, which encompass a larger number of platforms and hence have a much broader scope.

The data set description chapter titles are as follows:

- Radiance and Imagery Products;
- Precipitation, Atmospheric Humidity and Atmospheric Temperatures;
- Cloud and Aerosol Properties and Radiative Energy Fluxes;
- Lightning;
- Atmospheric Chemistry;
- Surface Temperature of Land and Oceans, Fire Occurrence, and Volcanic Effects;
- Vegetation Dynamics, Land Cover, and Land Cover Dynamics;
- Ocean Primary Productivity, Phytoplankton and Organic Matter;
- Snow and Ice Cover; and
- Data Assimilation System products.

Readers looking for derived geophysical data (e.g., Sea Surface Temperature) will be most interested in the data described in the topical sections (e.g., Surface Temperature of Land and Oceans), while readers interested in dealing with large-volume data sets, such as uncalibrated instrument counts and temperatures, calibrated radiances, and reflectivities can refer to the Radiance and Imagery section.

It is important to understand that the science themes given for the data products are by no means all-inclusive. The applications envisioned today for products will change as new uses are discovered and as the products themselves are improved. These improvements are likely to come through algorithm refinement, or enhancements to input data needed for product development. Many data sets are applicable to more than one theme. Where more than one application is appropriate, a listing of key science applications is provided for the data set within its product summary description.

Data Product Description

The data set descriptions contain the following information (Level 1 and radiance products contain a subset of this information):

- product description;
- research and applications;
- data set evolution;
- suggested reading; and
- product summary information
  - coverage
  - resolution
  - wavelengths (Level 1 products only)
  - key science applications (optional)
  - key (geophysical if applicable) parameters (Level 2, 3, 4 products)
  - processing level and availability
  - product type and production mode
  - science team contact.

The *Product Description* contains summary information about what is contained in the data set and a few details about the resolution, derivation, and accuracy of the data. *Research and Applications* briefly describes some of the science questions and applications for which the data set will be useful. *Data Set Evolution* provides information on precursor data sets and highlights ways in which the data sets improve upon current capabilities. *Suggested Reading* provides several references for more information. An effort has been made to include more recent publications, which are generally available to the broader science community.

Please note that the terms data set and data product are used interchangeably throughout this document. The data described in this document are distributed through the EOSDIS, and the EOSDIS science processing support office has assigned EOS identifiers (EOS-IDs) for each data product. These EOS-IDs are used throughout this document. These product IDs should not be confused with ATBD numbers assigned by the Project Science Office to identify each unique Algorithm Theoretical Basis Document which may contain multiple data products.

Note that CERES products use instrument IDs which do not use a numbering scheme.

Product Summary Information

The product summary information contains an overview of the processing level, coverage, resolution, and contact information for each data set.

Processing Level – Data set processing level is referred to throughout this document. The definitions of processing levels are shown in the box below. Level 1 data (e.g., Volts, Counts, Brightness Temperatures, etc.) require knowledge, agreed-upon algorithms, and computer processing capability for conversion to Level 2. Level 2 data measure the biogeophysical properties of Planet Earth. When a satellite instrument/algorithm is relatively new, the Level 2 product is heavily used. When the instrument/algorithm is mature, many users prefer the Level 3 product. Level 3 (mapped/gridded) and Level 4

Level 0 - Reconstructed unprocessed instrument/payload data at full resolution; any and all communications artifacts (e.g., synchronization frames, communications headers) removed.

Level 1A - Reconstructed unprocessed instrument data at full resolution, time-referenced, and annotated with ancillary information, including radiometric and geometric calibration coefficients and georeferencing parameters (e.g., platform ephemeris) computed and appended, but not applied, to the Level 0 data.

Level 1B - Level 1A data that have been processed to sensor units (not all instruments have a Level 1B equivalent).

Level 2 - Derived geophysical variables at the same resolution and location as the Level 1 source data.

Level 3 - Variables mapped on uniform space-time grid scales, usually with some completeness and consistency.

Level 4 - Model output or results from analyses of lower level data (e.g., variables derived from multiple measurements).

(modeled) products can be used by interdisciplinary scientists to combine data from different areas of knowledge without necessarily having to know the details or undertake all of the processing that would otherwise be necessary (to process Level 1 to Level 3 or 4). The availability of Level 3 and 4 data is a major advantage of EOSDIS in promoting data usage from outside the science field in which the data were generated. Some data sets are being produced and archived in both a Level 2 (unmapped) and Level 3 (mapped and/or temporally sampled) form.

The differences in products allow researchers to choose products available at a particular level, enabling them to work in coarser resolution to model global processes and events or in finely detailed resolution which allows for investigations at targeted regions.

Coverage – The Terra satellite is in a Sun-synchronous polar orbit and views the globe, daytime and nighttime, at the same time every day. TRMM, however, is in a precessing, inclined orbit and views the Earth from 36°N latitude to 36°S latitude. Many instruments have large swaths and view the entire globe every day. Some of the higher resolution instruments have a small swath width and as such only view the complete Earth's surface over a period of several days or weeks. For each data set described in this reference, a summary of the coverage characteristics (day/night, global/local, etc.) is provided.

Processing Level and Availability – Most of the data sets in this reference are EOS "standard data products." This means the products will be routinely processed for every applicable data acquisition. The science teams have identified the best available algorithms and methods for producing these data sets, given current understanding of physics and instrument performance; these are the "at-launch" data products. Some products, such as seasonal products or products describing variance from seasonal norms, cannot be implemented until some time after launch. In these cases, the data sets are referred to as "post-launch." All Level 1 data sets are standard at-launch products, while some Level 2, 3, and 4 data sets were phased in after launch.

Great improvements have been made in the derivation of geophysical data products in the first few years of satellite operation, and EOSDIS has been sized to enable reprocessing of standard products periodically as improved methods and instrument characterization are available.

Contacts For Further Information – To learn more about the data sets described in this guide, the ATBDs can be acquired from the EOS Project Science Office (PSO) website at eospso.gsfc.nasa.gov. In addition, a science team contact is listed for each data set described in this volume, and the phone, fax, and e-mail information for these investigators can be found in the EOS Directory, available from the PSO Web page.

Further Information Sources

The reader is referred to Volume 2 (Parkinson and Greenstone, 2000) for information about the data products from ACRIMSAT, Aqua, Jason-1, Landsat 7, Meteor 3M/SAGE III, and QuikScat. The reader is further referred to the *1999 EOS Reference Handbook* (King and Greenstone, 1999) for background on NASA's Earth Science Enterprise and for details on the entire EOS program, including its scope, purposes, individual mission elements and instruments, science teams, interdisciplinary science investigations, and educational outreach programs. Finally, the reader is referred to the *Science Strategy for the Earth Observing System* (Asrar and Dozier, 1994) and the *EOS Science Plan* (King, 1999) and its accompanying Executive Summary (Greenstone and King, 1999) for details on the science issues being addressed by the EOS program and the approaches being used.

Suggested Reading

(full references are listed in Appendix C)

Asrar, G., and J. Dozier, 1994.

Asrar, G., and R. Greenstone, 1995.

Greenstone, R., and M. D. King, 1999.

King, M. D., 1999.

King, M. D., and R. Greenstone, 1999.

Chapter 2

Background

TRMM
CERES
LIS
PR
TMI
VIRS

Terra
ASTER
CERES
MISR
MODIS
MOPITT

Data Assimilation System

Background

The Earth Science Enterprise

NASA's Earth Science Enterprise (ESE) program provides measurement systems and research initiatives to further the acquisition and synthesis of environmental data to address scientific issues related to global change and Earth system science. ESE programs include basic scientific research, development of Earth and space-based observing systems, field campaigns and experiments, state-of-the-art data set development, and data access and distribution systems. The Earth Observing System is a major program within ESE.

Among other programs of particular relevance to EOS are the New Millennium Program (NMP), the Earth System Science Pathfinder (ESSP) program, and Airborne Science. NMP was conceived to develop and flight-validate breakthrough technologies that will reduce the cost of high-priority science missions of the 21st century while enhancing their scientific capability. For example, the first mission, NMP/EO-1 (Earth Observing-1) carries an Advanced Land Imager (ALI) and other advanced imaging systems, looking forward to future improved Landsat follow-on missions. The Earth System Science Pathfinder Program (ESSP) was instituted to provide for Principle-Investigator-led missions of approximately three years duration addressing unique scientific problems that will complement, but not duplicate, the scientific objectives of EOS missions. For example, the first ESSP mission, the Gravity Recovery and Climate Experiment (GRACE), was launched to produce more accurate gravitational field maps of the Earth that will have important implications with respect to many climatic variables.

The National Polar-orbiting Operational Environmental Satellite System (NPOESS) Preparatory Project (NPP) is a joint mission to extend key measurements in support of long-term monitoring of climate trends and global biological productivity, and also to provide risk reduction for new NPOESS payloads. NPP spacecraft and instrument concepts are intended to provide a bridge between NASA's Earth Observing System mission and NPOESS.

NPP will extend the measurement series being initiated with the MODIS instrument on EOS Terra and the AIRS, AMSU, and HSB instruments that are flying on EOS Aqua. MODIS-like measurements will be continued using the Visible Infrared Imaging Radiometer Suite (VIIRS). AIRS-like measurements will be obtained from the Cross-track Infrared Sounder (CrIS). The NPOESS Integrated Program Office (IPO) will provide both of these sensors. The AMSU and HSB measurement series will be extended by the Advanced Technology Microwave Sounder (ATMS), which will be provided by NASA. Thus, NPP will provide NASA with a continuation of global-change observations that include monitoring of atmospheric and sea-surface temperatures, humidity sounding, land and ocean biological productivity, and cloud and aerosol properties.

In addition, the NPP mission will provide the NPOESS program with early access to the next generation of operational sensors, thereby greatly reducing the risks incurred during the transition from DMSP and POES. This will permit testing of the advanced ground operations facilities and validation of sensors and algorithms while the current operational systems are still in place. This new system will provide nearly an order of magnitude more data than the current operational system.

Launch is planned for late 2006 into an 824 km orbit with a 10:30 a.m. equator crossing time at the descending node. The orbit altitude is forward compatible with the NPOESS, while the crossing time is backward compatible with the EOS Terra mission. With a five-year design lifetime, NPP will provide data past the planned lifetime of EOS Terra and EOS Aqua and through the expected launch of the first NPOESS spacecraft in 2009.

Throughout all of these activities, ESE carries a strong commitment to make high quality, well documented Earth science data easily available to the global community to further environmental and global change research needs. The most pressing issues for global change research and NASA's Earth Science program are described in the "Earth Science Enterprise Strategic Plan," available at the following web site: www.earth.nasa.gov/visions/index.html

Three companion documents, the "Earth Science Enterprise Research Strategy," the "Technology Strategy," and the "Applications Strategy" are available on the same web site.

The Earth Observing System

The Earth Observing System (EOS) is a series of Earth-orbiting satellites which will provide global observations of the land surface, atmosphere, and oceans over 15 years or more, with the first satellites having been launched in the late 1990s. Complete information and details on the satellites and instruments included in EOS can be found in the 1999 EOS

Reference Handbook. This document can be directly accessed at:
eospso.gsfc.nasa.gov/eos_homepage/for_scientists/data_products/refbook1999.php.

EOS is complemented by missions and instruments from international partners, including Japan, Brazil, the European Space Agency (ESA), and ESA member countries. For example, the Tropical Rainfall Mapping Mission (TRMM) is a joint NASA/Japanese mission. In addition, some instruments flown on EOS satellites are provided by international partners, such as the Advanced Microwave Scanning Radiometer for EOS (AMSR-E) from Japan, and the Humidity Sounder for Brazil (HSB), both flying on Aqua. Together, these NASA and international programs form the basis for a comprehensive International Earth Observing System (IEOS).

The EOS satellites carry two classes of instruments: Facility Instruments supplied by NASA and the Ministry of Economy, Trade and Industry (METI)/National Space Development Agency of Japan (NASDA) in response to general mission requirements, and Principal Investigator (PI) Instruments selected through a competitive process and aimed at the focused research interests of the selected investigators. Two EOS instruments—Clouds and the Earth's Radiant Energy System (CERES) and Lightning Imaging Sensor (LIS)—are flown on the TRMM satellite, in addition to non-EOS instruments—Precipitation Radar (PR), TRMM Microwave Imager (TMI), and Visible Infrared Scanner (VIRS). However, data from all of the instruments on TRMM are part of the ESE research and data development program and are distributed through the EOSDIS archives. Consequently, this data product handbook includes descriptions of the data sets from all of the TRMM instruments. The Terra platform is in a polar orbit with a descending node equator crossing time of 10:40 a.m. Terra's sibling satellite, Aqua (described in Volume 2 of the EOS Data Products Handbook), was launched in May, 2002, and is in a complementary orbit crossing the equator at 1:30 p.m. local time. The TRMM satellite is in an inclined, equatorial orbit and only views the Earth from roughly 36°N to 36°S. Most of the Terra, Aqua and TRMM instruments operate in both daylight and darkness. However, some of the optical instruments collect visible data over areas of darkness.

The instruments have variable scanning and coverage characteristics. Depending on the swath width, some instruments provide global data daily, while some of the higher resolution instruments have smaller swaths and only cover a portion of the day. Within a repeat cycle of a few days, however, most of these instruments also provide global imaging. In the case of TRMM, the orbital processing is 30 days for the geographic and diurnal repeat, and for Terra and Aqua, the repeat cycle is roughly nine days.

EOS Validation

EOS manages a comprehensive Validation Program to verify geophysical measurements obtained by satellite sensors. The EOS Instrument Science Teams are responsible for algorithm validation and specification of the uncertainties in the high-level geophysical quantities derived from calibrated instrument measurements. Guidelines, policies, coordination, and the review process for EOS-wide validation activities are the responsibility of the EOS Validation Scientist within the EOS Project Science Office. Pre-launch activities include development and verification of algorithms and characterization of uncertainties resulting from parameterizations and their algorithmic implementation. Post-launch activities include refinement of algorithms and uncertainty estimates based on near-direct comparisons with correlative measurements and selected, controlled analyses or application implementations. Airborne measurements using specifically designed EOS instrument simulators and community airborne instruments also play an essential role in pre-launch and post-launch studies.

The Airborne Science program complements the Validation Program by providing aircraft capable of both *in situ* and remote sensing to perform scientific experiments that demonstrate the feasibility of new sensors before producing a space-based system, and validate the measurements of new satellite-borne sensors. Examples of recent airborne campaigns are studies of the Pacific tropospheric chemistry, the ecology of the Amazon region of Brazil, and biomass burning in southern Africa.

Science Data Sets

Data and data sets define mission success for the EOS. In more than 25 years of Earth observation, scientists have begun only recently to routinely use global data sets of moderate to coarse resolution (1-10 km) for global change research. It has taken computational advances, lowering of data cost, relaxation of data access restrictions, and proactive data set generation efforts (such as the Pathfinder programs of NOAA and NASA) to enable the research community to effectively use global, remotely sensed data sets. In the next decade, the EOS data sets and interdisciplinary investigations will advance the state-of-the-art use

of global Earth observation data to high to moderate resolution data sets (100-1000 m). These data sets present an unprecedented opportunity and challenge for the Earth science community.

The data sets for global change research that are being produced from the TRMM and Terra instruments have been selected by NASA through peer review. Investigators developing these data sets may be part of instrument teams or interdisciplinary science investigation teams.

The unprecedented science goals and volumes of these data sets drive several critical issues for the EOSDIS and its ground segment, which produces, archives, and distributes the data. The issues of producing and distributing these data sets fall into two basic categories: science and engineering. The science issues are being addressed in part through the development of Algorithm Theoretical Basis Documents (ATBDs) and the computation and engineering issues of data set production, archiving and distribution are being addressed by the EOS Data and Information System (EOSDIS) developers.

Algorithm Theoretical Basis Documents

Efforts defining the data sets' theoretical basis and science algorithms are taking place among the instrument and investigator teams under the coordinating direction of the EOS Senior Project Scientist. Each EOS instrument team for the Terra and TRMM platforms, as well as the Data Assimilation Office (DAO), has presented for peer review an ATBD which provides detailed descriptions of the data set science algorithm. These documents include:

- Overview and Technical Background;
- Science Rationale;
- Algorithm Theoretical Description;
  - Physics of the Problem
  - Mathematical Description
  - Uncertainty & Errors
- Practical Considerations;
  - Science Software Considerations
  - Calibration and Validation
  - Quality Control
  - Data Dependencies
  - Product Definition; and
- Implementation Schedule (pre- and post-launch).

Much of the information in this Data Products Handbook comes from the ATBDs, which are available over the Internet at the following address: eospso.gsfc.nasa.gov/eos_homepage/for_scientists/atbd/index.php.

EOS Data and Information System

Critical to the generation and distribution of the EOS data sets is the EOS Data and Information System (EOSDIS). The EOSDIS provides traditional flight operations, mission support, and data processing roles for EOS spacecraft and instruments and provides archiving and distribution services for EOS data and a variety of global change and Earth observation data.

The EOSDIS is taking advantage of recent advances in computational hardware, systems engineering, and national and international networking capabilities to implement a system of unprecedented capacity, user service, and openness.

EOSDIS Distributed Active Archive Centers

Key elements of EOSDIS are the Distributed Active Archive Centers (DAACs), the facilities responsible for producing, archiving, and distributing the data sets. The EOSDIS links these archives through high-speed networks and an open architecture to integrate and provide data services to the research community. "Open Architecture" means that the user community is able to access the system directly through its own customized interfaces as well as through standard data access interfaces.

There are currently nine DAACs representing a wide range of Earth science disciplines and socio-economic and educational applications. The geographic distribution of the DAACs is illustrated on the following page. Also refer to Appendix A, which provides access information for the DAACs. These institutions are custodians of EOS mission data, and ensure that data are easily accessible to users. Acting in concert, DAACs provide reliable, robust services to users whose needs may cross traditional discipline boundaries, while continuing to support the particular needs of their respective discipline communities. DAAC assignments were based primarily on the distribution of scientific expertise, institutional heritage, and capability. Each DAAC has a working group of users to provide recommendations on priorities for scientific data, levels of service, and the needed capabilities. The DAACs actively participate in the design, implementation, and operation of EOSDIS.

The EOSDIS Data Gateway provides information and ordering of data and documentation at the DAACs using a menu-driven interface. The service is open to the public with access to restricted data by authorization. The ordering service allows users to identify, browse, and then select data by time and

location, geophysical parameter, and processing level. The service is accessible via the internet at eos.nasa.gov/imswelcome. Access information for online and user support services for each of the DAACs is listed in Appendix A.

Data Set Distribution

The EOS data policy is to provide data to the global research community with few restrictions and at no cost or at most no more than the marginal cost of filling an order. Details of the EOS data policy can be found in the 1999 EOS Reference Handbook. EOS data are not copyrighted; however, it is requested that all researchers who publish data or results using EOS data sets include the following acknowledgment:

Data used in this research include data produced through the funding of NASA's Earth Science Enterprise Earth Observing System Program.

In addition, for publications using EOSDIS-provided data the following acknowledgment should be used:

Data used in this research include data provided to the authors by the NASA-funded EOS Data and Information System archive at [insert name of archive center providing data].

Reproducibility and Longevity

Since global change studies require access to Earth observation data over decades, one of the key directives of the EOSDIS is that all data archived and distributed will be sufficiently documented such that researchers looking at data 10 or 20 years after the launch of the spacecraft will be able to understand and read the data. Related to this is the principle that all software, documentation, ancillary data, etc., be available to users so that any data set will be reproducible by anyone in the research community. In addition to ensuring easy and open access, this will aid in the scientific peer review and validation process.

Suggested Reading

Asrar, G., and R. Greenstone, Eds., 1995.

Asrar, G., and J. Dozier, 1994.

Asrar, G. *et al.*, 2001.

Barry, R. G., and A. L. Varani, Eds., 1995.

King, M. D., and R. Greenstone, 1999.

Sellers, P. J. *et al.*, 1995.

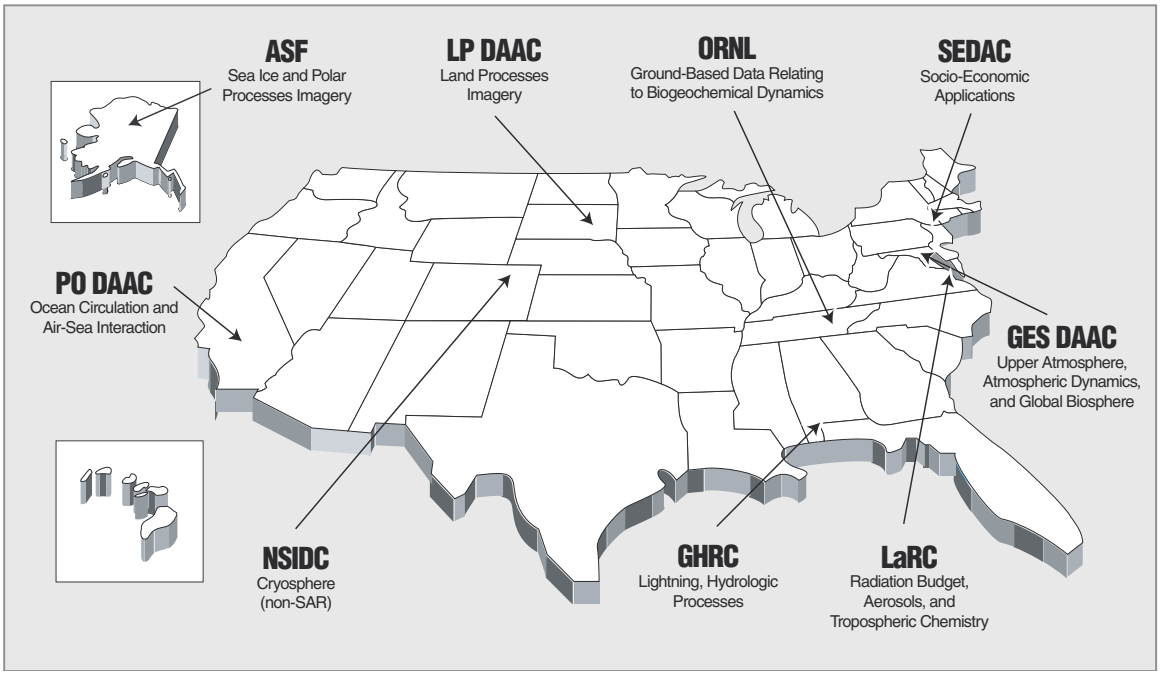

Distributed Active Archive Centers

Chapter 3

Instrument Descriptions and Data Processing Overviews

TRMM
CERES
LIS
PR
TMI
VIRS

Terra
ASTER
CERES
MISR
MODIS
MOPITT

Overview

The EOS system is designed to foster interdisciplinary use of Earth science data sets in ways that have been previously impossible. The science strategy identified early for ESE was to group instruments to exploit their capabilities for synergism in surface imaging and in determining related properties of the atmosphere. Cross-calibration of the instruments and validation of their resulting data products further enhance this synergism. Through EOSDIS, efforts to provide better data utilization include standardization of formats and media, consistency in standards and processing, and a platform of standard analysis tools to support investigation of the data.

Within the full EOS instrument suite, sets of instruments complement one another to produce desired observations. In some instances, certain instrument suites must generate correlative data; therefore, they must make their measurements simultaneously. For example, measurement of ocean circulation requires global altimeter data, precise orbit determination, and water vapor amounts. These observations also contain signals resulting from ocean tide deformation, atmospheric pressure and ocean surface interactions, and sea-level change, including long-term average sea level as well as interannual hemispherical variations. Such sets of observations dictate some minimum payload groupings.

The EOS science program combines the measurements from the assembled suite of instruments, using some instruments to refine the measurements of others or to provide data products derived from more than one instrument. This strategy permits the extraction of parameters that a single instrument cannot measure reliably. This flow of data, the product of one data set used as input to another, is critical to understanding the complex interrelationships of the Earth's system. Global and regional data assimilation models that function as part of EOSDIS use the observations from the EOS platforms to provide continuous calculations of the principal fluxes between components.

All EOS instruments have their own primary characteristics, and all fit together to complement each other. For example, compared with Moderate Resolution Imaging Spectroradiometer (MODIS), Advanced Spaceborne Thermal Emission and Reflection Radiometer (ASTER) has higher spatial resolution, but lower average duty cycle (8% day, 16% night). The Multi-Angle Imaging Spectroradiometer (MISR) is similar to MODIS in the 250-m bands. MODIS data can be used for atmospheric correction for ASTER and cloud screening for Clouds and the Earth's Radiant Energy System (CERES). Similarly, there are synergies between MISR and MODIS in characterizing aerosols over oceans. ASTER with its pointing, stereo mapping, and multi-spectral thermal infrared (IR) radiometer, provides synergism with MODIS and MISR, and acquires essential data for the study of volcanoes and surface climate. ASTER also provides simultaneous multispectral, high-resolution detail to support global mapping of surface vegetation by MODIS and MISR. Simultaneous data from ASTER are essential to understand the subpixel variability of MODIS and MISR data.

The synergy provided by EOS instruments may be used to obtain and apply atmospheric corrections to allow quantitative, rather than qualitative, remote sensing science (such atmospheric attenuation and cloud-screening corrections are applicable to multiple sensors, MODIS cloud cover for CERES and MOPITT, MODIS total-water vapor for ASTER). Also, they may be used to validate data product algorithms and maintain instrument calibrations over a 15-year period, leading to support of a broad range of interdisciplinary investigations describing the Earth's carbon, energy, and water cycles, and our impact on them.

For information about the products developed by the Data Assimilation Office, see Chapter 13.

Suggested Reading

Earth Observing System: Science and Mission Requirements Working Group Report.

Hobish, M. K. *et al.*, 1994.

King, M. D., ed., 1999.

Mission	Orbit Type	Altitude	Equatorial crossing time	Launch date
TRMM	Non sun-synchronous, 36° inclination	402 km	----------	November 27, 1997
Terra	Polar, sun-synchronous, 98.1° inclination	720 km	10:40 a.m.	December 18, 1999

Satellite missions covered in this volume

Satellite	Instrument	Description
TRMM	PR – Precipitation Radar	An electronically scanning radar operating at 13.8 GHz; 4.3 km instantaneous field-of-view at nadir; 220-km swath. Provided by NASDA (Japan).
TRMM	TMI – TRMM Microwave Imager	A nine-channel conical scanning passive microwave imager making measurements from 10 to 85 GHz, 37 to 4.6 km resolution respectively, covering 760 km swath.
TRMM	VIRS – Visible Infrared Scanner	A five-channel cross-track imaging radiometer (0.62, 1.63, 3.78, 10.83, and 12.03 µm) with nominal 2-km resolution at nadir and 720-km swath.
TRMM & Terra	CERES – Clouds & the Earth's Radiant Energy System	A three-channel radiometer (0.3 to > 50 µm, 0.3 to 5 µm, 8 to 12 µm). TRMM has one cross-track scanning radiometer and Terra has two instruments, one operating in cross-track mode and one in rotating azimuth plane mode. The spatial resolution at nadir is 10 km from the TRMM orbit and 20 km from the highest Terra orbit.
TRMM	LIS – Lightning Imaging Sensor	Staring telescope/filter imaging system (0.777 µm) with 5-km spatial resolution and 2-msec temporal resolution over an imaging area of 600 × 600 km.
Terra	ASTER – Advanced Spaceborne Thermal Emission & Reflection Radiometer	A three-radiometer sensor package with three vis/near-IR, six shortwave, and five thermal infrared channels with 15, 30, and 90-m resolution, respectively, and a 60-km swath. Provided by the Japanese Ministry of Economy, Trade and Industry (METI).
Terra	MISR – Multi-angle Imaging Spectroradiometer	Thirty-six channel instrument; nine pushbroom cameras with discrete view angles (to ± 70°) in four spectral bands (0.443 to 0.865 µm) with resolution of 275 m to 1.1 km.
Terra	MODIS – Moderate Resolution Imaging Spectroradiometer	Thirty-six channel imaging radiometer (0.4 µm to 14.5 µm) with 250-m, 500-m, or 1-km resolution and 2,300-km swath width.
Terra	MOPITT – Measurements of Pollution in The Troposphere	Eight-channel cross-track scanning gas correlation radiometer operating at three wavelengths (2.2, 2.3, and 4.7 µm).

Coverage characteristics of the instruments on TRMM and Terra

TRMM

Tropical Rainfall Measuring Mission

TRMM is a joint NASA/Japan satellite designed specifically to monitor rainfall and its associated latent heating in the tropics and subtropics. The total rainfall and its distribution are important, because the atmosphere gets three-fourths of its heat energy from the release of latent heat in the process of precipitation. The horizontal and vertical location at which this energy is released affects the weather around the world. Despite its fundamental importance to global climate, the total rainfall in the tropics is not well known, and the vertical distribution of latent heating can only be estimated imprecisely. Although the sensors on TRMM have utility beyond the primary rainfall parameters, the TRMM Science Team has defined and developed a set of "standard products" that are critical to monitoring rainfall and its vertical structure. These standard products are processed by the TRMM Science Data and Information System (TSDIS).

The figure on the following page shows how the various satellite sensors and algorithms interact in order to provide the TRMM satellite standard products. The algorithms are coded by members of the TRMM science team who have the responsibility to develop these products. As an example, the passive microwave (TMI) team has the responsibility for generating code to produce TMI calibrated brightness temperatures (1B-11), TMI rainfall structure products (2A-12), and TMI monthly surface rainfall maps (3A-11). This type of in-team algorithm development can be seen for each of the three instrument teams.

A key feature of TRMM is the combined algorithms. These algorithms include the "TRMM Combined Algorithm," which refers to an algorithm that combines TRMM sensor measurements; and "TRMM & Other Sensors," which refers to algorithms that take the best rain estimates from TRMM and use them to calibrate other available data, in order to reduce the sampling bias.

The TRMM mission has identified four main ground validation (GV) sites, which include ground-based radars and their associated rain gauge networks. These sites include Southern Florida, Australia (Darwin), Southeastern Texas, and the Marshall Islands (Kwajalein Atoll). GV data are processed at Goddard Space Flight Center in cooperation with the TRMM GV team. A flow diagram of these products and how they interact is shown in the second figure. All GV products for the different sites are processed using the same algorithms developed by the TRMM GV Team.

The TRMM mission recognizes that new sensor data often lead to significant improvements in interpretation of remotely sensed data and quality of products. To ensure that any improvements in the products are quickly passed on to the research community, TRMM reprocesses data periodically as better algorithms or calibration procedures become available. To provide the stable long time series of products needed for Earth system research, the entire TRMM data set is reprocessed each time starting from day one of the mission.

On August 22, 2001, the spacecraft orbit was boosted from 350 km to 402 km to conserve its remaining fuel and extend the mission's life into the 2005-2007 time frame. Note that the instrument swath sizes increased by about 15 percent with the altitude increase, but there are no other significant changes to the data products.

TRMM Home Page: trmm.gsfc.nasa.gov

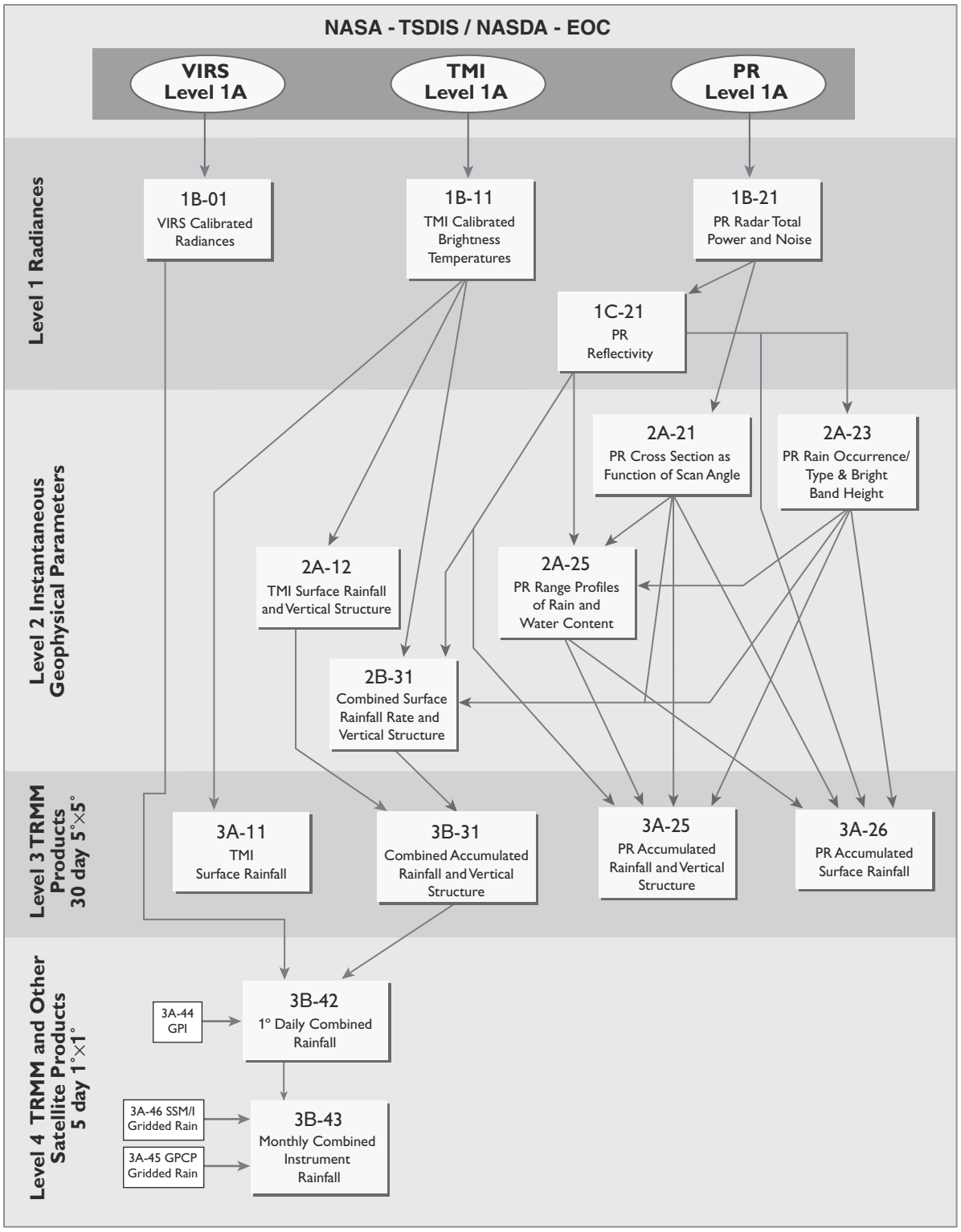

TRMM Instrument Algorithms and Products

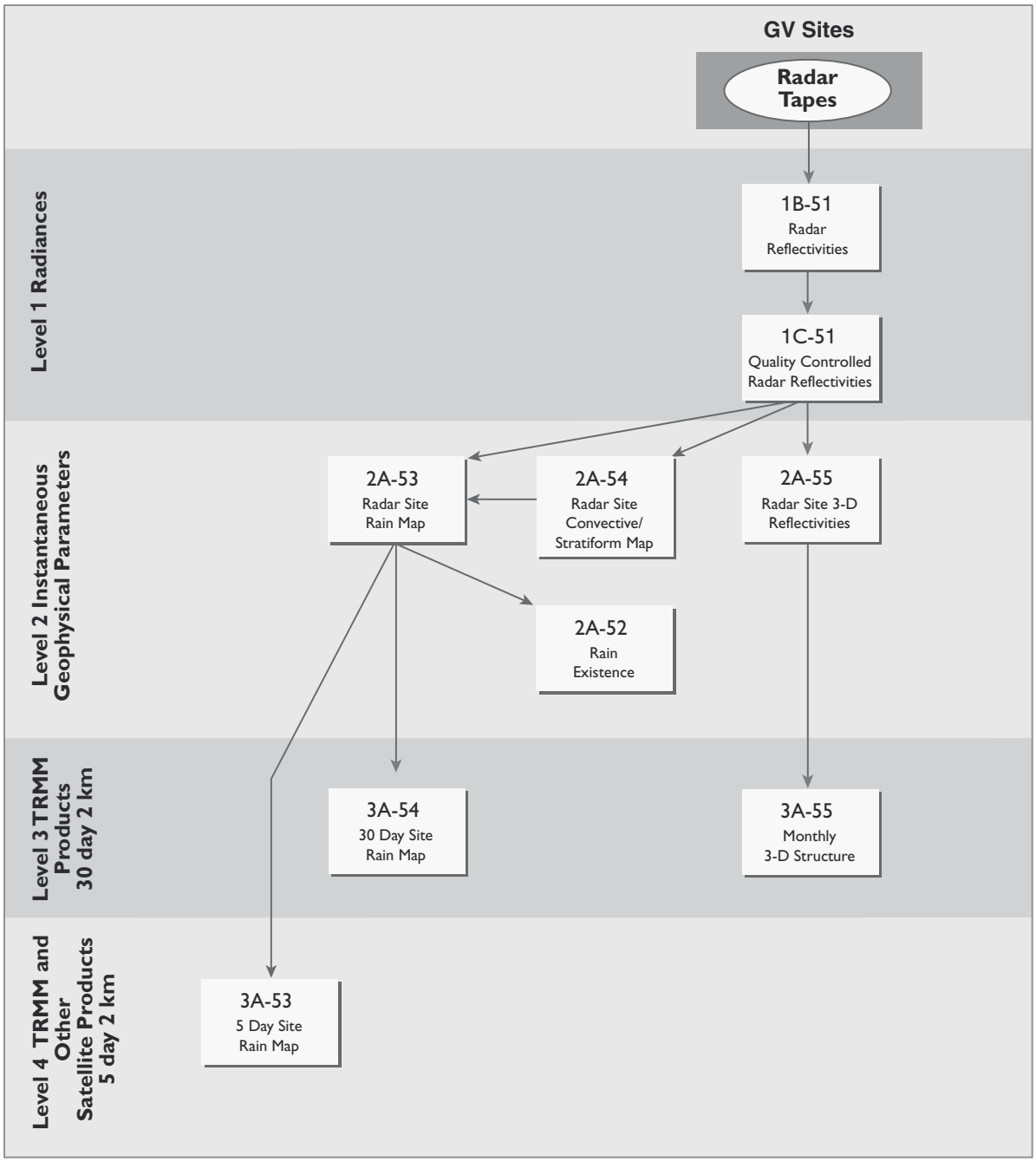

Interaction of TRMM Ground-Based Radar Validation Products

LIS

Lightning Imaging Sensor

The Lightning Imaging Sensor (LIS) is a calibrated, optical imager designed to measure the global incidence of lightning, and to investigate its correlation with rainfall and its relationship with the global electric circuit. Conceptually, LIS is a simple device, consisting of a staring imager optimized to locate both intracloud and cloud-to-ground lightning with storm-scale resolution over a large region of the Earth's surface, to mark the time of occurrence, and to measure the radiant energy. It was designed to monitor individual storms within its field-of-view (FOV) for more than 80 seconds, which is long enough to estimate the flashing rate of active storms. LIS was launched on TRMM in November 1997 and has performed flawlessly since that time. It has provided global maps of tropical lightning activity with location accuracies of greater than 5 km.

The LIS design uses an expanded-optics 100° FOV lens combined with a narrow-band width (1.0 nm) interference filter that focuses the image on a small, high-speed, charge-coupled-device (CCD) focal plane. The signal is read out from the focal plane into a real-time data processor for event detection and data compression. The unusual characteristics of the sensor design result from the requirement to detect weak lightning signals during the day when the background illumination, produced by sunlight reflecting from the tops of clouds, is much brighter than the illumination produced by the lightning.

A combination of four methods is used to take advantage of the significant differences in the temporal, spatial, and spectral characteristics between the lightning signal and the background noise. First, spatial filtering is used to match the instantaneous FOV of each detector element in the LIS focal-plane array to the typical cloud-top area illuminated by a lightning event (about 5 km). Second, spectral filtering is applied, using a narrow-band interference filter centered about the strong singly ionized oxygen emission line (OI [1]) multiplet in the lightning spectrum at 777.4 nm. Third, temporal filtering, using very short CCD integration times (2 milliseconds), is applied to further suppress the background noise.

The lightning pulse duration is of the order of 400 microseconds, whereas the background illumination tends to be constant on a time scale of seconds. Hence, the lightning signal-to-noise ratio improves as the CCD integration time approaches the pulse duration until a significant number of pulses start to be split between successive frames. The two-millisecond integration time helps maximize lightning detectability. Finally, a modified frame-to-frame background subtraction is used to remove the slowly varying background signal from the raw data coming off the LIS focal plane. If after background removal, the signal for a given pixel exceeds a specified threshold, that pixel is processed as if it contains a lightning event.

Since its launch, LIS investigations have furthered our understanding of processes related to, and underlying, lightning phenomena in the Earth/atmosphere system. These processes include the amount, distribution, and structure of deep convection on a global scale, and the coupling between atmospheric dynamics and energetics as related to the global distribution of lightning activity. These investigations have contributed to a number of important EOS mission objectives, including cloud characterization and hydrologic cycle studies. LIS studies have demonstrated that lightning activity is closely coupled to storm convection, dynamics, and microphysics, and can be correlated to the global rates, amounts, and distribution of ice phase precipitation, to the release and transport of latent heat, and to the natural production of NO_x. LIS standard products include the locations, times of occurrence, and intensities of lightning events.

Key LIS Facts

LIS Home Page: thunder.msfc.nasa.gov

EOS-funded instrument, launched on TRMM November 27, 1997

Staring telescope/filter imaging system that detects the rate, location, and radiant energy of lightning flashes

Investigates the distribution and variability of lightning over the Earth with storm-scale spatial resolution

80-90% detection efficiency under both day and night conditions using background remover and event processor

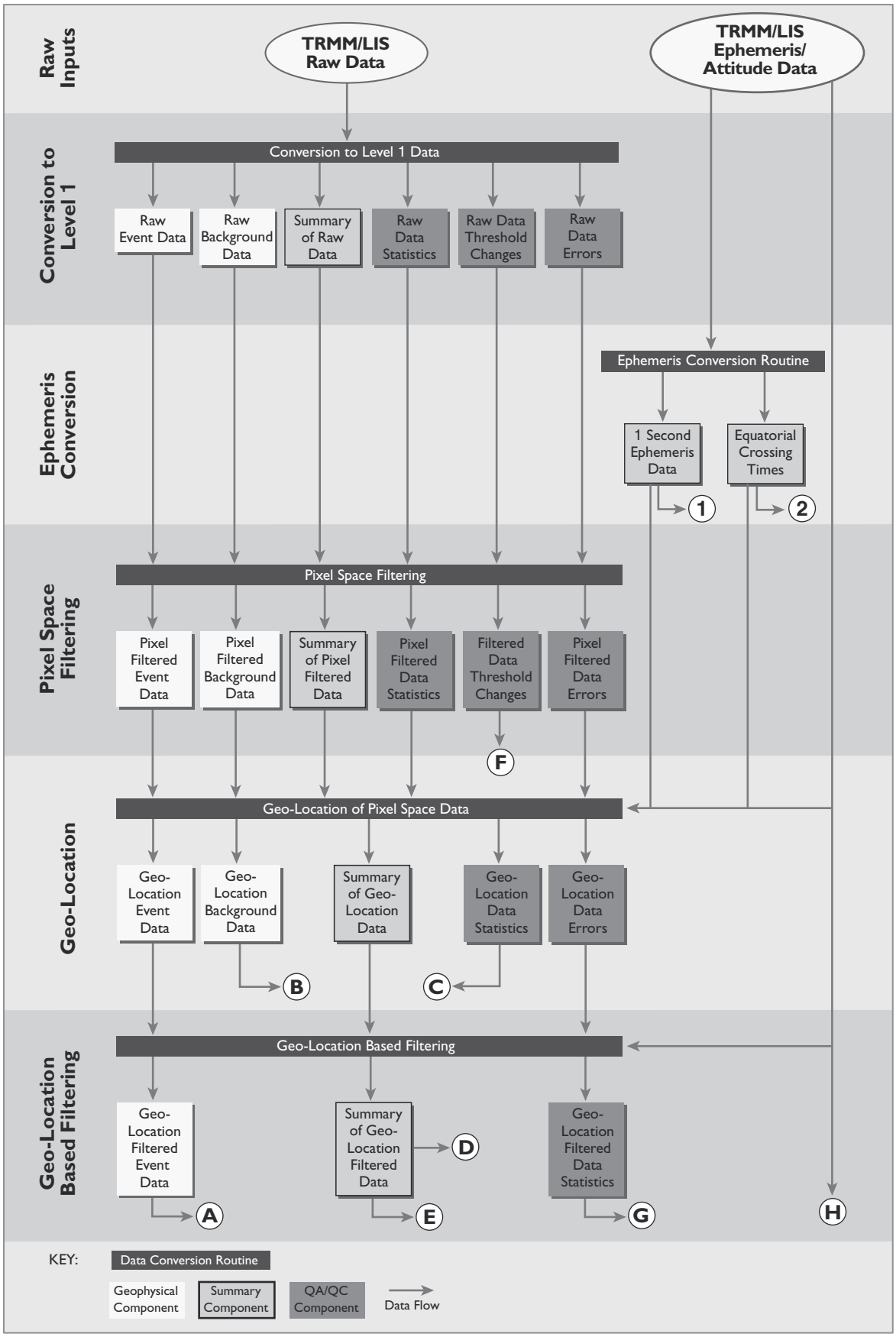

LIS Data Flow *(continued next page)*

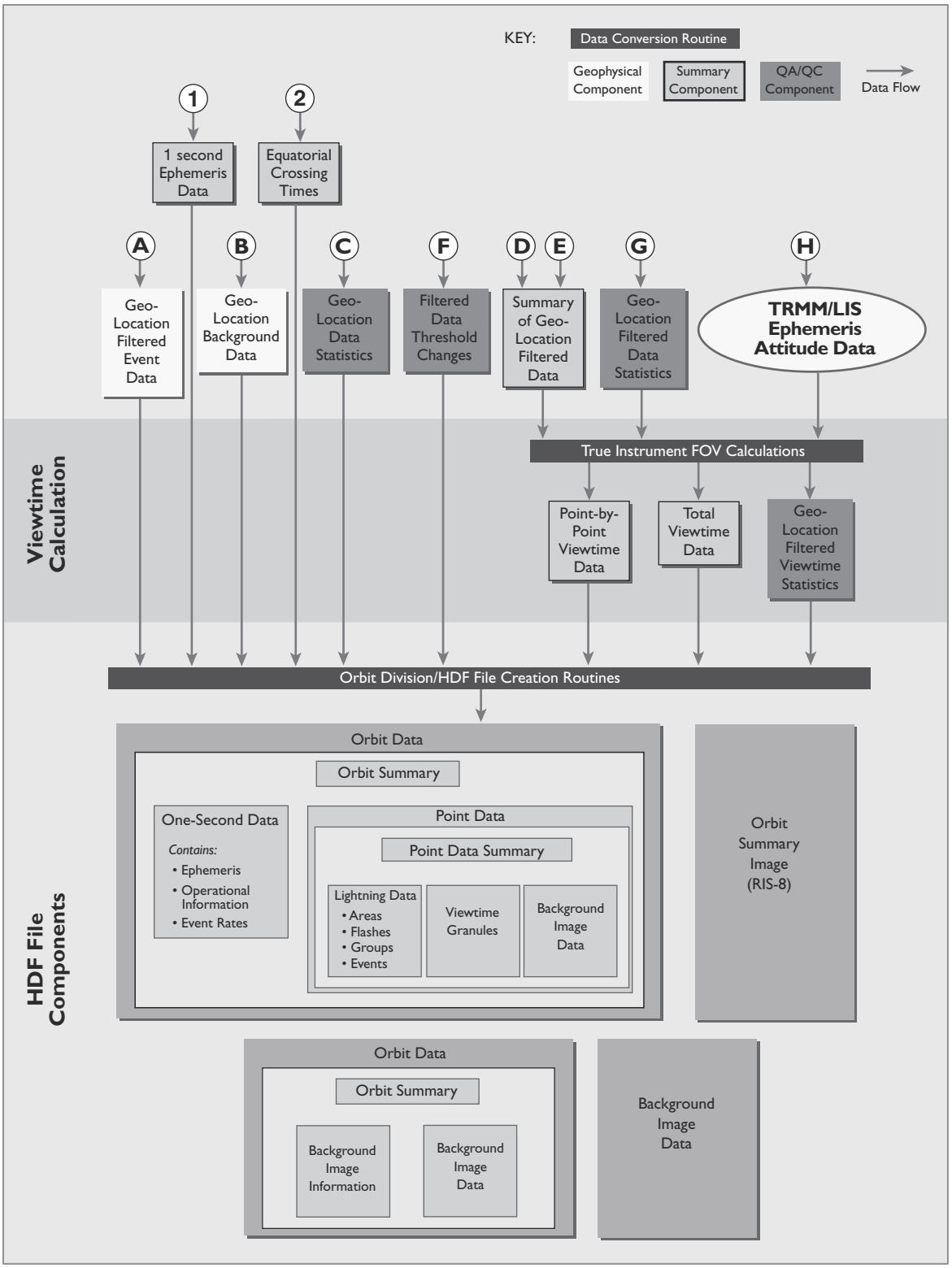

LIS Data Flow ***(continued)***

ASTER

Advanced Spaceborne Thermal Emission and Reflection Radiometer

ASTER is a Facility Instrument provided for the EOS Terra platform by the Japanese Ministry of Economy, Trade and Industry (METI). It provides high spatial resolution (15-90 m) multispectral images of the Earth's surface and clouds in order to better understand the physical processes that affect climate change. ASTER provides data at a scale that can be directly related to detailed physical processes. These data bridge the gap between field observations and data acquired by coarse spatial resolution instruments such as MODIS and MISR, and between local-process models and regional models.

Clouds are one of the most important variables in the global climate system. With its high spatial-resolution, broad spectral coverage, and stereo capability, ASTER provides essential measurements of cloud amount, type, spatial distribution, morphology, and radiative properties. ASTER data are also used for long-term monitoring of local and regional changes on the Earth's surface, which either lead to, or are in response to, global climate change (e.g., land use, deforestation, desertification, lake and playa water level changes) and other changes in vegetation communities, glacial movement, and volcanic processes. ASTER provides radiative (brightness) temperature, and the multispectral thermal infrared (TIR) data can be used to derive surface kinetic temperature and spectral emissivity. Radiative temperature is an element in the surface heat balance. Surface kinetic temperature can be used to determine elements of surface process models, sensible heat flux, latent heat flux, and ground heat conduction. Surface temperatures are also related to thermophysical properties (such as thermal inertia), vegetation health, soil moisture, temporal land classification (e.g., wet vs. dry, vegetated vs. bare soil) and evapotranspiration.

ASTER operates in three visible and near-infrared (VNIR) channels between 0.52 and 0.86 μm, with 15-m resolution; six shortwave infrared (SWIR)

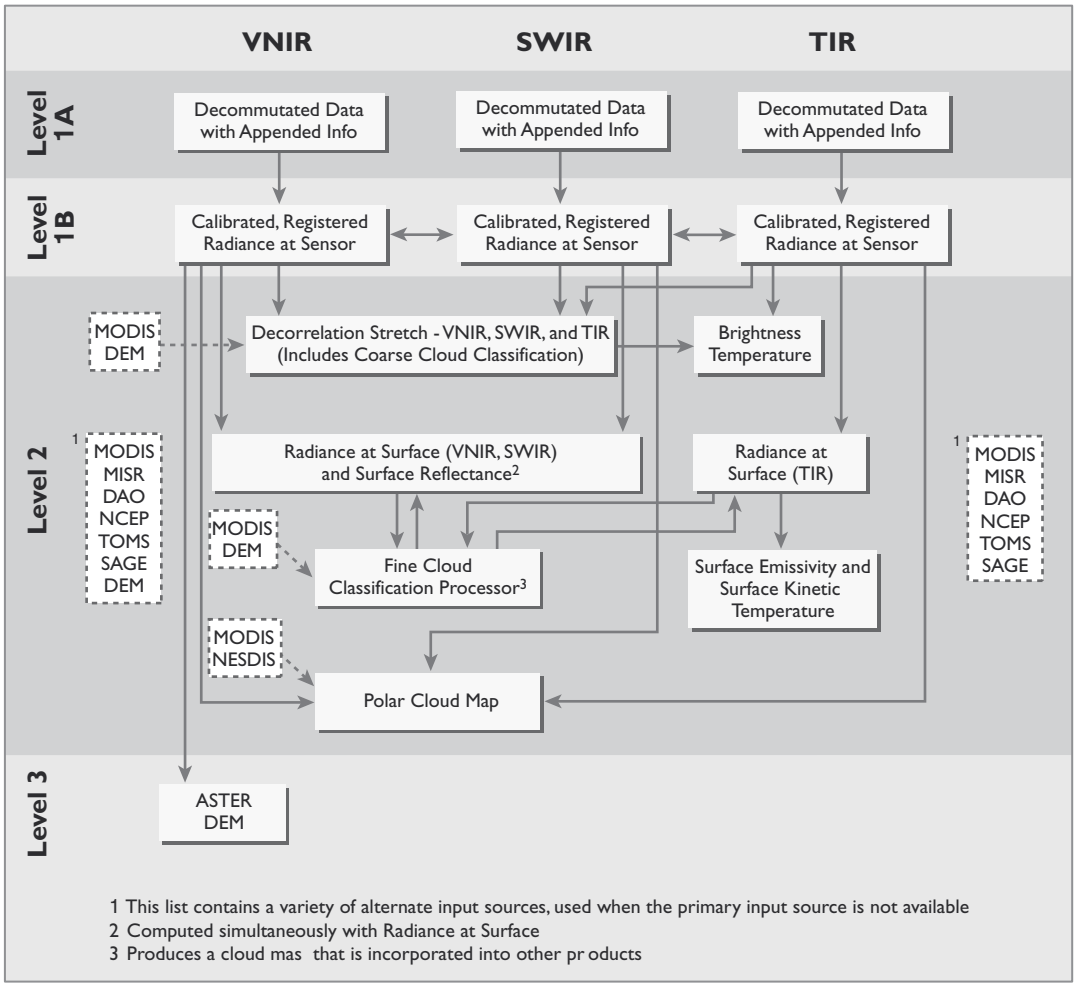

ASTER Data Product Architecture

channels between 1.60 and 2.43 μm, with 30-m resolution; and five TIR channels between 8.13 and 11.65 μm, with 90-m resolution. The instrument acquires data over a 60-km swath whose center is pointable (cross-track ± 8.55° in the SWIR and TIR, with the VNIR pointable out to ± 24°). An additional VNIR telescope (aft pointing) covers the wavelength range of Channel 3. By combining these data with those for Channel 3, stereo views can be created, with a base-to-height ratio of 0.6. ASTER's pointing capabilities are such that any point on the globe is accessible at least once every 16 days in all 14 bands on average every 4 days in the three VNIR channels.

ASTER data products exploit combinations of VNIR, SWIR, and TIR for cloud studies, surface mapping, soil and geologic studies, volcano monitoring, and for surface temperature, emissivity, and reflectivity determination. VNIR and SWIR bands are used for investigation of land use patterns and vegetation, VNIR and TIR combinations for the study of coral reefs and glaciers, and VNIR for digital elevation models (DEMs). TIR channels are used for study of evapotranspiration, and land and ocean temperature. The stereoscopic capability yields local topography, cloud structure, volcanic plumes, and glacial changes.

Since launch in 1999, the ASTER instrument has performed exceptionally well. No operational anomalies have occurred. Analyses of the data have revealed several characteristics not accounted for prior to launch. Most of these have been addressed, and software corrections implemented in the standard data processing algorithms. There remain a small number of factors that the ASTER Science Team is still addressing, and developing corrections.

1) Optical cross-talk in the SWIR spectrometer results in anomalous signal leaking into adjacent bands; this is most pronounced for energy falling on detectors for Band 4, and a small fraction reflecting onto detectors for Bands 5 and 9. The effect has been characterized, and software is being tested to correct the problem. It is anticipated that a revised standard higher level data product will incorporate the corrections.

2) A scratch has been detected on the filter in the SWIR detector package; it manifests itself as a squiggly line in harshly processed data. A software correction is being tested, and will be incorporated in the Level 1 software algorithms.

3) An error in the geo-location information in the metadata was found: there is a fixed error for the earth rotation angle in the coordinate transformation from the earth inertial frame to the earth fixed frame. The error is very small at mid-latitudes. A correction table will be made available to users to correct this error in the near future, and a modification of the Level 1 production software is planned.

Suggested Reading

Abrams, M., 2000.

Iwasaki, A. et al., 2002.

Yamaguchi, Y. et al., 2001.

ASTER Users Handbook, Version 2, asterweb.jpl.nasa.gov

ASTER Level 1 Users Guide, www.science.aster.ersdac.or.jp/users/defaulte.htm

Key ASTER Facts

ASTER Home Page: asterweb.jpl.nasa.gov

Launched on Terra December 18, 1999

Heritage: JERS-1 and Landsat

Imaging radiometer

Provides high-resolution images of the land surface, water, ice, and clouds

Earth-orbit stereo capability

14 multispectral bands from visible through thermal infrared

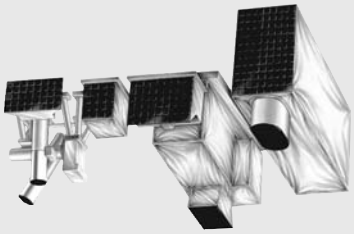

ASTER

CERES

Clouds and the Earth's Radiant Energy System

The U.S. Global Change Research Program classifies the role of clouds and radiation as its highest scientific priority (CEES, 1994). There are many excellent summaries of the scientific issues (IPCC, 1992; Hansen *et al*., 1993; Ramanathan *et al*., 1989; Randall *et al*., 1989, Wielicki *et al*., 1996) concerning the role of clouds and radiation in the climate system. These issues naturally lead to a requirement for improved global observations of both radiative fluxes and cloud physical properties. The CERES Science Team, in conjunction with the EOS Investigators Working Group representing a wide range of scientific disciplines from oceans, to land processes, to atmosphere, has examined these issues and proposed an observational system with the following objectives:

1) For climate-change analysis, provide a continuation of the Earth Radiation Budget Experiment (ERBE) record of radiative fluxes at the top of the atmosphere (TOA), analyzed using the same algorithms that produced the existing ERBE data.

2) Double the accuracy of estimates of radiative fluxes at TOA and the Earth's surface.

3) Provide the first long-term global estimates of the radiative fluxes within the Earth's atmosphere.

4) Provide cloud-property estimates which are consistent with the radiative fluxes from the surface to the top of the atmosphere.

To accomplish these goals, the CERES data products are divided into three major categories, as shown in the figure on page 34: ERBE-like Products (top row), CERES Surface/TOA Products (middle row), and CERES Surface/TOA/Atmosphere (bottom row).

The ERBE-like products address the first objective of long-term continuity of the ERBE TOA fluxes. The Surface/TOA Products address the second objective and attempt to provide the most direct tie between surface radiative-flux estimates and TOA flux measurements. The Surface/TOA/Atmosphere products focus on the last two objectives and attempt to derive an internally consistent set of atmosphere, cloud, and surface-to-TOA radiative fluxes, all within the context of a state-of-the-art radiative-transfer model. In this last case, the observed TOA fluxes are used as a direct constraint on the model calculations in order to implicitly account for non-plane-parallel and other poorly modeled atmospheric radiative effects. As in ERBE, CERES radiative fluxes will be separately determined for both clear- and cloudy-sky conditions.

One of the major advances of CERES over ERBE is the availability of high spatial and spectral resolution cloud imagers for cloud masking, cloud height, and cloud-optical-property determination (i.e., VIRS on TRMM, MODIS on Terra and Aqua; for more information about Aqua, see *EOS Data Products Handbook, Volume 2*.) A second major advance is the use of one CERES scanner in a cross-track mode (global spatial coverage) and a second scanner in a rotating-azimuth-plane mode (complete angular sampling of viewing zenith and azimuth). The rotating-azimuth-plane scanner data will be combined with nearly simultaneous cloud-imager data to develop a new set of improved empirical models of the shortwave (SW) and longwave (LW) anisotropy of radiation as a function of surface and cloud type. While it is estimated to take two years of these data to develop new angular models, they are expected to reduce instantaneous TOA flux errors by a factor of three from the ERBE levels.

A detailed listing of the CERES data products and their individual parameters can be found in the CERES Data Products Catalog (asd-www.larc.nasa.gov/DPC/DPC.html). Documentation of the Release 1 CERES analysis algorithms can be found in the CERES Algorithm Theoretical Basis Documents (ATBDs) Volumes 0 through 12, where each volume covers one of the CERES Data Products and its associated technical algorithms (eospso.gsfc.nasa.gov/atbd/cerestables.html). A summary of the CERES experiment can be found in Wielicki *et al*., *Bulletin of the American Meteorological Society*, May, 1996.

The two CERES instruments on the EOS Terra spacecraft have performed nominally since launch in December of 1999, with no in-flight anomalies to date. The single CERES instrument on the EOS TRMM spacecraft, launched in November of 1997, collected 9 complete months (January-August 1998, March 2000) of science data before a failing voltage converter resulted in the loss of science data transmission. All CERES radiometric performance goals have been met or exceeded on both platforms. Analysis of the collected radiometric science measurements has indicated minor drifts (~1%/yr) in two of the six radiometric channels on the Terra spacecraft. These drifts, which occur in the shortwave spectral regions (0.2-3.0 μm) of the broadband total channels (0.2 - >100 μm) on each of the CERES/Terra instruments, may cause errors in the CERES/Terra Daytime longwave data. The longwave portion of the CERES/Terra total channels (3.0 - >100 μm) are stable at the 0.25%/yr level while the shortwave and atmospheric window channels are stable at better than 0.10%/yr.

All channels on the CERES/TRMM instrument were stable over the 8 months of science data collection. A thorough radiometric validation protocol has been developed to continuously monitor the radiometric performance of the instruments. This protocol is able to characterize and quantify radiometric drifts, or instrument artifacts, so that they may be removed from the Level 1 and Level 1b data products. Data users are warned that these artifacts are not removed from the Terra Edition1 BDS, ES-8, ES-4, and ES-9 data sets. All other validated CERES data sets have these artifacts removed, including the Terra Edition2 BDS, ES-8, ES-4, and ES-9 data sets, as well as all validated TRMM data sets. A more detailed description of these artifacts and their impact on the data products are documented in the CERES Data Product Quality Summaries and may be found at the web pages listed below. These Quality Summaries are dynamic and will be updated to document future artifacts and quantify their impact on the data products.

Suggested Reading

Priestley, K. J. *et al.*, 2002.

Lee, R. B. *et al.*, 1998.

asd-www.larc.nasa.gov/ceres

asd-www.larc.nasa.gov/Instrument/intro.html

eosweb.larc.nasa.gov/PRODOCS/ceres/table_ceres.html

Key CERES Facts

CERES Home Page:
asd-www.larc.nasa.gov/ceres/docs.html

Launched on TRMM November 27, 1997; on Terra December 18, 1999; and on Aqua, May 4, 2002

Heritage: ERBE

Broadband, scanning radiometer capable of operating in cross-track mode, or rotating plane mode (bi-axial scanning)

Dual scanners on Terra

Measures Earth's radiation budget and atmospheric radiation from the top of the atmosphere to the surface

First instrument (cross-track scanning) will essentially continue the ERBE mission; the second (biaxially scanning) will provide angular radiance information that will improve the accuracy of angular models used to derive the Earth's radiative balance

CERES

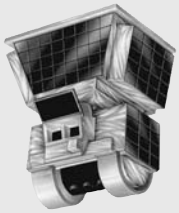

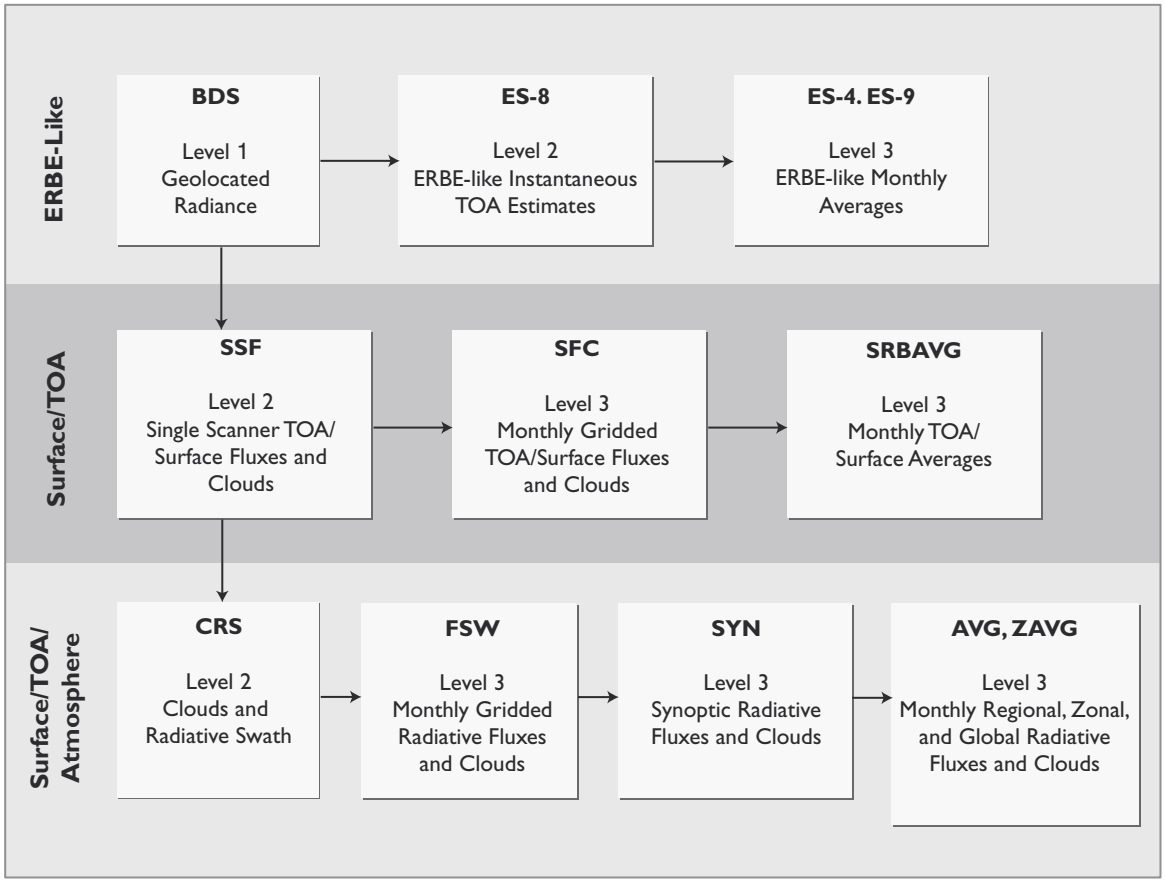

CERES Data Processing Architecture and Products

MISR

Multi-angle Imaging SpectroRadiometer

MISR routinely provides multiple-angle continuous coverage of the sunlit Earth with moderately high spatial resolution. The instrument obtains multi-directional observations of each scene within seven minutes, under virtually the same atmospheric conditions. MISR uses nine individual charge-coupled device (CCD)-based pushbroom cameras to observe the Earth at nine discrete view angles: one at nadir, plus eight other symmetrical views at 26.1°, 45.6°, 60.0° and 70.5° forward and aftward of nadir. Images at each angle are obtained in four spectral bands centered at 446, 558, 672, and 866 nm. Each of the 36 instrument data channels (four spectral bands in each of nine cameras) is capable of providing ground sampling of 275 m, 550 m, or 1.1 km. The actual observing configuration is selected by commands to the instrument.

The swath width of the MISR imaging data is 360 km, providing global multi-angle coverage of the entire Earth in nine days at the equator, and two days at the poles.

The instrument design and calibration strategies maintain absolute radiometric uncertainty to ±3% over bright surfaces and ±6% over dark surfaces, with smaller uncertainties in relative band-to-band and angle-to-angle radiances. These objectives are met by deploying the instrument's On-Board Calibrator (OBC) on a bimonthly basis; the calibrator consists of solar diffuser panels and an array of radiation-resistant and high-quantum-efficiency diodes. Semiannual field calibration exercises provide ground-truth verification of diode performance.

MISR images are acquired in two observing modes: global and local. Global mode provides continuous planet-wide observations, with 24 channels operating at 1.1-km resolution and 12 selected channels operating at 275 m. Local mode provides data at the highest resolution in all spectral bands and all cameras for selected 360 km (cross-track) × 300 km (along-track) regions. In addition to radiometrically calibrated and geo-rectified image products, global mode data are used to generate two standard Level 2 science products during ground data processing: the Top-of-Atmosphere (TOA)/Cloud Product and the Aerosol/Surface Product.

The TOA/Cloud Product provides global information about cloud types (classified by heterogeneity and altitude) and their effects on the solar radiance and irradiance reflected to space. These are key factors that determine cloud effects on Earth's climate. This product also provides stereoscopically-derived cloud-top heights and cloud-tracked winds, as well as a cloud screen for MISR aerosol and surface retrievals.

The Aerosol/Surface Product contains global aerosol parameters describing the magnitude and natural variability in space and time of sunlight absorption and scattering by aerosols in the Earth's atmosphere. These parameters help determine aerosol effects on climate and improve our knowledge of the sources, sinks, and global budgets of natural and anthropogenic aerosols. They also provide atmospheric correction inputs for surface imaging data acquired by MISR and other instruments. The surface parameters within the Aerosol/Surface Product characterize land surface radiative properties, particularly bidirectional and hemispherical reflectances, on a global basis. In conjunction with MODIS, they provide improved measures of land surface classification, dynamics, canopy photosynthesis, and transpiration rates over vegetated terrain. They also supplement MODIS studies of the biogeochemical cycle in the tropics by providing atmospherically-corrected ocean color data.

This handbook describes three ancillary products (MIS10, MIS11, and MIS12) that are produced at the MISR Science Computing Facility (SCF) and used in the generation of other MISR products. These products are available from the Langley Atmospheric Sciences Data Center as aids in interpreting MISR data.

Overall, the MISR instrument performance is excellent. However, there are several factors affecting science data quality that users should take into consideration:

1) Uncertainties in low-light-level radiometry. The MISR radiometric scale has been validated to 4% uncertainty through comparisons with AirMISR, AVIRIS, MODIS, and vicarious calibrations over medium to bright land targets. For uniform dark targets (equivalent reflectances ~0.05), uncertainties are estimated to be about 10%. For very dark targets (equivalent reflectances <0.05), especially those embedded in heterogeneous scenes, percentage uncertainties are larger due to the challenge of identifying robust calibration standards and the effects of errors in system linearity and video offset determination, imperfect point-spread function deconvolution, and optical ghosting. Specific studies are planned to quantify and reduce these uncertainties.

2) South Atlantic Anomaly effects on radiometry. Proton impingement on the MISR focal plane CCD's can induce random bright points in the imagery. Converting these bright values to equivalent reflectance, 0.00007% of pixels outside of the SAA

have equivalent reflectance errors associated with such hits >0.004; during transit through the SAA the frequency of pixels increases to 0.06%. These rare events do not correlate from one band or angle to another, and can be ignored for most applications. Certain high level processing algorithms such as aerosol retrievals contain data filters that safeguard against the use of affected pixels.

3) "Bit flips" and instrument "out-of-synchronization" events. Random occurrences of bit flips in packet headers, or instrument out-of-sync events which occur when the data throughput exceeds the flight computer's ability to process packet headers properly, can cause momentary data gaps a few lines in duration. Most affected image lines are flagged in ground data processing, and appear as dark stripes across Level 1 imagery. Typically about 0.02% of image lines are affected, and usually only in those orbits that contain Local Mode sequences.

4) 70° aft camera pointing anomalies. For eight of the nine MISR cameras, camera-to-camera co-registration uncertainty is less than 1 pixel (275 m). Time-varying co-registration errors in the 70° aft camera have been observed, with errors typically less than two pixels, though larger on occasion. Image matching algorithms using "reference orbit imagery" have been implemented and usually successfully correct these errors. However, they may be present in portions of some orbits, and a geometric data quality indicator is being implemented within the Level 1 georectified radiance product to alert users.

Suggested Reading

Diner, D. J. *et al*., 2002.

Bruegge, C. J. *et al*., 2002.

Jovanovic, V. M. *et al*., 2002.

Bothwell, G. W. *et al*., 2002.

Key MISR Facts

MISR Home Page: www-misr.jpl.nasa.gov

Launched on Terra December 18, 1999

Heritage: Galileo, Wide-Field/Planetary Camera

Provides radiometrically and geometrically calibrated multi-angle radiance measurements of the atmosphere, clouds, and surface with moderately high resolution

Provides global aerosol properties, cloud-top heights and cloud-tracked winds, top-of-atmosphere and land-surface albedo, and vegetation properties

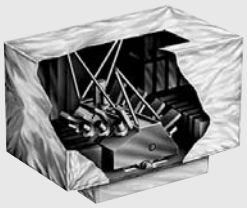

MISR

The new Diamond Valley Lake Reservoir near the city of Hemet in Riverside County is billed as the largest earthworks construction project in U.S. history. Construction began in 1995 and involved 31 million cubic meters of foundation excavation and 84 million cubic meters of embankment construction. The above set of MISR images captures a phase in the reservoir's activation. At the upper left is a view acquired by the instrument's vertical-viewing (nadir) camera on March 14, 2000, shortly after the Metropolitan Water District began filling the reservoir with water from the Colorado River and Northern California. Water appears darker than the surrounding land. The image at the upper right was acquired nearly one year later on March 1, 2001, and shows a clear increase in the reservoir's water content. When full, the lake will hold nearly a trillion liters of water. On the internet, visit visibleearth.nasa.gov to view a variety of MISR data images.

MODIS

Moderate Resolution Imaging Spectroradiometer

MODIS is an EOS facility instrument designed to measure biological and physical processes on a global basis every one to two days. Currently flying onboard the Terra and Aqua satellites, the instrument will provide long-term observations from which to derive an enhanced knowledge of global dynamics and processes occurring on the surface of the Earth and in the lower atmosphere. This multidisciplinary instrument will yield simultaneous, congruent observations of high-priority atmospheric (cloud cover and associated properties), oceanic (sea-surface temperature and chlorophyll), and land-surface features (land-cover changes, land-surface temperature, and vegetation properties). The instrument is continuing to make major contributions to the understanding of the global Earth system, including interactions between land, ocean, and atmospheric processes.

The MODIS instrument employs a conventional imaging-radiometer concept, consisting of a cross-track scan mirror and collecting optics, and a set of linear detector arrays with spectral interference filters located in four focal planes. The optical arrangement provides imagery in 36 discrete spectral bands from 0.4 to 14.5 μm, selected for diagnostic significance in Earth science. The spectral bands have spatial resolutions of 250 m, 500 m, or 1 km at nadir; signal-to-noise ratios of greater than 500 at 1-km resolution (at a solar zenith angle of 70°); and absolute irradiance accuracies of ±5% from 0.4 to 3 μm (2% relative to the Sun) and 1% or better in the thermal infrared (3 to 14.5 μm). Each of the MODIS instruments, operating continuously, provides daylight reflection and day/night emission spectral imaging of any point on the Earth at least once every two days.

Many MODIS products are made over time intervals ranging from about one week to a month or a season. These products are better suited for use by investigators interested in seasonal phenomena. In some cases these products are made to reduce data volume; in others they are made to provide cloud-free coverage within a defined time period. Because the ground track of the EOS spacecraft follows a 16-day repeat cycle, and because there may be biases in the multiday data sets, based on viewing geometry at specific locations, the MODIS "week" has been defined as an 8-day period. The land and ocean data products are based upon 8-day weeks beginning on January 1 of each year. The atmosphere products are also based on 8-day weeks, but these begin with the first 8-day period of the Aqua MODIS sensor that is concurrent with the Terra MODIS schedule and run in an unbroken sequence thereafter. Thus, the land and ocean weeks will not, in general, coincide with the atmosphere weeks.

MODIS will provide specific global data products, which include the following:

- Surface temperature with 1-km resolution, day and night, with absolute accuracy of 0.2 K for oceans and 1 K for land;
- Ocean color, defined as ocean-leaving spectral radiance within 5% from 415 to 653 nm, enabled by atmospheric correction from near-infrared sensor channels;
- Chlorophyll fluorescence within 50% at surface-water concentrations of 0.5 mg m^{-3};
- Concentrations of chlorophyll *a* within 35%;
- Daily and annual ocean primary productivity.
- Vegetation/land-surface cover, conditions, and productivity
  - Net primary productivity, leaf-area index, and intercepted photosynthetically active radiation
  - Land cover type, with change detection and identification
  - Vegetation indices with improved sensitivity to the global range of biomes;
- Snow cover and sea ice cover;
- Land-surface reflectance (atmospherically corrected) with bidirectional reflectance and albedo;
- Cloud cover with 250-m resolution by day and 1,000-m resolution at night;
- Cloud properties characterized by cloud-droplet phase, optical thickness, droplet size, cloud-top pressure, and emissivity;
- Aerosol properties defined as optical thickness, particle size, and mass transport;
- Fire occurrence, size, and temperature;
- Global distribution of precipitable water; and
- Cirrus-cloud cover.

The data-product descriptions in the main part of this handbook refer to MODIS spectral bands by number. These are all defined in the table on the following page.

Since the launch of the MODIS instrument on the EOS Terra spacecraft in December 1999 the overall instrument operation has been very good. However, analyses of the data from the instrument starting immediately after the first observations were received on February 24, 2000 revealed several factors in the data that needed improvement in order to reach the full potential inherent in MODIS observations. Several of the factors have been manifested in images or the MODIS data as striping or noise. Examples of the several specific factors that have been examined include optical cross-talk from band 31 into bands 32-26 and shortwave infrared (SWIR) thermal leaks, electronic cross-talk among bands 5-7 and 20-26, non-uniform channel to channel response within a band, sensor time-dependent, gain changes, mirror-rotation correlated noise, etc. These effects have largely been analyzed and corrections instituted into the MODIS Level 1 and related data products so that the specified uncertainly levels in radiance and reflectances have been achieved and the products now available from the data archives are validated for scientific studies. References providing more extended descriptions of these factors and attendant corrections and related instrument performance are listed below. Monitoring of the instrument performance continues so as to make adjustments for time-dependent behavior or other changes. Where significant changes occur, adjustments in the relevant algorithms will be made and included as appropriate in processing and reprocessing of the MODIS data set.

Suggested Reading

Guenther, B. *et al*., 2002.

Barnes, W. L. *et al*., 1998.

Esaias, W. E. *et al*., 1998.

Guenther, B. *et al*., 1998.

Wolfe, R. E. *et al*., 2002.

www.mcst.ssai.biz/mcstweb/performance/terra_instrument.html

www.mcst.ssai.biz/mcstweb/L1B/product.html

www.mcst.ssai.biz/mcstweb/index.html

Key MODIS Facts

MODIS Home Page: modis.gsfc.nasa.gov

Launched on Terra December 18, 1999, and on Aqua May 4, 2002

Heritage: AVHRR, HIRS, Landsat TM, and Nimbus 7 CZCS

Medium-resolution, multi-spectral, cross-track-scanning radiometer

Measures biological and physical processes

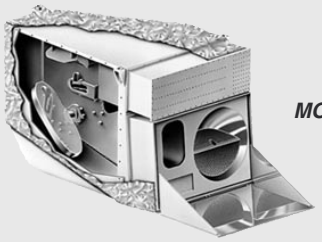

MODIS

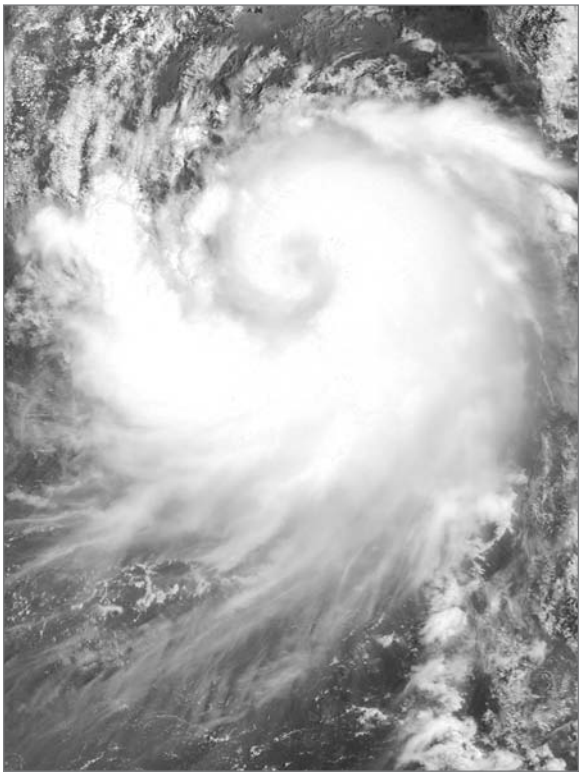

Typhoon Yutu seems to span the entire South China Sea from the Philippines (lower right) to Taiwan (upper right) and eastward to the Chinese mainland in this MODIS image from July 24, 2001.

On the internet, visit visibleearth.nasa.gov to view a variety of MODIS data images in color.

Primary Use	Band	Center Wavelength (nm)	Bandwidth (nm)	Pixel Size (m)	L_{typ}	SNR @ L_{typ}
Land/Cloud/Aerosol Boundaries	1	645	48	250	21.8	129
	2	857	38	250	24.7	201
Land/Cloud/Aerosol Properties	3	466	19	500	35.3	243
	4	554	20	500	29.0	228
	5	1242	24	500	5.4	74
	6	1629	29	500	7.3	270
	7	2114	56	500	1.0	111
Ocean Color/ Phytoplankton/ Biogeochemistry	8	411	15	1000	44.9	880
	9	442	10	1000	41.9	838
	10	487	11	1000	32.1	803
	11	530	12	1000	27.9	754
	12	547	10	1000	21.0	750
	13	666	10	1000	9.5	914
	14	677	11	1000	8.7	1088
	15	746	10	1000	10.2	600
	16	866	16	1000	6.2	517
Atmospheric Water Vapor	17	904	35	1000	10.0	167
	18	936	14	1000	3.6	57
	19	935	46	1000	15.0	250
Cirrus Clouds	26	1383	35	1000	6.0	150

Primary Use	Band	Center Wavelength (µm)	Bandwidth (µm)	Pixel Size (m)	$L_{typ}(T_{typ})$	SNR @ L_{typ} = $L_{typ}/NE\Delta L$
Surface/Cloud	20	3.79	.19	1000	0.45(300K)	900
Temperature	21	3.99	.08	1000	2.38(335K)	203
	22	3.97	.09	1000	0.67(300K)	838
	23	4.06	.09	1000	0.79(300K)	988
Atmospheric Temperature	24	4.47	.09	1000	0.17(250K)	142
	25	4.55	.09	1000	0.59(275K)	454
Water Vapor	27	6.75	.25	1000	1.16(240K)	252
	28	7.33	.33	1000	2.18(250K)	641
Cloud Properties	29	8.52	.35	1000	9.58(300K)	2661
Ozone	30	9.74	.30	1000	3.69(250K)	445
Surface/Cloud Temperature	31	11.02	.54	1000	9.55(300K)	2809
	32	12.03	.52	1000	8.94(300K)	1825
Cloud Top Altitude	33	13.36	.31	1000	4.52(260K)	452
	34	13.68	.33	1000	3.76(250K)	298
	35	13.91	.33	1000	3.11(240K)	221
	36	14.19	.29	1000	2.08(220K)	107

MODIS Spectral Band Properties and Applications

SNR = Signal-to-Noise Ratio
NE = Noise Equivalent
L_{typ} (in W/m^2-µm-sr) = Spectral radiance at typical conditions for this product
T_{typ} = Temperature at typical conditions for this product

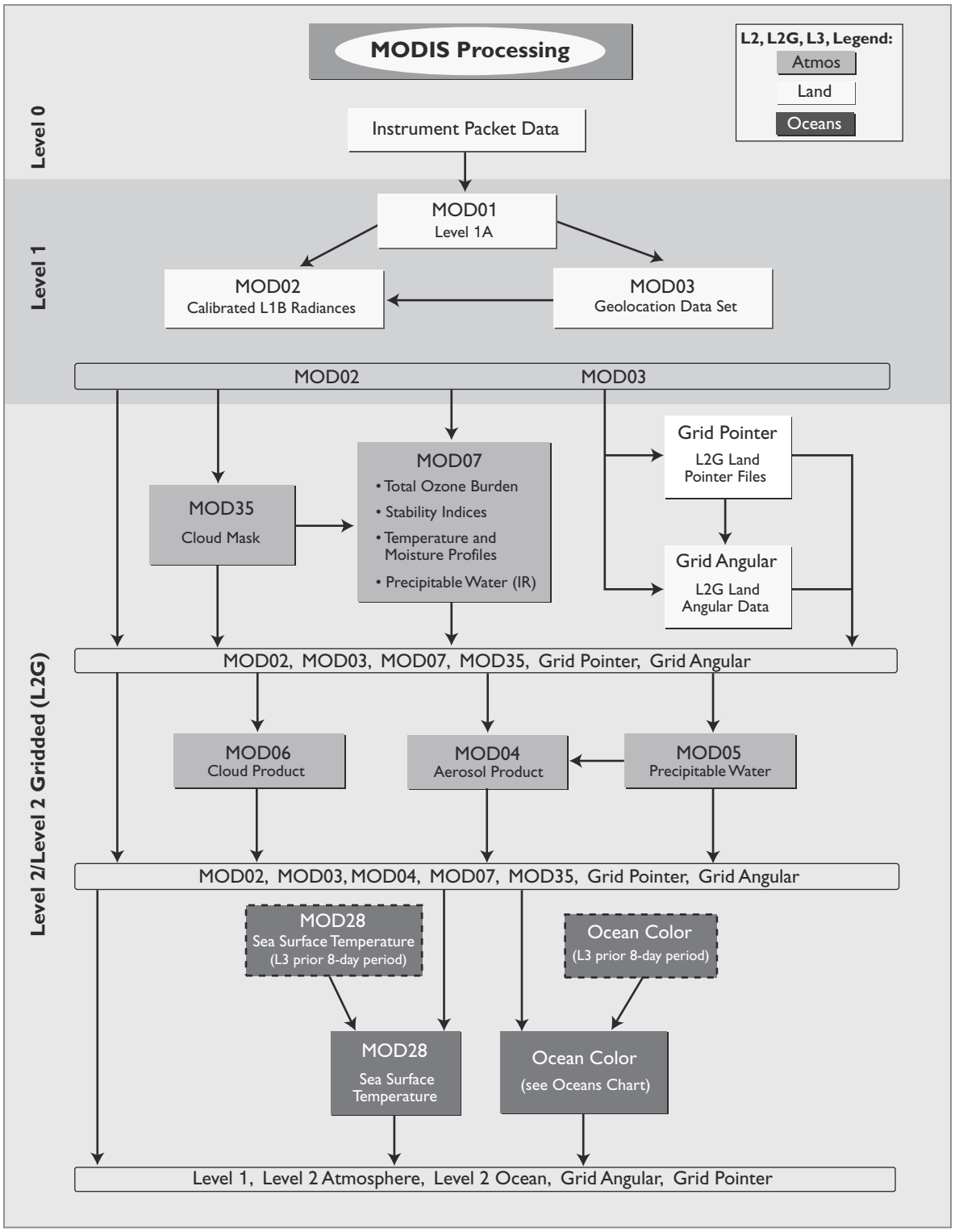

MODIS Data Processing Architecture and Products, general

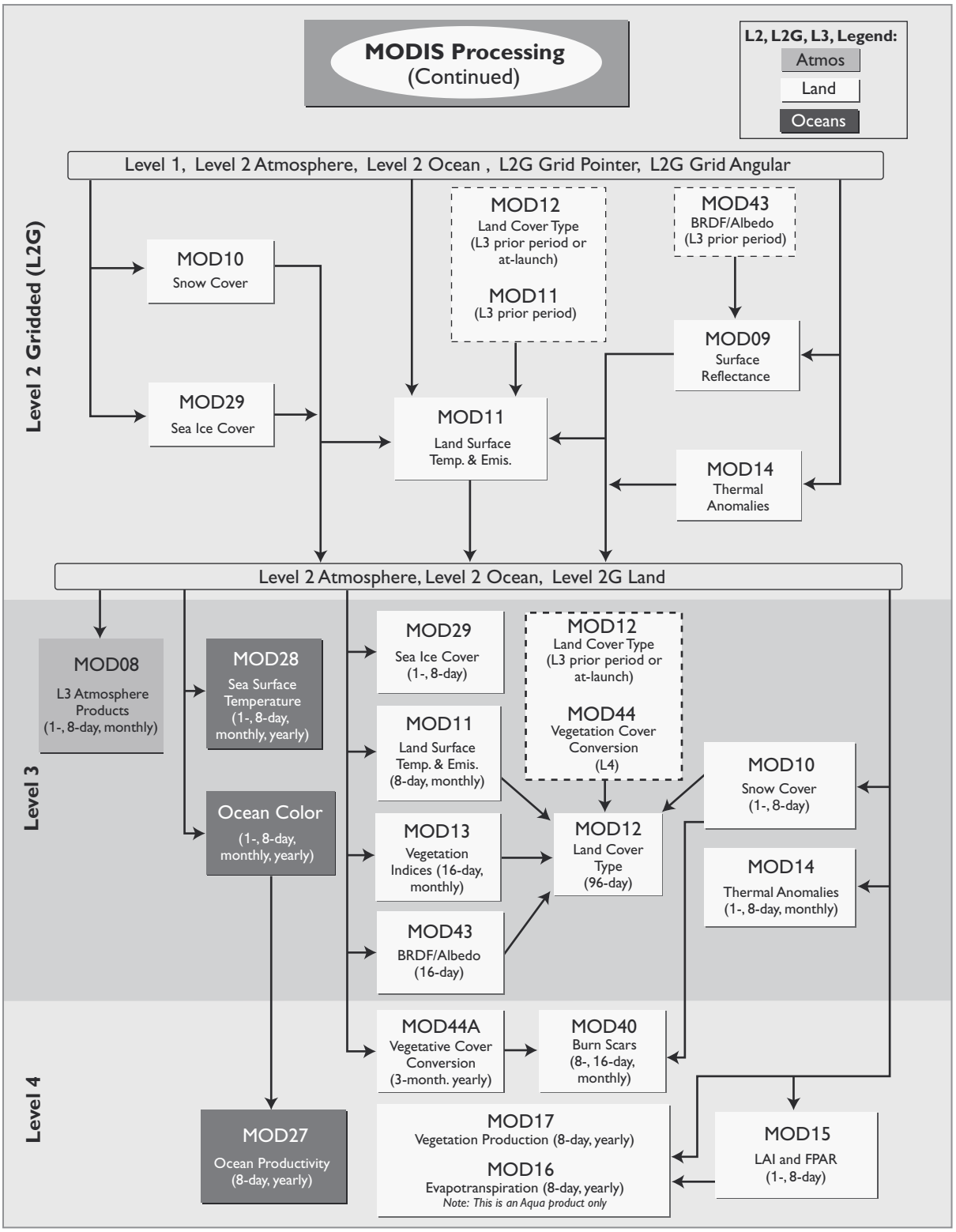

MODIS Data Processing Architecture and Products, general (continued)

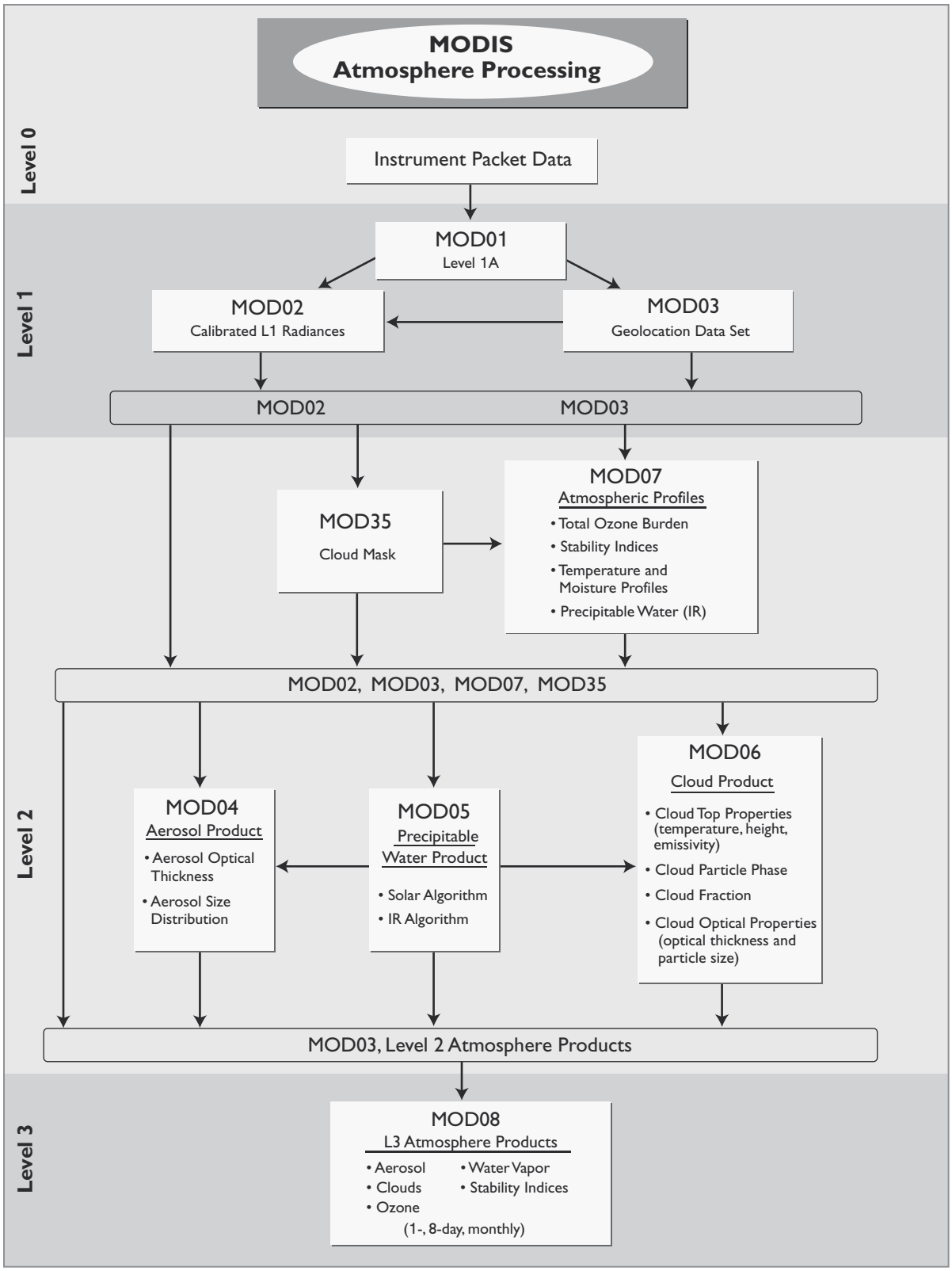

MODIS Data Processing Architecture and Products, land

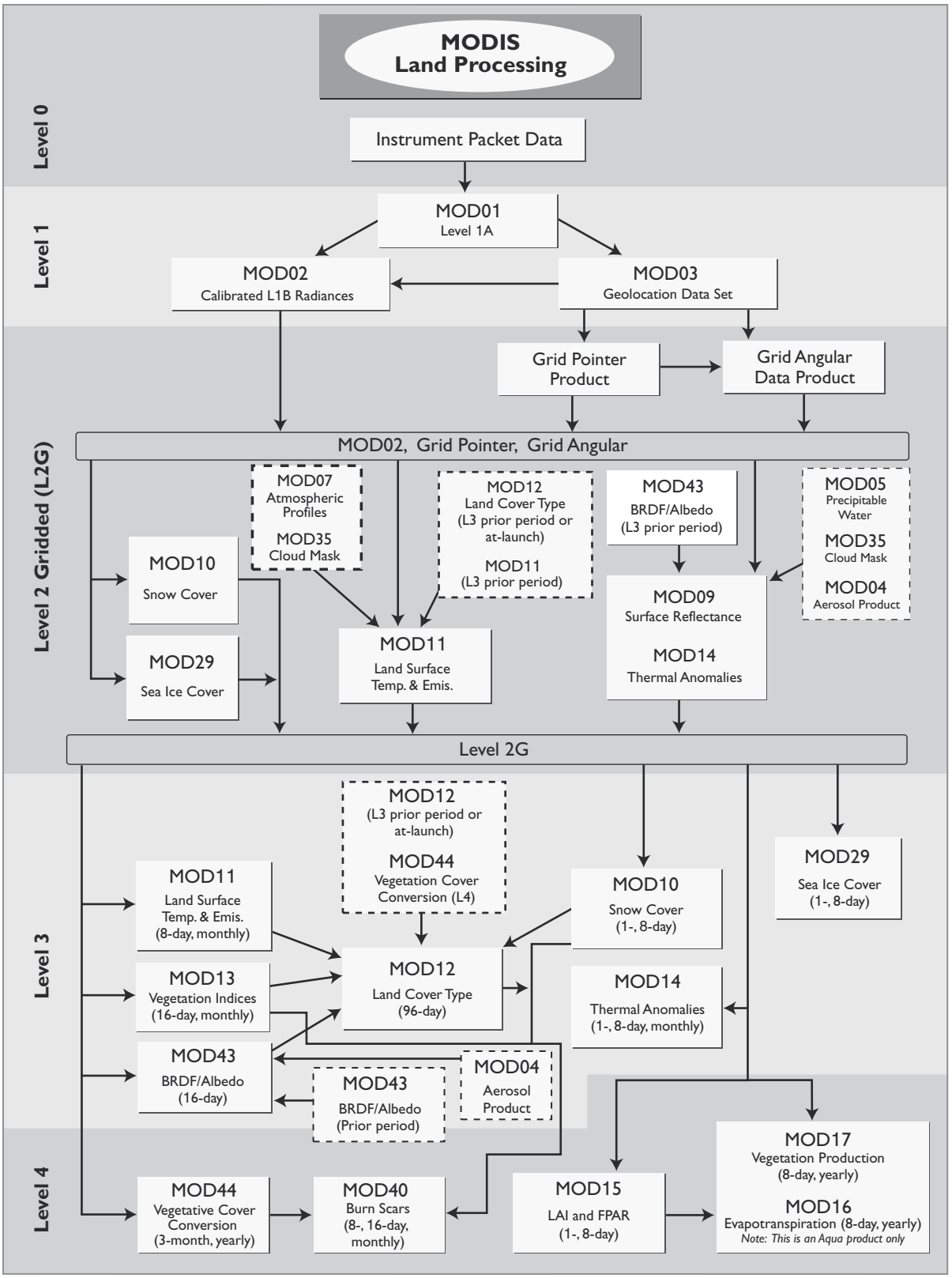

MODIS Data Processing Architecture and Products, atmosphere

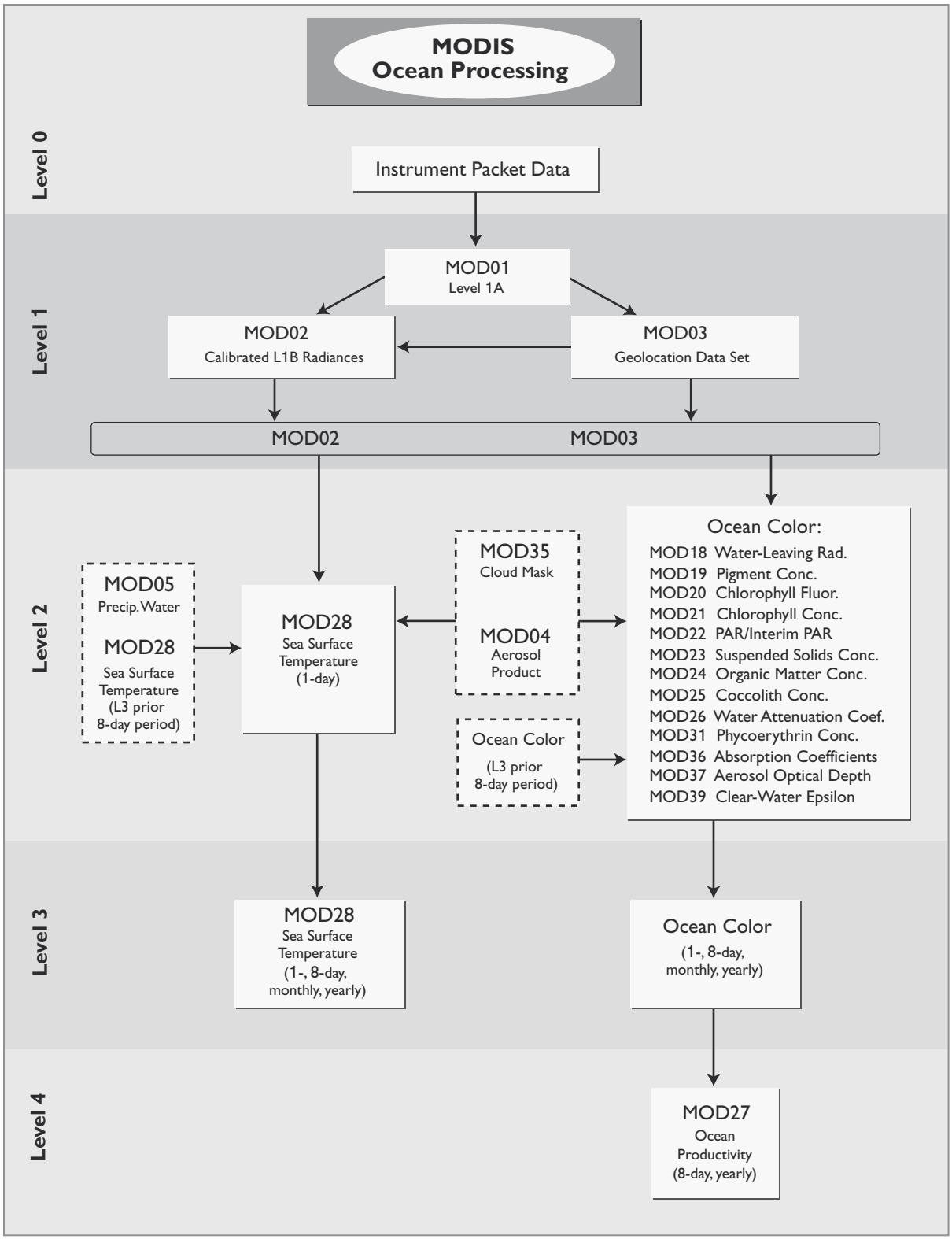

MODIS Data Processing Architecture and Products, oceans. A complete set of these products will be produced for both Terra and Aqua MODIS sensor data. In addition, a merged Terra/Aqua MODIS Ocean product set will be produced at Levels 3 and 4 in the post-Aqua launch period.

MOPITT

Measurements of Pollution in The Troposphere

The MOPITT experiment is provided under a Memorandum of Understanding with the Canadian Space Agency (CSA). MOPITT measures thermal emission in the 4.6-μm band of carbon monoxide (CO) and reflected solar radiation in the 2.3-μm band of CO and 2.2-μm band of methane (CH_4). Tropospheric CO profile and total columns of CO and CH_4 are derived from those measurements in the retrieval process.

CO is one of the most important trace species in tropospheric chemistry. The full range of the effects of the increased/decreased concentration of CO is not fully understood at the present time, but it is known that CO is photochemically active and plays a major part in the concentration of hydroxyl (OH) radicals in the troposphere. Increased CO may deplete tropospheric OH radicals, thereby reducing the yearly removal of many natural and anthropogenic trace species. In particular, this effect may add to the increase of CH_4, which in turn could further reduce OH concentration. Increased CO may also indirectly intensify global warming and perturb the stratospheric ozone layer by increasing the lifetime of trace gases such as CH_4, methyl chloride (CH_3Cl), and chlorofluorocarbons (CFCs). CH_4 is also a very effective greenhouse gas, and the change of its concentration due to human activities will impact global climate change. Measurements of CO and CH_4 will enhance our knowledge of the chemistry of the troposphere, and particularly how it interacts with the surface/ocean/biomass systems, atmospheric transports, and the carbon cycle.

MOPITT operates on the principle of correlation spectroscopy, a non-dispersive spectroscopy technique. It uses the target gas itself contained in a gas cell as the filter to achieve high spectral resolution as well as high signal to noise. Both pressure modulation cells (PMC) and length modulation cells (LMC) are used in MOPITT. By cycling the amount of gas in the absorption cell between two states (low and high pressure in the case of the PMC, and long and short path in the case of the LMC), the detector will be alternately looking through two different filters that exactly correlate with the target gas spectra. The difference of the two signals will be identical to the output of a system in which the gas cell and its modulator are replaced by an optical filter with nonzero transmission only at the spectral line positions of the target gas (CO and CH_4 for MOPITT). Therefore, the difference signal is most sensitive to the contributions by the target gas and is not sensitive to the contributions of other gases. The average of the two signals can also be obtained. It has the property that its transmittance is near unity away from the lines in the cell, but it reduces the signals at the centers of the lines. Thus, it is sensitive to other gases, and especially to the surface contribution to the upwelling radiation in the spectral regions of interest.

MOPITT is a cross-track scanning instrument which collects data with a scan line of four adjacent 22-km square pixels at nadir and at 14 "stare" positions on either side of nadir. The pixels are arranged in the along-track direction. The stare positions are interleaved so as to produce nearly contiguous coverage in the cross-track and along-track directions. For each orbit, a swath ~640 km wide is sampled. This allows complete sampling of the Earth's surface about every three days.

MOPITT Level 2 products include: 1) tropospheric CO profiles with a resolution of 22 km horizontally, 4 km vertically and with an accuracy of 10% throughout the troposphere; 2) total column of CO with a 10% accuracy and 22-km horizontal resolution; and 3) total column of CH_4 with a precision of 1% and horizontal resolution of 22 km. The column amounts of CO and CH_4 will only be available on the sunlit side of the orbit. Level 3 products to be developed postlaunch will include gridded three-dimensional global maps of CO and global maps of CH_4 total column.

The MOPITT instrument began operations on March 2, 2000 and continued in full operation until May 7, 2001 when a cooler issue caused one half of the instrument to be shut down. From August 23, 2001 to the present time, the other side of the instrument has continued to produce satisfactory data and recent analysis shows that the planned redundancy permits almost complete restoration of the data quality. During the first few months of instrument operation several artifacts in the data stream were detected and dealt with, including issues of filter changes with temperature and data issues with the pressure modulator channels. These have been resolved, and the carbon monoxide data for the 4.7 μm band are being routinely processed. Carbon monoxide data up to May 7, 2001 has been validated. Work continues on the shortwave channels which have proved to have a number of issues, both instrumental and geophysical, which have delayed release of the data products. Instrument performance analysis shows that there has been virtually no degradation of optics, filters, or detectors since launch. Periodic removal of the water ice which accumulates on the cold filter assemblies has been required less and less often and is now projected to be performed about once per year.

Suggested Reading

Edwards, D. P. *et al.*, 2002.

Key MOPITT Facts

MOPITT Home Page:

www.atmosp.physics.utoronto.ca/MOPITT/home.html

www.eos.ucar.edu/mopitt

Launched on Terra December 18, 1999

Heritage: Pressure-modulated cell elements used in the PMR, SAMS, and ISAMS instruments, using similar correlation spectroscopy techniques

Eight-channel correlation radiometer with cross-track scanning

Instrument provided by the Canadian Space Agency

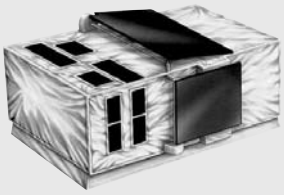

MOPITT

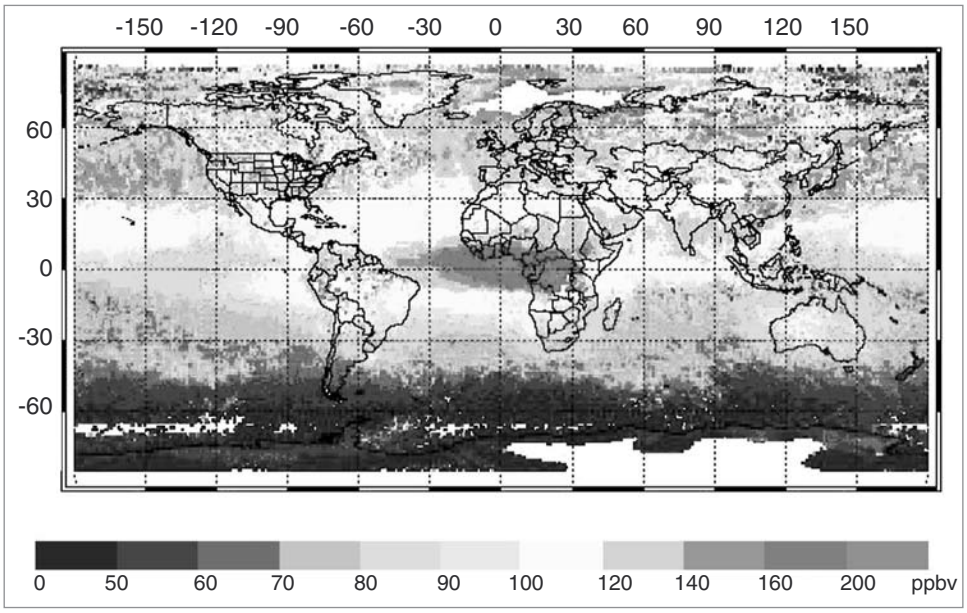

This is a global image of carbon monoxide averaged over the month of January 2001 at an altitude of about 3 km (700 hPa). The high concentrations of CO in the northern regions of the United States are mainly due to industrial processes and urban emissions, and over western central Africa they are due to widespread biomass burning. Areas of missing data show the presence of persistent cloud which inhibit retrievals. On the internet, visit visibleearth.nasa.gov and www.eos.ucar.edu/mopitt/dataimages/index.html to view a variety of MOPITT images.

Chapter 4

Radiance and Imagery Products

TRMM
CERES
LIS
PR
TMI
VIRS

Terra
ASTER
CERES
MISR
MODIS
MOPITT

Radiance and Imagery Products – An Overview

Relationship to Global Change Issues

The instruments on TRMM and Terra detect electromagnetic radiation in the visible, infrared, and microwave wavelengths. Each type of wavelength data provides different information about the Earth-atmosphere system. Because there are dozens of geophysical parameters such as atmospheric composition, surface properties, and biological attributes, many independent wavelength measurements are required to monitor the Earth system. Radiances may be thought of as the intensity or brightness of the radiation. Accurate radiances are a fundamental and essential requirement for deriving correct values for all the higher-level geophysical parameters monitored by the Earth Science Enterprise (ESE). To ensure that correct geophysical measurements are made, it is crucial to have well-calibrated radiances within spectral bands of individual instruments, across instruments, across platforms, and for time intervals from days to decades.

In addition to the radiances, there are a number of ancillary data products such as cloud cover, surface reflectivity and topography, aerosols, and scene type that are important input data sets in the derivation of other geophysical quantities. These ancillary data sets are used for data processing within a single instrument or are transferred from one instrument to another as part of their input data streams. For our purposes we can call these ancillary geophysical data sets "imagery products." In addition, many of the land and ocean radiance products are grouped here. In this section, we review some of the radiance and imagery data products from nine satellite sensors on two satellite platforms and explain how the products support the overall global change program.

Product Overview

Radiances: Electromagnetic energy detected by satellites arises in the Earth-atmosphere system by one of four processes: 1) reflection of solar radiation off the land and oceans or from the atmosphere, 2) thermal infrared to microwave radiation by surface and atmosphere, 3) non-thermal emission of radiation, most prominently by lightning discharges, and 4) return of radiation emitted by the sensor (such as a radar). Detecting each of these four types of electromagnetic energy requires a completely different instrument design and technique. The first three techniques involve passive sensors which take advantage of electromagnetic radiation already present. The last technique uses active sensors that generate their own radiation and monitor the return signals from echoes off the surface and atmosphere. TRMM uses all four techniques. The Terra platform concentrates on the first two using high spectral and spatial resolutions.

On the Terra satellite, radiances are derived using MODIS, ASTER, MOPITT, CERES, and MISR sensors. The reflected solar and thermal spectrum is very sensitive to changes in water vapor, ozone, and aerosol concentrations, to surface reflectivity, emissivity, and temperature, and to cloud properties such as droplet size.

TRMM has five sensors: 1) the Precipitation Radar (PR), 2) the TRMM Microwave Imager (TMI), 3) the Visible Infrared Scanner (VIRS), 4) CERES, and 5) LIS. Information on tropical precipitation, the radiation budget, and the Earth's lightning climatology is an important goal for this satellite.

Imagery Data: In the List of Products, there are a number of geophysical parameters that can be classified as imagery products, which are used as input in the derivation of higher-level geophysical data products. These imagery products include masking-type data such as cloud cover and scene type. They include intermediate-type products such as water-leaving radiances used in the derivation of oceanic biological activity and photosynthetically active radiation (PAR) used in biological studies, and they include geolocation data allowing comparisons between instruments of the same location or across time.

Input Data to Other Instruments: Radiance and imagery data from one instrument are often used as input for processing data from another instrument. For example, the ASTER calibration uses atmospheric absorption and scattering properties derived from simultaneous MISR and MODIS observations. In part then, the calibration of the ASTER radiances may have a dependence on MISR and MODIS radiances.

Product Interdependency and Continuity with Heritage Data

The radiance values are the first physical quantity derived from the raw instrument counts. The accuracy and self-consistency of the higher-level geophysical products are dependent on the accuracy of the radiances and, hence, upon the calibration of the sensors.

Image products from one instrument often influence the data processing paths used by other instruments. For example, CERES data processing uses MODIS scene classification input. ASTER calibration may have a dependency upon MODIS calibration. Topographic information such as MISR's digital elevation model (MIS10) is used in the interpretation of satellite radiances. In addition, a rough topography will have a different reflectivity in different directions (referred to as the bi-directional reflectance distribution function or BRDF) than will a smooth topography. The topographic information is a required input for the interpretation of MISR and many other types of satellite observations.

The detection of changes in the Earth's environment requires accurate and self-consistent observations of physical phenomena over many years. The EOS and TRMM programs have placed much emphasis on making well-calibrated measurements. Calibrating the measurements over many years is complicated because many satellites are involved, which may or may not have overlapping observations; the instruments themselves are changing (because of degradation, for example); and there are numerous wavelength bands from the visible to the microwave requiring different calibration methods.

Radiation flux and budget observations began with the Earth Radiation Budget (ERB) and Earth Radiation Budget Experiment (ERBE) and continue with the CERES instruments on TRMM and Terra, along with the Aqua mission. Calibrated radiances from all these instruments are fundamentally important for the documentation of subtle changes in the Earth's radiation budget. ASTER advances the technology of imagers such as Landsat and France's Systeme pour l'Observation de la Terre (SPOT). MODIS provides improved spectral resolution compared to the Advanced Very High Resolution Radiometer (AVHRR), the Coastal Zone Color Scanner (CZCS), Sea-viewing Wide Field-of-view Sensor (SeaWiFS), and earlier scanning spectroradiometers. MOPITT, MISR, and the TRMM instruments represent significant advances over their predecessors as well. A significant portion of these improvements can be directly attributed to the increased emphasis on calibration of all the sensors coming online in the EOS era.

Suggested Reading

Brest, C. L., and S. N. Goward, 1987.

Boccippio, D.J. *et al.*, 2000.

Christian, H. J. *et al.*, 1989.

Gillespie, A. R. *et al.*, 1986.

Goodman, A. H., and A. Henderson-Sellers, 1988.

Gordon, H. R., 1978.

Kummerow, C. *et al.*, 1998.

Kummerow, C. *et al.*, 2000.

Slater, P. N. *et al.*, 1987.

LIS Background Product (LIS01)

Product Description

The Level 1A product consists of LIS background images, reported intermittently by the instrument as memory buffers allow (lightning event data have storage priority over background image data). Typical time between backgrounds is 15-30 sec, although during high lightning-rate scenes, backgrounds may not be reported at all. The purpose of this product is to provide a "snapshot" of the LIS field-of-view when the lightning data volume is low. When available, backgrounds are also used for calibration of lightning event radiances; between backgrounds, cloud brightness (and hence LIS radiance calibration for transient events) is approximated by a solar zenith angle relationship.

Backgrounds are organized into orbit granules, segmented at the southernmost nadir point of each orbit. Data include the same orbit summary and one-second Level 1 and 3 data from the primary LIS product granules, a background image summary record containing the time, nadir point, and corner locations of each image, and the actual background images themselves, containing 12-bit background amplitudes of the 128 × 128 CCD array at the time of scene reporting. Navigation transform matrices in the one-second data container allow full geolocation of these images, while diagnostic records in the one-second data provide status flags for various instrument, platform, environmental, and processing conditions.

LIS Background Product Summary

Coverage: Global, 35°N to 35°S

Processing Level: 1A

Spatial/Temporal Characteristics: 4 km × 4 km, orbit granules, intermittent reporting

Key Measurements: Background, summary, navigation and status data

Product Type: Standard, at-launch

Maximum File Size: 5.54 MB

File Frequency: 1/orbit

Primary Data Format: HDF-EOS

Browse Available: Yes

Additional Product Information: thunder.nsstc.nasa.gov/data/

DAAC: Global Hydrology Resource Center, ghrc.msfc.nasa.gov

Science Team Contacts: H. Christian, S. Goodman

PR Radar Total Power, Noise, and Reflectivity (PR 1B-21, 1C-21)

Product Description

The Level 1B Precipitation Radar (1B-21) data set contains returned power and noise information, along with satellite information such as navigation (spacecraft position and velocity) and radar calibration information. The Level 1C PR data (1C-21) are radar reflectivity derived from the Level 1B data where data are excluded if no significant echoes are found (i.e., little or no rain activity) and noisy data are suppressed and set to predefined values.

Suggested Reading

Kozu, T. *et al*., 2001.

PR Radar Total Power, Noise, and Reflectivity Summary

Coverage: 36°S to 36°N; 15-16 orbits per day with a swath width of 220 km before August 2001 and 253 km after August 2001 (satellite altitude was raised from 350 km to 402.5 km)

Spatial/Temporal Characteristics: 5 km (after August 2001)

Key Geophysical Parameters: Rainfall profile

Processing Level: 1B

Frequency: 13.8 GHz

Product Type: Standard, at-launch

Maximum File Size: 160 MB

File Frequency: 1/orbit

Primary Data Format: HDF

Browse Available: Yes

Additional Product Information:
trmm.gsfc.nasa.gov
tsdis.gsfc.nasa.gov

DAAC: Goddard Space Flight Center Earth Sciences DAAC, daac.gsfc.nasa.gov

Science Team Contact: K. Okamoto

TMI Calibrated Brightness Temperatures (TMI 1B-11)

Product Description

This Level 1B data set contains calibrated brightness temperatures, in degrees Kelvin, from the high- and low-resolution TMI channels. Pixel geolocation, calibration, and instrument pointing and location information are also included.

The TMI is similar to the SSM/I instrument flown on the DMSP satellites with two key differences: 1) the addition of vertically and horizontally polarized 10-GHz channels; and 2) the scan geometry is the same for every scan instead of alternating between an A scan and a B scan. The TMI Level 1B data format is similar to the SSM/I Wentz Antenna Temperature data; however, some changes were made due to instrument characteristics and feedback from the investigator community.

Aside from the rainfall parameters derived as part of the TRMM mission, TMI data may also be used to derive sea surface wind speed, atmospheric water vapor content and cloud liquid water content over the ocean. Over land, passive microwave frequencies found on TMI can be useful for monitoring soil moisture and vegetation.

TMI Calibrated Brightness Temperatures Summary

Coverage: 38°S to 38°N; 15-16 orbits per day with a swath width of 760 km before August 2001 and 875 km after August 2001 (satellite altitude was raised from 350 km to 402.5 km)

Spatial/Temporal Characteristics: 5 km

Key Geophysical Parameters: Rainfall profile

Processing Level: 1B

Frequency: 10.65, 19.35, 37.0, 85.5 GHz (vertical, horizontal); 21.3 GHz (vertical only)

Product Type: Standard, at-launch

Maximum File Size: 15 MB

File Frequency: 1/orbit

Primary Data Format: HDF

Browse Available: Yes

Additional Product Information:
trmm.gsfc.nasa.gov
tsdis.gsfc.nasa.gov

DAAC: Goddard Space Flight Center Earth Sciences DAAC, daac.gsfc.nasa.gov

Science Team Contact: J. Shiue

VIRS Calibrated Radiances (VIRS 1B-01)

Product Description

This Level 1B data set contains calibrated radiances in mW/(cm^2 μm sr) from the five channels of the VIRS instrument. Geolocation, data quality, and solar and scan geometry information are appended to the five channels. Data are collected continuously from all 5 channels (0.62, 1.61, 3.78, 10.83, and 12.03 μm). Radiometric calibration is performed using ground testing and in-flight data. In-flight calibration of channels 1 and 2 is via an onboard solar diffuser and occasional views of the moon. Channels 3-5 use an onboard blackbody and a space view to update calibration parameters before each scan line. Processing to compensate for undesirable sensor effects is performed, but the data are not geometrically corrected or resampled.

The VIRS channels are similar to those of AVHRR and MODIS, and as such the radiance data may be used for a variety of atmospheric, terrestrial, and oceanographic research. This product is an input to TRMM 3B-42, which generates surface rainfall derived from geostationary satellites and calibrated by the data from the TRMM sensors.

Suggested Reading

Barnes, R. *et al*., 2000.

Lyu, C. *et al*., 2000.

Lyu, C., and W. Barnes, 2003.

VIRS Calibrated Radiances Summary

Coverage: 38°S to 38°N; 15-16 orbits per day with a swath width of 720 km before August 2001 and 830 km after August 2001 (satellite altitude was raised from 350 km to 402.5 km)

Spatial/Temporal Characteristics: 2 km

Key Geophysical Parameters: Rainfall rate

Processing Level: 1B

Wavelengths: 0.62, 1.61, 3.78, 10.83, 12.03 µm

Product Type: Standard, at-launch

Maximum File Size: 95 MB

File Frequency: 1/orbit

Primary Data Format: HDF

Browse Available: Yes

Additional Product Information:
trmm.gsfc.nasa.gov
tsdis.gsfc.nasa.gov

DAAC: Goddard Space Flight Center Earth Sciences DAAC, daac.gsfc.nasa.gov

Science Team Contact: J. Xiong

ASTER Reconstructed, Unprocessed Instrument Data (AST01)

Product Description

The ASTER Level 1A raw data (AST01) are reconstructed, unprocessed instrument digital counts with ground resolution of 15 m, 30 m, and 90 m for 3 VNIR (0.52-0.86 μm), 6 SWIR (1.60-2.43 μm), and 5 TIR (8.13-11.65 μm) channels. This product contains depacketized, demultiplexed, and realigned instrument image data with geometric correction coefficients and radiometric calibration coefficients appended but not applied. This includes correcting for SWIR parallax as well registration within and between telescopes. The spacecraft ancillary and instrument engineering data are also included. This product is the responsibility of Japan.

The radiometric calibration coefficients consisting of offset and sensitivity information are generated from a database for all detectors. The geometric correction is the coordinate transformation for band-to-band coregistration.

Suggested Reading

Yamaguchi, Y. *et al.*, 2001.

ASTER Reconstructed, Unprocessed Instrument Data Product Summary

Coverage: Regional up to 780 60 km × 60 km scenes per day (daytime for all channels, daytime and nighttime TIR channels, nighttime SWIR and TIR channels for volcano observation)

Processing Level: 1A

Spatial/Temporal Characteristics: 15 m (VNIR), 30 m (SWIR), 90 m (TIR)

Wavelengths: VNIR–0.52-0.86 µm (3 channels plus 1 stereo channel); SWIR–1.60-2.43 µm (6 channels); TIR–8.13-11.65 µm (5 channels)

Product Type: Standard, at-launch

Maximum File Size: 107 MB

File Frequency: N/A

Primary Data Format: HDF-EOS

Browse Available: Yes

Additional Product Information: edcdaac.usgs.gov/aster/asterdataprod.html

www.gds.aster.ersdac.or.jp/gds_www2000/service_eset_service_e.html

DAAC: EDC Land Processes DAAC, edcdaac.usgs.gov

Science Team Contact: H. Watanabe

ASTER Registered Radiance at Sensor (AST03)

Product Description

This Level 1B product (AST03) contains radiometrically calibrated and geometrically coregistered data for all ASTER channels. This product is created by applying the radiometric and geometric coefficients to the Level 1A data. The bands have been coregistered both between and within telescopes, and the data have been resampled to apply the geometric corrections. As for the Level 1A product, these Level 1B radiances are generated at 15-m, 30-m, and 90-m resolutions corresponding to the VNIR, SWIR, and TIR channels. Calibrated, at-sensor radiances are given in W/(m^2 μm sr). This product serves as input to derived geophysical products.

Suggested Reading

Yamaguchi, Y. *et al.*, 2001.

ASTER Registered Radiance at Sensor Product Summary

Coverage: Regional up to 310 60 km × 60 km scenes per day (daytime and nighttime)

Processing Level: 1B

Spatial/Temporal Characteristics: 15 m (VNIR), 30 m (SWIR), 90 m (TIR)

Wavelengths: VNIR–0.52-0.86 µm (3 channels plus 1 stereo channel); SWIR–1.60-2.43 µm (6 channels); TIR–8.13-11.65 µm (5 channels)

Product Type: Standard, at-launch

Maximum File Size: 118 MB

File Frequency: N/A

Primary Data Format: HDF-EOS

Browse Available: Yes

Additional Product Information: edcdaac.usgs.gov/aster/asterdataprod.html

DAAC: EDC Land Processes DAAC, edcdaac.usgs.gov

Science Team Contact: H. Watanabe

ASTER Brightness Temperature at Sensor (AST04)

Product Description

This Level 2 product includes brightness temperature in degrees Celsius (C) at 90-m resolution for ASTER's 5 thermal-infrared channels (8-12 μm). This is an on-request product and is generated only when requested. Brightness temperature is the apparent temperature of the surface assuming a surface emissivity of 1.0. Setting the emissivity to 1.0 is equivalent to assuming the target is a black body, so the brightness temperature is defined as the temperature a blackbody would have in order to produce the radiance perceived by the sensor.

Brightness temperature has been used to observe volcanic ash clouds, detect ice leads in the Arctic, and to identify anthropogenic and natural fires, to name a few examples. The ASTER brightness temperature is used as an alternate to radiance in the temperature/emissivity separation algorithm to report relative cloud top temperature because there is no routinely available applicable atmospheric correction to enable a calculation of exact cloud-top temperature.

ASTER brightness temperatures can be acquired during the day or night and over all surface types (land, water, cloud, etc.).

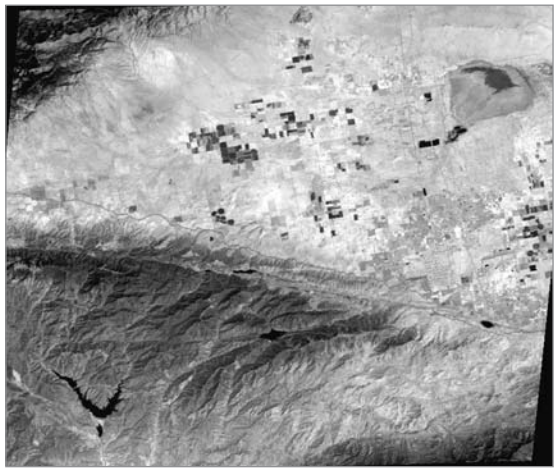

This is an image of Antelope Valley, California, which was acquired by ASTER on May 4, 2001. This image shows the brightness temperatures for ASTER Band 11. Prominent features in the scene include the San Andreas Fault, which forms the southern boundary of the valley floor, and Castaic Lake, the V-shaped reservoir in the lower left corner of the scene. On the internet, visit visibleearth.nasa.gov to view a variety of color ASTER data images.

ASTER Brightness Temperature at Sensor Product Summary

Coverage: Regional up to 70 64 km × 60 km scenes per day (daytime and nighttime)

Processing Level: 2

Spatial/Temporal Characteristics: 90 m

Wavelengths: Brightness temperatures (°C) derived for each thermal infrared channel

Product Type: Standard, at-launch

Maximum File Size: 7 MB

File Frequency: On demand

Primary Data Format: HDF-EOS

Browse Available: Yes

Additional Product Information: edcdaac.usgs.gov/aster/asterdataprod.html

DAAC: EDC Land Processes DAAC, edcdaac.usgs.gov

Science Team Contact: R. Alley

ASTER Browse Data – Decorrelation Stretch Product (AST06)

Product Description

This Level 2 browse product contains decorrelation stretch images of ASTER VNIR, SWIR, and TIR radiance data. These images are produced at pixel resolutions of 15 m for VNIR, 30 m for SWIR, and 90 m for TIR. Decorrelation stretched images provide an overview that enhances reflectance and emissivity variations and subdues variations due to topography and temperature.

Research and Applications

The decorrelation stretch is a process that is used to enhance the spectral differences found in multi-spectral image data sets. These images are used as a visual aid in browsing the ASTER scene data and making the selection of suitable scenes for further analysis and research. In particular, a decorrelation-stretched image would show the potential user which scenes have spectral variations large enough to be useful for subsequent spectral analysis.

Data Set Evolution

The algorithm used removes the interchannel correlation found in the input pixels. The decorrelation-stretched images are color coded producing a color composite containing the maximum contrast for the features in the original set of bands. The user may request as an on-demand product a decorrelation-stretched image generated from any three ASTER channels that share a single telescope (VNIR, SWIR, or TIR).

Suggested Reading

Gillespie, A. R. *et al.*, 1986.

Mather, P. M., 1999.

Rothery, D. A., 1987.

ASTER Browse Data – Decorrelation Stretch Product Summary

Coverage: Regional, three images available per scene

Processing Level: 2

Spatial/Temporal Characteristics: 15 m (VNIR), 30 m (SWIR), 90 m (TIR)

Wavelengths: Any three ASTER channels within a single telescope for on-demand products

Product Type: Standard, at-launch

Maximum File Size: 85 MB

File Frequency: On demand

Primary Data Format: HDF-EOS

Browse Available: Yes

Additional Product Information: edcdaac.usgs.gov/aster/asterdataprod.html

DAAC: EDC Land Processes DAAC, edcdaac.usgs.gov

Science Team Contact: R. Alley

ASTER Surface Reflectance (AST07) and Surface Radiance (AST09)

Product Description

The Level 2 surface reflectance data set (AST07) contains surface reflectance for VNIR and SWIR channels at 15-m and 30-m resolutions, respectively, derived by applying an atmospheric correction to observed satellite radiances. The data product is recorded as percent reflectance. The method uses a look-up table approach based upon a radiative transfer model capable of estimating the magnitude of scattering and absorption given atmospheric turbidity parameters. The needed section of the lookup table is selected using a set of atmospheric parameters (e.g., scattering optical depths, columnar ozone, and water vapor) known at the time and location of the satellite measurements. The retrieved surface reflectance is only of known accuracy for cloud-free pixels because inputs are known for clear-sky pixels only.

The Level 2 surface radiance data set (AST09) contains surface radiance, in W/(m^2 μm sr), for VNIR, SWIR, and TIR channels at 15-m, 30-m, and 90-m resolutions, respectively. The product is derived by applying an atmospheric correction to satellite radiances. The atmospheric correction used to derive AST09 for the VNIR and SWIR bands is similar to that used to drive AST07. The approach for atmospheric correction in the thermal infrared uses a radiative transfer model capable of estimating the magnitude of atmospheric emission, absorption, and scattering using a set of atmospheric parameters (e.g., temperature, water vapor, ozone, profiles, and scattering optical depths) known at the time and location of the satellite measurements. The retrieved surface radiance is only of known accuracy for cloud-free pixels because inputs are known for clear-sky pixels only.

Both AST07 and AST09 are generated only upon request. The products based on VNIR data are available only for daytime satellite overpasses. Those from SWIR data are available for daytime overpasses, and, in cases of high temperature sources (e.g., volcanoes or fires), available for nighttime overpasses. Surface radiance from TIR data are available for both daytime and nighttime overpasses.

Research and Applications

The objective of these ASTER products is to provide estimates of the surface radiance and reflectance. The thermal infrared radiance includes both

surface-emitted and surface-reflected components. After accurate atmospheric correction, seasonal and annual surface changes can be studied and surface kinetic temperature and emissivity can be extracted. Surface radiances and reflectances can also be used for surface classification, desertification studies, and surface energy-balance work.

Data Set Evolution

This product, as well as similar products for other Terra instruments, mark the first implementations of operational atmospheric corrections in environmental satellites. Past work to retrieve surface reflectance from satellite imagery has focused on small sets of satellite data for highly studied ground targets. The primary reason for this is that atmospheric correction is a computationally intensive process. Methods for reducing the computational requirements include using look-up tables and making assumptions about the horizontal homogeneity of the atmosphere.

Research into developing future versions of code to produce AST07 and AST09 focuses on attempting pixel-by-pixel corrections using pixel-by-pixel atmospheric input parameters rather than assuming horizontal homogeneity. Because of ASTER's small ground instantaneous field of view, versions of the atmospheric correction include corrections for multiple scatter effects from adjacent pixels of differing reflectance, also known as the adjacency effect. Look-up tables have also been expanded to include other parameters such as surface bidirectional reflectance characteristics.

Suggested Reading

Abrams, M. *et al*., 2000.

Deschamps, P., and T. Phulpin, 1980.

Hilland, J. E. *et al*., 1985.

Price, J. C., 1984.

Thome, K. *et al*., 1998a, b.

ASTER Surface Reflectance and Surface Radiance Product Summary

Coverage: Regional; 16 days required for global coverage; 70 scenes per day

Processing Level: 2

Spatial/Temporal Characteristics: 15 m (VNIR), 30 m (SWIR), 90 m (TIR)

Wavelengths: VNIR–0.52-0.86 µm (4 channels); SWIR–1.60-2.43 µm (6 channels); TIR–8.125-11.65 µm (5 channels)

Product Type: Standard, at-launch

Maximum File Size: 189 MB (VNIR), 79 MB (SWIR)

File Frequency: On demand

Primary Data Format: HDF-EOS

Browse Available: Yes

Additional Product Information: edcdaac.usgs.gov/aster/asterdataprod.html

DAAC: EDC Land Processes DAAC, edcdaac.usgs.gov

Science Team Contacts: K. Thome (VNIR, SWIR), F. Palluconi (TIR)

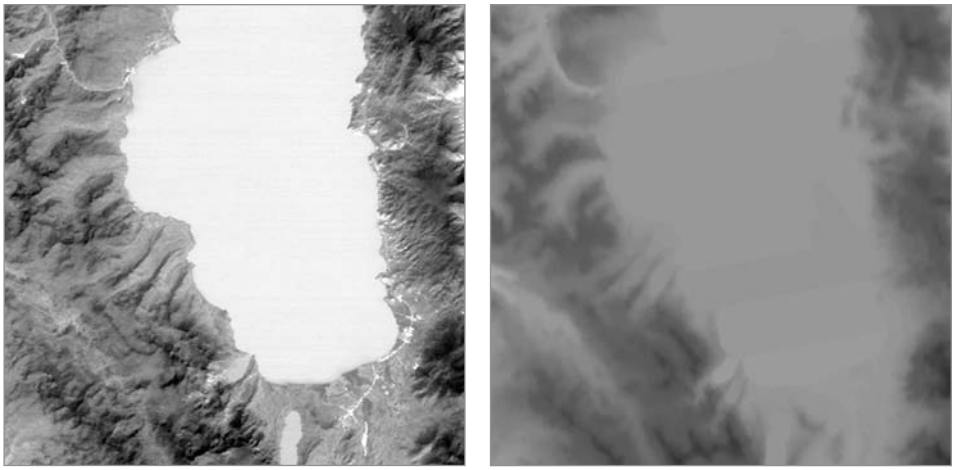

These two images are of Lake Tahoe, taken on 27 February 2002, using TIR on ASTER, band 13. The left image represents Surface Leaving Radiance, in W/(m^2 μm sr), and the right image represents Sky Irradiance in W/m2/μm.

ASTER Digital Elevation Models (DEMs)(AST14)

Product Description

This data set contains topographic information derived from the along-track, 15-m ASTER optical stereo data acquired in the near-infrared. These high spatial resolution DEMs (up to 7-m absolute horizontal and vertical accuracy with appropriate ground control, and up to 10-m relative accuracy without ground control) can be used to derive absolute slope and slope aspect good to 5º over horizontal distances of more than 100 m. ASTER DEMs meet 1:50,000 to 1:250,000 map accuracy standards. Postings are at 30-m.

This is an on-request product which is generated by the Land Processes DAAC at EROS Data Center only when requested and at a rate of 1-2 DEMs per day. Based on 3-years' experience with actual instrument operations, mission planning, cloud cover, and illumination, the ASTER digital stereo data with a base/height ratio of 0.6 should be acquired for all of the Earth's land surface below 85º latitude by the end of the 5-year mission. These data are appropriate for users interested in generating DEMs themselves.

Research and Applications

Topographic data as well as derived slope and slope aspect are basic to all aspects of land surface research including cartography, climate modeling, biogeochemistry, biogeography, geophysics, geology, geomorphology and soil science. Digital elevation data are also required for atmospheric and radiometric correction of most satellite-acquired observations of the land surface. Digital elevation data are also used for practical engineering applications such as studies of drainage and runoff, and site suitability studies for buildings or waste containment sites.

Data Set Evolution

Generation of elevation models from stereo photographic data, now a routine adjunct to standard surveying methods, has been developed over the past 60 years based on the principles of photogrammetry. Extensions of these principles to the generation of DEMs from optical stereo satellite data have been implemented in past decades. Examples of these satellite stereo systems include SPOT and JERS-1 OPS. At one time, there were large areas of the globe for which no consistent, high-resolution, widely avail-

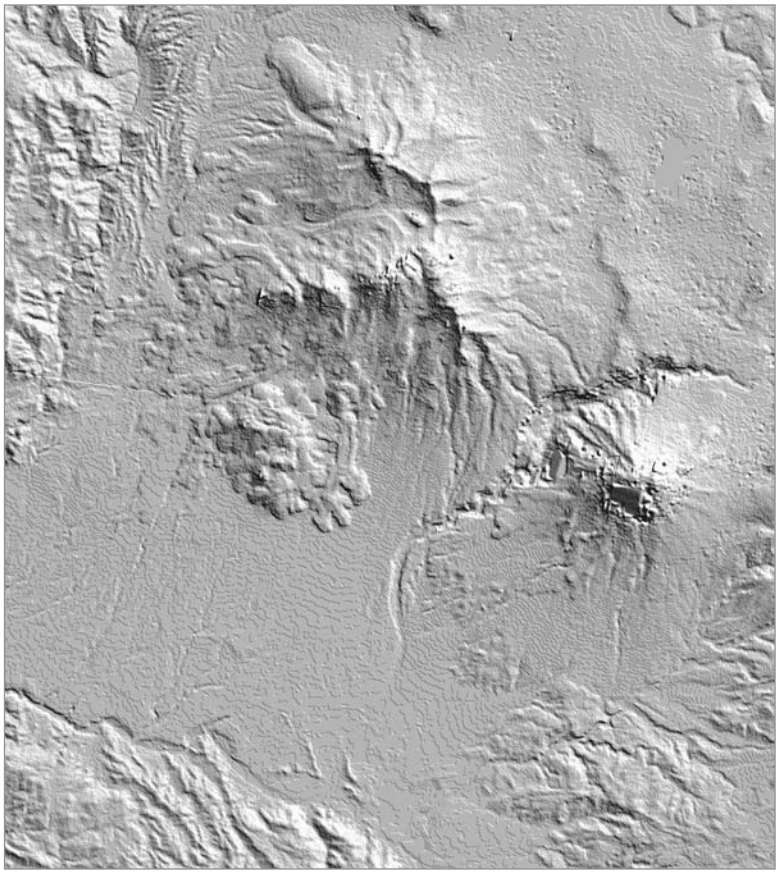

This image is a shaded relief of an ASTER Digital Elevation Model (DEM). The area covers Arequipa, Peru and El Misti volcano. Visit visibleearth.nasa.gov to view a variety of color ASTER data images.

able elevation models existed. ASTER DEMs now help provide much-needed coverage over many of these remote areas.

Suggested Reading

Abrams, M., 2000.

Bohme, R., 1993.

Kaab, A., 2002.

Kahle, A. *et al*., 1991.

Fujisada, H., 1994.

Fujisada, H., 1998.

Hirano, A. *et al*., 2003.

O'Neill, M. A., and I. J. Dowman, 1993.

Toutin, T., 2002.

Welch, R., and H. Lang, 1994.

Yamaguchi, Y. *et al*., 1993.

Yamaguchi, Y. *et al*., 1994.

Yamaguchi, Y. *et al*., 1998.

ASTER Digital Elevation Models (DEMs) Product Summary

Coverage: Global

Processing Level: 3

Spatial/Temporal Characteristics: 30 m

Wavelengths: VNIR Band 3 nadir and Band 3 aft-looking

Product Type: Standard, at-launch

Maximum File Size: 25 MB

File Frequency: On demand

Primary Data Format: HDF-EOS

Browse Available: No

Additional Product Information: edcdaac.usgs.gov/aster/asterdataprod.html

DAAC: EDC Land Processes DAAC, edcdaac.usgs.gov

Science Team Contact: M. Abrams

CERES Bi-Directional Scans Product (BDS)

Product Description

The Bi-Directional Scans (BDS) Product contains 24 hours of instantaneous Level 1B Clouds and the Earth's Radiant Energy System (CERES) data for a single scanner instrument. The BDS contains instantaneous radiance measurements recorded every 0.01 second for views of space, internal calibration, solar calibration, and Earth. It contains all elevation scan modes, which include the normal Earth scan and the short Earth scan modes and both the fixed and rotating azimuth-plane scan modes. The BDS also contains Level 0 raw (unconverted) science and instrument data as well as the geolocation of the radiance measurements. The BDS product contains additional data not found in the Level 0 input file, including converted satellite position and velocity data, celestial data, converted digital status data, and parameters used in the equations for radiance count conversions.

A complete listing of parameters for this data product can be found in the CERES Data Products Catalog at asd-www.larc.nasa.gov/DPC/DPC.html, and detailed definitions of each parameter can be found in the CERES Collection Guide at asd-www.larc.nasa.gov/ceres/collect_guide/list.html.

Research and Applications

These radiance data products are the primary inputs to all the CERES product algorithms. The spacecraft ephemeris and sensor telemetry are inputs to this subsystem, which uses instrument calibration coefficients to convert the spacecraft telemetry inputs into geolocated filtered radiances and housekeeping data into engineering units.

Data Set Evolution

The BDS product algorithm operates on the Level 0 reformatted raw sensor counts and produces calibrated radiances in the three channels. The steps in

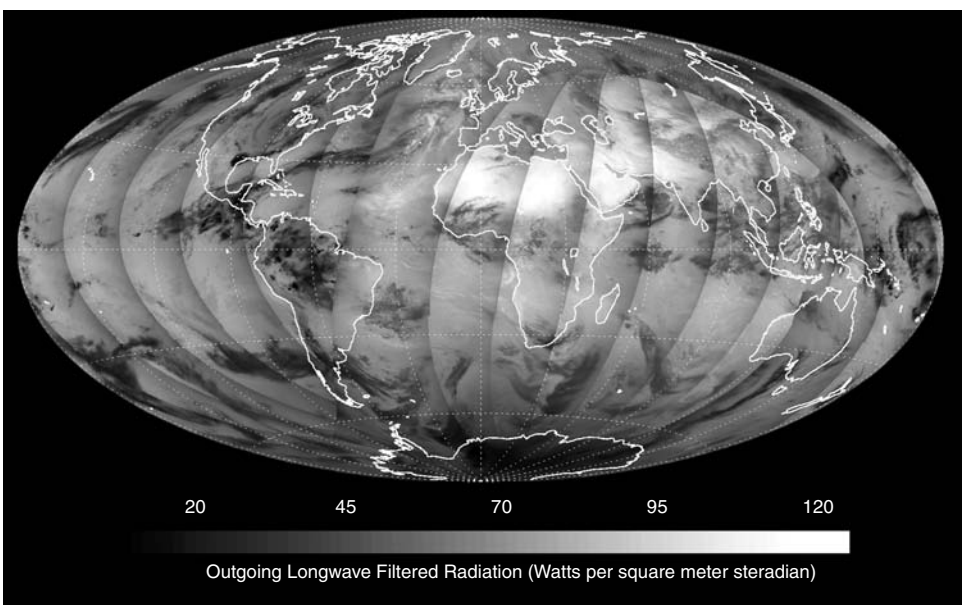

The image above shows thermal emitted longwave radiance escaping the top of the Earth's atmosphere as measured by the Clouds and the Earth's Radiant Energy System (CERES) instrument on May 25, 2001. Record-breaking heat waves in southern Asia, northern Africa, and southwestern U.S. killed dozens of people during May. The smallest amounts of radiation emitted to space are over Antarctica where the entire surface/atmosphere column is cold, and over deep convective clouds in the tropics seen in this image over Brazil. These clouds have the largest greenhouse effect on the Earth. The highest emission levels are from clear hot desert regions during daylight hours. The pronounced banding of the images between orbits is produced because the effective radiating temperature of the Earth depends on viewing angle as the CERES instrument scans the earth from orbit. On the internet, visit visibleearth.nasa.gov to view a variety of CERES data images.

the processing are: 1) Convert the raw housekeeping telemetry into engineering units; 2) calculate the geographical location of the CERES footprints; 3) revise the radiometric detector count conversion coefficients when required; 4) convert the radiometric detector signals into filtered radiances; and 5) archive the BDS standard products.

Documentation on the BDS algorithms can be found in the CERES ATBD for Subsystem 1.0, in PDF format, at eospso.gsfc.nasa.gov/atbd/cerestables.html.

Suggested Reading

Hoffman, L. H. *et al*., 1987.

Jarecke, P. J. *et al*., 1991.

Lee III, R. B. *et al*., 1996.

Priestley, K. J. *et al*., 2000.

Smith, G. L. *et al*., 1986.

Wielicki, B. A. *et al*., 1998.

CERES Bi-Directional Scans Product Summary

Coverage: Global

Spatial/Temporal Characteristics: 20 km at nadir/0.01 second

Key Geophysical Parameters: Filtered total, shortwave, and window radiances, geolocation data

Processing Level: 0, 1

Product Type: Standard, at-launch

Maximum File Size: 900 MB

File Frequency: 1/day

Primary Data Format: HDF-EOS

Browse Available: No

Additional Product Information: eosweb.larc.nasa.gov/PRODOCS/ceres/table_ceres.html

DAAC: Langley Atmospheric Sciences Data Center, eosweb.larc.nasa.gov

Science Team Contact: K. J. Priestley

MISR Reformatted Annotated Product (MIS01)

Product Description

The Level 1A Reformatted Annotated Product contains raw MISR data which are decommutated, reformatted (12-bit L0 data shifted to byte boundaries, reversal of square-root encoding applied, and converted to 16-bits) and annotated (e.g., with time information, etc.). The MISR Level 1A data set is the primary archive of MISR instrument Charge-Coupled Device (CCD) science data, instrument engineering data (e.g., instrument temperatures, electrical status, command verification, etc.), calibration data, motor data, and navigation data (raw spacecraft position and attitude). These data are used by the Level 1B1 processing algorithm to generate calibrated radiances. The science data output preserves the spatial sampling rate of the Level 0 raw MISR CCD Science data.

CCD data are collected during routine science observations of the sunlit portion of the Earth. Each product represents one "granule" of data. A "granule" is defined to be the smallest unit of data required for MISR processing. Also included in the Level 1A product will be pointers to calibration coefficient files provided for Level 1B processing.

Suggested Reading

Bruegge, C. J. *et al.*, 2002.

MISR Reformatted Annotated Product Summary

Coverage: Daytime; 378-km swath width (nadir), 413-km swath width (off nadir), providing global coverage in 9 days

Processing Level: 1A

Spatial/Temporal Characteristics: The spatial sampling of the nadir-viewing camera is 250 m (cross-track) × 275 m (along-track), while for the 8 off-nadir cameras the sampling is 275 m in both directions. Onboard averaging up to 1.1 km is selectable by ground command.

Wavelengths: 446, 558, 672, 866 nm

Product Type: Standard, at-launch

Maximum File Size: 900 MB (nadir), 400 MB (oblique)

File Frequency: 135/day

Primary Data Format: HDF-EOS Swath

Browse Available: No

Additional Product Information: eosweb.larc.nasa.gov/PRODOCS/misr/table_misr.html

DAAC: Langley Atmospheric Sciences Data Center, eosweb.larc.nasa.gov

Science Team Contact: C. Bruegge

MISR Radiometric Product (MIS02)

Product Description

The MISR Radiometric Product (MIS02) is produced during Level 1B1 processing. Here Level 1A data are converted from digital counts to radiances, using coefficients that are updated periodically to account for instrument degradation. The Radiometric Product contains spectral radiances for all MISR channels (four spectral bands and nine cameras), given in units of W/(m^2 μm sr). Each radiance value represents the incident radiance averaged over the sensor's total band response. The radiometric coefficients are derived primarily from use of the On-Board Calibrator (OBC). The OBC contains Spectralon calibration panels which are deployed at bimonthly intervals and reflect sunlight into the cameras. Detector standards measure this reflected light to provide the calibration. Vicarious field campaigns are additionally used to adjust the radiometric scale. These experiments are conducted less frequently, but provide an independent methodology useful for reducing systemic errors.

Suggested Reading

Bruegge, C. J. *et al.*, 1998.

Jovanovic, V. M. *et al.*, 2002.

MISR Radiometric Product Summary

Coverage: Daytime; 378-km swath width (nadir), 413-km swath width (off nadir), providing global coverage in 9 days

Processing Level: 1B1

Spatial/Temporal Characteristics: The spatial sampling of the nadir viewing camera is 250 m (cross-track) × 275 m (along-track), while for the 8 off-nadir cameras the sampling is 275 m in both directions. Onboard averaging up to 1.1 km is selectable by ground command.

Wavelengths: 446, 558, 672, 866 nm

Product Type: Standard, at-launch

Maximum File Size: 1300 MB (nadir), 400 MB (oblique), Local Mode Radiance Data: 30 MB

File Frequency: 135/day, Local Mode Radiance Data, 15/day

Primary Data Format: HDF-EOS Swath

Browse Available: No

Additional Product Information: eosweb.larc.nasa.gov/PRODOCS/misr/table_misr.html

DAAC: Langley Atmospheric Sciences Data Center, eosweb.larc.nasa.gov

Science Team Contact: C. Bruegge

MISR Geo-rectified Radiance Product (MIS03)

Product Description

The Geo-rectified Radiance Product (GRP) consists of parameters that have had geometric corrections applied and have been projected to a Space-Oblique Mercator (SOM) map grid. Included in this product is the surface-projected TOA radiance, which is the calibrated radiance from the Level 1B1 data (MIS02) that has had a geometric correction applied to remove spacecraft position and pointing knowledge errors as well as effects due to topography. The radiance is then orthorectified on a reference ellipsoid at the surface. Also part of the GRP is the ellipsoid-projected TOA radiance that uses supplied spacecraft position and pointing and is not corrected for topography, but is resampled at surface reference ellipsoid. In addition, geometric parameters such as solar and view zenith and azimuth angles are included.

Resampling of MISR data at Level 1B2 is critical because the pushbroom images from the nine cameras are obtained at widely separated locations along the subspacecraft track. However, derivation of geophysical products requires that the multiangle, multispectral radiances for any single ground target be coregistered.

Suggested Reading

Jovanovic, V. M. *et al.*, 1998.

MISR Geo-rectified Radiance Product Summary

Coverage: Daytime, 378-km swath width (nadir), 413-km swath width (off nadir), providing global coverage in 9 days

Processing Level: 1B2

Spatial/Temporal Characteristics: The resampled data are provided on a 275 m × 275 m Space Oblique Mercator grid in certain channels, and a 1.1 km × 1.1 km grid in the remaining channels, as established by the instrument observing configuration.

Wavelengths: 446, 558, 672, 866 nm

Product Type: Standard, at-launch

Maximum File Size:
Ellipsoid Data: 600 MB (nadir), 200 MB (oblique)
Terrain Data: 350 MB (nadir), 100 MB (oblique)
Geometric Parameters: 6 MB
Radiometric Cloud Mask: 10 MB

File Frequency: 135/day, 15/day (geometric parameters)

Primary Data Format: HDF-EOS Swath

Browse Available: Yes

Additional Product Information: eosweb.larc.nasa.gov/PRODOCS/misr/table_misr.html

DAAC: Langley Atmospheric Sciences Data Center, eosweb.larc.nasa.gov

Science Team Contact: D. Diner

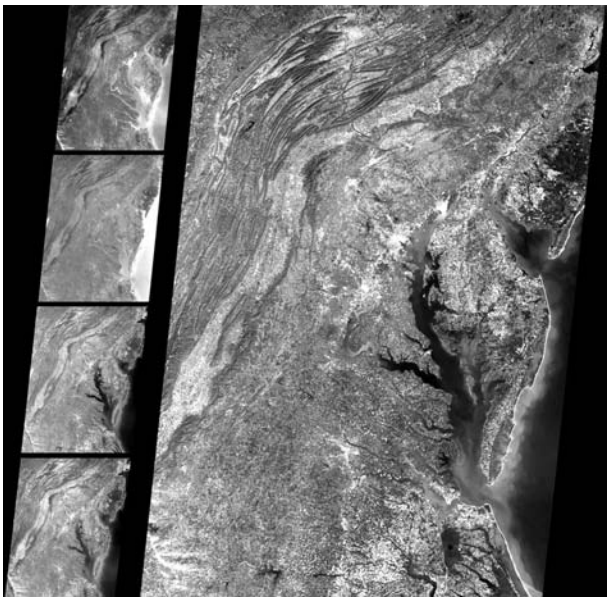

MISR Geo-rectified Radiance Products over Delaware Bay, Chesapeake Bay, and the Appalachian Mountains acquired on March 24, 2000 during Terra orbit 1417. The larger image was taken by the MISR camera viewing straight down (nadir). The series of smaller images, from top to bottom, respectively, were taken by cameras viewing 70.5° forward, 45.6° forward, 45.6° aftward, and 70.5° aftward of nadir. These images cover the environs of Newark, Philadelphia, Baltimore, Washington and Richmond. Differences in brightness and contrast as a function of view angle are visible over both land and water. On the internet, visit visibleearth.nasa.gov to view a variety of MISR data images.

MISR Ancillary Geographic Product (MIS10)

Product Description

The MISR Ancillary Geographic Product (AGP) contains terrain data (generated from a high resolution DEM), referenced to the WGS84 reference ellipsoid and mapped onto a SOM grid. It is an archival product generated once preflight at the MISR Science Computing Facility (SCF), but which can be distributed to the scientific community through the DAAC as an aid in interpreting MISR retrievals. The AGP is used as input to Level 1B2 and Level 2 processing. Its contents include latitude, longitude, scene elevation (average and standard deviation relative to a horizontal plane and the local slope), surface-normal zenith angle, surface-normal azimuth angle, and a land/ocean/inland water/ephemeral water/coastline mask. All of these parameters are given on 1.1-km centers. Average and standard deviation of scene elevation over 17.6-km areas are also provided.

MISR Ancillary Geographic Product Summary

Coverage: Global, one time only

Spatial/Temporal Characteristics: 1.1 km for most parameters, 17.6 km for coarse-resolution elevation information

Wavelengths: N/A, parameters include latitude, longitude, elevation, and land/water classification

Product Type: Internal, on request

Maximum File Size: 110 MB

File Frequency: N/A

Primary Data Format: HDF-EOS Grid

Browse Available: No

Additional Product Information: eosweb.larc.nasa.gov/PRODOCS/misr/table_misr.html

DAAC: Langley Atmospheric Sciences Data Center, eosweb.larc.nasa.gov

Science Team Contact: D. Diner

MISR Ancillary Radiometric Product (MIS11)

Product Description

The MISR Ancillary Radiometric Product (ARP) contains coefficients and data variables that are used in the Level 1B1 processing. Updated ARP parameters include the sensor radiometric calibration coefficients, uncertainties in calibration, signal-to-noise ratios, pixel data quality indicators, and quality assessment threshold parameters. Static ARP parameters include spectral response parameters, point-spread-functions (PSF), fields-of-view, passband-weighted solar irradiance values, and photosynthetically active radiation (PAR) integration weights. The ARP is regenerated periodically at the MISR SCF to update the instrument performance report. The ARP is used as input to Level 1B1 as well as Level 2 processing.

MISR Ancillary Radiometric Product Summary

Coverage: N/A, generated periodically

Spatial/Temporal Characteristics: Per pixel

Key Parameters: Radiometric calibration coefficients, uncertainties, signal-to-noise ratios, spectral response parameters, PSF, fields-of-view, band-averaged solar irradiance, and PAR weights

Product Type: Internal

Maximum File Size: 5 MB

File Frequency: N/A

Primary Data Format: HDF-EOS Grid

Browse Available: No

Additional Product Information: eosweb.larc.nasa.gov/PRODOCS/misr/table_misr.html

DAAC: Langley Atmospheric Sciences Data Center, eosweb.larc.nasa.gov

Science Team Contact: C. Bruegge

MODIS Level 1A Radiance Counts (MOD01)

Product Description

This Level 1A data set contains counts for 36 MODIS spectral bands, along with raw instrument engineering and spacecraft ancillary data. The Level-1A data are used as input for geolocation, calibration, and processing. Quality indicators are added to the data to indicate missing or bad pixels and instrument modes. Visible, SWIR, and NIR measurements are made during daytime only, while radiances for TIR are measured during both the day and the night portions of the orbit. This product includes all MODIS data in digitized (counts) form for all bands, all spatial resolutions, all time tags (converted), all detector views (Earth, solar diffuser, spectroradiometric calibration assembly, black body, and space view), and all engineering and ancillary data.

MODIS Level 1A Radiance Counts Summary

Coverage: Global

Spatial/Temporal Characteristics: 0.25, 0.5, and 1 km resolutions/ daily (daytime and nighttime)

Wavelengths: 20 channels 0.4-3.0 µm, 16 channels 3-15 µm

Processing Level: 1A

Product Type: Standard, at-launch

Maximum File Size: 534 MB

File Frequency: 288/day

Primary Data Format: HDF-EOS

Additional Product Information: daac.gsfc.nasa.gov/MODIS/

DAAC: Goddard Space Flight Center Earth Sciences DAAC, daac.gsfc.nasa.gov

Science Team Contact: V. V. Salomonson

MODIS Level 1B Calibrated, Geolocated Radiances (MOD02)

Product Description

The Level 1B data set contains calibrated and geolocated output for the 36 spectral bands generated from MODIS Level 1A sensor counts (MOD01). The primary product of the reflected solar bands (1-19 and 26) is the Earth view (EV) reflectance factor, $\rho_{EV}\cos(\theta_{EV})$. The primary product for the thermal emissive bands (20-25 and 27-36) is spectral radiance. The radiances are in $W/(m^2\,\mu m\,sr)$. In addition, EV spectral radiance may be determined for the solar reflective bands through knowledge of the solar irradiance. Additional data are provided, including quality flags, error estimates, and calibration data.

Visible, SWIR, and NIR measurements are made during daytime only, while radiances for TIR are measured continuously. Only Channels 1 and 2 have 250-m resolution, Channels 3-7 have 500-m resolution, and the rest have 1-km resolution.

MODIS Level 1B Calibrated, Geolocated Radiances Summary

Coverage: Global

Spatial/Temporal Characteristics: 0.25, 0.5, and 1 km resolutions/daily (daytime and nighttime)

Wavelengths: 20 bands 0.4-3.0 µm, 16 bands 3-15 µm

Processing Level: 1B

Product Type: Standard, at-launch

Maximum File Size: 345 MB (1 km), 276 MB (500 m), 287 MB (250 m)

File Frequency: 288/day (1 km), 144/day (500 m), 144/day (250 m)

Primary Data Format: HDF-EOS

Additional Product Information: daac.gsfc.nasa.gov/MODIS/

DAAC: Goddard Space Flight Center Earth Sciences DAAC, daac.gsfc.nasa.gov

Science Team Contacts: X. Xiong

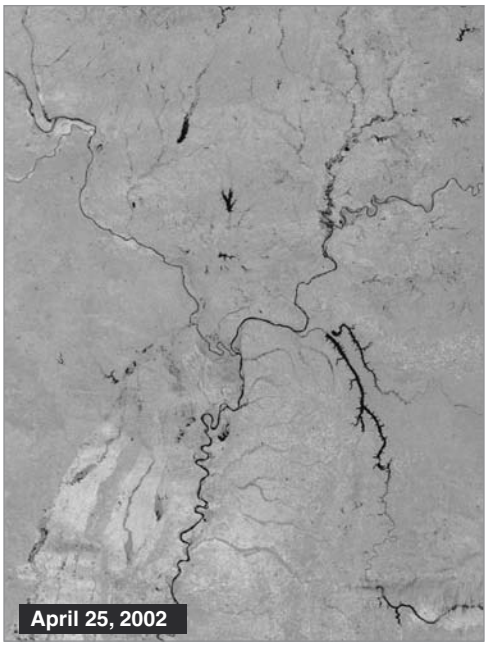

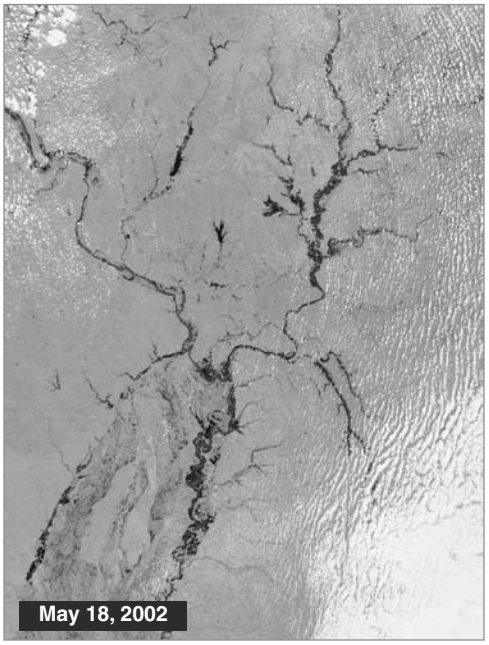

The images above show the junction of the Ohio River and the Mississippi River where Spring floods were at their worse. The images compare April 25, 2002, to May 18, 2002, with data from MODIS. The Mississippi River rose up to 12 feet above flood stage in the area shown here. Normally, all the rivers in this image would resemble thin black lines (top image). Image courtesy Jacques Descloitres, MODIS Land Rapid Response Team at NASA Goddard Space Flight Center. On the internet, visit visibleearth.nasa.gov to view a variety of MODIS data images.

MODIS Geolocation Data Set (MOD03)

Product Description

The MODIS Geolocation product contains geodetic coordinates, ground elevation, land/sea mask, satellite range, and solar and satellite zenith, and azimuth angle for each MODIS 1-km sample. These data are provided as a 'companion' data set to the Level 1B calibrated radiances and the Level 2 data sets to enable further processing. These geolocation fields are determined using the spacecraft attitude and orbit, instrument telemetry, and a digital elevation model. Additional data are provided, including quality flags and error estimates.

Suggested Reading

Wolfe, R. E. *et al*., 2002.

MODIS Geolocation Data Set Summary

Coverage: Global

Spatial/Temporal Characteristics:
1 km resolution/daily (daytime and nighttime)

Wavelengths: N/A

Processing Level: 1B

Product Type: Standard, at-launch

Maximum File Size: 60 MB

File Frequency: 288/day

Primary Data Format: HDF-EOS

Additional Product Information:
daac.gsfc.nasa.gov/MODIS/Terra/rad_geo/MOD03.shtml

DAAC: Goddard Space Flight Center Earth Sciences DAAC, daac.gsfc.nasa.gov

Science Team Contacts:
V. V. Salomonson, R. E. Wolfe, A. J. Fleig

MODIS Normalized Water-Leaving Radiance (MOD18) and Aerosol Optical Depth (MOD37)

Product Description

This Level 2 and Level 3 product contains ocean water-leaving radiances for bands 8-14 of MODIS (wavelengths 412-681 nm). These are the "ocean" bands; the water-leaving radiances in these bands are used to derive nearly all of the MODIS ocean products. In addition, another key parameter generated by the algorithm is provided as product MOD37: Aerosol Optical Depth. The Level 2 product is provided daily at 1-km resolution for cloud-free pixels, while the Level 3 product is provided daily, 8-day weekly, monthly, and yearly. The product constraints are that only cloud-free pixels are used (with Sun glitter below a threshold), and all valid pixels are outside a distance threshold from land.

Research and Applications

Normalized Water-Leaving Radiance is approximately the radiance that would exit the ocean in the absence of the atmosphere, if the Sun were at the zenith. It is used in the bio-optical algorithms to estimate chlorophyll *a* concentration and ocean primary productivity on a global scale. The algorithm evolved from experience from the CZCS experiment, which proved the feasibility of measuring ocean color from space. Extensive testing of the algorithm has been conducted using SeaWiFS imagery and is continuing using the Terra and Aqua MODIS instruments. This is the fundamental product for recovering most of the MODIS ocean products.

Data Set Evolution

Inputs to the algorithm are the Level 1 radiances in Bands 8-14, screened for clouds and land, and estimates of the surface wind speed, atmospheric pressure, and ozone concentration derived from National Centers for Environmental Prediction (NCEP, formerly the NMC) products. The success of the algorithm depends on the accurate characterization of the atmospheric effect, which typically constitutes 90 percent of the at-satellite radiance over the ocean. The algorithm includes single scattering, multiple scattering effects, and whitecap removal, and uses six types of ancillary data. There are three major sources of uncertainty in the product: 1) The candidate aerosol models chosen to describe the aerosol may be unrepresentative of the natural aerosol, e.g., wind-blown dust; 2) there is uncertainty in the estimate of the whitecap reflectance/radiance, 3) there is uncertainty in the sensor's radiometric calibration, and 4) there are unaccounted bi-directional effects related to the angular distribution of upwelling radiance just beneath the sea surface. Efforts to reduce these uncertainties include development of improved aerosol models, direct measurements of the properties of oceanic whitecaps, utilization of the Marine Optical Buoy (MOBY) calibration site to improve radiometric calibration, and direct measurement of the upwelling radiance distribution at the MOBY site and during validation experiments. The product is validated by comparing simultaneous surface-based measurements (including drifting-buoy radiometers) and MODIS-derived values at a set of locations. The validation activity will continue throughout the mission to assure stability of this data product, and all other ocean products derived from the water-leaving radiances.

Suggested Reading

Chomko, R., and H. R. Gordon, 1998.

Deschamps, P. Y. *et al.*, 1983.

Evans, R. H., and H. R. Gordon, 1994.

Gordon, H. R., 1997.

Gordon, H. R., and D. K. Clark, 1981.

Gordon, H. R., and A. Y. Morel, 1983.

Gordon, H. R., and M. Wang, 1994.

Gordon, H. R. *et al.*, 1997.

Morel, A., and B. Gentili, 1991.

Morel, A., and B. Gentili, 1993.

Morel, A., and B. Gentili, 1996.

Morel, A. *et al.*, 1995.

MODIS Normalized Water-Leaving Radiance and Aerosol Optical Depth Product Summary

Coverage: Global ocean surface, clear-sky only

Spatial/Temporal Characteristics: 1 km/daily (Level 2), 4.6 km, 36 km, 1°/daily, 8-day, monthly, yearly (Level 3)

Key Science Applications: Ocean chlorophyll, ocean productivity

Key Geophysical Parameters: Water-leaving radiances in the ocean bands, aerosol optical depth

Processing Level: 2, 3

Product Type: Standard, at-launch

Maximum File Size: 88 MB (Level 2); 640 MB binned, 134 MB mapped (Level 3)

File Frequency: 144/day (Daily Level 2); 7/day (Daily Level 3), 7/8-day (8-day Level 3), 7/month (Monthly Level 3), 7/year (Yearly Level 3)

Primary Data Format: HDF-EOS

Additional Product Information: modis-ocean.gsfc.nasa.gov/dataprod.html

DAAC: Goddard Space Flight Center Earth Sciences DAAC, daac.gsfc.nasa.gov

Science Team Contacts: H. R. Gordon, K. Voss

MODIS Photosynthetically Active Radiation (PAR)(MOD22)

Product Description

This Level 2 and 3 product consists of two parameters related to the solar radiation entering the ocean that is available for photosynthesis. The first is Instantaneous Photosynthetically Active Radiation (IPAR), which is the total downwelling flux of photons just below the sea surface at the instant MODIS views the pixel, integrated over the wavelength range of 400 to 700 nm. The second is Absorbed Radiation by Phytoplankton (ARP) averaged over the first optical depth at 685 nm. This parameter is used by the MOD20 product in the calculation of fluorescence efficiency. This product is produced at 1 km daily for Level 2 and gridded at 4.6 km, 36 km, and 1° daily, 8-day weekly, monthly and yearly for Level 3.

Research and Applications

Knowledge of the photosynthetically available radiation (PAR) is critical for determining the photosynthetic rate of phytoplankton, and thus for estimating ocean primary production. Primary productivity algorithms use a variety of forms of PAR (Behrenfeld and Falkowski, 1997). The most highly resolved models require an instantaneous PAR, such as that provided by this product. Other algorithms, such as those used in the MODIS Primary Productivity product (MOD27), use a daily integrated PAR. For this product, it was decided to provide only instantaneous PAR (IPAR) since measurements are available only at the time of the satellite overpass. Having two MODIS instruments in orbit, together with other similar satellite missions (SeaWiFS, MERIS, GLI), the time course of IPAR throughout the day can be estimated to compute daily primary productivity using the highly resolved models.

Radiation absorbed by the phytoplankton (ARP) is utilized for photosynthesis, fluorescence, and heat. Efficiencies of these processes are determined by dividing their respect rates by ARP. The Chlorophyll Fluorescence product (MOD20) uses ARP together with the Fluorescence Line Height to estimate a Fluorescence Efficiency, with the goal of relating this to photosynthetic efficiency (see MOD20). Neglecting variations in the heating efficiency, photosynthetic efficiency is inversely related to the fluorescence efficiency.

Data Set Evolution

The model of Gregg and Carder (1990) is used to estimate the downwelling solar irradiance at the ocean surface. Product generation begins with solar-irradiance data at 1-nm resolution taken from the revised Neckel and Labs data and corrected for Earth-Sun distance for the current day. Atmospheric correction is made for the effects of scattering, absorption by ozone, absorption by gas, and water vapor. This spectrum is then reflected and refracted at the air-sea interface and the below-surface values are computed and summed to give IPAR. The phytoplankton absorption spectrum is then applied to IPAR to obtain ARP. Inputs to the algorithm are Water-Leaving Radiance (MOD18) and Absorption Coefficients (MOD36).

Suggested Reading

Behrenfeld, M. J., and P. F. Falkowski, 1997b.

Gordon, H. R., and M. Wang, 1994.

Gregg, W. W., and K. L. Carder, 1990.

Iqbal, M., 1983.

Paltridge, G. W., and C. M. R. Platt, 1976.

Neckel, H., and D. Labs, 1984.

Thomas, D. *et al*., 2002.

MODIS Photosynthetically Active Radiation Summary

Coverage: Global ocean surface, clear-sky only

Spatial/Temporal Characteristics: 1 km/daily (Level 2); 4.6 km, 36 km, 1°/daily, 8-day, monthly, yearly (Level 3)

Key Science Applications: Ocean chlorophyll, productivity

Key Geophysical Parameters: Photosynthetically available irradiance

Processing Level: 2, 3

Product Type: Validation, at-launch

Maximum File Size: 83 MB (Level 2); 640 MB binned, 134 MB mapped (Level 3)

File Frequency: 144/day (Daily Level 2); 2/day (Daily Level 3), 2/8-day (8-day Level 3), 2/month (Monthly Level 3), 2/year (Yearly Level 3)

Primary Data Format: HDF-EOS

Browse Available: 36-km sample imagery available at the GES DAAC (Level 3 only)

Additional Product Information: modis-ocean.gsfc.nasa.gov/dataprod.html

DAAC: Goddard Space Flight Center Earth Sciences DAAC, daac.gsfc.nasa.gov

Science Team Contacts: K. Carder, D. Tanré, W. Esaias, M. Abbott

MODIS Processing Framework and Match-up Database (MOD32)

Product Description

This Level 2 product consists of the calibration data set to be used in the generation of all the MODIS Ocean products. It consists of a database which contains *in situ* observations of ocean parameters matched with satellite measurement data. This matchup database was initially populated with existing ocean-surface data matched temporally and spatially with CZCS, AVHRR, and SeaWiFS data, and then with MODIS data postlaunch. The product includes the definition of the processing framework in which all the MODIS ocean product algorithms will operate. It is produced daily and supports ocean products at 1 km, but the product itself does not have a spatial resolution.

Research and Applications

This is a calibration product for MODIS ocean processing. It is used through a vicarious calibration scheme to update MODIS radiometric calibration coefficients, which directly relate MODIS Level 1A raw counts to Level 2 calibrated water-leaving radiances, and to monitor long-term performance of the MODIS instrument. MOD32, as a match-up database, is also used to validate derived ocean geophysical parameters such as SST and for quality control of the ocean product suite.

Data Set Evolution

Heritage programs provide the basis for MODIS algorithms. A program developed for the Pathfinder ocean SST product forms the framework for analyzing AVHRR-derived SST, algorithm development and validation, and application of the match-up database. Development for ocean-color algorithms was based on experience gained during the transition from CZCS to SeaWiFS algorithms. Development of the SeaWiFS program involved integration of algorithms generated by H. Gordon (atmospheric correction) and K. Carder (chlorophyll). In addition, daily validity tests were developed through collaboration of the SeaWiFS calibration/validation team and the MODIS Ocean Science Team members. To create the match-up database, *in situ* records are first temporally matched against the satellite retrievals. The satellite data for the match-up database are extracted for 3 × 3 pixel boxes centered at each *in situ* measurement location. Sea-surface temperature observations are from two main types of platforms: moored buoys and drifting buoys. The primary source of match-up bio-optical measurements is the Marine Optical Buoy (MOBY), but measurements made from ship surveys are also included in this database. Prior to the launch of MODIS, algorithms were validated using data from the SeaWiFS and AVHRR Pathfinder programs. Computer codes were then generated to produce each algorithm product, in accordance with EOS coding standards and accounting for the sequence of data production required by product interdependencies.

Suggested Reading

Brown, O. *et al.*, 2002.

Evans, R. H., and H. R. Gordon, 1994.

Gordon, H. R., 1987.

Gordon, H. R., and A. Y. Morel, 1983.

Kilpatrick, K. A. *et al.*, 2001.

Kearns, E. *et al.*, 2001.

Slater, P. N. *et al.*, 1987.

MODIS Processing Framework and Match-up Database Product Summary

Coverage: Global ocean surface

Spatial/Temporal Characteristics: 1 km/daily

Key Science Applications: Ocean chlorophyll, ocean productivity, all ocean products

Key Geophysical Parameters: Match-up databases, water-leaving radiances, *in situ* measurements

Processing Level: 2

Product Type: Standard, at-launch

Science Team Contacts: R. H. Evans, H. R. Gordon

MODIS Clear-Water Epsilon (MOD39)

Product Description

This product provides a single parameter, the ratio of clear-water-leaving radiance at 531 nm to that at 667 nm and is called the clear-water epsilon. This quantity relates directly to the iron content of aerosols over clear waters mostly in the ±35° latitude range. The Level 2 product is produced daily, at 1 km spatial resolution, whereas the Level 3 product is produced daily, 8-day weekly, monthly, and yearly, at 4.6 km, 36 km, and 1° resolution.

Research and Applications

The primary purpose of this algorithm is to estimate aerosol iron content over ocean waters. The aerosol iron influences the validity of other MODIS products. The secondary objective is to flag instances when normalized water-leaving-radiance retrievals may need adjustment due to aerosol absorption at blue and green wavelengths. Such errors will affect chlorophyll *a* calculations. The third objective is to provide a check on the Angstrom exponent derived at red and infrared wavelengths. The algorithm is valid for pigment concentrations up to 2 mg/m^3. When pigment concentrations are larger than this, the algorithm can no longer be applied.

Data Set Evolution

The algorithm is based on methods developed for obtaining clear-water epsilon values from CZCS data. Modifications for the MODIS algorithm include extension of the clear-water concept to include waters with higher pigment concentrations and modification of the values of the normalized water-leaving radiance at 520, 550, and 670 nm for CZCS to the slightly different MODIS bands by means of the water-absorption curve. Product validation used SeaWiFS data in the pre-launch period and MODIS data postlaunch. Scattering and optical-thickness data plus ship data of water-leaving radiances are acquired to test the clear-water radiance assumptions.

Suggested Reading

Carder, K. L. *et al*., 1991.

Carder, K. L., 2001.

Carder, K. L., 2002.

Gordon, H. R., 1978.

Gordon, H. R., and D. K. Clark, 1981.

Gordon, H. R., and A. Y. Morel, 1983.

Gordon, H. R., and M. Wang, 1994.

MODIS Clear-Water Epsilon Summary

Coverage: Global ocean surface, clear-sky only

Spatial/Temporal Characteristics: 1 km/daily (Level 2); 4.6 km, 36 km, 1°/daily, 8-day, monthly, yearly (Level 3)

Key Science Applications: Aerosol iron estimation, water-leaving radiance correction

Key Geophysical Parameters: Clear-water epsilon, aerosol iron content

Processing Level: 2, 3

Product Type: Validation, at-launch

Maximum File Size: 88 MB (Level 2); 865 MB binned, 134 MB mapped (Level 3)

File Frequency: 144/day (Daily Level 2); 36/day (Daily Level 3), 36/8-day (8-day Level 3), 36/month (Monthly Level 3), 36/year (Yearly Level 3)

Primary Data Format: HDF-EOS

Browse Available: 36-km sample imagery available at the GES DAAC (Level 3 only)

Additional Product Information: modis-ocean.gsfc.nasa.gov/dataprod.html

DAAC: Goddard Space Flight Center Earth Sciences DAAC, daac.gsfc.nasa.gov

Science Team Contact: K. Carder

MOPITT Geolocated Radiances (MOP01)

Product Description

This product contains geolocated Level 1B radiances for the eight spectral channels of the MOPITT instrument. Radiances are obtained at three different wavelengths using two different methods of gas correlation radiometry. Reflected solar radiation is measured at 2.2 and 2.3 μm using length-modulated cells to determine the total atmospheric columns of methane and carbon monoxide respectively. Thermal radiation at 4.6 μm is measured in four channels using a combination of length-modulated and pressure-modulated cells to provide information on the vertical profile of carbon monoxide. Engineering data describing the state of the gas cells and calibration are also provided to support transformation of the radiances into Level 2 products.

Radiances are acquired by cross-track scanning about the nadir resulting in an interlaced swath of pixels approximately 640 km wide. All channels are simultaneously measured on four separate pixels each with a resolution of 22 × 22 km. Each channel measures radiance in two states of its correlation cell. The states correspond to long and short optical paths through the gas cell. An average and a difference radiance are derived from these two.

Suggested Reading

Deeter, M. N. *et al*., 2002.

MOPITT Science Team, 1996.

MOPITT Geolocated Radiances Product Summary

Coverage: Global

Spatial/Temporal Characteristics: 650-km swath centered at nadir; interlaced crosstrack scan of 4 pixels, each 22 × 22 km at nadir

Wavelengths:
2.258 µm center, ±0.355 width
2.334 µm center, ±0.011 width
4.627 µm center, ±0.055 width

Processing Level: 1B

Product Type: Standard, at-launch

Maximum File Size: 83 MB

File Frequency: 1/day

Primary Data Format: HDF-EOS

Browse Available: No

Additional Product Information:
www.eos.ucar.edu/mopitt/index.html

www.atmosp.physics.utoronto.ca/MOPITT/home.htm

DAAC: Langley Atmospheric Sciences Data Center, eosweb.larc.nasa.gov

Science Team Contact: J. R. Drummond

Chapter 5

Precipitation, Atmospheric Humidity and Atmospheric Temperatures

TRMM
PR
TMI

Terra
MODIS

Precipitation, Atmospheric Humidity and Atmospheric Temperatures – An Overview

Relationship to Global Change Issues

The hydrological cycle is one of three key Earth system processes that are components of global climate; the carbon and energy cycles are the others. Monitoring precipitation and atmospheric humidity is critical to obtaining hydrological-cycle parameters needed for developing global climate models and detecting climate change. The processes that generate rainfall are central to the dynamical, biological, and chemical processes in the atmosphere, in the oceans, and on the land surfaces. Space-based measurements give a more accurate global documentation of tropical rainfall. The TRMM instruments are designed to provide greatly-improved measurements of rain rates over both land and ocean compared to current methods. TRMM, often referred to as a "flying rain gauge," makes an important contribution to the World Climate Research Program's rain climatology initiative. This section describes the TRMM and Terra products that support the monitoring of rainfall and atmospheric humidity, including the TRMM ground-truth validation data acquisition.

Precipitation: The majority of global precipitation occurs in the tropics, between latitudes of 30˚N and 30˚S. Tropical rain is one of the key parameters that affects the global heat balance and the global water cycle. To understand and predict large variations in weather and climate, it is critical to understand the coupling between the atmosphere and the surface below, which is approximately 29% land and 71% ocean. Atmospheric circulation transports both energy and water, moving heat from the tropics to the polar regions. Water that has evaporated from the oceans and the land surface falls as rain or snow, often in places far removed from its point of origin. There is evidence that tropical rainfall variability, apparently coupled with changes in the underlying surface (particularly sea surface temperature), is associated with significant alterations in wind patterns and rainfall. Fluctuations in rainfall amount impact climate on both short and long time scales.

Unlike the small-scale general features that appear on daily weather maps, the long-term, time-averaged circulation and precipitation fields show large-scale features associated with the annual evolution of the monsoons, trade wind systems, and oceanic convergence zones. Large-scale features are also evident on a monthly and seasonal scale. Interannual variability is dominated by tropical Pacific ocean-atmosphere interactions. These interactions are associated with the El Niño-Southern Oscillation (ENSO) cycle, whose major swings, which occur at irregular intervals of two to seven years, are associated with pronounced year-to-year precipitation variations over large areas of the tropics. The large-scale spatial coherence and systematic evolution of both intraseasonal and interannual tropical precipitation anomalies is of great significance to climate prediction. They are also important in the development of optimal sampling strategies for estimating accumulated precipitation over periods of a few weeks to a few months.

The characterization of rainfall in tropical regimes is fundamental to improving techniques of radar-rainfall measurements as well. Not only are there regional and seasonal differences, but significant differences also occur within tropical rain systems. These differences can be broadly classified as 1) morphological, referring to sizes, lifetimes, and spatial structures of rain-producing systems; and 2) microphysical, referring to raindrop formation processes, and the raindrop size distribution. Rainfall rates display a highly variable structure in both time and space, meaning radar surveillance systems must take frequent measurements to accurately assess rainfall totals. Three-dimensional volume scans (like the WSR-88D radar scans on the nightly weather reports) every five minutes are desirable, although scans at 15-minute intervals provide useful data. The hydrological and severe weather monitoring requirements of most operational radar systems satisfy these criteria, providing invaluable ground-based validation data with nominal additional expenditure.

Humidity: Atmospheric circulation redistributes moisture and heat. Water vapor evaporates from the ocean and land surfaces, and is transported to other parts of the atmosphere where condensation occurs, clouds form, and precipitation ensues. There is a net outflow of atmospheric moisture from the tropics, where sea-surface temperatures are high and the warm atmosphere can hold large amounts of water vapor, to higher latitudes, where condensation and precipitation remove the moisture. Current numerical weather prediction models give inconsistent results about the future distribution of precipitation.

Humidity is the amount of water vapor in the atmosphere. Water vapor concentration depends on temperature, which determines the total amount of

water that the atmosphere can hold without saturation. Hence, water vapor amounts decrease from Equator to Pole and with increasing altitude. Generally, water amounts are less over the continents than over the oceans, and the upper atmosphere is drier than the near-surface atmosphere. Superimposed on this general behavior are smaller variations of water vapor amounts that determine the formation and properties of clouds and rainfall. Simultaneous imaging of clouds and water vapor by TRMM and Terra can provide the data necessary to understand better the interactions between cloud processes and the large-scale flow and distribution of water vapor.

Temperatures: The atmosphere is not physically uniform; it has significant variations in temperature and pressure with altitude. The regions where temperature is either increasing or decreasing with height define the different layers of the atmosphere. The lowest 10 km of the atmosphere is called the troposphere, and the region from about 10 to 50 km is known as the stratosphere. The transition region between the two is known as the tropopause.

Atmospheric temperature has a critical influence on the hydrological cycle and is a key input parameter in global climate models. Tropospheric and stratospheric temperatures are central to the problem of greenhouse warming. Global Circulation Models (GCMs) predict that temperature changes due to higher concentrations of greenhouse gases will have characteristic profiles in the different layers of the atmosphere, with warming in the mid-troposphere and cooling in the stratosphere. Cooler stratospheric temperatures are an expected consequence of the increased trapping of terrestrial radiation in the troposphere. In addition, most ozone depletion occurs in the lower part of the stratosphere (15 to 25 km) so an accurate knowledge of the fluctuations in stratospheric temperature on a global scale is therefore required for an overall understanding of global warming.

The most important data required for initializing forecast models are the 3-D horizontal wind and temperature profiles. Other desirable parameters are the 3-D moisture distribution, surface pressure and wind fields, and sea-surface temperature. Problems exist in the establishment of a 3-D global temperature field because of data gaps over the ocean. In addition, sharp temperature inversions exist in the atmosphere, which are difficult to infer from satellite.

Product Overview

The products included in this section are primarily produced by the TRMM instruments, with MODIS on the Terra satellite providing two products giving humidity data.

The TRMM mission is designed to use the measurements of multiple instruments flying on its platform to quantify the distribution of the two-thirds of global precipitation estimated to fall in the tropics and subtropics. PR measures the three-dimensional rainfall distribution over both land and ocean. More specifically, this instrument provides information about the vertical structure of precipitation, the key to determining the latent heat input to the atmosphere. A unique feature is that it permits the measurement of rain over land where passive microwave precipitation estimation techniques are difficult.

The fundamental data set obtained from the TRMM program is a three-year sequence of instantaneous rainfall rates as well as monthly, tropical rainfall accumulations averaged over geographical grid squares 500 km on a side. These gridded monthly averages are being used to validate climate forecasting models. The TRMM data product sequence begins with the TMI data and the precipitation radar data, which form the basis of the improved rainfall estimation promised by the mission. Rainfall estimates from TMI and the PR are combined in TRMM product 3B-31, and then combined with Sun-synchronous low-orbit satellite microwave data (SSM/I), geostationary satellite IR data (e.g., GOES) and rain gauge data to produce the final rainfall product (3B-43).

The MODIS products provide water vapor measurements (MOD05) needed for atmospheric correction algorithms for all surface parameter retrieval tasks. They are also used to improve understanding of the hydrological cycle, energy budget, and climate. The atmospheric stability parameter in MOD07 gives information on convection and instability which, along with temperature and moisture profiles, also contained in product MOD07, is needed by the atmospheric correction algorithms.

A set of TRMM ground validation products from approximately ten independent sites is included. These products provide the rainfall data used to validate the data obtained from PR on TRMM. Included are the instantaneous surface rainfall maps (2A-53), the radar site Convective/Stratiform Map (2A-54), and the radar site gridded reflectivities (2A-55) used to validate the vertical hydrometeor and latent-heating retrievals of TMI and PR. Five-day and 30-day rainfall data at the radar sites (3A-53, 54) and monthly 3-D radar reflectivity distributions (3A-55) complete the set of products that are needed to validate and improve all the TRMM rainfall products.

Product Interdependency and Continuity with Heritage Data

TRMM carries the first quantitative precipitation radar to be flown in space. Previous measurements from space of rain rate have used passive microwave measurements from instruments on Nimbus and the Defense Meteorological Satellites, which are in polar orbits and cannot capture the diurnal variability of rainfall in the tropics. TMI on TRMM provides continuity with these earlier data, which are used in conjunction with PR and the heritage instrument data to provide greatly-improved accuracy in rainfall mapping. The radiometers on TRMM give good measurements of rainfall rates over the oceans, but such measurements continue to be less reliable over land where the surface emissivity inhomogeneities make interpretation more difficult. VIRS, which was derived from AVHRR heritage technology, is also included in the TRMM instrument complement so that the rainfall measurements from the radar and passive microwave instruments can be used to better interpret VIS/IR measurements from past and future operational satellites.

The MODIS humidity products are being used by atmospheric characterization and climate modeling researchers in conjunction with the rainfall data, even though there is not a direct product dependence between MODIS and TRMM.

The present series of atmospheric sounders (TOVS) aboard NOAA polar satellites are limited by their vertical resolution. NOAA and the Defense Meteorological Satellite Program (DMSP) operational satellites have provided temperature and humidity profiles and surface products for ingest into assimilation models. Three important NOAA instruments are: AVHRR since 1981; TOVS since 1979; the Geostationary Operational Environmental Satellite (GOES) Visible Infrared Spin-Scan Radiometer (VISSR) and its VISSR atmospheric sounder version since 1978. Considerable progress was also made with the deployment of the three-axis stabilized high-resolution infrared sounder on geostationary satellites. Lastly, the 20-channel Advanced Microwave Sounding Unit (AMSU) on NOAA-K, provides higher-resolution temperature profiles than its predecessor, the four-channel MSU.

Suggested Reading

Chiu, L. S., 1988.

Inoue, T., 1997.

Kummerow, C. *et al.*, 1998.

Kummerow, C. *et al.*, 2000.

Li, J., and K. Nakamura, 2002.

Liao, L. *et al.*, 2001.

Pfaendtner, J. *et al.*, 1995.

Rasmusson, E. M., 1985.

Schubert, S. D. *et al.*, 1993.

Simpson, J. *et al.*, 1996.

Takacs, L. L. *et al.*, 1994.

Tao, W.-K. *et al.*, 2001.

PR Surface Cross-Section as Function of Scan Angle (PR 2A-21)

Product Description

This Level 2 product provides an estimate of the path attenuation and its reliability by using the surface as a reference target. Path attenuation is estimated by comparing the apparent surface cross section measured in the presence of rain, with the averaged surface cross section measured in the absence of rain. A reliability parameter is also provided based on the variability of the surface cross section in the absence of rain. The product includes the spatial and temporal statistics of the surface scattering cross section, and classification of the cross sections into land/ocean, rain/no rain categories. Output parameters consist of attenuation, reliability, and surface cross section (σ_0).

Research and Applications

One of the ways by which attenuating-wavelength radars such as TRMM can correct for attenuation is by means of the surface reference method. In this method, the path-integrated attenuation caused by rain is estimated by a ratio of the apparent surface cross section, σ_0, in the raining region to a temporally or spatially averaged value of this quantity in rain-free regions.

As the surface cross sections are closely related to the vegetation and soil moisture conditions over land, and the wind speed and directions over oceans, a number of TRMM-related studies can be undertaken with these data sets.

Data Set Evolution

There have been limited σ_0 measurements made from aircraft radars, but systematic global maps had not previously been compiled.

Relation to Other TRMM Products

This product is used as input for the PR rain profiling algorithm (2A-25). For areas far away from rainfall, σ_0 is a unique product of TRMM.

Suggested Reading

Caylor, I. J. *et al*., 1997.

Iguchi, T., and R. Meneghini, 1994.

Kozu, T., 1995.

Marzoug, M., and P. Amayenc, 1994.

Meneghini, R., and K. Nakamura, 1990.

Meneghini, R., and T. Kozu, 1990.

Meneghini, R. *et al*., 2000.

PR Surface Cross-Section as Function of Scan Angle Product Summary

Coverage: 36°S to 36°N; 15-16 orbits per day with a swath width of 220 km before August 2001 and 253 km after August 2001 (satellite altitude was raised from 350 km to 402.5 km)

Spatial/Temporal Characteristics: 5 km (after August 2001)

Key Geophysical Parameters: Rainfall profile

Processing Level: 2

Product Type: Standard, at-launch

Maximum File Size: 12 MB

File Frequency: 1/orbit

Primary Data Format: HDF

Browse Available: Yes

Additional Product Information:
trmm.gsfc.nasa.gov
tsdis.gsfc.nasa.gov

DAAC: Goddard Space Flight Center Earth Sciences DAAC, daac.gsfc.nasa.gov

Science Team Contact: K. Okamoto

PR Rain Occurrence and Rain Type and Bright Band Height (PR 2A-23)

Product Description

The Level 2 product 2A-23 indicates the presence of a "bright band," which in turn indicates the presence of stratiform rain. If the bright band is detected, its height is determined. This information is used to classify the rain type (stratiform type, convective type, or warm rain). The TRMM Science Data and Information System (TSDIS) supplies information as to the background type: land, ocean, or indeterminate. The height of the bright band is useful to the TMI algorithms to identify the height of the freezing level.

Research and Applications

PR provides information on the distribution and characterization of rainfall and latent heating over the global tropics and subtropics. This information is used to advance the Earth system science objective to understand global energy and water cycles. In addition, it provides understanding of the mechanism through which tropical rainfall and its variability influence global atmospheric circulation by improving the modeling of rainfall and atmospheric circulation interactions. This enables the improved prediction of monthly and longer global circulation and rainfall variability. Finally, it improves modeling of convectively-driven precipitating systems in the tropics, including their organization on the mesoscale and their interactions with the ocean and the atmosphere.

Data Set Evolution

There have been a number of airborne radars that have flown on field campaigns in previous years. Most notably, ARMAR is a 13.8 GHz radar that flew on the NASA DC-8 and was built specifically to simulate TRMM observations.

Relationship to Other TRMM Products

Product 2A-23 is a qualitative description not previously available. It is useful to passive microwave determinations as well as input to the PR rain algorithm.

Suggested Reading

Awaka, J. *et al*., 1998.

Furuhama, Y. *et al*., 1982.

Iguchi, T., and R. Meneghini, 1994.

Steiner, M. *et al*., 1995.

Theon, J. S. *et al*., Eds., 1992.

PR Rain Occurrence and Rain Type and Bright Band Height Product Summary

Coverage: 36°S to 36°N; 15-16 orbits per day with a swath width of 220 km before August 2001 and 253 km after August 2001 (satellite altitude was raised from 350 km to 402.5 km)

Spatial/Temporal Characteristics: 5 km (after August 2001)

Key Geophysical Parameters: Rainfall profile

Processing Level: 2

Product Type: Standard, at-launch

Maximum File Size: 15 MB

File Frequency: 1/orbit

Primary Data Format: HDF

Browse Available: Yes

Additional Product Information:
trmm.gsfc.nasa.gov
tsdis.gsfc.nasa.gov

DAAC: Goddard Space Flight Center Earth Sciences DAAC, daac.gsfc.nasa.gov

Science Team Contact: K. Okamoto

PR Range Profiles of Rain and Water Content (PR 2A-25)

Product Description

Level 2 product 2A-25 retrieves rain parameters over each PR resolution cell (4 km × 4 km × 250 m). Products 1C-21, 2A-21, and 2A-23 are input to this product. In the presence of rain, these parameters include rainfall structure, estimated path attenuation, and its reliability.

Research and Applications

PR provides information on the distribution and characterization of rainfall and latent heating over the global tropics and subtropics. This information is used to advance the Earth system science objective to understand global energy and water cycles. In addition, it provides understanding of the mechanism through which tropical rainfall and its variability influence global atmospheric circulation by improving the modeling of rainfall and atmospheric circulation iterations. This enables the improved prediction of monthly and longer global circulation and rainfall variability. Finally, it improves modeling of convectively-driven precipitating systems in the tropics, including their organization on the mesocale and their interactions with the ocean and the atmosphere.

Data Set Evolution

There have been a number of airborne radars that have flown on field campaigns in previous years. Most notably, ARMAR is a 13.8 GHz radar that flew on the NASA DC-8 and was built specifically to simulate TRMM observations.

Relationship to Other TRMM Products

Product 2A-25 provides the best single-instrument rain profile information. Over the narrow swath of the radar it is used to improve the passive microwave algorithm (2A-12), thereby extending the usefulness of PR to the wide swath of TMI.

Suggested Reading

Iguchi, T. *et al*., 1998.

Iguchi, T., and R. Meneghini, 1994.

Iguchi, T. *et al*., 2000.

Kozu, T. *et al*., 1991.

Kozu, T., and T. Iguchi, 1996.

Theon, J. S. *et al*., Eds., 1992.

PR Range Profiles of Rain and Water Content Product Summary

Coverage: 36°S to 36°N; 15-16 orbits per day with a swath width of 220 km before August 2001 and 253 km after August 2001 (satellite altitude was raised from 350 km to 402.5 km)

Spatial/Temporal Characteristics: 5 km (after August 2001)

Key Geophysical Parameters: Rainfall profile

Processing Level: 2

Product Type: Standard, at-launch

Maximum File Size: 260 MB

File Frequency: 1/orbit

Primary Data Format: HDF

Browse Available: Yes

Additional Product Information:
trmm.gsfc.nasa.gov
tsdis.gsfc.nasa.gov

DAAC: Goddard Space Flight Center Earth Sciences DAAC, daac.gsfc.nasa.gov

Science Team Contact: K. Okamoto

PR Monthly Accumulated Rainfall and Vertical Structure (PR 3A-25) and Monthly Combined Accumulated Surface Rainfall (PR 3A-26)

Product Description

Statistics of rain data are provided in this Level 3 product, including probability distributions of rain rates, to help identify and characterize sampling errors, and to determine patterns in precipitation movement and latent heat transfer. The statistical nature of the rainfall is characterized by the outputs from the Level 2 radar algorithms. Four categories of output products are computed over 5° × 5° × 1 month domains. The four categories are:

1) mean and variance of the rain rate at five heights above the surface;
2) fractional rain areas (stratiform, convective, both);
3) histograms of the rain rates, reflectivity factors, heights of the bright-band and storm top, and path attenuation; and
4) correlation coefficients between rain rates at the various heights.

Research and Applications

This product is designed to provide the temporal continuity and spatial coverage necessary for routine evaluation of time-space mean precipitation. Applications include quantitative estimates of large-scale, time-averaged precipitation over the global tropics, analyses of the seasonal, interannual, and diurnal variability of precipitation, and the establishment of multiyear time series data for global climate change.

Relationship to Other TRMM Products

Inputs to algorithm 3A-25 are the output products from the Level 2 PR algorithms. A few of the output products from 3A-25 and 3A-26 provide estimates of the same quantity, e.g., the monthly mean rain rate at the 5° × 5° boxes over the TRMM domain. The approach used in 3A-25 is that of a straightforward sample mean of the individual measurements obtained during the month whereas 3A-26 uses a somewhat more involved statistical approach. Comparisons of these products over the TRMM ground-validation sites are obviously important. As the TMI 3A-11 algorithm outputs monthly means over the same 5° × 5° cells as does 3A-25 and 3A-26, comparisons of the output products should be made. To reduce the effects of sampling errors on 3A-25 and 3A-26, comparisons of these outputs with those of 3A-11 should also be made over longer time periods (3 months, 6 months, and yearly).

Data Set Evolution

Approaches for measuring statistically averaged rain rates for TRMM have their heritage in the GARP Atlantic Tropical Experiment (GATE) measured rain rates experiments, as well as the Florida Area Cumulus Experiment (FACE). The GATE and FACE radar rain distributions were the heritage data sets used to describe some of the key statistics characteristics of the precipitation that TRMM is intended to measure. Additionally, by identifying the ranges of rain rates measured in these experiments, they served to enable instrument designers to better specify the parameters and performance of the observing system.

Suggested Reading

Atlas, D. *et al.*, 1990.

Kedem, B. *et al.*, 1990.

Meneghini, R., 1998.

Short, D. *et al.*, 1993.

Meneghini, R. *et al.*, 2001.

Meneghini, R., and J. A. Jones, 1993.

Wilheit, T. T. *et al.*, 1991.

PR Monthly Accumulated Rainfall and Vertical Structure and Monthly Combined Accumulated Surface Rainfall Product Summary

Coverage: 40°N to 40°S

Spatial/Temporal Characteristics: 5° × 5° and 0.5° × 0.5°, monthly

Key Geophysical Parameters:
Low Resolution – mean and standard deviation of rain rate, storm height, x_i, brightband height and NWBF correction, rain fraction, histograms of above, correction coefficients
High Resolution – mean and standard deviation of rain rate, rain fraction

Processing Level: 3

Product Type: Standard, at-launch

Maximum File Size: 30 MB (3A-25), 6 MB (3A-26)

File Frequency: 1/month

Primary Data Format: HDF

Browse Available: Yes

Additional Product Information:
trmm.gsfc.nasa.gov
tsdis.gsfc.nasa.gov

DAAC: Goddard Space Flight Center Earth Sciences DAAC, daac.gsfc.nasa.gov

Science Team Contact: K. Okamoto

TMI Surface Rainfall and Vertical Structure (TMI 2A-12)

Product Description

This product contains vertical hydrometeor profiles from the TMI obtained by blending the radiometric data with dynamical cloud model data. The results consist of the surface rainfall rate and a confidence parameter, as well as three-dimensional results, with five hydrometeor classes and the associated latent heating derived at approximately 14 vertical layers. The layer information must be viewed as approximate since it is inferred through the cloud model rather than from direct measurements. This is a Level 2 product that has not been resampled; scan time, latitude, longitude, and scan line/pixel number are included for each pixel in this product.

Research and Applications

The research objectives of this product are to:

- improve the ability to obtain rainfall and latent heat release over the global tropics;
- validate and improve models that promote the understanding of the formation and organization of convection and their interactions with the ocean and ambient atmosphere and the climate system; and
- advance understanding of the Earth's global energy and water cycles by determining how tropical rainfall and its variability influence global circulation.

Relationship to other TRMM products

This product generates output similar to 2A-25 and 2B-31. Product 2A-25, the PR rainfall vertical structure has better vertical resolution (250 m), but is limited to a relatively narrow swath of approximately 250 km as compared to the approximately 870 km swath of the TMI (after the altitude of the satellite was raised from 350 km to 402.5 km in August 2001). Sensitivity to the integrated ice content is also greater from the TMI product than the PR product.

Product 2B-31 combines information from both the radar and radiometer over the narrow swath of the radar. In this region, 2B-31 should ultimately provide the best surface rainfall and structure products. Problems related to co-registration of the sensors, as well as the lack of PR heritage, made this product (2B-31) less reliable at the onset of the mission.

Data Set Evolution and Applications

The TMI is similar to several spaceborne microwave instruments that have flown over the past decade, including the SSM/I onboard the DMSP satellites and the SMMR onboard Nimbus-7. The major changes are the addition of 10 GHz dual-polarized channels and increased spatial resolution, which reduce the footprint filling uncertainty that affects passive microwave algorithms.

Suggested Reading

Hong, Y. *et al*., 1999.

Kummerow, C. *et al*., 1998.

Kummerow, C. *et al*., 1996.

Olson, W. *et al*., 1999.

Kummerow, C., and L. Giglio, 1994.

Kummerow, C. *et al*., 2001.

Mugnai, A. *et al*., 1993.

Smith, E. A. *et al*., 1994a,b.

TMI Surface Rainfall and Vertical Structure Product Summary

Coverage: 38°S to 38°N; 15-16 orbits per day with a swath width of 760 km before August 2001 and 874 km after August 2001 (satellite altitude was raised from 350 km to 402.5 km).

Spatial/Temporal Characteristics: 5 km

Key Geophysical Parameters: Surface rainfall

Processing Level: 2

Product Type: Standard, at-launch

Maximum File Size: 105 MB

File Frequency: 1/orbit

Primary Data Format: HDF

Browse Available: Yes

Additional Product Information:
trmm.gsfc.nasa.gov
tsdis.gsfc.nasa.gov

DAAC: Goddard Space Flight Center Earth Sciences DAAC, daac.gsfc.nasa.gov

Science Team Contact: C. Kummerow

TMI Monthly Surface Rainfall (TMI 3A-11)

Product Description

This product consists of mean monthly rainfalls over 5° × 5° cells. Retrievals are only possible over oceanic areas, where data are needed most for climate model verification. The frequency of occurrence of rain intensities in different rate categories over a specified area can be plotted as a histogram or as a smoothed curve that fits the histogram. This curve is called the probability density function (pdf) of the rain rates. In the case of tropical rainfall, the pdfs are always highly skewed such that a large fraction of the total rainfall is concentrated into a relatively small number of storms of high intensity or in a small fraction of the time or of the area in which it is raining. This product is obtained by considering histograms of 19-GHz, 21-GHz and 19-21-GHz combinations. Monthly rainfall indices are computed by statistically matching the histograms with the model calculated pdfs. The main purpose of this product is to provide a robust baseline of surface rainfall rates.

Research and Applications

This product is designed to advance understanding of the Earth's global energy and water cycles by determining how tropical rainfall and its variability influence global circulation. A reliable measurement of rainfall, particularly over the oceans, provides for the first time space-time variability of vertically integrated latent heating. This, coupled with information on the nature of synoptic disturbances in different regions of the tropics, can help determine the vertical structure of the diabatic heating.

Data Set Evolution

The TMI is similar to several spaceborne microwave instruments that have flown over the past decade including the SSM/I onboard the DMSP satellites and the SMMR onboard Nimbus-7. The major changes are the addition of 10-GHz polarized channels and increased spatial resolution, which reduce the footprint filling uncertainty that affects passive microwave algorithms. The surface rainfall algorithm is very similar to the one developed and applied as part of the Global Precipitation Climatology Project (GPCP) program for the past eight years.

Relationship to Other TRMM Products

This product generates monthly surface rainfall with sampling corresponding to the wide swath of the TMI. This parameter may also be obtained from the TRMM combined sensor algorithm but is included as a standard product to serve as a very robust baseline.

Suggested Reading

Chang, A. T. C. *et al*., 1999a,b.

Chiu, Long S. *et al*., 1993.

Wilheit, T. T. *et al*., 1991.

TMI Monthly Surface Rainfall Product Summary

Coverage: Day and night, 40°N to 40°S over oceans only

Spatial/Temporal Characteristics: 5° × 5°, monthly

Key Geophysical Parameters: Surface rainfall and statistics

Processing Level: 3

Product Type: Standard, at-launch

Maximum File Size: 60 MB

File Frequency: 1/month

Primary Data Format: HDF

Browse Available: Yes

Additional Product Information:
trmm.gsfc.nasa.gov
tsdis.gsfc.nasa.gov

DAAC: Goddard Space Flight Center Earth Sciences DAAC, daac.gsfc.nasa.gov

Science Team Contact: A. Chang

TRMM Combined Surface Rainfall Rate and Vertical Structure (PR 2B-31)

Product Description

This is a Level 2 product, which combines information from more than one sensor. This product contains vertical hydrometeor profiles obtained by blending reflectivities obtained by PR with brightness temperatures from the TMI instrument. The results consist of the surface rainfall rate and a confidence parameter. Also included are the three-dimensional results, with five hydrometeor classes and the associated latent heating derived at the vertical resolution of the PR (250 m).

This product is designed to improve our ability to obtain rainfall and latent heat release over the global tropics. Additionally, it is used to validate and improve models that promote the understanding of the formation and organization of convection and their interactions with the ocean and ambient atmosphere and the climate system. Finally, it advances our understanding of the Earth's global energy and water cycles by determining how tropical rainfall and its variability influence global circulation.

Research and Applications

The vertical distribution of hydrometeors is an important part of any surface rainfall rate retrieval algorithm, because the distribution strongly affects the microwave radiances. The intent is that this product should constitute the best product available from the TRMM mission.

Relationship to Other TRMM Products

This product generates output similar to 2A-12 and 2A-25. Product 2A-12 (the TMI rainfall vertical structure) has wider coverage (approximately 870 km vs. 250 km, after the alititude of the satellite was raised from 350 km to 402.5 km in August 2001).

Data Set Evolution and Applications

The simultaneous use of active and passive microwave sensors can yield dramatic improvements over either sensor alone. Some limited aircraft studies have demonstrated this point. The opportunity to merge radiances from active and passive sensors, as

well as visible and infrared radiances on a global data set, is a capability that is unique to the TRMM satellite.

Suggested Reading

Haddad, Z. *et al*., 1997a,b.

Schols, J. L., and J. A. Weinman, 1994.

Smith, E. A. *et al*., 1994b.

Smith, E. A. *et al*., 1997.

Smith, E. A. *et al*., 2003.

TRMM Combined Surface Rainfall Rate and Vertical Structure Product Summary

Coverage: 36°N to 36°S; 15-16 orbits per day with a swath width of 220 km before August 2001 and 253 km after August 2001 (satellite altitude was raised from 350 km to 402.5 km).

Spatial/Temporal Characteristics: 5 km (after August 2001)

Key Geophysical Parameters: Rainfall profile

Processing Level: 2

Product Type: Standard, at-launch

Maximum File Size: 170 MB

File Frequency: 1/orbit

Primary Data Format: HDF

Browse Available: Yes

Additional Product Information:
trmm.gsfc.nasa.gov
tsdis.gsfc.nasa.gov

DAAC: Goddard Space Flight Center Earth Sciences DAAC, daac.gsfc.nasa.gov

Science Team Contact: E. Smith

TRMM Monthly Combined Accumulated Rainfall and Vertical Structure (3B-31)

Product Description

This Level 3 product consists of rainfall accumulations over 5° × 5° areas and monthly time scales of surface rainfall, as well as the three-dimensional hydrometeor structure and measurements of latent heating. Retrievals are made over both land and ocean using the sampling characteristics of the TMI instrument. The product is a calibration of the TMI profiling algorithm (2A-12), where the calibration is obtained by comparing the coincident geophysical products from the TMI 2A-12 with those of the combined sensors approach (2B-31). The calibration coefficients are then applied to the entire 2A-12 data set and monthly accumulations are computed.

The simultaneous use of active and passive microwave sensors can yield dramatic improvements over either sensor alone, as demonstrated by earlier aircraft studies. The opportunity to merge radiances from active and passive sensors as well as visible and infrared radiances on a global data set is a capability that is unique to the TRMM satellite. As the algorithm has matured, this product has formed the cornerstone of TRMM retrievals and serves as the transfer standard to calibrate previous satellite measurements.

Research and Applications

Before the launch of TRMM there were no reliable data sets for either monthly or seasonal mean rainfall or for their interannual variability to validate the global atmospheric models. Latent heat derived from precipitation is the major source of energy within the atmosphere, and its vertical distribution affects the stability of the atmosphere and hence the propagation pattern of Rossby waves, which influence the climate in regions that are located far from the tropical storms where the latent energy is released. This product allows latent heating to be calculated from condensation. The direct observation of precipitation, and the cloud systems that produce it in varying amounts, permits researchers to know exactly where the latent heat is being released. This information can be used as input to climate models to determine higher latitude effects and possible interannual changes.

Relationship to Other TRMM Products

This product generates monthly surface rainfall and latent heating with sampling corresponding to the wide swath of the TMI. Product 3A-25 generates similar products but only uses the narrower swath of the PR.

Data Set Evolution

Precipitation distributions have already been retrieved from spaceborne microwave radiometers, and TMI builds on that earlier work. The primary instrument currently used to retrieve volumetric rainfall from space is the SSM/I passive radiometer system on the DMSP. The TRMM Combined Monthly Rainfall product overcomes the limitation of radiometric measurements, which include difficulty in measuring light rain and snowfall over land. Combining radar and radiometric measurements in a common precipitation retrieval algorithm takes advantage of the strengths of both types of measurements.

Suggested Reading

Smith, E. A. *et al*., 1994b.

Smith, E. A. *et al*., 1997.

Smith, E. A. *et al*., 2003.

Schols, J. L., and J. A. Weinman, 1994.

TRMM Monthly Combined Accumulated Rainfall and Vertical Structure Product Summary

Coverage: Day and night, 40°N to 40°S

Spatial/Temporal Characteristics: 5° × 5°, 14 levels, monthly

Key Geophysical Parameters: Surface rainfall and hydrometeor profiles

Processing Level: 3

Product Type: Standard, at-launch

Maximum File Size: 500 KB

File Frequency: 1/month

Primary Data Format: HDF

Browse Available: Yes

Additional Product Information:
trmm.gsfc.nasa.gov
tsdis.gsfc.nasa.gov

DAAC: Goddard Space Flight Center Earth Sciences DAAC, daac.gsfc.nasa.gov

Science Team Contact: E. Smith

TRMM 1° Daily Combined Rainfall (TRMM 3B-42) and Monthly Combined Instrument Rainfall (TRMM 3B-43)

Product Description

This pair of products implements the "flying rain gauge" aspect of TRMM by calibrating other precipitation estimates with the "best" TRMM estimate of precipitation to provide improved rainfall estimates on finer scales than TRMM can provide by itself. The TRMM 1° Daily Combined Rainfall (3B-42) product uses TRMM estimates of surface rain and hydrometeor structure to calibrate and adjust rain estimates made from geosynchronous infrared observations. The Monthly Combined Instrument Rainfall (3B-43) product combines 3B-42 with rain gauge analyses (where available) to objectively determine the best estimate of rainfall on the space and time scales indicated. This includes adjustments for bias between the satellite and gauge fields, where feasible, and objective combination based on the random errors estimated for each field. Each product has an associated field of estimated random error that reflects the local sampling of the various input fields and the reliability of each data source.

Research and Applications

Surface rainfall in many parts of the world is very poorly documented on the time and space scales that these products provide. These products provide considerably more detail for validation of numerical weather and climate predictions, accumulations into seasonal-scale climatologies, and input to surface hydrology models. Also, these products provide systematic insight into the accuracy of the independent input fields, both regionally and seasonally, which motivates fresh research to improve the precipitation estimation process.

Relationship to Other TRMM Products

The Surface Rainfall and Vertical Structure (2B-31), and consequently all of the products antecedent to 2B-31, is key to making 3B-42 (and hence 3B-43) as accurate as possible. The TRMM VIRS 11-μm temperatures (1B-01) provide key data in the calibration step of 3B-42. The TRMM Daily and Monthly Rainfall products provide finer space and time scales than pure TRMM products, but at the expense of depending on data sources outside TRMM.

Data Set Evolution

The analysis procedures for 3B-42 and 3B-43 were developed for rainfall estimates from the SSM/I, which has flown on selected Defense Meteorological Satellite Program (DMSP) polar-orbiting platforms since mid-1987. The TRMM versions of both procedures are third-generation code; further development is expected as researchers gain experience with the new data sources.

Suggested Reading

Adler, R. F. *et al*., 1994.

Adler, R. F. *et al*., 2000.

Huffman, G. J. *et al*., 1995.

Huffman, G. J. *et al*., 1997a,b.

TRMM 1° Daily Combined Rainfall and Monthly Combined Instrument Rainfall Product Summary

Coverage: Day and night, 40°N to 40°S

Spatial/Temporal Characteristics: 1° × 1°; daily (3B-42), monthly (3B-43)

Key Geophysical Parameters: Surface rainfall

Processing Level: 3

Product Type: Standard, at-launch

Maximum File Size: 150 KB (3B-42), 250 KB (3B-43)

File Frequency: 1/day (3B-42), 1/month (3B-43)

Primary Data Format: HDF

Browse Available: Yes

Additional Product Information:
trmm.gsfc.nasa.gov
tsdis.gsfc.nasa.gov

DAAC: Goddard Space Flight Center Earth Sciences DAAC, daac.gsfc.nasa.gov

Science Team Contact: R. Adler

TRMM Instantaneous Radar Site Rain Map (TRMM 2A-53)

Product Description

The Level 2A ground validation Radar Site Rain Map (2A-53) product contains instantaneous (highest temporal, 2-km horizontal resolution) rainmaps produced from the 1C-51 reflectivity fields. These require application of an appropriate reflectivity (Z) to rain (R) transformation, determined separately for each site on the basis of rain gauge, radar, and raindrop size information.

Research and Applications

This product is used to determine the intensity, duration, and spatial extent of rain-producing systems at each ground validation site.

Relationship to Other TRMM Products

This product is necessary to validate instantaneous rainfall retrievals derived from measurements by instruments on the TRMM satellite (2A-12, 2A-25, 2B-31).

Data Set Evolution

Rainfall estimations from surface-based radar observations have been used operationally for several decades in short-term forecasting and for hydrological purposes. Recent upgrades to the operational systems and rainfall algorithms are used in the TRMM Ground Validation Program.

Suggested Reading

Krajewski, W. F., 1987.

Rosenfeld, D. *et al.*, 1994.

Steiner, M. *et al.*, 1995.

TRMM Instantaneous Radar Site Rain Map Product Summary

Coverage: 150-km radius of ground validation radar, continuous

Spatial/Temporal Characteristics: 2 km (minimum)

Key Geophysical Parameters: Surface rainfall

Processing Level: 2A

Product Type: Validation, at-launch

Maximum File Size: 2 MB

File Frequency: 1/hour

Primary Data Format: HDF

Browse Available: Yes

Additional Product Information:
trmm.gsfc.nasa.gov
tsdis.gsfc.nasa.gov

DAAC: Goddard Space Flight Center Earth Sciences DAAC, daac.gsfc.nasa.gov

Science Team Contact: R. Houze

TRMM Instantaneous Radar Site Convective/Stratiform Map (TRMM 2A-54)

Product Description

The Level 2A ground validation Radar Site Convective/Stratiform Map identifies rainfall from TRMM 2A-53 as occurring from either convective- or stratiform-type clouds and generated from the reflectivity product 1C-51.

Research and Applications

Characterization of precipitation types as stratiform or convective is essential for determining the vertical profile of heating associated with these two major classifications. Classification methods include information on the vertical and horizontal structure of reflectivity fields.

Relationship to Other TRMM Products

Product 2A-54 is used to validate the convective/stratiform separation derived by the PR algorithm 2A-23. The convective stratiform classification map performs as input to 3A-55 to be used in evaluation of the vertical heating profile, which is of interest to large-scale models for initialization and validation studies.

Data Set Evolution

Convective/stratiform classification methods have been developed for use in studies of the structure, dynamics, and evolution of tropical mesoscale convective systems.

Suggested Reading

Churchill, D. D., and R. A. Houze, Jr., 1984.

Houze, R. A. Jr., 1989.

Rosenfeld, D. *et al*., 1995.

Steiner, M. *et al*., 1995.

TRMM Instantaneous Radar Site Convective/Stratiform Map Product Summary

Coverage: 150-km radius of ground validation radar, continuous

Spatial/Temporal Characteristics: 2 km (minimum)

Key Geophysical Parameters: Surface rainfall

Processing Level: 2A

Product Type: Validation, at-launch

Maximum File Size: 1 MB

File Frequency: 1/hour

Primary Data Format: HDF

Browse Available: Yes

Additional Product Information:
trmm.gsfc.nasa.gov
tsdis.gsfc.nasa.gov

DAAC: Goddard Space Flight Center Earth Sciences DAAC, daac.gsfc.nasa.gov

Science Team Contact: R. Houze

TRMM Instantaneous Radar Site 3-D Reflectivities (TRMM 2A-55)

Product Description

The Level 2A ground validation Radar Site 3-D Reflectivity (2A-55) product contains instantaneous (highest temporal, 2-km horizontal resolution) 3-D Cartesian-gridded reflectivities, interpolated from volume-scan reflectivities (1C-51). The origin and outer boundaries of the 3-D Cartesian grid are determined by the TRMM Ground Validation Team. In addition to the 3-D gridded reflectivity data, this product includes vertical profiles of the mean reflectivity and the frequency distribution at each height. The frequency distribution is provided in the form of contoured frequency by altitude diagrams (CFADs). Vertical profiles and CFADs are provided for the following categories: total, total-land, total-ocean, total-convective, total-stratiform, total-anvil, land-convective, land-stratiform, land-anvil, ocean-convective, ocean-stratiform, and ocean-anvil.

Research and Applications

The 3-D structure of radar reflectivity is determined by hydrometeor distributions within cloud systems and is indicative of both microphysical and dynamical processes within such systems. The reflectivity structure can be used to simulate satellite observations of precipitating cloud systems, given assumptions about the hydrometeor distributions.

Relationship to Other TRMM Products

This product is used to validate the vertical hydrometeor and latent heating retrievals of the TMI (2A-12), PR (2A-25), and combined product (2B-31) vertical hydrometeor and latent heating retrievals.

Data Set Evolution

Pre-operational tests within TSDIS began in August 1995 and continued until the launch of TRMM in November 1997.

Suggested Reading

Yuter, S. E., and R. A. Houze, Jr., 1995.

TRMM Instantaneous Radar Site 3-D Reflectivities Product Summary

Coverage: 150-km radius of ground validation radar, continuous

Spatial/Temporal Characteristics: 2 km horizontal (minimum), 1.5 km vertical (minimum)

Key Geophysical Parameters: 3-D reflectivity

Processing Level: 2A

Product Type: Validation, at-launch

Maximum File Size: 19 MB

File Frequency: 1/hour

Primary Data Format: HDF

Browse Available: Yes

Additional Product Information:
trmm.gsfc.nasa.gov
tsdis.gsfc.nasa.gov

DAAC: Goddard Space Flight Center Earth Sciences DAAC, daac.gsfc.nasa.gov

Science Team Contact: R. Houze

TRMM 5-Day Site Rain Map (TRMM 3A-53)

Product Description

5-day, 2 km × 2 km surface rainfall at site.

Research and Applications

Significant variations in tropical rainfall patterns have been found to occur at periods longer than 5 days. These patterns frequently have large-scale structure and persistence that could be useful for weather prediction and validation of general circulation models.

Relationship to Other TRMM Products

Although TRMM sampling by itself is not sufficient to accurately represent 5-day rainfall totals, supplementary observations of proxy rainfall data observed continuously by other satellites can be calibrated regionally by the validation product to globally map and monitor variations in rainfall patterns occurring at periods in the range of weeks to a month or two. Directly, this product will validate the estimates for the TRMM and other satellite algorithms (3B-42 and 3B-43).

Suggested Reading

Huffman, G. J. *et al.*, 1995.

Rosenfeld, D. *et al.*, 1994.

Steiner, M. *et al.*, 1995.

TRMM 5-Day Site Rain Map Product Summary

Coverage: 150-km radius of ground validation radar, continuous

Spatial/Temporal Characteristics: 5-day accumulations, 2 × 2 km

Key Geophysical Parameters: Surface rainfall

Processing Level: 3

Product Type: Validation, at-launch

Maximum File Size: 500 KB

File Frequency: 1/5 days

Primary Data Format: HDF

Browse Available: Yes

Additional Product Information:
trmm.gsfc.nasa.gov
tsdis.gsfc.nasa.gov

DAAC: Goddard Space Flight Center Earth Sciences DAAC, daac.gsfc.nasa.gov

Science Team Contact: R. Houze

TRMM 30-Day Site Rain Map (TRMM 3A-54)

Product Description

30-day, 2 km × 2 km surface rainfall at site.

Research and Applications

This product is used to validate the satellite algorithms and to provide independent validation to climate and forecast models.

Relationship to Other TRMM Products

This product is the principal means of validating all the TRMM monthly 5° × 5° rainfall estimates.

Suggested Reading

Huffman, G. J. *et al*., 1995.

Rosenfeld, D. *et al*., 1994.

Steiner, M. *et al*., 1995.

TRMM 30-Day Site Rain Map Product Summary

Coverage: 150-km radius of ground validation radar, continuous

Spatial/Temporal Characteristics: 30-day accumulations, 2 × 2 km

Key Geophysical Parameters: Rain vertical structure and latent heating

Processing Level: 3

Product Type: Validation, at-launch

Maximum File Size: 500 KB

File Frequency: 1 per month

Primary Data Format: HDF

Browse Available: Yes

Additional Product Information:
trmm.gsfc.nasa.gov
tsdis.gsfc.nasa.gov

DAAC: Goddard Space Flight Center Earth Sciences DAAC, daac.gsfc.nasa.gov

Science Team Contact: R. Houze

TRMM Monthly 3-D Structure (TRMM 3A-55)

Product Description

This product contains vertical profiles of the mean reflectivity and the frequency distribution at each height. The frequency distribution is provided in the form of contoured frequency by altitude diagrams (CFADs). Vertical profiles and CFADs are provided for the following categories: total, total-land, total-ocean, total-convective, total-stratiform, total-anvil, land-convective, land-stratiform, land-anvil, ocean-convective, ocean-stratiform, and ocean-anvil.

Research and Applications

The 3-D structure of radar reflectivity is determined by hydrometeor distributions within cloud systems and is indicative of both microphysical and dynamical processes within such systems. The reflectivity structure can be used to simulate satellite observations of precipitating cloud systems, given assumptions about the hydrometeor distributions.

Relationship to Other TRMM Products

This product is necessary to cross-check the vertical structure retrieved by TRMM satellite instruments (3A-25, 3A-26, 3B-31).

Suggested Reading

Keenan, T. D. *et al*., 1988.

Yuter, S. E., and R. A. Houze, Jr., 1995.

TRMM Monthly 3-D Structure Product Summary

Coverage: 150-km radius of ground validation radar, continuous

Spatial/Temporal Characteristics: 30-day accumulations, 2 × 2 km

Key Geophysical Parameters: 3-D reflectivity

Processing Level: 3

Product Type: Validation, at-launch

Maximum File Size: 400 KB

File Frequency: 1/month

Primary Data Format: HDF

Browse Available: Yes

Additional Product Information:
trmm.gsfc.nasa.gov
tsdis.gsfc.nasa.gov

DAAC: Goddard Space Flight Center Earth Sciences DAAC, daac.gsfc.nasa.gov

Science Team Contact: R. Houze

MODIS Total Precipitable Water (MOD05)

Product Description

The MODIS Precipitable Water product (MOD05) consists of column water-vapor amounts. During the daytime, a near-infrared algorithm is applied over clear land areas of the globe and above clouds over both land and ocean. Over clear ocean areas, water-vapor estimates are provided over the extended glint area. An infrared algorithm for deriving atmospheric profiles is also applied both day and night for Level 2.

The Level 2 data are generated at the 1-km spatial resolution of the MODIS instrument using the near-infrared algorithm during the day, and at 5 × 5 1-km pixel resolution both day and night using the infrared algorithm when at least five FOVs are cloud free. The infrared-derived precipitable water vapor is generated as one component of product MOD07, and simply added to product MOD05 for convenience.

The solar retrieval algorithm relies on observations of water-vapor attenuation of reflected solar radiation in the near-infrared MODIS bands so that the product is produced only over areas where there is a reflective surface in the near IR.

Research and Applications

The near-infrared total-column precipitable water is very sensitive to boundary-layer water vapor since it is derived from attenuation of reflected solar light from the surface. This data product is essential to understanding the hydrological cycle, aerosol properties, aerosol-cloud interactions, energy budget, and climate. Of particular interest is the collection of water-vapor data above cirrus cloudiness, which has important applications to climate studies. MODIS also provides finer horizontal-scale atmospheric water-vapor gradient estimates than are available from the Polar-orbiting Operational Environmental Satellites (POES).

Data Set Evolution

The near-IR column water-vapor parameter is derived from the attenuation by water vapor of near-IR solar radiation. Techniques employing ratios of water-vapor-absorbing bands 17, 18, and 19 with the atmospheric window bands 2 and 5. The ratios remove largely the effects of variation of surface reflectance with wavelength and result in the atmospheric water-vapor transmittances. The column-water-vapor amounts are derived from the transmittances based on theoretical radiative-transfer calculations and using look-up-table procedures. MODIS is the first space instrument to use near-IR bands together with the traditional IR bands to retrieve total precipitable water. Experience in this retrieval is based on the AVIRIS instrument aboard the NASA ER-2 aircraft. Atmospheric water vapor is determined with an accuracy of 5-10%.

The thermal column water-vapor parameter is derived by integrating the moisture profile through the atmospheric column. Other, split-window, methods also exist. This class of techniques uses the difference in water-vapor absorption that exists between channel 31 (11 μm) and channel 32 (12 μm).

Data validation is conducted by comparing these data with water-vapor measurements from the National Weather Service (NWS) radiosonde network, from ground-based upward-looking microwave radiometers, from a ground-based GPS network, and from a ground-based sunphotometer network. Quality control is performed in two dimensions. The first is comparisons of specific validation sites across as many different climatic and geographic regions as possible. The second is a statistical analysis of the entire data set.

The related MODIS Precipitable Water ATBDs can be found in PDF format at eos.nasa.gov/atbd/modistables.html.

Suggested Reading

Gao, B. C., and A. F. H. Goetz, 1990.

Gao, B. C., and Y. J. Kaufman, 2003.

Green, R. O., and J. E. Conel, 1995.

Jedlovec, G. J., 1987.

Kaufman, Y. J., and B. C. Gao, 1992.

King, M. D. *et al*., 1992.

King, M. D. *et al*., 2003.

Kleepsies, T. J., and L. M. McMillan, 1984.

MODIS Total Precipitable Water Summary

Coverage: Global

Spatial/Temporal Characteristics: Varies with retrieval technique; 1 km near-infrared daylight only, and 5 km infrared day and night

Key Science Applications: Hydrological cycle climatology, effect on aerosol and clouds, atmospheric correction, characterization of the atmosphere

Key Geophysical Parameters: Atmospheric total column water vapor

Processing Level: 2

Product Type: Standard, at-launch

Maximum File Size: 20.15 MB (daytime granules), 3.56 MB (nighttime granules)

File Frequency: 288/day

Primary Data Format: HDF-EOS

Browse Available: modis-atmos.gsfc.nasa.gov/MOD08_D3/browse.html

Additional Product Information: modis-atmos.gsfc.nasa.gov/MOD05_L2/index.html

DAAC: Goddard Space Flight Center Earth Sciences DAAC, daac.gsfc.nasa.gov

Science Team Contacts: B. C. Gao, Y. J. Kaufman, D. Tanré, W. P. Menzel

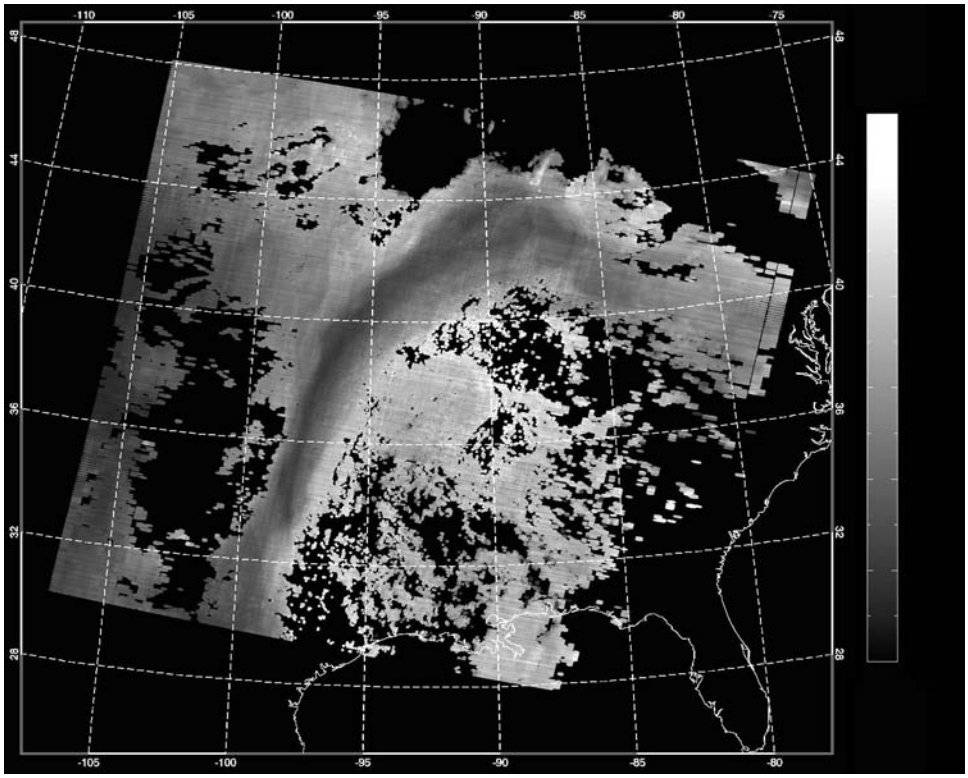

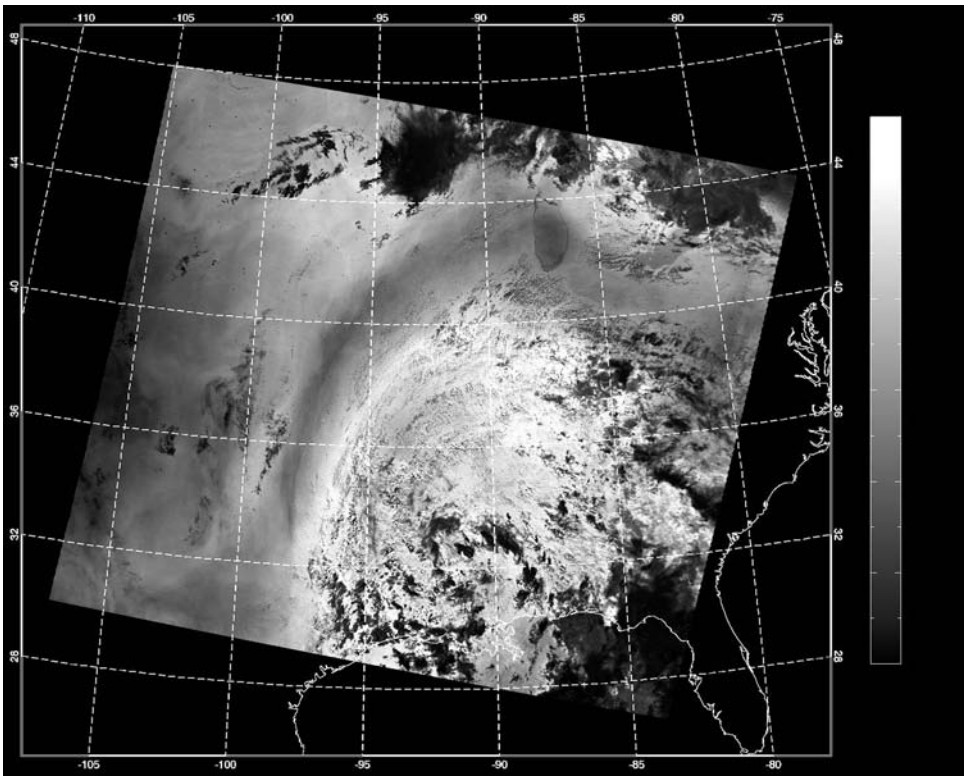

Water vapor over the eastern United States on June 24, 2002. The image at top shows total precipitable water (in cm) derived from the cloud-free pixels over land using the near-infrared algorithm. The bottom image shows total precipitable water (in cm) derived from the thermal infrared algorithm. On the internet, visit visibleearth.nasa.gov to view a variety of MODIS data images.

MODIS Atmospheric Profiles (MOD07)

Product Description

The MODIS Atmospheric Profiles product (MOD07) consists of several parameters: they are total-ozone burden, atmospheric stability, temperature and moisture profiles, and atmospheric water vapor. All of these parameters are produced day and night for Level 2 at 5 × 5 1-km pixel resolution when at least 5 FOVs are cloud free.

The MODIS total-ozone burden is an estimate of the total-column tropospheric and stratospheric ozone content. The MODIS atmospheric stability consists of three daily Level 2 atmospheric stability indices. The Total Totals (TT), the Lifted Index (LI), and the K index (K) are each computed using the infrared temperature- and moisture-profile data, also derived as part of MOD07. The MODIS temperature and moisture profiles are produced at 20 vertical levels. A statistical regression algorithm based on the infrared radiative-transfer equation in a cloudless sky is used. The MODIS atmospheric water-vapor product is an estimate of the total tropospheric column water vapor made from integrated MODIS infrared retrievals of atmospheric moisture profiles in clear scenes.

Research and Applications

Total-column ozone estimates at MODIS resolution are required by MODIS investigators developing atmospheric correction algorithms. This information is crucial for accurate land and ocean-surface-parameter retrievals. Furthermore, strong correlations have been found to exist between the meridional gradient of total ozone and the wind velocity at tropopause levels, providing the potential to predict the position and intensity of jet streams. Total-column ozone monitoring is also important due to the potential harm to the environment caused by anthropogenic depletion of ozone.

Atmospheric instability measurements are predictors of convective-cloud formation and precipitation. The MODIS instrument offers an opportunity to characterize gradients of atmospheric stability at high resolution and greater coverage. Radiosonde-derived stability indices are limited by the coarse spacing of the point-source data, too large to pinpoint local regions of probable convection.

Atmospheric temperature and moisture sounding data at high spatial resolution from MODIS and high-spectral-resolution sounding data from AIRS (flying onboard Aqua, launched May 4, 2002) provide a wealth of new information on atmospheric structure in clear skies. The profiles are used to correct for atmospheric effects for some of the MODIS products (e.g., sea-surface and land-surface temperatures, ocean aerosol properties, water-leaving radiances, and photosynthetically-active radiation) as well as to characterize the atmosphere for global greenhouse studies.

Total-column precipitable-water estimates at MODIS resolution are required by MODIS investigators developing atmospheric-correction algorithms. This information is crucial for accurate land and ocean surface-parameter retrievals. MODIS also provides finer horizontal-scale atmospheric water-vapor gradient estimates than are available from the POES satellites.

Data Set Evolution

Temperature and moisture profile retrieval algorithms are adapted from the International TOVS Processing Package (ITPP), taking into account MODIS' lack of stratospheric channels and far higher horizontal resolution. The algorithm uses a statistical regression using synthetic radiances derived from a global radiosonde data base. The profile retrieval algorithm requires calibrated, navigated, and coregistered 1-km FOV radiances from MODIS bands with wavelengths between 4.47 μm (band 24), and 14.24 μm (band 36). The MODIS cloud-mask product (MOD35) is used for cloud screening. The algorithm requires NCEP model analysis of surface pressure.

Atmospheric water vapor, or precipitable water, is determined by integrating the moisture profile through the atmospheric column. Atmospheric stability estimates are derived from the MODIS temperature and moisture retrievals contained in this product. Layer temperature and moisture values are used to estimate the temperature lapse rate of the lower troposphere and the low-level moisture concentration.

A statistical regression algorithm is used for the MODIS total ozone retrieval. Global ozone soundings from ozone sondes and SBUV profiles are used for training, and an empirical regression of calculated MODIS spectral band radiances against ozone mixing ratio profiles is created for the retrieval.

Data validation is conducted by comparing results to *in situ* radiosonde measurements, NOAA HIRS and GOES sounder operational retrievals, NCEP analyses, and retrievals from the AIRS/AMSU-A/HSB instrument package on the Aqua platform. Comparisons are made with ground-based measurements at the Atmospheric Radiation Measurement-Cloud and

Radiation Testbeds (ARM-CART) at Oklahoma, Alaska, and the Tropical Western Pacific. A field campaign using a profiler network in the central U.S. and an aircraft equipped with the MODIS Airborne Simulator (MAS) was initiated in the first year after launch and continues to be active.

Suggested Reading

Hayden, C. M., 1988.

King, M. D. *et al*., 2003.

Li, J. *et al*., 2000.

Li, J. *et al*., 2001.

Li, J., and H. L. Huang, 1999.

Prabhakara, C. *et al*., 1970.

Seemann, S. W. *et al*., 2003.

Smith, W. L., and F. X. Zhou, 1982.

Smith, W. L. *et al*., 1985.

Sullivan, J. *et al*., 1993.

MODIS Atmospheric Profiles Summary

Coverage: Global, clear-sky only

Spatial/Temporal Characteristics: 5 km

Key Science Applications:

- Ozone: atmospheric correction, prediction of cyclogenesis, anthropogenic ozone depletion
- Atmospheric stability: atmospheric correction, prediction of convective cloudiness and precipitation, characterization of the atmosphere
- Soundings: atmospheric correction algorithm development and use, characterization of the atmosphere
- Total-column water vapor: atmospheric- correction algorithm development and use, characterization of the atmosphere

Key Geophysical Parameters: Total-column ozone, atmospheric stability (Total Totals, Lifted Index, and K index), atmospheric profiles of temperature and moisture, atmospheric total-column water vapor

Processing Level: 2

Product Type: Standard, at-launch

Maximum File Size: 32.2 MB

File Frequency: 288/day

Primary Data Format: HDF-EOS

Browse Available: modis-atmos.gsfc.nasa.gov/MOD07_L2/sample.html

Additional Product Information: modis-atmos.gsfc.nasa.gov/MOD07_L2/index.html

DAAC: Goddard Space Flight Center Earth Sciences DAAC, daac.gsfc.nasa.gov

Science Team Contact: W. P. Menzel

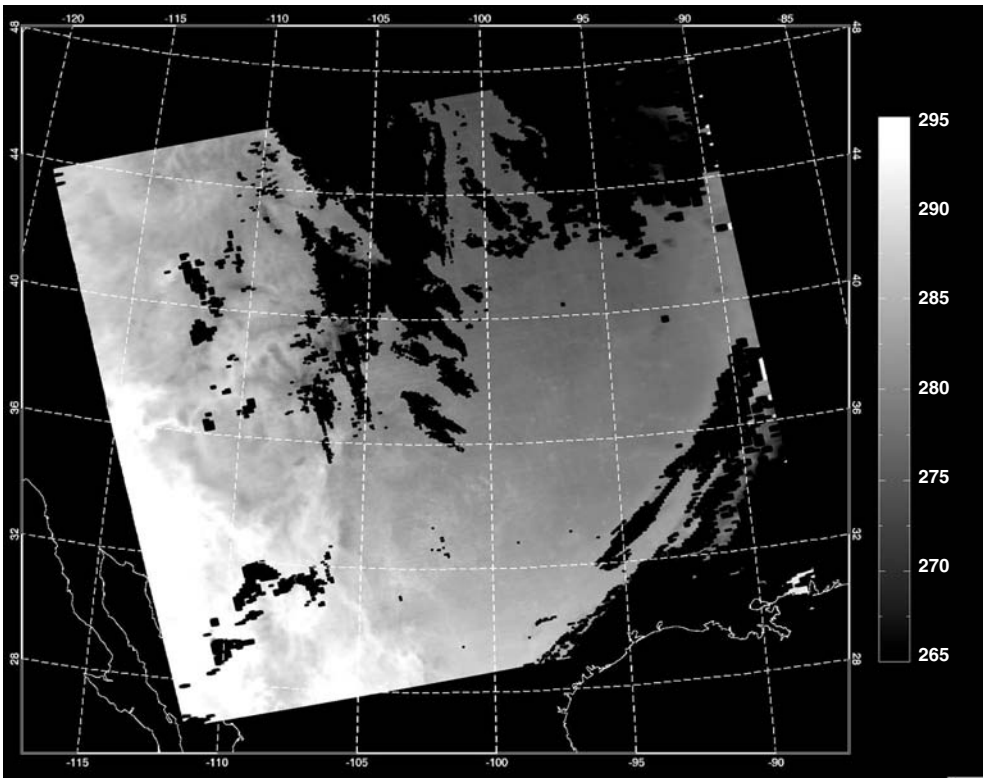

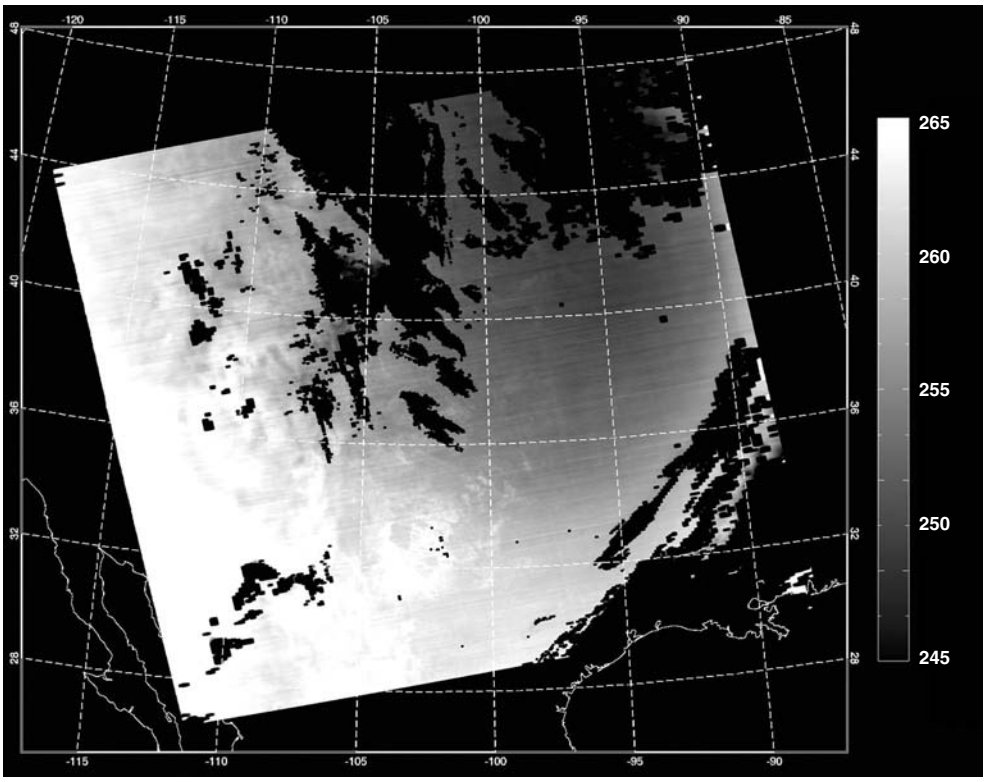

Atmospheric temperatures retrieved from Terra-MODIS radiances on May 22, 2001 at 850 hPa (top image) and 500 hPa (bottom image) in K. On the internet, visit visibleearth.gsfc.nasa.gov to view a variety of MODIS data images.

Chapter 6

Cloud and Aerosol Properties and Radiative Energy Fluxes

TRMM
CERES

Terra
ASTER
CERES
MISR
MODIS

Cloud and Aerosol Properties and Radiative Energy Fluxes – An Overview

Relationship to Global Change

The flow of energy to and from the Earth is modulated by clouds and aerosols. As such, measuring and understanding these elements is key to predicting climate change and to testing global climate models. The technology for accurately measuring radiative fluxes, cloud properties, and aerosol properties from space has advanced to the point that these observations can be used to greatly advance our ability to address critical global change issues. For example, if the global climate changes, do clouds act to result in a positive or negative feedback? Do aerosols offset some of the expected warming due to the increase in greenhouse gases? The products described below provide key global observations needed to explore these questions.

Clouds: A key step in measuring cloud properties from space is to determine where clouds exist, how they are distributed through the atmosphere, and what their dimensions are. Once clouds are identified and mapped, cloud properties, such as effective particle size, thermodynamic phase (water, ice), cloud top properties, and optical thickness (which all help determine how much radiation passes through them), may be measured. The MODIS, MISR, and ASTER instruments on the Terra satellite and the VIRS instrument on TRMM provide these key cloud measurements. The daily observations provided by these instruments also provide the sampling needed to drive and verify climate models.

Aerosols: The measurement of aerosols, suspended particles in the atmosphere (e.g., dust, sulfate, smoke, etc.), is an important element in describing energy transmission through the atmosphere. Aerosols are a significant source of uncertainty in climate modeling because they affect cloud microphysics by acting as condensation nuclei, thereby affecting cloud radiative properties, the hydrological cycle and atmospheric dynamics. They also interact directly with solar radiation, thus affecting the radiative balance. The location of anthropogenic aerosols is also an important consideration in their impact on climate. Aerosol products described here, derived from MODIS and MISR on Terra, provide new information on aerosol formation, distribution, and sinks over both the land and ocean.

Radiation: The flow of radiation from the Sun to the Earth, its absorption, reflection, and emission, determines the energy balance of the Earth, and hence the nature of the life of its inhabitants. The information from products describing optical and physical properties of clouds and aerosols is combined with broadband radiation measurements from CERES to provide estimates of solar and infrared radiative fluxes, and the associated heating and cooling of the Earth and the atmosphere. The radiation estimates needed to do this are both shortwave and longwave fluxes at the surface and at the top of the atmosphere, both downwelling and upwelling, so that the net flow can be determined.

Product Overview

The physical quantities that must be measured for the cloud, aerosol, and radiation categories are discussed in the previous section. In this section we relate the data products to these measurement needs and explain how the product groups support the overall global change program. An evolutionary approach to product generation for the CERES cloud and radiation products was used to implement a progression from ERBE to CERES algorithms. The ERBE program has produced a 14-year record of cloud and radiation budget information and CERES continues with these measurements.

Six months after the Terra launch (following instrument and analysis validation) CERES began production of ERBE-Like data products. These TOA fluxes use the ERBE analysis algorithms to allow consistent comparisons to historical ERBE data. The first 24 months after launch were used to develop a new set of CERES angular distribution models (ADMs). These ADMs are used to convert broadband CERES radiances (i.e., radiative energy at a single viewing direction) into estimates of broadband hemispheric fluxes. The CERES rotating-azimuth-plane scan mode was used along with the cloud properties derived using VIRS for CERES/TRMM measurements and MODIS for CERES/Terra measurements to derive a new and much more accurate set of ADMs. Beginning 24 months after launch, these more accurate CERES estimated TOA fluxes were produced in addition to the ERBE-Like data. Finally, starting 30 months after launch, CERES routinely provides

estimates of radiative fluxes at the surface and at a selected number of levels within the atmosphere. The number of atmospheric levels depends on the accuracies determined during post-launch validation.

All the CERES products except the ERBE-like products are classed as "post-launch" for the reasons discussed above. The MODIS, MISR, and ASTER products are "at-launch" except for the gridded MISR products (MIS07, MIS08) and AST13. The following section discusses how these products satisfy the measurement needs in the three categories: cloud products, aerosol properties, and radiant energy flux products.

The *cloud products* provide the parameters needed to determine how much solar radiation reaches the Earth and how much escapes back to space. The parameters also supply information on factors that influence cloud formation and forces driving circulation and global climate. The cloud products fall into two classes: 1) cloud detection and delineation, and 2) cloud property retrieval. Cloud detection and delineation produces masks indicating where clouds exist and information on layering and overlap to give a geometric picture of global cloud coverage. Cloud property retrieval quantifies the physics of the cloud by means of parameters such as optical thickness, temperature, liquid water content, ice water content, particle radius, cloud top altitude, and phase, which all relate to the radiative transmission, reflection, and emission of the cloud.

The CERES cloud detection process uses either TRMM VIRS or Terra MODIS observations to produce a global binary mask indicating the presence or absence of a cloud in each pixel. The MISR cloud products provide along-track directional reflectance measurements of clouds that will enable development of bidirectional models for different cloud types, especially for horizontally inhomogeneous cloud fields. Stereo matching of MISR multi-angle imagery enables cloud top elevations to be obtained. These parameters are provided in products MIS04 and MIS07. The ASTER cloud product (AST13) also provides stereo views of cloud cover, which complement the MISR data and will permit cloud top elevation estimation. The major advantage of the ASTER cloud product is the high spatial resolution that allows the study of individual cloud cells. The disadvantage is very limited spatial and time coverage. The ASTER products are also tuned to the difficult polar cloud detection task, which will include the detection of water clouds and ice clouds. The MODIS cloud mask (MOD35) is a global product that provides a probability that a view of the Earth is obstructed by cloud and whether cloud shadow is detected. It also provides information on the processing path taken by the algorithm (land/sea, day/night, etc.), along with individual spectral test results used in the determination of the final cloud mask product.

Cloud physical properties are obtained using a set of algorithms operating on multispectral imagery data from multiple sources including MODIS or VIRS. CERES cloud properties include cloud layer mapping, cloud top and cloud base pressure, infrared emissivity, liquid water path, particle radius, and cloud overlap, all derived from MODIS or VIRS data and remapped onto the broadband CERES fields of view for studies of the Earth's atmosphere energy distribution. The MODIS cloud property parameters include particle size and phase, optical thickness, cloud top height, emissivity and temperature, and cloud fraction in a region, all of which support specific MODIS science tasks that complement the radiation studies and products from other instruments.

Aerosol Properties are provided by MODIS (MOD04) and MISR (MIS05). Aerosols must be accounted for during the retrieval of surface and atmospheric parameters. The MODIS aerosol products document one of the most elusive and least understood radiatively active components of the atmosphere by providing information on aerosol optical thickness, aerosol size distribution, and aerosol sources and sinks. MISR provides aerosol information on absorption and scattering in the lower atmosphere that aids in the understanding of how sunlight is absorbed by aerosols, determining global aerosol budgets, and improving correction for aerosol effects in the retrieval of surface parameters.

The *Radiant Energy Flux Products* provide estimates of the radiative flux downward and upward at the top-of-atmosphere, at the Earth's surface, and at selected intermediate altitudes, as well as the net flux, which is used to determine the radiation budget. This budget determines the overall heating and cooling of the atmosphere and Earth's surface and subsequent changes in climate. These parameters are generated from CERES data and from the final averaged flux and radiation budget products AVG, ZAVG and CRH. The radiation algorithms use the cloud and aerosol products in the process of determining how much solar radiation is transmitted, reflected, and absorbed in the cloud/atmosphere/Earth surface system, and are thus critical to the success of the global climate monitoring task.

Product Interdependency and Continuity with Heritage Data

The products from these instruments, especially the cloud products from MODIS, CERES, MISR, and ASTER, are interrelated on a number of levels. First, many algorithms require output products from other instruments as ancillary input data. For example, CERES cloud parameters (SSF) require MODIS and VIRS ancillary radiances such as the cloud products (MOD06) and microwave water path (MWP). MISR aerosol optical depth products require MODIS input. The MODIS cloud mask may be used in the viewing decisions of high-resolution instruments like ASTER. In many cases, output data from one instrument become input data for another. This permits the formatting necessary to permit the generation of higher-level products, and does not represent a duplication of data products.

Second, surface-viewing instruments use ancillary data in atmospheric correction algorithms to reduce contamination of surface retrievals. Similar products from different instruments may use different algorithms and are useful for mutual comparison and validation. Finally, a degree of redundancy for principal (especially cloud) products used as ancillary input is necessary to permit alternative sources of ancillary data in the event of instrument failure or degradation.

The CERES instruments on TRMM, Terra, and Aqua are a continuation of the ERBE project, extending a heritage of radiation budget products dating back more than a decade. Several CERES data products use ERBE algorithms to ensure continuity. As with other EOS-era missions, the data sets produced by continuing past missions will provide valuable information on long-term trends. Analysis of the trends will provide valuable input to long-term predictive models, and will enable scientists to interpret better the possible causes or consequences of changes to clouds, aerosols, and radiation budget on global climate change.

Suggested Reading

Ackerman, S. A. *et al*., 1998.

Kaufmann, Y. J. *et al*., 2002.

King, M. D. *et al*., 1992.

King, M. D. *et al*., 1997.

King, M. D. *et al*., 2003.

Kummerow, C. *et al*., 1998.

Kummerow, C. *et al*., 2000.

Platnick, S. *et al*., 2003.

Wielicki, B. A. *et al*., 1995.

Wielicki, B. A. *et al*., 2002.

ASTER Polar Surface and Cloud Classification Product (AST13)

Product Description

This Level 4 product is a polar classification map, consisting of the following classes: water, wet/slush ice, snow/ice, land, shadow, water cloud, and ice cloud. Each pixel is classified using a bit map for each of the above classes. Therefore, for complex scenes such as cirrus over broken sea ice, the water, ice, and ice cloud bits would be set. This product is produced at 30-m spatial resolution and uses a combination of visible, near-infrared, and infrared channels. The polar regions are defined as all land and water regions lying poleward of 60°N or 60°S. Both daytime and nighttime classifications are available, with the daytime algorithm applied for solar zenith angles less then 85°, and the nighttime algorithm applied in all cases. This is an on-request product.

Research and Applications

Since greenhouse forcings are expected to be amplified in the polar regions, these regions may act as early warning indicators of global climate shifts. Cloud cover can be expected to be altered by greenhouse forcings, and cloud changes are expected to have a significant effect on sea ice conditions and regional ice-albedo feedbacks, especially to the polar heat balance which directly affects surface melting. ASTER polar data will be used to monitor changes in surface conditions, notably temperature, albedo, and sea ice breakup.

Data Set Evolution

This data set builds on work over the past decade with data from Landsat TM, AVIRIS, TIMS, and MAS. The improved spectral coverage, resolution, and radiometric accuracy enable ASTER to provide remotely sensed polar data of unprecedented accuracy.

The ASTER polar data set are also used to validate the global-scale polar data and cloud property retrievals from MODIS. In particular, this data set is used to validate the MODIS cloud optical thickness and effective particle sizes, which directly impact the Earth's radiative budget. Only ASTER has the spatial resolution necessary to fully analyze the cloud 3-D effects.

Suggested Reading

Ebert, E., 1987.

Tovinkere, V. R. *et al*., 1993.

Welch, R. M. *et al*., 1990.

Welch, R. M. *et al*., 1990.

ASTER Polar Surface and Cloud Classification Product Summary

Coverage: Regional (poleward from 60° N or S)

Spatial/Temporal Characteristics: 30 m over 60 km × 60 km scenes

Key Science Applications: Climate modeling, polar heat balance

Key Geophysical Parameters: Polar clouds, thick cloud, thin cloud, shadow, ice, wet ice

Processing Level: 4

Product Type: Standard, on-request

Maximum File Size: 42 MB

File Frequency: On demand

Primary Data Format: HDF-EOS

Browse Available: Yes

Additional Product Information: edcdaac.usgs.gov/aster/asterdataprod.html

DAAC: EDC Land Processes DAAC, edcdaac.usgs.gov

Science Team Contact: R. Welch

CERES ERBE-like Instantaneous TOA Estimates (ES-8)

Product Description

The ERBE-like Instantaneous TOA Estimates (ES-8) product contains 24 hours of instantaneous CERES data for a single scanner instrument. The ES-8 product contains filtered radiances recorded every 0.01 seconds for the total, shortwave (SW), and window (WN) channels and the unfiltered SW, longwave (LW), and WN radiances. The SW and LW radiances at spacecraft altitude are converted to top-of-the-atmosphere (TOA) fluxes with a scene-identification algorithm and Angular Distribution Models (ADMs), which are "like" those used for the Earth Radiation Budget Experiment (ERBE). The TOA fluxes, scene identification, and angular geometry are included in the ES-8 product.

A complete listing of parameters for this data product can be found in the CERES Data Products Catalog at asd-www.larc.nasa.gov/DPC/DPC.html, and detailed definitions of each parameter can be found in the CERES Collection Guide at asd-www.larc.nasa.gov/ceres/collect_guide/list.html.

Research and Applications

This product is a CERES-produced equivalent to the instantaneous fluxes derived from the ERBE scanners on ERBS, NOAA-9, and NOAA-10. ES-8 flux data are directly comparable to ERBE fluxes and thus effectively extend the time series of ERBE flux measurements, allowing global-change experiments to continue using ERBE algorithms without the errors associated with comparing fluxes estimated by two different algorithms. Improved TOA flux-estimation algorithms for CERES (using improved ADMs and VIRS/MODIS cloud identification) are available in the Single-Scanner Footprint (SSF) product. Producing the two versions of TOA fluxes will allow continuity with the previous ERBE data along with improved accuracy of CERES TOA flux data.

Data Set Evolution

The ERBE-like Inversion Subsystem consists of algorithms that convert filtered radiometric measurements to instantaneous flux estimates at the TOA. The basis for this procedure is the ERBE Data Management System, which produced TOA fluxes from the ERBE scanning radiometers. The system consists of algorithms for Spectral Correction, Observed Scene

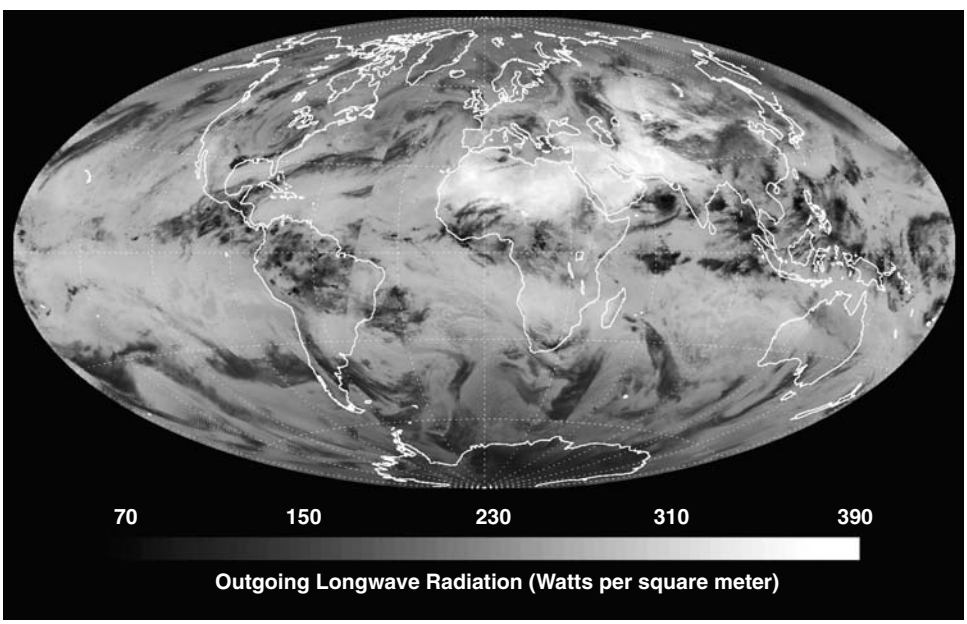

The image above shows thermal emitted longwave flux of energy escaping the top of the Earth's atmosphere as measured by the Terra CERES instrument on May 25, 2001. Radiative flux is the sum of energy emitted by the earth in all angles. Compare to the CERES BDS longwave radiance figure for the same day to show the reduction in orbit banding as directional radiances are converted to radiative fluxes. The ES-8 product contains both thermal emitted energy as well as solar reflected energy to allow studies of the Earth's radiative energy balance at the top of the atmosphere that can be compared with the ERBE experiment data from the 1980s. This is also the earliest validated data product available from each CERES instrument.

Type, Radiance-to-Flux Conversion using Angular Distribution Models, and finally the Regional Averaging algorithm, which produces regional fluxes. A linear-estimation scheme is used to relate the filtered and unfiltered radiances. Ancillary parameter files are required for processing, including ADMs and spectral correction coefficients for converting filtered radiances to unfiltered radiances.

Documentation on the ES-8 algorithms can be found in CERES ATBD Subsystem 2.0, in PDF format, at eospso.gsfc.nasa.gov/atbd/cerestables.html.

Suggested Reading

Avis, L. M. *et al*., 1984.

Barkstrom, B. R., and G. L. Smith, 1986.

Smith, G. L. *et al*., 1986.

Wielicki, B. A. *et al*., 1998.

CERES ERBE-like Instantaneous TOA Estimates Summary

Coverage: Global

Spatial/Temporal Characteristics: 20 km at nadir/0.01 second

Key Geophysical Parameters: TOA SW, LW fluxes and radiances, scene type

Processing Level: 2

Product Type: Standard, at-launch

Maximum File Size: 490 MB

File Frequency: 1/day

Primary Data Format: HDF

Browse Available: No

Additional Product Information: eosweb.larc.nasa.gov/PRODOCS/ceres/table_ceres.html

DAAC: Langley Atmospheric Sciences Data Center, eosweb.larc.nasa.gov

Science Team Contacts: N. G. Loeb, K. J. Priestley

CERES ERBE-like Monthly Regional Averages (ES-9) and ERBE-like Monthly Geographical Averages (ES-4)

Product Description

The ERBE-like Monthly Regional Averages (ES-9) product contains a month of space-and-time-averaged CERES data for a single scanner instrument. The ES-9 product is also produced for combinations of scanner instruments. All instantaneous shortwave and longwave fluxes at the top of the atmosphere (TOA) from the CERES ES-8 product for a month are sorted by 2.5° spatial regions, by day number, and by the local hour of observation. The mean of the instantaneous fluxes for a given region-day-hour bin is determined and recorded in the ES-9 product along with other flux statistics and scene information. For each region, the daily average flux is estimated from an algorithm that uses the available hourly data, scene identification data, and diurnal models. This algorithm is "like" the algorithm used for the Earth Radiation Budget Experiment (ERBE). The ES-9 product also contains hourly average fluxes for the month and an overall monthly average for each region. These average fluxes are given for both clear-sky and total-sky scenes.

The ERBE-like Monthly Geographical Averages (ES-4) product contains a month of space-and-time-averaged CERES data for a single scanner instrument. The ES-4 product is also produced for combinations of scanner instruments. For each observed 2.5-degree spatial region, the daily average, the hourly average over the month, and the overall monthly average of shortwave and longwave fluxes at the TOA from the CERES ES-9 product are spatially nested up from 2.5° regions to 5° and 10° regions, to 2.5°, 5°, and 10° zonal averages, and to global monthly averages. For each nested area, the albedo and net flux are given. For each region, the daily average flux is estimated from an algorithm that uses the available hourly data, scene-identification data, and diurnal models. This algorithm is "like" the algorithm used for the ERBE.

A complete listing of parameters for these data products can be found in the CERES Data Products Catalog at asd-www.larc.nasa.gov/DPC/DPC.html, and detailed definitions of each parameter can be found in the CERES Collection Guide at asd-www.larc.nasa.gov/ceres/collect_guide/list.html.

Research and Applications

These products are designed to provide continuity with the historical ERBE radiation budget data. They use the same algorithms to provide the most consistent possible analysis of changes in radiation budget from the 80s through the EOS era. These products are often used to verify the accuracy and limitations of climate models, especially with respect to the effect of clouds on radiation. These CERES products are some of the earliest available, but lack the accuracy improvements, surface radiative fluxes, atmosphere radiative fluxes, and matching cloud and aerosol information in the more advanced CERES SRBAVG and AVG products.

The ES-9 and ES-4 products are equivalent to their ERBE analogs (S-9, and S-4) and effectively extend the time series of ERBE flux measurements through the EOS era. Various spatial scales are provided to simplify intercomparisons with earlier Nimbus and ERBE non-scanner time series.

Data Set Evolution

These data sets are generated using heritage ERBE algorithms operating on inputs from CERES calibrated Level 1 data and ancillary data. Data processing uses CERES Subsystem 3.0, which temporally interpolates CERES measurements using linear interpolation over oceans and half-sine-curve fit over land and desert regions. Monthly and monthly-hourly means are then computed using the combination of observed and interpolated values.

Documentation on the algorithms used to create the data products can be found in CERES ATBD Subsystem 3.0, in PDF format, at eos.nasa.gov/atbd/cerestables.html.

Suggested Reading

Brooks, D. R. *et al*., 1986.

Harrison, E. F. *et al*., 1990a,b.

Harrison, E. F. *et al*., 1995.

Ramanathan V. *et al*., 1989.

Wielicki, B. A. *et al*., 1998.

CERES ERBE-like Monthly Regional Averages and ERBE-like Monthly Geographical Averages Products Summary

Coverage: Global

Spatial/Temporal Characteristics: 2.5°, 5.0°, 10.0°, region and zone, global/monthly (by day and hour)

Key Geophysical Parameters: TOA shortwave and longwave radiant flux, scene type, albedo, solar incidence, cloud condition

Processing Level: 3

Product Type: Standard, at-launch

Maximum File Size: 27 MB (ES-4), 1100 MB (ES-9)

File Frequency: 1/month

Primary Data Format: HDF

Browse Available: No

Additional Product Information: eosweb.larc.nasa.gov/PRODOCS/ceres/table_ceres.html

DAAC: Langley Atmospheric Sciences Data Center, eosweb.larc.nasa.gov

Science Team Contacts: D. F. Young, T. Wong

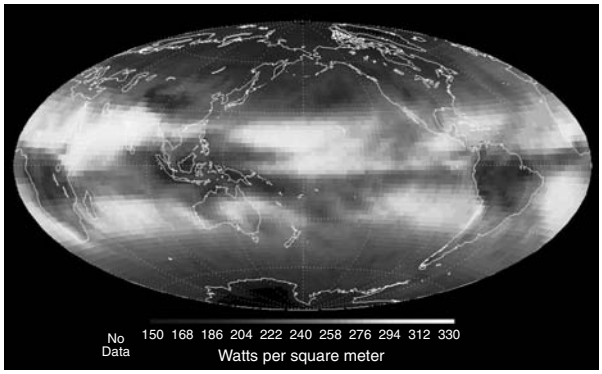

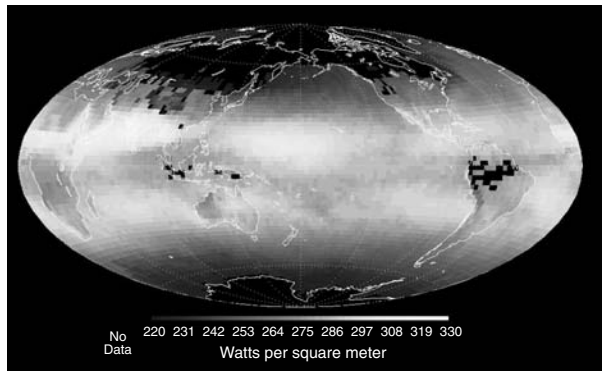

(Left) **Sample CERES ERBE-like Monthly Geographical Averages, presenting the TOA longwave flux for March 2000.** *(Right)* **Sample CERES ERBE-like Monthly Regional Average, presenting the TOA clear-sky longwave flux for March 2000. Both images are from data from the Terra CERES. On the internet, visit visibleearth.nasa.gov to view a variety of CERES data images.**

CERES Single Scanner TOA/ Surface Fluxes and Clouds (SSF)

Product Description

The Single Scanner Footprint TOA/Surface Fluxes and Clouds (SSF) product contains one hour of instantaneous CERES data for a single scanner instrument. The SSF combines instantaneous CERES data with scene information from a higher-resolution imager such as the Visible/Infrared Scanner (VIRS) on TRMM or MODIS on Terra and Aqua. Scene identification and cloud properties are defined at the higher imager resolution and these data are averaged over the larger CERES footprint. For each CERES footprint, the SSF contains the number of cloud layers, and, for each layer, the cloud amount, height, temperature, pressure, optical depth, emissivity, ice and liquid-water path, and water-particle size. The SSF also contains the CERES filtered radiances for the total, shortwave (SW), and window (WN) channels and the unfiltered SW, longwave (LW), and WN radiances. The SW, LW, and WN radiances at spacecraft altitude are converted to top-of-the-atmosphere (TOA) fluxes based on the imager-defined scene. These TOA fluxes are used to estimate surface fluxes. Only footprints with adequate imager coverage are included on the SSF, which is much less than the full set of footprints on the CERES ES-8 product.

A complete listing of parameters for this data product can be found in the CERES Data Products Catalog at asd-www.larc.nasa.gov/DPC/DPC.html, and detailed definitions of each parameter can be found in the CERES Collection Guide at asd-www.larc.nasa.gov/ceres/collect_guide/list.html. The algorithms are described in CERES ATBDs 4.0-4.6, located, in PDF format, at eospso.gsfc.nasa.gov/atbd/cerestables.html.

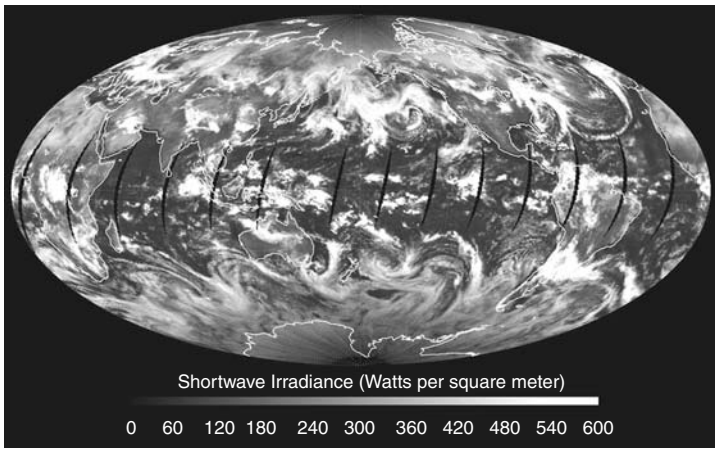

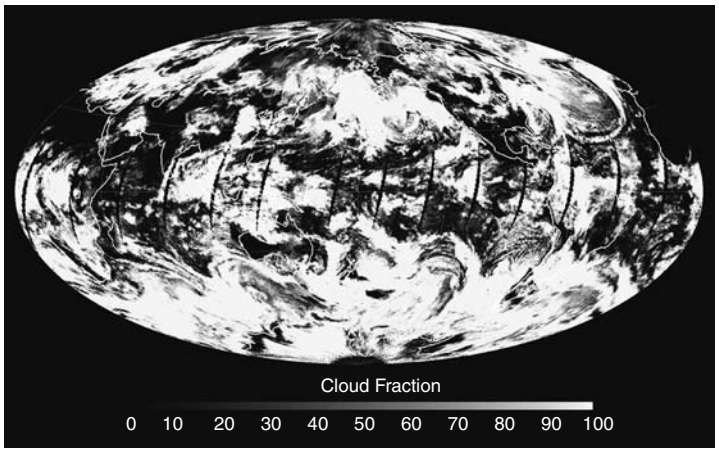

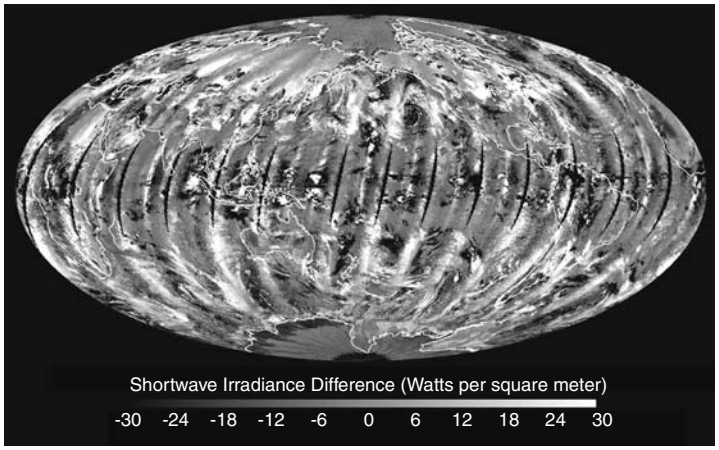

The CERES SSF provides a new level of integration and accuracy in radiation budget data. Cloud imager data from VIRS on TRMM and MODIS on Terra are used to derive the cloud and surface properties accurately matched to each CERES field of view. These properties are then used with a new generation of angular dependence models developed from the CERES hemispheric scanning capability to provide much more accurate TOA fluxes. These images show results from Terra SSF for March 22, 2001: TOA shortwave reflected flux (top left), cloud fraction (top right), and the difference in reflected flux from the simpler ERBE-Like TOA flux on the ES-8 data product to the more accurate fluxes on the SSF product (left). One of the major new capabilities of the SSF product is the ability to provide accurate fluxes for individual cloud or surface types, where the simpler ERBE data was only accurate for large ensemble monthly means.

On the internet, visit visibleearth.nasa.gov to view a variety of CERES data images.

Research and Applications

The SSF data product has instantaneous cloud, aerosol, TOA radiative fluxes, and simple parameterization surface radiative fluxes for each CERES field of view. This data set is optimal for research on the radiative properties of different types of cloudiness, aerosols, or surface properties. It can be compared to numerical weather prediction models, cloud resolving models, and field experiment data. The properties and the fluxes are matched so that space/time matching noise is reduced to 1% or less. The product also adds surface radiative flux estimates from simple radiative transfer parameterizations that attempt to depend as directly as possible on the TOA fluxes. More rigorous full radiative transfer constrained surface and atmosphere fluxes are found in the CRS data product. SSF provides the basis for the remainder of the new generation of radiation budget data products that go far beyond the earlier ERBE capability.

Data Set Evolution

This product is the first step in the sequence of processes from the geolocated radiances to estimates of the global radiation budget.

The SSF analysis uses coarse-spatial-resolution broadband radiance data from CERES, matched with simultaneous high-spatial-resolution narrowband radiance data from MODIS on Aqua.

Analysis proceeds in five basic steps:

1) Cloud masking and clear-sky map update;
2) Simultaneous determination of cloud height, layer, phase, and optical properties;
3) Convolution of imager pixel-level cloud/surface properties with the CERES point-spread function for each CERES field of view;
4) Use of convolved cloud/surface properties to select a broadband anisotropic model for conversion of CERES radiance to TOA flux (Loeb, N. *et al.*, 2003); and
5) Estimation of radiative fluxes at the surface, using theoretical/statistical relationships to TOA fluxes.

The SSF data product contains the matched cloud and radiative-flux data, which will also be used for later determination of radiative fluxes within the atmosphere.

Suggested Reading

Dong, X. *et al.*, 1999.

Green, R. N., and B. A. Wielicki, 1995.

Green, R. N. *et al.*, 1995.

Loeb, N. *et al.*, 2003.

Minnis, P. *et al.*, 1995.

Minnis, P. *et al.*, 1998.

Minnis, P. *et al.*, 1999.

Wielicki, B. A. *et al.*, 1995.

Wielicki, B. A. *et al.*, 1998.

Young, D. F. *et al.*, 1998.

CERES Single Scanner TOA/Surface Fluxes and Clouds Summary

Coverage: Global

Spatial/Temporal Characteristics: 20 km at nadir/0.01 second

Key Geophysical Parameters: Radiance and flux (TOA and surface); cloud and clear-sky statistics, optical depth, infrared emissivity, liquid-water path, ice-water path, cloud-top pressure, cloud effective pressure, cloud temperature and cloud height, cloud-bottom pressure, water and ice-particle radius

Processing Level: 2

Product Type: Standard, post-launch

Maximum File Size: 260 MB

File Frequency: 1/hour

Primary Data Format: HDF

Browse Available: No

Additional Product Information: eosweb.larc.nasa.gov/PRODOCS/ceres/table_ceres.html

DAAC: Langley Atmospheric Sciences Data Center, eosweb.larc.nasa.gov

Clouds Science Team Contact: P. Minnis

Angular Models Science Team Contact: Norman Loeb

CERES Clouds and Radiative Swath (CRS)

Product Description

The Clouds and Radiative Swath (CRS) product contains one hour of instantaneous CERES data for a single scanner instrument. The CRS contains all of the CERES SSF product data. For each CERES footprint on the SSF the CRS also contains vertical flux profiles evaluated at four levels in the atmosphere: the surface, 500-, 70-, and 1-hPa. The CRS fluxes and cloud parameters are adjusted for consistency with a radiative-transfer model, and adjusted fluxes are evaluated at the four atmospheric levels for both clear-sky and total-sky.

A complete listing of parameters for this data product can be found in the CERES Data Products Catalog at asd-www.larc.nasa.gov/DPC/DPC.html.

Research and Applications

The surface and atmospheric radiation budget (SARB) is the primary driver of the hydrological cycle and the general circulation of the atmosphere. Anthropogenically induced changes in the radiatively active trace gases and aerosols will affect the SARB and will therefore force a climate response. The 68 radiance and radiant flux and cloud parameters provided by this product are inputs to higher level algorithms which produce gridded, averaged flux and cloud-property products. This product contains a further enhancement of the basic data on radiation and cloud characteristics from SSF needed for determination of the amount of energy passing from space through the atmosphere to the Earth and flowing from the Earth back to space, which is provided by products SRBAVG, AVG, and ZAVG. It is a global product and is used as the input to the hourly gridded computation of surface, multiple atmosphere levels, and TOA radiative fluxes.

The analysis algorithms are described in CERES ATBD Subsystem 5.0, which can be found in PDF format at eospso.gsfc.nasa.gov/atbd/cerestables.html.

The online CERES ARM Validation Experiment (CAVE) provides easy-to-read subsets of these CERES products at over 30 ground sites; plots of surface radiometer and meteorology time series for validation; "point and click" facilities for radiative transfer calculations; and a library of the latest reports on CERES SARB (www-cave.larc.nasa.gov/cave/).

Data Set Evolution

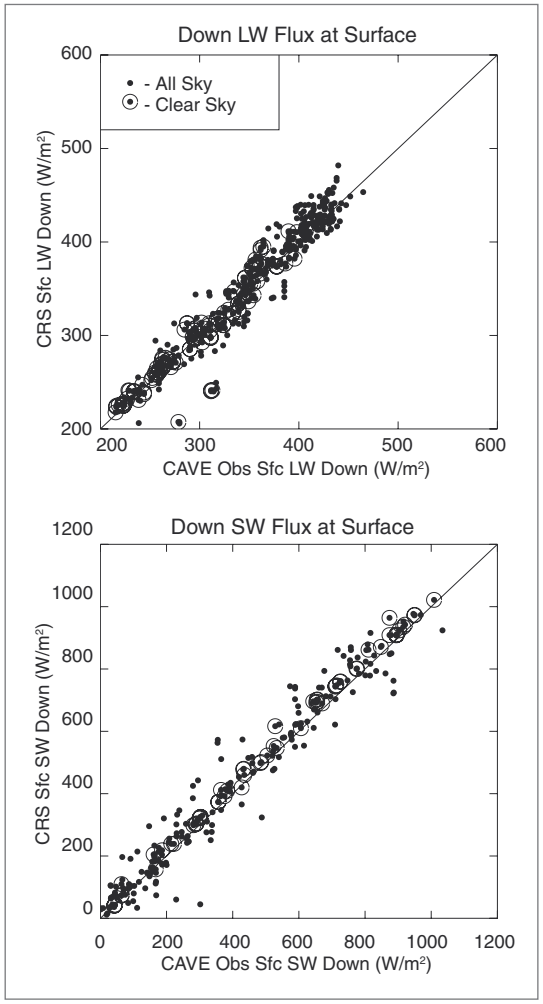

Surface Comparisons*

All Sky					Clear Sky				
	N	*Mean*	*Bias (Obs-CRS)*	*RMS*		*N*	*Mean*	*Bias (Obs-CRS)*	*RMS*
LW Down	455	349.3	-3.0	18.4	LW Down	17	303.9	-4.8	8.4
LW Up	430	416.3	-2.8	16.4	LW Up	17	397.8	5.9	11.4
SW Down	260	427.9	-21.2	60.3	SW Down	17	324.5	-14.3	17.1
SW Up	260	87.2	10.8	19.9	SW Up	17	71.6	5.6	13.0

TOA Comparisons*

All Sky					Clear Sky				
	N	*Mean*	*Bias (Obs-CRS)*	*RMS*		*N*	*Mean*	*Bias (Obs-CRS)*	*RMS*
LW Up	457	246.7	-0.4	4.0	LW Up	17	273.9	-1.8	3.2
SW Up	260	225.5	-2.2	8.1	SW Up	17	108.8	1.2	1.3

*** Complete comparison results at: www-cave.larc.nasa.gov/cave/ (under "Site Statistics")**

Comparison of CERES/TRMM (Jan-Aug 1998) Edition-2B SARB calculated downwelling flux to observations at ARM/SGP E13 site (ARM Central Facility). Clear Sky points in tables are identified clear if both CERES (VIRS) cloud mask and surface radiometry cloud amount (Long/Ackerman algorithm) equal to 0%. Clear Sky in plots are clear by virtue of CERES (VIRS) cloud mask equal to 0%. "Obs" refers to surface flux measured by up-looking pyrgeometer (LW), pyranometer (SW) and at TOA measured by the CERES instrument.

The inputs to this product come from the SSF product, and the cloud parameters are further corrected and adjusted. The TOA and surface values are corrected for satellite and cloud effects to produce observed TOA and tuned surface estimates. This data set is tailored to provide the needed inputs to the hourly gridded flux and surface radiation budget Level 3 product, FSW.

Suggested Reading

Charlock, T. P., and T. L. Alberta, 1996.

Charlock, T. P. *et al*., 1993.

Charlock, T. P. *et al*., 1995.

Fu, Q., and K. Liou, 1993.

Liou, K.-N., 1992.

Whitlock, C. H. *et al*., 1995.

Wielicki, B. A. *et al*., 1998.

Wu, M., and L.-P. Chang, 1992.

CERES Clouds and Radiative Swath Summary

Coverage: Global

Spatial/Temporal Characteristics: 20 km at nadir/0.01 second

Key Geophysical Parameters: Shortwave and longwave radiant flux at the surface, multiple atmosphere levels, and TOA, scene identification, cloud parameters

Processing Level: 2

Product Type: Standard, post-launch

Maximum File Size: 354 MB

File Frequency: 1/hour

Primary Data Format: HDF

Browse Available: No

Additional Product Information: eosweb.larc.nasa.gov/PRODOCS/ceres/table_ceres.html

DAAC: Langley Atmospheric Sciences Data Center, eosweb.larc.nasa.gov

Science Team Contact: T. P. Charlock

CERES Monthly Gridded Radiative Fluxes and Clouds (FSW)

Product Description

The Monthly Gridded Radiative Fluxes and Clouds (FSW) product contains a month of space-and-time-averaged CERES data for a single scanner instrument. The FSW is also produced for combinations of scanner instruments. All instantaneous fluxes from the CERES CRS product for a month are sorted by 1° spatial regions, by day number, and by the Universal Time (UT) hour of observation. The mean of the instantaneous fluxes for a given region-hour bin is determined and recorded on the FSW along with other flux statistics and scene information. The mean adjusted fluxes at the four atmospheric levels defined by CRS are also included for both clear-sky and total-sky scenes. In addition, four cloud-height categories are defined by dividing the atmosphere into four intervals with boundaries at the surface, 700-, 500-, 300-hPa, and the top of the atmosphere (TOA). The cloud layers from CRS are put into one of the cloud-height categories and averaged over the region. The cloud properties are also column averaged and included on the FSW.

A complete listing of parameters for this data product can be found in the CERES Data Products Catalog at asd-www.larc.nasa.gov/DPC/DPC.html.

Research and Applications

This product provides a 1° gridded version of the CRS data. The data volume is an order of magnitude smaller, but it retains the ability to compare to weather or climate model results at 1° resolution. It can also serve as a smaller browse product. This data set is a primary input to the SYN and AVG data products which merge the CERES data with 3 hourly geostationary data to provide more accurate diurnal cycles and time averages. Care is taken to let the geostationary data provide the relative diurnal cycle magnitude, but for CERES to provide the absolute accuracy of the fluxes.

Data Set Evolution

The algorithm is based on ERBE algorithms and carries out aggregation of the high-resolution 20-km (nadir) data products to 1° (110 km) data cells using weighted averaging and linear interpolation to produce the flux and cloud data in this grid-cell format chosen for final products. This is an equal-angle grid consisting of regions that are 1° in latitude by 1° in longitude. The parameter list is essentially the same as for CRS.

The analysis algorithms are described in CERES ATBD Subsystem 6.0, which can be found at eospso.gsfc.nasa.gov/atbd/cerestables.html.

Suggested Reading

Stowe, L. *et al*., 1993.

Wielicki, B. A. *et al*., 1998.

CERES Monthly Gridded Radiative Fluxes and Clouds Product Summary

Coverage: Global

Spatial/Temporal Characteristics: 1° region/hour

Key Geophysical Parameters: Gridded surface, atmosphere layer, and TOA fluxes, clear-sky and total-sky cloud parameters in CRS, (e.g., cloud overlap, cloud pressure, cloud altitude, cloud temperature, ice-water properties, ice-particle properties, liquid-water properties)

Processing Level: 3

Product Type: Standard, post-launch

Maximum File Size: 1130 MB

File Frequency: 11/month

Primary Data Format: HDF

Browse Available: No

Additional Product Information: eosweb.larc.nasa.gov/PRODOCS/ceres/table_ceres.html

DAAC: Langley Atmospheric Sciences Data Center, eosweb.larc.nasa.gov

Science Team Contact: D. F. Young

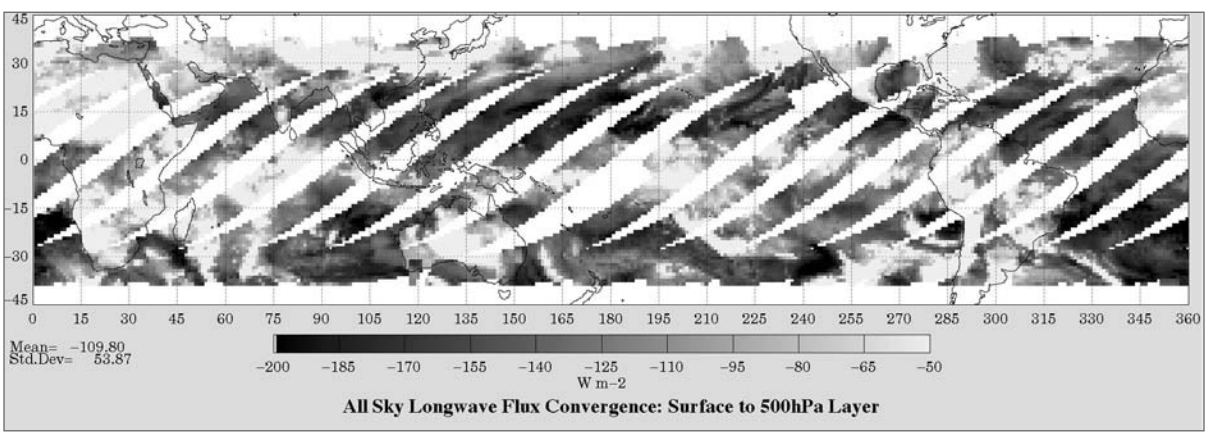

Convergence of longwave flux into the atmospheric layer from the surface to 500hPa level for all-sky conditions. The results are from TRMM data for February 3, 1998. Gaps between orbit tracks show the limit of the VIRS imager scan swath. The FSW data product contains 1° gridded data for TOA, surface, and atmosphere products along with matching surface, aerosol, and cloud data for each grid box. The LW convergence represents the most accurate construction consistent with the CERES LW and window fluxes, VIRS cloud properties, and ECMWF temperature and humidity profiles. On the internet, visit visibleearth.nasa.gov to view a variety of CERES data images.

CERES Synoptic Radiative Fluxes and Clouds (SYN)

Product Description

The Synoptic Radiative Fluxes and Clouds (SYN) product contains a day of space-and-time-averaged CERES data for a single scanner instrument. The SYN is also produced for combinations of scanner instruments. The 1° regional flux at the hour of observation from the CERES FSW product and concurrent diurnal data from geostationary satellites are used to estimate the regional flux at 3-hour intervals. Also at 3-hour intervals are estimates of the adjusted fluxes at the four atmospheric levels as defined by the CERES CRS product for both clear-sky and total-sky scenes, estimates of the average cloud parameters in four cloud-height categories, and column-averaged cloud parameters.

A complete listing of parameters for this data product can be found in the CERES Data Products Catalog at asd-www.larc.nasa.gov/DPC/DPC.html.

Research and Applications

The synoptic format of this product provides data which are global and simultaneous in time. This is preferred by climate modelers since the synoptic times ensure consistency with ground-truth meteorological observations from weather stations and radiosondes as well as with geostationary satellites, which provide images at synoptic hours. The production of a CERES synoptic data product is important because synoptic views provide a basis for studying the life cycle of cloud systems and for validating the CERES data processing, and it provides a regular data structure that simplifies the design of algorithms and operation of the data processing system. Synoptic fields of radiation and clouds are potentially valuable in developing and understanding the role of clouds in the generation and dissipation of available potential energy, since the calculation of this quantity requires integration over approximately horizontal layers within the atmosphere.

Data Set Evolution

The CERES time-space averaging and time-interpolation algorithm is based on techniques used in previous systems for deriving the Earth radiation budget, such as ERBE. The chief input to the time interpolation process is the gridded SW and LW TOA clear-sky and total-sky fluxes and cloud information provided by the FSW product. Data from the three systems which carry CERES simultaneously in orbit (TRMM, Terra, and Aqua) provide up to six samples per day. This significantly reduces temporal sampling errors. Estimates of the cloud properties at synoptic times are also provided. The cloud-mask output defines clear-sky conditions for the 1° cells for the radiative fluxes, which are averaged over 3-hour periods. Interpolation to the synoptic times uses geostationary data to assist in modeling meteorological variations between times of observations.

The analysis algorithms are described in CERES ATBD Subsystem 7.0, which can be found at eospso.gsfc.nasa.gov/atbd/cerestables.html.

Suggested Reading

Breigleb, B. P., and V. Ramanathan, 1982.

Brooks, D. R. *et al*., 1986.

Harrison, E. F. *et al*., 1988.

Minnis, P., and E. F. Harrison, 1984.

Smith, G. L. *et al*., 1995.

Wielicki, B. A. *et al*., 1998.

Young, D. F. *et al*., 1995a.

CERES Synoptic Radiative Fluxes and Clouds Summary

Coverage: Global

Spatial/Temporal Characteristics: 1° region/ 3-hour, monthly

Key Geophysical Parameters: Synoptic time- interval clear-sky, total-sky fluxes at surface, atmosphere levels, and TOA, cloud parameters including cloud overlap, cloud pressure, cloud altitude, cloud temperature, optical depth, ice-water properties, ice-particle properties, liquid-water properties, photosynthetically active radiation

Processing Level: 3

Product Type: Standard, post-launch

Maximum File Size: 240 MB

File Frequency: 1/3-hour (3-hour Level 3), 1/month (Monthly Level 3)

Primary Data Format: HDF

Browse Available: No

Additional Product Information: eosweb.larc.nasa.gov/PRODOCS/ceres/table_ceres.html

DAAC: Langley Atmospheric Sciences Data Center, eosweb.larc.nasa.gov

Science Team Contact: T. Wong

CERES Monthly Regional Radiative Fluxes and Clouds (AVG) and Monthly Zonal and Global Radiative Fluxes and Clouds (ZAVG)

Product Description

The Monthly Regional Radiative Fluxes and Clouds (AVG) product contains a month of space-and-time-averaged CERES data for a single scanner instrument. The AVG is also produced for combinations of scanner instruments. The 1° regional flux at the hour of observation from the CERES SYN product and concurrent diurnal data from geostationary satellites are used to estimate the daily regional flux, which is averaged to yield the monthly average flux. Adjusted fluxes at the four atmospheric levels defined by the CERES CRS product are also estimated for both clear-sky and total-sky scenes. In addition, four cloud-height categories are defined by dividing the atmosphere into four intervals with boundaries at the surface, 700-, 500-, 300-hPa, and the top of the atmosphere. The cloud layers from SYN are put into one of the cloud-height categories and diurnally averaged. The cloud properties are also column averaged. The AVG also contains, for each region, the hourly average fluxes for the month and an overall monthly average.

The Monthly Zonal and Global Radiative Fluxes and Clouds (ZAVG) product contains a month of space-and-time-averaged CERES data for a single scanner instrument. The ZAVG is also produced for combinations of scanner instruments. The space-and-time-averaged fluxes and cloud parameters on the CERES AVG product are spatially averaged from 1° regions to 1° zonal averages and a global monthly average.

A complete listing of parameters for these data products can be found in the CERES Data Products Catalog at asd-www.larc.nasa.gov/DPC/DPC.html.

Research and Applications

These products will be used by meteorological researchers to study climate and improve global climate models. Zonal quantities are needed for studying energy transport since averaging on large spatial scales minimizes the effects of regional-scale anomalies in studying climate change and global dynamics. Global averages can be compared with other historical data sets derived from different regional scales to detect climate temperature trends and evaluate large-scale climate anomalies such as the effects of major volcanic eruptions.

Data Set Evolution

The product algorithm first calculates the means on a regional (1° equal-angle grid) basis from one month of synoptic maps from the SYN 3-hourly product. Regional means are then combined to obtain zonal and global averages. The main steps of the monthly averaging process are: 1) regionally sort the synoptically ordered data, 2) linearly average all flux data to produce monthly and monthly-hourly means, 3) average the cloud properties using the proper weighting schemes, and 4) combine and average the regional means into zonal and global means. Once regional means are computed for all parameters and all regions, these means are combined into zonal and global means. Area-weighting factors are used to correct for the variation of grid-box size with latitude.

The analysis algorithms are described in CERES ATBD Subsystem 8.0, which can be found at eospso.gsfc.nasa.gov/atbd/cerestables.html.

Suggested Reading

Harrison, E. F. *et al.*, 1990b.

Li, Z., and H. Leighton, 1993.

Wielicki, B. A. *et al.*, 1998.

Young, D. F. *et al.*, 1995b.

CERES AVG and ZAVG Products Summary

Coverage: Global

Spatial/Temporal Characteristics: 1° region, 1° zone, global/month

Key Geophysical Parameters: Averaged clear-sky, total-sky surface, TOA, and standard CERES pressure-level fluxes; cloud parameters include: cloud overlap, pressure, temperature, optical depth, ice-particle properties, liquid-water properties, PAR

Processing Level: 3

Product Type: Standard, post-launch

Maximum File Size: 1500 MB

File Frequency: 3/month

Primary Data Format: HDF

Browse Available: No

Additional Product Information: eosweb.larc.nasa.gov/PRODOCS/ceres/table_ceres.html

DAAC: Langley Atmospheric Sciences Data Center, eosweb.larc.nasa.gov

Science Team Contact: T. Wong

CERES Monthly Gridded TOA/ Surface Fluxes and Clouds (SFC)

Product Description

The Monthly Gridded TOA/Surface Fluxes and Clouds (SFC) product contains a month of space-and-time averaged CERES data for a single scanner instrument. The SFC is also produced for combinations of scanner instruments. All instantaneous shortwave, longwave, and window fluxes at the top of the atmosphere (TOA) and surface from the CERES SSF product for a month are sorted by 1° spatial regions, by day number, and by the local hour of observation. The mean of the instantaneous fluxes for a given region-day-hour bin is determined and recorded in the SFC product along with other flux statistics and scene information. These average fluxes are given for both clear-sky and total-sky scenes. The regional cloud properties are column averaged and are included in the SFC product.

A complete listing of parameters for this data product can be found in the CERES Data Products Catalog at asd-www.larc.nasa.gov/DPC/DPC.html.

Research and Applications

This product provides a 1° gridded version of the instantaneous footprint SSF data. The data volume is an order of magnitude smaller, but it retains the ability to compare to weather or climate model results at 1° resolution. It can also serve as a smaller browse product. This data set is a primary input to the SRBAVG data product which merges the CERES data with 3 hourly geostationary data to provide more accurate diurnal cycles and time averages. Care is taken to let the geostationary data provide the relative diurnal cycle magnitude, but for CERES to provide the absolute accuracy of the fluxes. Users who need within atmosphere fluxes or the most consistent set of surface to atmosphere to TOA fluxes should use the FSW, SYN, and AVG CERES data products. Validated data for SRBAVG will be available earlier than the more complete AVG product. Finally, the AVG product uses GMT defined day boundaries, while the SRBAVG product uses local solar time.

Data Set Evolution

The parameters generated for this product are derived from the SSF product, which contains all the flux and cloud parameters. Each of the parameters from SSF is averaged to the 1° grid using equal weighting, which results in approximately 50 footprints being averaged for each geographic cell. These parameters are all inputs to the SRBAVG final radiation-budget product.

The analysis algorithms are described in CERES ATBD Subsystem 4.6, which can be found at eospso.gsfc.nasa.gov/atbd/cerestables.html.

Suggested Reading

Barkstrom, B. R., and B. A. Wielicki, 1995.

Cess, R. *et al*., 1991.

Gupta, S. K. *et al*., 1992.

Gupta, S. K. *et al*., 1995.

Inamdar, A. K., and V. Ramanathan, 1994.

Inamdar, A. K., and V. Ramanathan, 1995.

Kratz, D. P., and Z. Li, 1995.

Li, Z. *et al*., 1993.

Wielicki, B. A. *et al*., 1998.

CERES Monthly Gridded TOA/Surface Fluxes and Clouds Summary

Coverage: Global

Spatial/Temporal Characteristics: 1° region/hour

Key Geophysical Parameters: Total-sky, clear-sky, and angular-model scene radiative fluxes (TOA and surface), cloud parameters, including cloud pressure, cloud altitude, cloud temperature, optical depth

Processing Level: 3

Product Type: Standard, post-launch

Maximum File Size: 615 MB

File Frequency: 18/month

Primary Data Format: HDF

Browse Available: No

Additional Product Information: eosweb.larc.nasa.gov/PRODOCS/ceres/table_ceres.html

DAAC: Langley Atmospheric Sciences Data Center, eosweb.larc.nasa.gov

Science Team Contacts: D. F. Young, D. P. Kratz

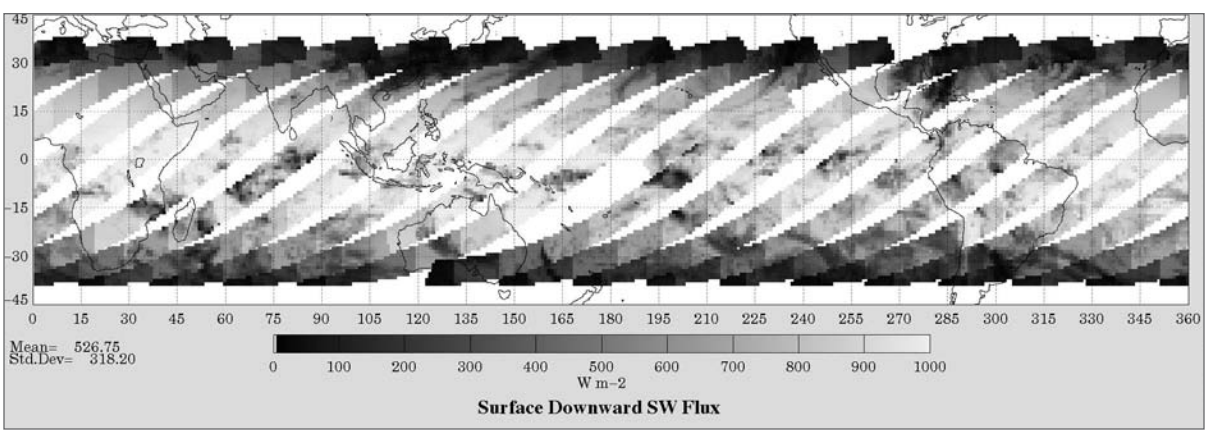

Downward shortwave flux at the surface for all-sky conditions. The results are from TRMM data for Feb 03, 1998. Gaps between orbit tracks show the limit of the VIRS imager scan swath. The SFC data product contains 1° gridded data for TOA and surface fluxes along with matching surface, aerosol, and cloud data for each grid box. Surface flux algorithms are simpler than those in the CRS and FSW products. On the internet, visit visibleearth.nasa.gov to view a variety of CERES data images.

CERES Monthly TOA/Surface Averages (SRBAVG)

Product Description

The Monthly TOA/Surface Averages (SRBAVG) product contains a month of space-and-time-averaged CERES data for a single scanner instrument. The SRBAVG is also produced for combinations of scanner instruments. The monthly average regional flux is estimated using diurnal models and the 1° regional fluxes at the hour of observation from the CERES SFC product. A second set of monthly average fluxes is estimated using concurrent diurnal information from geostationary satellites. These fluxes are given for both clear-sky and total-sky scenes and are spatially averaged from 1° regions to 1° zonal averages and a global average. For each region, the SRBAVG also contains hourly average fluxes for the month and an overall monthly average. The cloud properties from SFC are column averaged and are included on the SRBAVG.

A complete listing of parameters for this data product can be found in the CERES Data Products Catalog at asd-www.larc.nasa.gov/DPC/DPC.html.

Research and Applications

SRBAVG provides the next generation of TOA fluxes beyond the ERBE capability. Improvements include the advanced angular dependence models used in the SSF input TOA fluxes, advanced models of the dependence of albedo on solar zenith angle based on the SSF data, and improved diurnal sampling achieved using the 3-hourly geostationary data for the relative diurnal shape while the CERES data defines the absolute accuracy and broadband direct measurements. SRBAVG is also advanced over ERBE ES-4 and ES-9 in that it contains cloud and aerosol properties, as well as surface radiative flux estimates derived using simple efficient parameterizations. This product should be broadly useful for climate and weather model verification, as well as for studying the role of clouds and aerosols in climate change. Users who need atmospheric fluxes or more rigorously constrained surface flux estimates should use the AVG gridded product.

Data Set Evolution

This product is obtained from the chain of processes which start with the 1B radiances and flow through products BDS, SSF, SFC, and the CERES Instrument Earth Scans (IES), ultimately producing the final averaged radiative flux and surface-radiation-budget (SRB) product. The regional fluxes are calculated using two different methods, which will help produce very stable, accurate long-term data sets and averages for use in detailed regional studies of radiation and clouds and interdisciplinary studies. This is a post-launch product. Currently, there is no adopted method available for producing total-sky surface LW flux from TOA flux. Data required for parameterization must be obtained from either Meteorological Ozone and Aerosol (MOA) atmo-

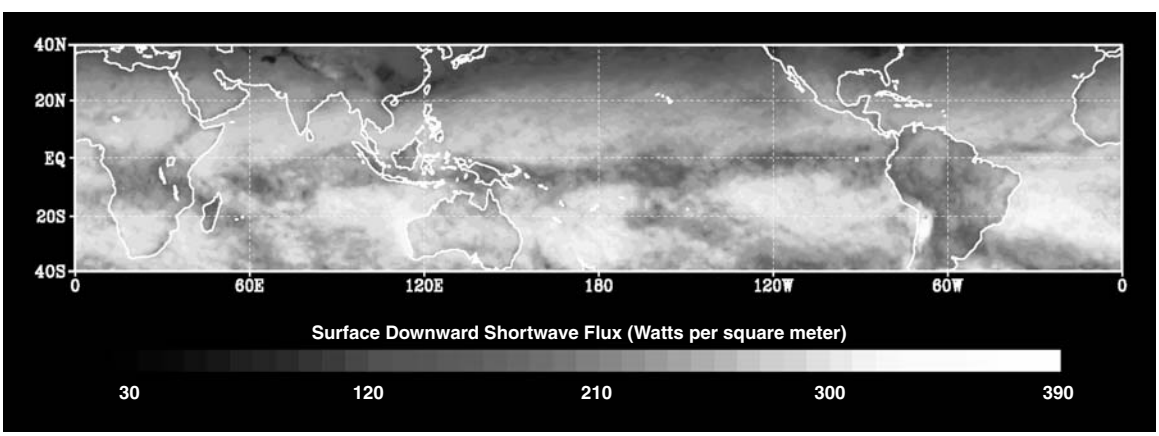

February 1998 monthly average downward shortwave flux at the surface for all-sky conditions. The data are from TRMM and is restricted to 40N to 40S by the TRMM spacecraft orbit. Surface SW downward fluxes decrease as cloud cover and cloud optical thickness increase. The figure for February 1998 is near the peak of the large 1997/98 El Niño. The dark band south of the equator shows the anomalous continuous band of convective cloud across the entire Pacific and Indian Oceans. On the internet, visit visibleearth.nasa.gov to view a variety of CERES data images.

spheric data sets or from CERES and International Satellite Cloud Climatology Project (ISCCP) cloud properties. In addition, data used in this product are limited to days in which there is at least one observation. The cloud parameters are also averaged monthly and monthly-daily. The surface radiation budget is the net radiative flux at the surface and is computed using the hourly gridded TOA and surface fluxes from SFC, parameterized models, atmospheric profiles, cloud parameters, and surface temperatures and emissivities to produce the downward and net shortwave and longwave fluxes at the surface. The LW algorithm is based on parameterized equations developed expressly for computing surface LW fluxes in terms of meteorological parameters obtained from satellite and/or other operational sources.

The analysis algorithms are described in CERES ATBD Subsystem 10.0, which can be found at eospso.gsfc.nasa.gov/atbd/cerestables.html.

Suggested Reading

Cess, R. *et al*., 1991.

Gupta, S. K. *et al*., 1992.

Harrison, E. F. *et al*., 1995.

Li, Z. *et al*., 1993.

Suttles, J. T., and G. Ohring, 1986.

Wielicki, B. A. *et al*., 1998.

CERES Monthly TOA/Surface Averages Summary

Coverage: Global

Spatial/Temporal Characteristics: 1° region/month

Key Geophysical Parameters: Averaged total-sky, radiative fluxes (TOA and surface), net surface radiative fluxes (surface radiation budget), averaged cloud parameters

Processing Level: 3

Product Type: Standard, post-launch

Maximum File Size: 1000 MB

File Frequency: 3/month

Primary Data Format: HDF

Browse Available: No

Additional Product Information: eosweb.larc.nasa.gov/PRODOCS/ceres/table_ceres.html

DAAC: Langley Atmospheric Sciences Data Center, eosweb.larc.nasa.gov

Science Team Contact: D. F. Young

MISR Top-Of-Atmosphere (TOA)/Cloud Product (MIS04, MIS06, MIS07)

Product Description

The Level 2 Top-of-Atmosphere (TOA)/Cloud Product (MIS04) consists of TOA radiation and cloud information including: stereoscopically derived cloud-top altitudes at 1.1-km sampling with simultaneous cloud-tracked winds at 70.4-km sampling; Reflecting Level Reference Altitude (RLRA), texture indices, top-of-atmosphere (TOA) bidirectional reflectance factors and albedos at 2.2-km sampling; altitude-binned (high, middle, and low) and total cloud fractions at 17.6 km; and coarsely-sampled (35.2 km) TOA albedos. The coarse TOA albedos include a restrictive albedo, derived from the nine multiangle observations of a single region, and an expansive albedo, which is calculated including contributions from surrounding regions at the appropriate angles. Data from MIS04 are mapped to produce Level 3 globally gridded products (MIS06, MIS07).

Research and Applications

The main purpose of the MISR TOA/Cloud Product is to produce accurate measures of spectral albedo and bidirectional reflectance classified by scene type. These enable study of the global effects of different types of cloud fields, including spatial and temporal dependencies, and determination of their effects on Earth's climate. Bidirectional reflectances of clear and cloudy regions obtained by MISR can be used to develop anisotropic reflectance models classified by cloud type, determine the spatial and temporal variability of cloud albedo, and validate coarse spatial resolution angular-reflectance models generated by other instruments. Automated stereo matching of multi-angle imaging is used to retrieve cloud-top elevations and cloud-tracked winds. MISR data can help to obtain a better understanding of the nonlinear scaling between sub-grid and grid-scale processes in GCMs and provide improved parameterization in these models.

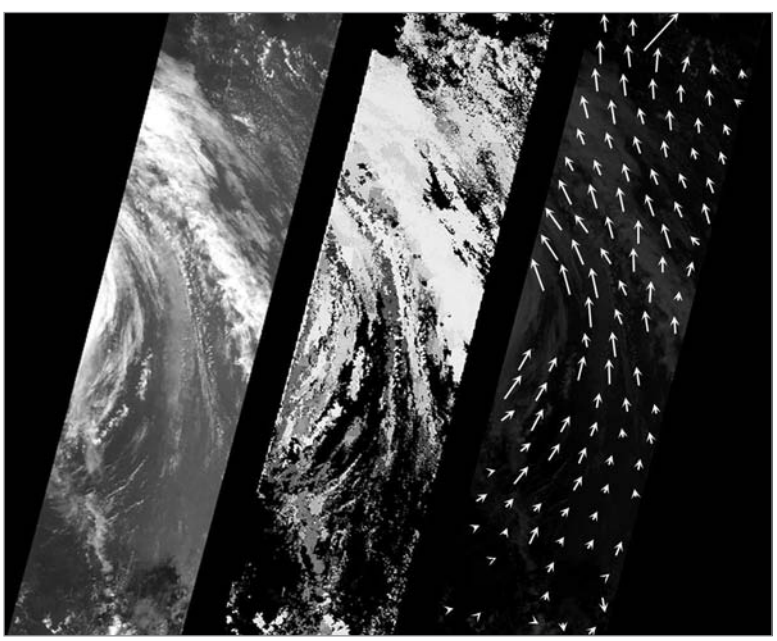

MISR images of Hurricane Debby in the Atlantic Ocean, acquired on August 21, 2000, during Terra orbit 3600. The first panel on the left is the MISR downward-looking (nadir) view of the storm's eastern edge. The next two panels show results obtained using MISR's stereoscopic observations and an operational retrieval algorithm to retrieve cloud heights and winds. The highest wind speed measured is nearly 100 kilometers/hour. On the internet, visit visibleearth.nasa.gov to view a variety of MISR data images.

Data Set Evolution

Earlier satellites, notably Nimbus-7 (ERB) and the NOAA-9 Earth Radiation Budget Experiment (ERBE), marked the beginning of techniques to directly integrate radiances from the same scene, measured more or less coincidentally at several different angles to yield the hemispherical flux. The Nimbus-7 scanner reduced its FOV to keep the viewed area about the same size, but had to look at different scenes across track and build up directional models. In its alongtrack mode, the NOAA-9 scanner obtained a very limited data set looking at fixed regions, but since its scanner had a fixed FOV the size of the target area changed systematically with angle. The presently available models have been painstakingly constructed from Nimbus-7 data, but cannot accommodate different cloud types, and define only a few categories of cloud cover amounts.

Suggested Reading

Di Girolamo, L., and R. Davies, 1994.

Horvath, A., and R. Davies, 2001.

Horvath, A., and R. Davies, 2001.

Loeb, N. G., and R. Davies, 1997.

Moroney, C. *et al*., 2002.

MISR TOA and Cloud Product Summary

Coverage: Daytime, 9-day for global repeat coverage

Spatial/Temporal Characteristics: 9-day for global coverage with 1.1 km, 2.2 km, 17.6 km, 35.2 km sampling, and 70.4 km sampling (various parameters) at Level 2; monthly and seasonal globally gridded products at Level 3

Key Geophysical Parameters: TOA albedo, TOA bidirectional reflectance factor, cloud-top height, cloud-tracked wind, cloud screens, reflecting level reference altitude, altitude-binned cloud fraction

Processing Level: 2, 3

Product Type: Standard, at-launch (MIS04) post-launch gridded products (MIS06, MIS07)

Maximum File Size: 90 MB, (TOA/Cloud Stereo Parameters); 5 MB (TOA/Cloud Classifier Parameters); 370 MB (TOA/Cloud Albedo Parameters)

File Frequency: 15/day

Primary Data Format: HDF-EOS

Browse Available: No

Additional Product Information: eosweb.larc.nasa.gov/PRODOCS/misr/table_misr.html

DAAC: Langley Atmospheric Sciences Data Center, eosweb.larc.nasa.gov

Science Team Contact: R. Davies

MISR Aerosol and Surface Product (MIS05, MIS08, MIS09)

Product Description

The Level 2 Aerosol/Surface Product (MIS05) contains a variety of information on the Earth's atmosphere and surface. The aerosol data include tropospheric aerosol optical depth on 17.6-km centers, archived with compositional model identifiers and retrieval residuals, ancillary data including atmospheric pressure and surface wind speed, and retrieval flags. The land surface data are mostly on 1.1-km centers and include hemispherical directional reflectance factor, bihemispherical reflectance (i.e., albedo), bidirectional reflectance factor, directional hemispherical reflectance, BRF model parameters, albedo-based NDVI, Fraction of Photosynthetically Active Radiation (FPAR), and Leaf Area Index (LAI).

Research and Applications

MIS05, MIS08, and MIS09 products are used to study absorption and scattering in the lower atmosphere and at the surface for use in climate and biosphere-atmosphere interaction studies. The MISR aerosol data sets enable: 1) the study of the global magnitude and variability of sunlight absorption and scattering by aerosols in the Earth's atmosphere (particularly tropospheric aerosols) and their effect on climate; 2) improved understanding of the sources, sinks, and global budgets of aerosols; and 3) improved atmospheric correction for surface imaging data acquired by MISR and other instruments (e.g., MODIS and ASTER).

The MISR surface data sets enable: 1) the study of the global magnitude and variability of sunlight absorption and scattering by the Earth's surface, particularly through determination of the surface hemispherical reflectance (albedo); 2) improved measures of land surface classification and dynamics; and 3) improved observations of ocean color in the tropics by providing data in equatorial regions to supplement MODIS observations.

Data Set Evolution

MISR builds on earlier work with satellite and aircraft optical sensors such as the AVHRR and the Advanced Solid-state Array Spectroradiometer (ASAS). Surface hemispherical reflectance (spectral albedo) is retrievable with much higher accuracy from MISR multi-angle observations than it can be inferred from solely nadir spectral reflectance factors. In addition, current aerosol retrievals (e.g., from AVHRR) are unable to distinguish different particle types, since they are based on measurements at a single wavelength and angle of view, and the algorithm to convert observed radiance to aerosol optical depth assumes particles of a fixed composition and size. MISR retrievals are based on more extensive coverage in both wavelength and view angle, providing greater ability to distinguish different particle types based on their physical and optical properties.

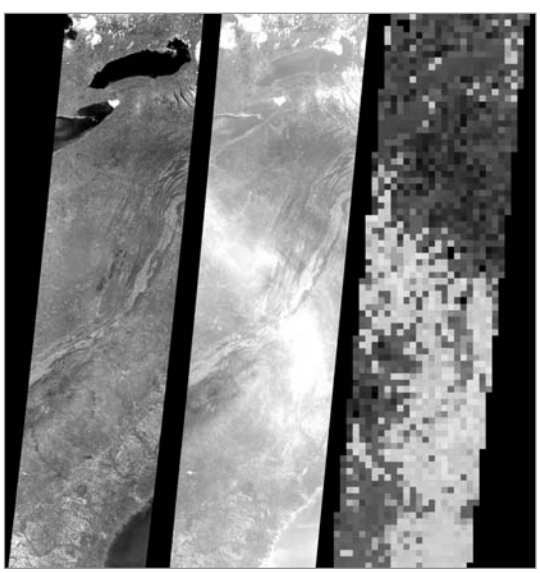

MISR images of the eastern United States acquired on March 6, 2000, during Terra orbit 1155. The first panel is the downward-looking (nadir) view, covering the region from Lake Ontario to northern Georgia, and spanning the Appalachian Mountains. The middle panel is the image taken by the forward-viewing 70.5° camera. At this increased slant angle, the line-of-sight through the atmosphere is three times longer, and a thin haze over the Appalachians is significantly more apparent. The third panel shows the airborne particle (aerosol) amount, derived using MISR's operational aerosol retrieval algorithm. On the internet, visit visibleearth.gsfc.nasa.gov to view a variety of MISR data images.

Suggested Reading

Diner, D. J. *et al*., 2001.

Kahn, R. *et al*., 1997.

Kahn, R. *et al*., 1998.

Kahn, R. *et al*., 2001.

Knyazikhin, Y. *et al*., 1998.

Martonchik, J. V. *et al*., 1998.

Martonchik, J. V. *et al*., 2002.

MISR Aerosol and Surface Product Summary

Coverage: Daytime

Spatial/Temporal Characteristics: 9-day for global coverage with 1.1-km, 17.6-km, and 70.4-km sampling (various parameters) at Level 2; 16-day, monthly, and seasonal globally gridded products at Level 3

Key Geophysical Parameters: Column aerosol optical depth, aerosol compositional model identifiers, directional hemispherical reflectance factors, hemispherical reflectances, BRF model parameters, NDVI, FPAR, LAI

Processing Level: 2, 3

Product Type: Standard, at-launch (MIS05); post-launch (MIS08, MIS09)

Maximum File Size: 40 MB (Aerosol Parameters); 500 MB (Surface Parameters)

File Frequency: 15/day

Primary Data Format: HDF-EOS Grid

Browse Available: No

Additional Product Information: eosweb.larc.nasa.gov/PRODOCS/misr/table_misr.html

DAAC: Langley Atmospheric Sciences Data Center, eosweb.larc.nasa.gov

Science Team Contact: J. Martonchik

MISR Aerosol Climatology Product (MIS12)

Product Description

The Aerosol Climatology Product (ACP)(MIS12) is generated at the MISR Scientific Computing Facility (SCF) and occasionally updated. It is used for interpretation of the aerosol data contained in MIS05. The ACP contains the physical and optical properties that define common atmospheric aerosol types. The parameters reported in the ACP include an aerosol model identifier (name, number, and composition); a water activity identifier (hygroscopic or not, and if so, how hydrophilic); a particle shape identifier (spherical, polyhedral, or irregular); a grid of relative humidity values for which all optical properties have been calculated; particle size distribution parameters; particle density (volume-weighted for mixtures); complex index of refraction; scattering and extinction cross-section; single scattering albedo; scattering anisotropy parameter; and phase function. It also includes the definitions of the aerosol mixtures used during generation of MIS 05.

Suggested Reading

Kahn, R. *et al*., 2001.

MISR Aerosol Climatology Product Summary

Coverage: N/A, one-time only, with possible infrequent updates

Resolution: N/A

Wavelengths: 446, 558, 672, and 866 nm; parameters include aerosol optical properties

Product Type: Internal

Maximum File Size: 0.2 MB

File Frequency: N/A

Primary Data Format: HDF-EOS Grid

Browse Available: No

Additional Product Information: eosweb.larc.nasa.gov/PRODOCS/misr/table_misr.html

DAAC: Langley Atmospheric Sciences Data Center, eosweb.larc.nasa.gov

Science Team Contact: R. Kahn

MODIS Aerosol Product (MOD04)

Product Description

The MODIS Aerosol Product (MOD04) monitors the ambient aerosol optical thickness over the oceans globally and over a portion of the continents. Further, the aerosol size distribution is derived over the oceans, and the aerosol type is derived over the continents. Daily Level 2 (MOD04) data are produced at the spatial resolution of 10 km, although made up from data at a resolution of 1 km (at nadir).

Research and Applications

Aerosols are one of the greatest sources of uncertainty in climate modeling. Aerosols modify cloud microphysics by acting as cloud condensation nuclei (CCN), and, as a result, impact cloud radiative properties and climate. Aerosols scatter back to space and absorb solar radiation. The MODIS aerosol product is used to study aerosol climatology, sources and sinks of specific aerosol types (e.g., sulfates and biomass-burning aerosol), interaction of aerosols with clouds, the hydrological cycle and atmospheric dynamics, and atmospheric corrections of remotely sensed surface reflectance over the land.

Data Set Evolution

Prior to MODIS, satellite aerosol measurements were limited to reflectance measurements in one (GOES, METEOSAT) or two (AVHRR) channels. There was no real attempt to retrieve aerosol content over land on a global scale. Algorithms had been developed for use only over dark vegetation. The blue channel on MODIS, not present on AVHRR, offers the possibility to extend the derivation of optical thickness over land to additional surfaces. The algorithms uses MODIS bands 1 through 7 and require prior cloud screening using MODIS data. Over the land, the dynamic aerosol models are derived from ground-based sky measurements and used in the net retrieval process.

Over the ocean, three parameters that describe the aerosol loading and size distribution are retrieved. Pre-assumptions on the general structure of the size distribution are required in the inversion of MODIS data, and the volume-size distribution are described with two log-normal modes: a single mode to describe the accumulation mode particles (radius <0.5 μm) and a single coarse mode to describe dust and/or salt particles (radius >1.0 μm). The aerosol parameters retrieved are: the ratio between the two modes, the spectral optical thickness, and the mean particle size.

The quality control of these products are based on comparison with ground stations and climatology.

The related MODIS Aerosol Product ATBD, *Algorithm for Remote Sensing of Tropospheric Aerosol from MODIS: Optical thickness over land and ocean and aerosol size distribution over the ocean*, can be found in PDF format at eospso.gsfc.nasa.gov/atbd/modistables.html.

Suggested Reading

Chu, D. A. *et al.*, 1998.

Chu, D. A. *et al.*, 2002.

Dubovik, O. *et al.*, 2002.

Gao, B. C. *et al.*, 2002b.

Holben, B. N. *et al.*, 1998.

Ichoku, C. *et al.*, 2002.

Kaufman, Y. J. *et al.*, 1997a.

Kaufman, Y. J. *et al.*, 1997b.

Kaufman, Y. J. *et al.*, 2002.

King, M. D. *et al.*, 1992.

King, M. D. *et al.*, 1999.

King, M. D. *et al.*, 2003.

Martins, J. V. *et al.*, 2002.

Rao, C. R. N. *et al.*, 1989.

Remer, L. A. *et al.*, 1996.

Remer, L. A. *et al.*, 2002.

Tanré, D. *et al.*, 1997.

MODIS Aerosol Product Summary

Coverage: Global over oceans, nearly global over land

Spatial/Temporal Characteristics: 10 km for Level 2

Key Science Applications: Aerosol climatology, biomass-burning aerosols, atmospheric corrections, cloud radiative properties, cloud and atmospheric dynamics, climate modeling

Key Geophysical Parameters: Atmospheric aerosol optical depth (global) and aerosol size distribution (oceans)

Processing Level: 2

Product Type: Standard, at-launch

Maximum File Size: 11.99 MB

File Frequency: 144/day

Primary Data Format: HDF-EOS

Browse Available: modis-atmos.gsfc.nasa.gov/MOD08_D3/browse.html

Additional Product Information: modis-atmos.gsfc.nasa.gov/MOD04_L2/index.html

DAAC: Goddard Space Flight Center Earth Sciences DAAC, daac.gsfc.nasa.gov

Science Team Contacts: Y. J. Kaufman, D. Tanré, L. A. Remer

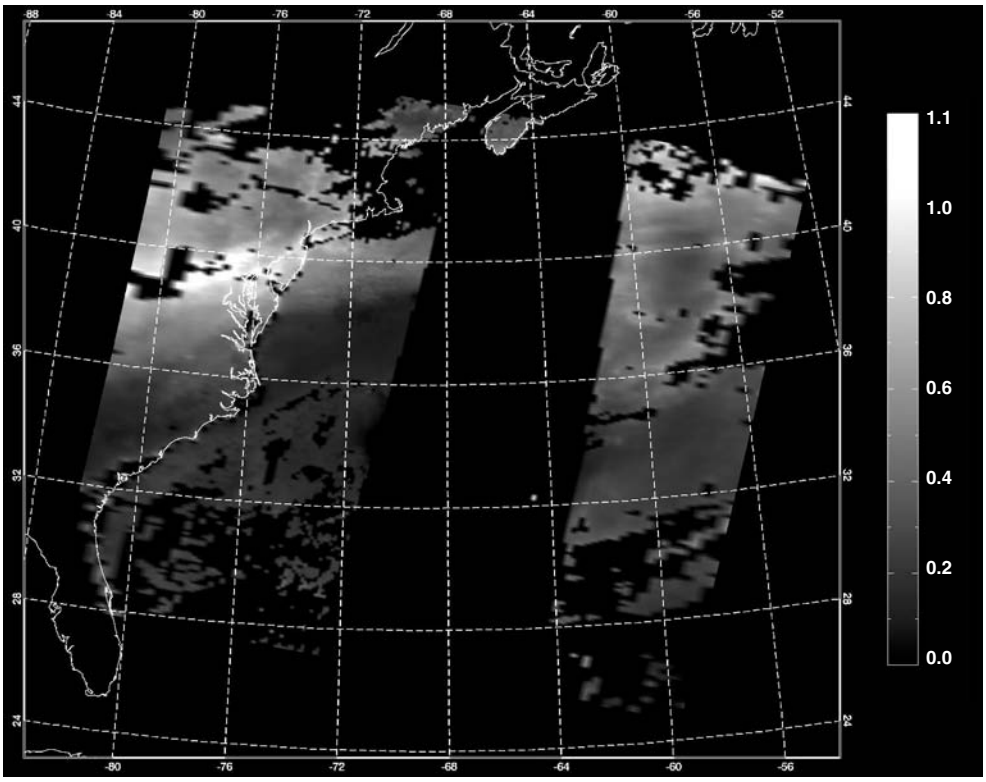

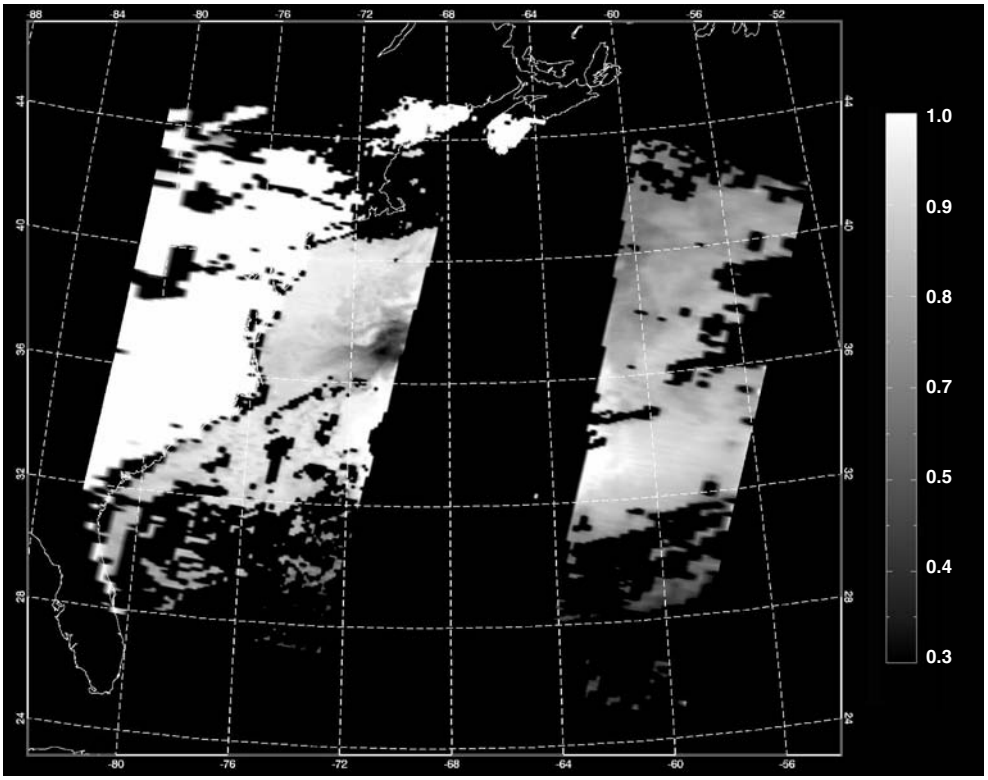

Aerosol optical properties. The image at top depicts the aerosol optical thickness at 0.56 μm over the Eastern United States on May 4, 2001, showing pollution along the Ohio Valley and transport to the north Atlantic. The bottom image shows the ratio of aerosol optical thickness of the fine mode to the total aerosol optical thickness. On the internet, visit visibleearth.nasa.gov to view a variety of MODIS data images.

MODIS Cloud Product (MOD06)

Product Description

The MODIS Cloud Product (MOD06) combines infrared and visible techniques to determine both physical and radiative cloud properties. Daily global Level 2 (MOD06) data are provided. Cloud-particle phase (ice vs. water, clouds vs. snow), effective cloud-particle radius, and cloud optical thickness are derived using the MODIS visible and near-infrared channel radiances. Cloud-top temperature, height, effective emissivity, phase (ice vs. water, opaque vs. non-opaque), and cloud fraction are produced by the infrared retrieval methods both day and night at 5 × 5 1-km-pixel resolution. Finally, the MODIS Cloud Product includes the cirrus reflectance in the visible at the 1-km-pixel resolution, which is useful for removing cirrus scattering effects from the land-surface reflectance product.

Research and Applications

A thorough description of global cloudiness and its associated properties is essential to the MODIS mission for two reasons. First, clouds play a critical role in the radiative balance of the Earth and must be accurately described in order to assess climate and potential climate change accurately. In addition, the presence or absence of cloudiness must be accurately determined in order to retrieve properly many atmospheric and surface parameters. For many of these retrievals, cloud cover, even thin cirrus, represents contamination. Key radiative properties of clouds such as phase, optical thickness, and temperature may be retrieved using MODIS instruments with unprecedented resolution.

Data Set Evolution

The determination of cloud-top properties will require the use of MODIS bands 29 and 31-36, along with the cloud-mask product (MOD35), to screen for clouds. In addition, NCEP or Data Assimilation Office global model analyses of surface temperature and pressure, profiles of temperature and moisture, and blended SST analyses will be required in the calculation of cloud forcing as a function of atmospheric pressure and emissivity. The Menzel cloud-phase algorithm requires MODIS bands at 8.55 μm (band 29) and 11.0 μm (band 31).

Validation of MODIS cloud top pressure will be conducted by comparisons with stereo determinations from MISR and O_2 A-band cloud heights from the Medium Resolution Imaging Spectrometer (MERIS) and lidar estimates as well as with two GOES determinations, aircraft lidar estimates plus observations of cirrus heights. Cloud emissivity will be compared to lidar-determined values. These interim products will be used in concert with field campaigns with the MAS instrument. The Menzel cloud-phase parameter will be validated using *in situ* data and by comparison to the King cloud-phase parameter.

The King cloud-phase algorithm requires product MOD02, calibrated multispectral radiances. Cloud-particle size and optical thickness require these radiances plus the cloud-top parameters within MOD06. In addition, these parameters require NCEP or DAO analyses and profiles described above. The validation and quality control of these products will be performed primarily through the use of *in situ* measurements obtained during field campaigns and with the use of the MAS instrument.

The related MODIS Cloud Product ATBDs, *MODIS: Cloud Top Properties and Cloud Phase* and *Cloud Retrieval Algorithms for MODIS: Optical Thickness, Effective Particle Radius, and Thermodynamic Phase*, can be found in PDF format at modis-atmos.gsfc.nasa.gov/reference_atbd.html.

Suggested Reading

Gao, B. C. *et al*., 1998.

Gao, B. C. *et al*., 2002a.

Gao, B. C. *et al*., 2003.

King, M. D. *et al*., 1992.

King, M. D. *et al*., 1996.

King, M. D. *et al*., 2003.

Nakajima, T. Y., and T. Nakajima, 1995.

Platnick, S. *et al*., 2000.

Platnick, S. *et al*., 2003.

Strabala, K. I. *et al*., 1994.

Wylie, D. P., and W. P. Menzel, 1998.

MODIS Cloud Product Summary

Coverage: Global

Spatial/Temporal Characteristics: Resolutions of 1 km or 5 km/once or twice per day (varies with parameter)

Key Science Applications: Cloud parameterization, climate modeling, climate monitoring, increasing accuracy of other MODIS retrievals

Key Geophysical Parameters: Cloud-particle phase (two algorithms), cloud-particle size and optical thickness, cirrus reflectance at 0.66 µm, and cloud-top temperature, emissivity, and height

Processing Level: 2

Product Type: Standard, at-launch

Maximum File Size: 69.60 MB (daytime granules), 14.15 MB (nighttime granules)

File Frequency: 288/day

Primary Data Format: HDF-EOS

Browse Available:
modis-atmos.gsfc.nasa.gov/MOD08_D3/browse.html

Additional Product Information:
modis-atmos.gsfc.nasa.gov/MOD06_L2/index.html

DAAC: Goddard Space Flight Center Earth Sciences DAAC, daac.gsfc.nasa.gov

Science Team Contacts: M. D. King, S. Platnick, W. P. Menzel, B. C. Gao

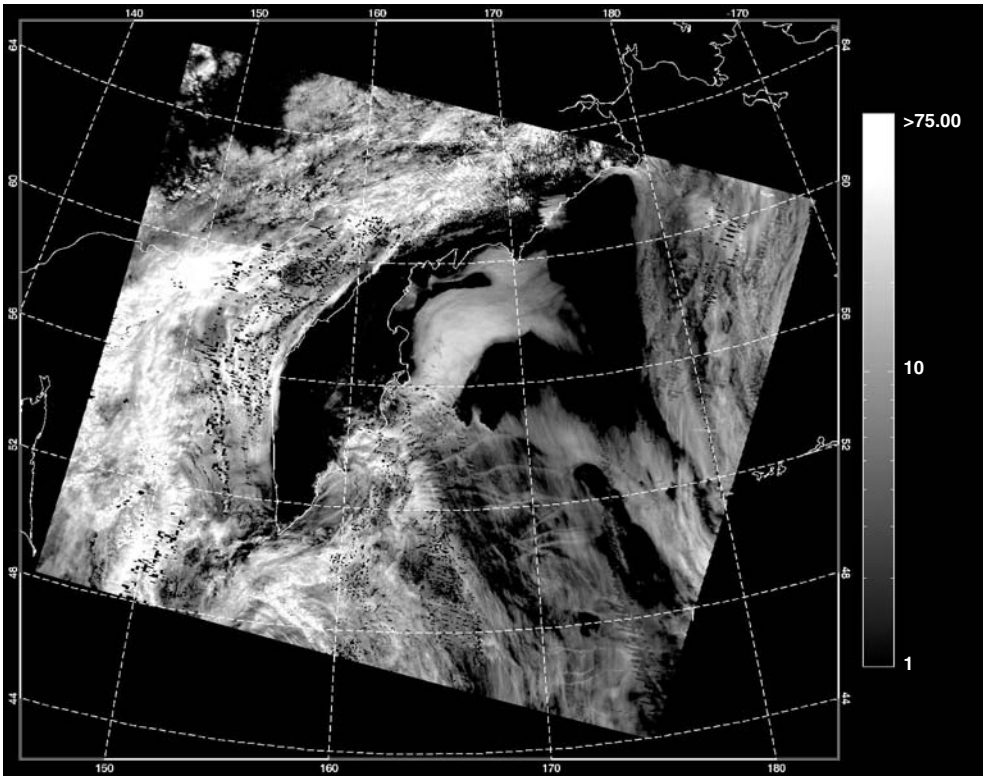

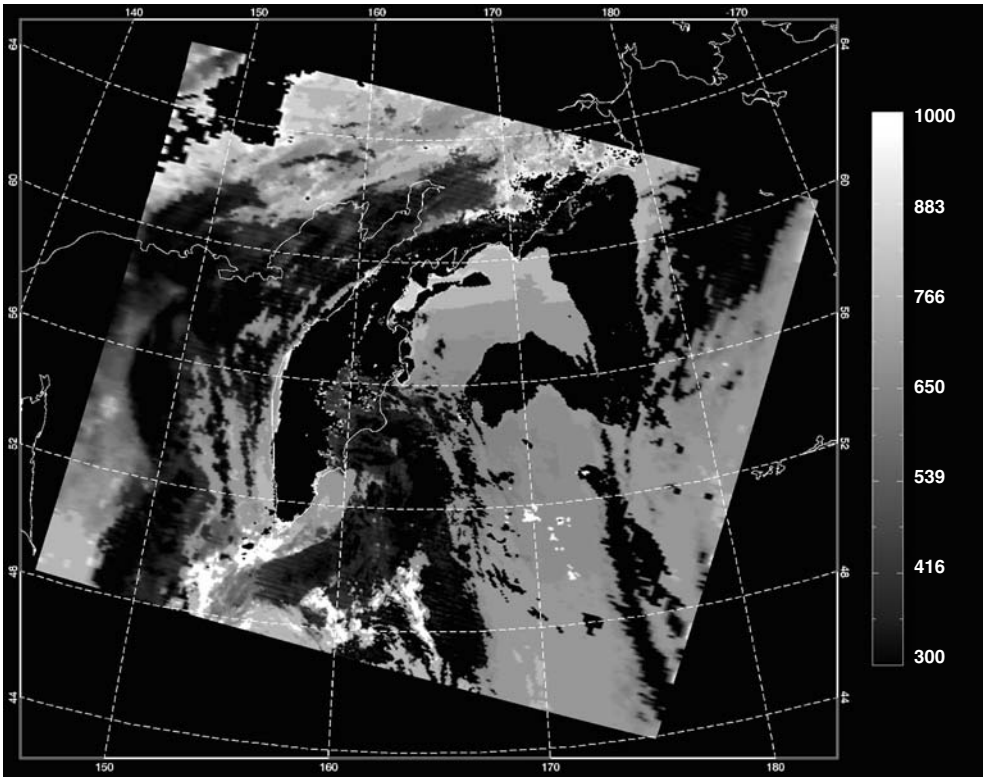

Cloud properties over the western Pacific Ocean off the Kamchatka Peninsula on August 10, 2001. The image at top shows the cloud optical thickness derived from all cloudy pixels. The bottom image shows the cloud top pressure (in hPa) for all clouds in this scene. On the internet, visit visibleearth.nasa.gov to view a variety of MODIS data images.

MODIS Level 3 Atmosphere Products (MOD08)

Product Description

There are three MODIS Level 3 Atmosphere Products, each covering a different temporal scale. The Earth Science Data Type names (and time spans) for each of the products are: MOD08_D3 (Daily), MOD08_E3 (8-Day), MOD08_M3 (Monthly).

Each of these Level 3 products contains statistics derived from over 50 science parameters from the Level 2 Atmosphere products: MOD04_L2, MOD05_L2, MOD06_L2, and MOD07_L2.

A range of statistical summaries is computed, depending on the Level 2 science parameter being considered. Statistics for a given Level 2 measurement might include:

- Simple (mean, minimum, maximum, standard deviation) statistics
- Parameters of normal and log-normal distributions
- Fraction of pixels that satisfy some condition (e.g., cloudy, clear)
- Histograms of the quantity within each grid box
- Histograms of the confidence placed in each measurement
- Histograms and/or regressions derived from comparing one science parameter to another; statistics may be computed for a subset that satisfies some condition
- Pixel counts

Statistics are sorted into 1° × 1° cells on an equal-angle grid and then summarized over the globe. The equal-angle grid has a fixed dimension of 360×180 pixels.

The daily product contains nearly 500 statistical summary parameters. The 8-day and monthly products, which are identical in format, include over 700 statistical summary parameters.

Additional information on the MODIS Level 3 Atmosphere products can be obtained from the MODIS-Atmosphere web site at: modis-atmos.gsfc.nasa.gov.

Research and Applications

Users should refer to the research applications of Level 2 Atmosphere products from MOD04, MOD05, MOD06, and MOD07 listed in this handbook. Level 3 statistical products derived from Level 2 measurements lend themselves to longer-term time-series studies that help monitor variations in environmental conditions and aid research for assessing both natural and human-induced global change.

Data Set Evolution

Definition of Time Spans

For the daily product (MOD08_D3), Level 2 granules that overlap any part of the data day (0000 to 2400 UTC) are included in the computation of statistics. Therefore a particular Level 2 granule may be included in two consecutive MOD08_D3 products.

The 8-day product (MOD08_E3) is computed by manipulating and summarizing the daily product over eight consecutive days. The running 8-day interval begins with the first day of MODIS data on Terra (February 25, 2000). The 8-day intervals for MODIS on Aqua will be the same 8-day intervals as for MODIS on Terra for the period of data overlap. It should be noted that the starting day of the 8-day interval is not reset to the 1st, during the rollover of a calendar month. However, during the rollover of a calendar year, the 8-day interval is reset to begin on January 1st. It should also be noted that the final 8-day interval of any year includes 8 full days even if they extend into a new year; this rule will, in general, cause some overlap of the 8-day interval around every new year.

The monthly product (MOD08_M3) is computed by manipulating and summarizing the daily product over a calendar month.

Definition of Daily Statistics

For the daily product, assume that $x_1, x_2, \ldots, x_n$ represent the retrieved pixel values of a Level 2 parameter over a 1° × 1° grid box, Q_i is the quality flag for each retrieved pixel value, and w_i is the weighting factor (1 for the daily case), then the simple statistics are defined as:

$$\overline{X_d} = \frac{\Sigma_i^n w_i \cdot x_i}{\Sigma_i^n w_i} \qquad (1)$$

$$\overline{X_{dQ}} = \frac{\Sigma_i^n Q_i \cdot x_i}{\Sigma_i^n Q_i} \qquad (2)$$

$$X_{std} = \frac{\Sigma_1^n (w_i \cdot x_i - w_i \cdot \overline{X_d})^2}{\Sigma_i^n w_i^2} \qquad (3)$$

$$X_{stdQ} = \frac{\Sigma_1^n (Q_i \cdot x_i - Q_i \cdot \overline{X_{dQ}})^2}{\Sigma_i^n Q_i^2} \qquad (4)$$

$$X_{min} = min\ (x_1, x_2, \ldots, x_n) \qquad (5)$$

$$X_{max} = max\ (x_1, x_2, \ldots, x_n) \qquad (6)$$

In these equations, (1) will be referred to as the "regular" mean, (2) as the QA-weighted mean, (3) as the regular standard deviation, (4) as the QA-weighted standard deviation, (5) as the minimum, and (6) as the maximum.

The simple statistics also include daily log regular mean, log standard deviation, log QA mean, and log QA standard deviation. These log quantities are calculated as shown in equations (1-4), except that x_1, x_2, …, x_n are replaced by their logarithms.

Regression statistics, based on the pixels within each 1° × 1° grid cell, include the slope, intercept, mean squared error (MSE), and the coefficient of determination (R^2).

The histograms and joint histograms report the counts of the pixels falling into predetermined numerical intervals.

The pixel counts are used to represent the number of pixels for the parameters that do not have QA flags, while the confidence-histograms-counts are used to represent the number of counts for each parameter that fall within each QA bin (e.g., good, very good, marginal, and total).

Definition of 8-day and Monthly Statistics

The 8-day and monthly statistics are based on the daily statistics with the assumption that the daily statistics from retrieved pixels can represent the statistics of the "populations" of each 1° × 1° grid cell. In other words, it is assumed that the samples composed of retrieved pixels can represent the "populations" composed of all the pixels within each grid cell.

The simple statistics for 8-day and monthly quantities include mean, standard deviation, and minimum and maximum values of the corresponding daily means (i.e., daily mean, daily QA mean, daily log mean, and daily log QA mean).

For example, if X_{d1}, X_{d2}, …,X_{dn} are the daily means for a Level 3 parameter, then their monthly simple statistics (i.e., mean, standard deviation, minimum, and maximum) are represented by equations (1, 3, 5, and 6) with X_i replaced by X_{di}. It should be noted that in the monthly case, the weights in equations (1) and (2) are taken either as unweighted (i.e., $w_i = 1$), pixel weighted (e.g., weighted by the number of pixels over the total pixels), or fraction weighted (e.g., weighted by the cloud fraction).

The fraction statistics represent the mean and standard deviation of the daily fraction values.

The regression statistics, which include four components (slope, intercept, mean-squared-error, and the coefficient of determination), are calculated by using the daily mean values of the first parameter versus the daily mean values of the second parameter. Therefore, two daily mean time series are used to calculate monthly regression attributes.

Histogram and joint-histogram statistics represent the number of times a parameter falls into each predefined interval.

The total counts are reported. This is simply the summation of all the counts from each interval for the parameter.

The 8-day and monthly product has an additional statistical parameter called "mean daily standard deviation." This parameter is used to represent the mean values of the daily standard deviations, such as the mean of daily standard deviation, mean of daily QA standard deviation, mean of log standard deviation, and mean of log QA standard deviation. The standard deviation of the mean is used to describe the variation of a parameter around its monthly mean, while the mean of the standard deviation is used to describe the average daily variation of a parameter. For example, a parameter may have a large daily standard deviation on each day, but those variations may be similar to each other. In this case, the mean daily standard deviation will be large, but its standard deviation will be small.

The related MODIS data product ATBDs can be found in PDF format at modis-atmos.gsfc.nasa.gov/reference_atbd.html.

Suggested Reading

Ackerman, S. A. *et al*., 1998.

Gao, B. C., and A. F. H. Goetz, 1990.

Gao, B. C. *et al*., 1993a.

Gao, B. C. *et al*., 1998.

Green, R. O., and J. E. Conel, 1995.

Gustafson, G. B. *et al*., 1994.

Hayden, C. M., 1988.

Kaufman, Y. J., and B. C. Gao, 1992.

Kaufman, Y. J., and L. A. Remer, 1994.

Kaufman, Y. J. *et al*., 1997a,b.

King, M. D. *et al*., 1992.

King, M.D. *et al*., 1996.

King, M. D. *et al*., 1998.

King, M. D. *et al*., 1999.

King, M. D. *et al*., 2003.

Kleepsies, T. J., and L. M. McMillan, 1984.

Nakajima, T. Y., and T. Nakajima, 1995.

Platnick, S. *et al*., 2000.

Prabhakara, C. *et al*., 1970.

Rao, C. R. N. *et al*., 1989.

Remer, L. A. *et al*., 1996.

Rossow, W. B., and L. C. Garder, 1993.

Saunders, R. W., and K. T. Kriebel, 1988.

Shapiro, M. A. *et al*., 1982.

Smith, W. L., and F. X. Zhou, 1982.

Smith, W. L. *et al*., 1985.

Stowe, L. L. *et al*., 1991.

Strabala, K. I. *et al*., 1994.

Sullivan, J. *et al*., 1993.

Tanré, D. *et al*., 1997.

MODIS Level 3 Atmosphere Products Summary

Coverage: Global

Spatial/Temporal Characteristics: 1.0° latitude-longitude equal-angle grid/daily, 8-day, and monthly

Key Science Applications: Climate and ecosystem monitoring and modeling, cloud radiative properties, atmospheric properties, and atmospheric corrections

Key Geophysical Parameters: Aerosol properties, cloud radiative properties, atmospheric water vapor and temperature

Processing Level: 3

Product Type: Standard, at-launch

Maximum File Size: 474.77 MB (Daily Level 3), 883.22 MB (8-day and Monthly Level 3)

File Frequency: 1/day (Daily Level 3), 1/8-day (8-Day Level 3), 1/month (Monthly Level 3)

Primary Data Format: HDF-EOS

Browse Available:
modis-atmos.gsfc.nasa.gov/ MOD08_D3/ browse.html (daily)

modis-atmos.gsfc.nasa.gov/MOD08_E3/ browse.html (8-day)

modis-atmos.gsfc.nasa.gov/MOD08_M3/ browse.html (monthly)

Additional Product Information:
modis-atmos.gsfc.nasa.gov/MOD08_D3 (daily)

modis-atmos.gsfc.nasa.gov/MOD08_E3 (8-day)

modis-atmos.gsfc.nasa.gov/MOD08_M3 (monthly)

DAAC: Goddard Space Flight Center Earth Sciences DAAC, daac.gsfc.nasa.gov

Science Team Contact: M. D. King

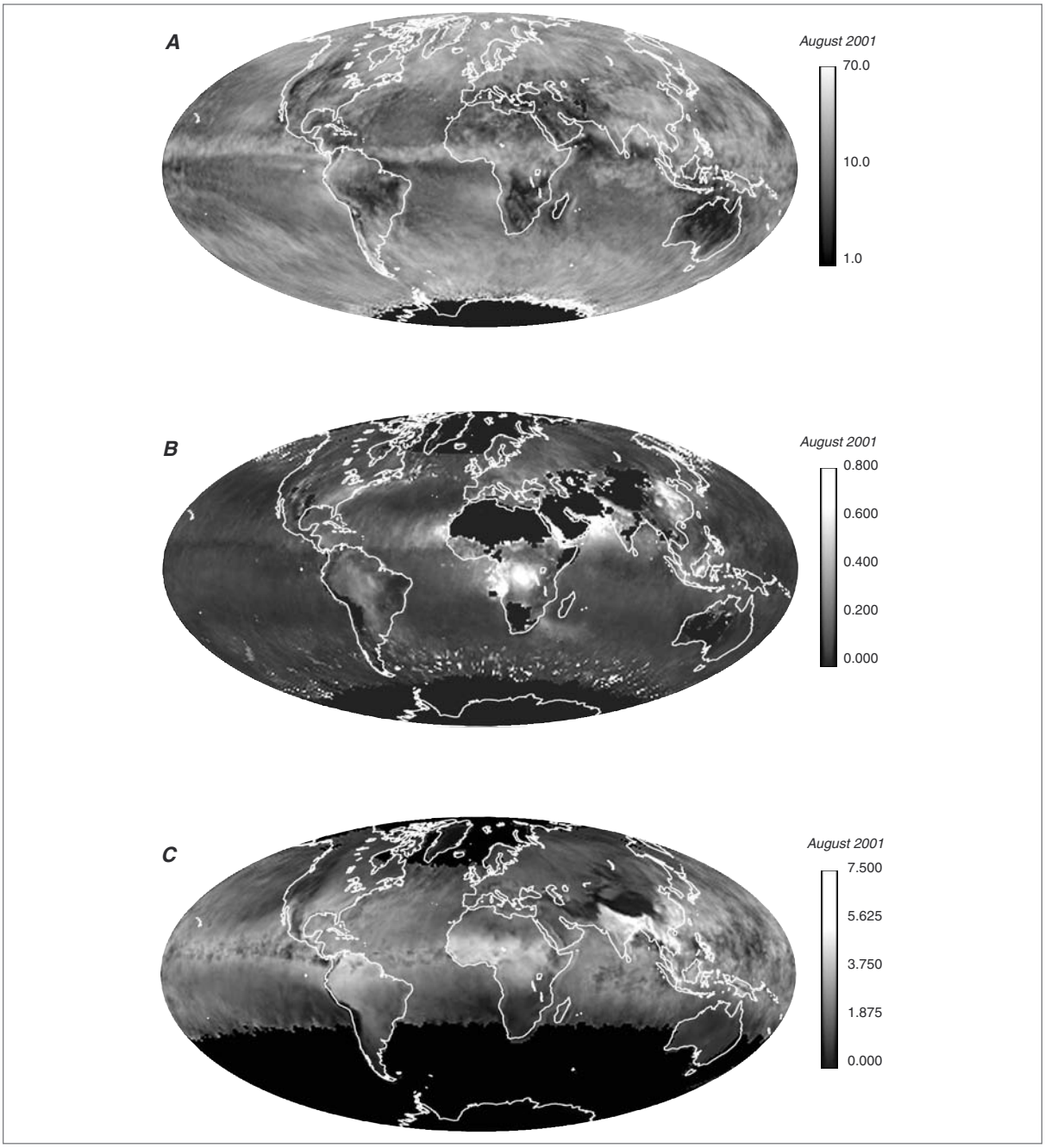

The images above depict Level 3 Atmosphere Monthly Mean for August 2001.

Figure A depicts Cloud Optical Thickness for combined water, ice, and undetermined phase clouds. Optical thickness, a unit-less parameter, is a measure of the attenuation of solar radiation through a column of atmosphere. Thicker, more opaque clouds (white) can be clearly seen over the inter-tropical convergence zone (ITCZ) and roaring 40's (latitude).

Figure B depicts Aerosol Optical Depth (AOD). Aerosols, one of the greatest sources of uncertainty in climate modeling, vary in time in space and can lead to variations in cloud microphysics, which could impact cloud radiative properties and climate. Large scale transport of dust, pollution and/or smoke can be detected moving west over the Atlantic from the Sahara; and east over the Pacific from China. Corresponding retrieved size parameters (not shown) can help identify aerosol type. It should be noted that AOD algorithms were developed for use over dark vegetation and ocean; leaving gaps in the image clearly visible over the (bright) deserts.

Figure C depicts Total Atmospheric Column Water Vapor in centimeters. Also called total column precipitable water, this parameter is derived from a near-infrared algorithm. It should be noted that the near-infrared is very sensitive to boundary-layer water vapor since it is derived from attenuation of reflected solar light from the surface. This product is essential to understanding the hydrological cycle, aerosol properties, aerosol-cloud interactions, energy budget, and climate. On the internet, visit visibleearth.nasa.gov to view a variety of MODIS data images.

MODIS Cloud Mask (MOD35)

Product Description

The MODIS Cloud Mask product (MOD35) is a daily, global Level 2 product generated at 1-km and 250-m (at nadir) spatial resolutions. The algorithm employs a series of visible and infrared threshold and consistency tests to specify confidence that an unobstructed view of the Earth's surface is observed. The 250-m cloud-mask flags are based on visible channel data but use 1-km cloud mask results as ancillary information. Radiometrically accurate radiances are required, so holes in the Cloud Mask will appear wherever the input radiances are incomplete or of poor quality.

Research and Applications

A determination of the presence of global cloudiness is essential to the MODIS mission for two reasons. First, clouds play a critical role in the radiative balance of the Earth and must be accurately described to assess climate and potential climate change. Second, the presence of cloudiness must be accurately determined to retrieve properly many atmospheric and surface parameters. For many of these retrieval algorithms even thin cirrus represents contamination.

Data Set Evolution

The MODIS cloud-mask algorithm employs a battery of spectral tests, which use methodology applied developed for the AVHRR Processing scheme Over cLoud Land and Ocean (APOLLO), International Satellite Cloud Climatology Project (ISCCP), CLoud Advanced Very high resolution Radiometer (CLAVR), and Support of Environmental Requirements for Cloud Analysis and Archive (SERCAA) to identify cloudy FOVs. From these a clear-sky confidence level (high confident clear, probably clear, undecided, cloudy) is assigned to each FOV. For inconclusive results, spatial- and temporal-variability tests are applied. The spectral tests rely on radiance (temperature) thresholds in the infrared and reflectance thresholds in the visible and near-infrared. Thresholds vary with surface type, atmospheric conditions (moisture, aerosol, etc.), and viewing geometry. Along with MOD02 calibrated radiances, a 1-km land/water mask, DEM, ecosystem analysis, and snow/ice cover maps are required as inputs.

Cloud-mask validation has been conducted using MAS data from several field campaigns, radar and lidar observations from the SGP CART site, and comparisons with cloud products from NOAA operational instruments.

The related MODIS Cloud Mask ATBD, Discriminating Clear Sky from Cloud with MODIS, can be found in PDF format at modis.gsfc.nasa.gov/data/atbd/atbd_mod06.pdf.

MODIS Cloud Mask Summary

Coverage: Global

Spatial/Temporal Characteristics: 250 m and 1 km/daily

Key Science Applications: Cloud determination and screening, climate modeling, climate monitoring, increasing accuracy of other MODIS retrievals

Key Geophysical Parameters: Presence of cloud

Processing Level: 2

Product Type: Standard, at-launch

Maximum File Size: 47.42 MB

File Frequency: 288/day

Primary Data Format: HDF-EOS

Additional Product Information: modis-atmos.gsfc.nasa.gov/MOD35_L2/index.html

DAAC: Goddard Space Flight Center Earth Sciences DAAC, daac.gsfc.nasa.gov

Science Team Contacts: W. P. Menzel, S. A. Ackerman

Suggested Reading

Ackerman, S. A. *et al*., 1998.

Gao, B. C. *et al*., 1993a.

Gao, B. C. *et al*., 2002a,b.

Gao B. C. *et al*., 2003.

Gao, B. C. and Y. J. Kaufman, 2003.

Gustafson, G. B. *et al*., 1994.

King, M. D. *et al*., 1998.

King, M. D. *et al*., 2003.

Platnick, S. *et al*., 2003.

Rossow, W. B., and L. C. Garder, 1993.

Saunders, R. W., and K. T. Kriebel, 1988.

Stowe, L. L. *et al*., 1991.

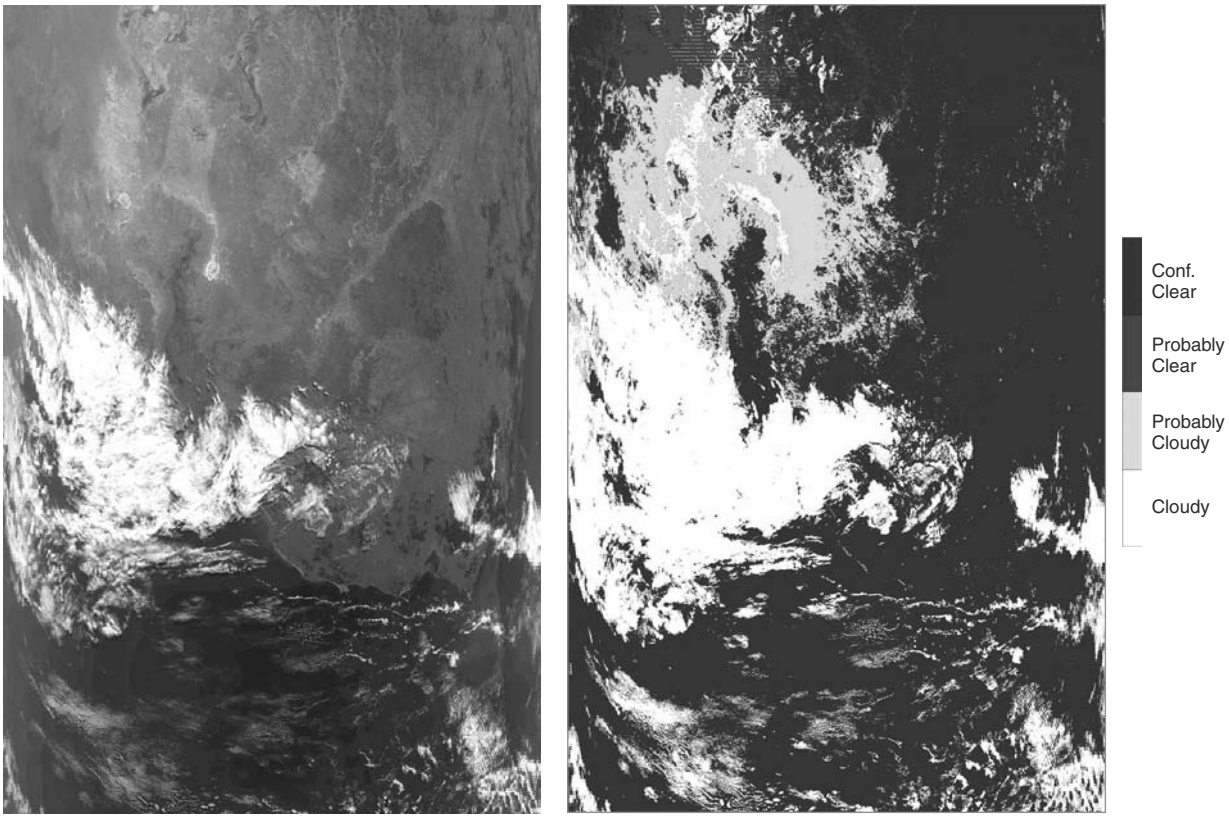

These images depict L1B (left) and Unobstructed FOV Cloud Mask (right) from August 1, 2002. Visible image and corresponding cloud mask for a scene over eastern Australia. A determination of the presence of global cloudiness is essential to the MODIS mission for two reasons. First, clouds play a critical role in the radiative balance of the Earth and must be accurately described to assess climate and potential climate change. Second, the presence of cloudiness must be accurately determined to properly retrieve many atmospheric and surface parameters. For many of these retrieval algorithms even thin cirrus represents contamination. On the internet, visit visibleearth.nasa.gov to view a variety of MODIS data images.

Chapter 7

Lightning

TRMM
LIS

Lightning – An Overview

Relationship to Global Change

Understanding lightning is a way to understand the interplay of some key components of atmospheric dynamics. Lightning is closely coupled to storm convection dynamics and can be correlated to the global rates, amounts, and distribution of convective precipitation. It points to where strong convection is occurring, when large quantities of water are growing in the mixed phase regions of storms, and suggests how latent heat is being released during the storm's life cycle. Since the microscales on which particles interact to generate electricity are coupled through storm-scale processes to synoptic-scale systems, lightning activity should provide information on the development of the atmosphere over many scale sizes, especially in the tropics.

The Lightning Imaging Sensor (LIS) on the TRMM Observatory is designed to detect, locate, and measure the intensity of lightning for scientific investigation of the distribution and variability of total lightning over the Earth and to increase our understanding of the Earth's atmosphere system. LIS provides a global lightning and thunderstorm climatology from which changes (even subtle temperature variations) might be detected. These data are used in a variety of global change studies, including cloud characterization, hydrologic cycle studies, storm convection, microphysics and dynamics, and the seasonal and interannual variability of thunderstorms.

LIS represents a significant advance over any previous satellite-borne lightning detectors. Those instruments could provide only a relative global distribution of lightning of a strictly statistical, and often biased, nature. Additionally, they required collecting data for long periods of time before they could be meaningfully interpreted in terms of global distributions. It was not possible to compare the lightning frequency of a particular storm with the earlier estimates. Lightning observations from LIS can be readily associated with the thunderstorms that produce them, and the detection of even a single discharge is significant and provides important information (e.g., storm location, precipitation estimates, storm height, the presence of ice, lightning frequency, electrical output, etc.).

LIS has been designed to study the distribution and variability of total lightning on a global basis. Its staring imager is optimized to locate and detect lightning with storm-scale resolution of 5-10 km over a large region (600 × 600 km) of the Earth's surface. The field of view (FOV) is sufficient to observe a point on the Earth or a cloud for 83 seconds, adequate to estimate the flashing rate of many storms. This makes it possible to estimate lightning frequency even for storms with flash rates as low as 1-2 discharges per minute.

Product Interdependency and Continuity with Heritage Data

During the 1980s, extensive optical and electrical observations of lightning were made from high-altitude NASA U-2 aircraft with the primary objective of defining a baseline design criterion for a space sensor capable of mapping lightning discharges from geostationary orbit during day and night, with high spatial resolution and high detection efficiency. The results, combined with parametric trade-off studies and other research, have clearly established the feasibility of making this kind of lightning measurement from space with present state-of-the-art technology.

Global lightning signatures from the Defense Meteorological Satellite Program (DMSP) Optical Linescan System (OLS) have been analyzed from the filmstrip imagery and digital DMSP tapes archived at the NOAA National Geophysical Data Center (NGDC) National Snow and Ice Data Center in Boulder, Colorado. This global lightning database is a useful reference data set for LIS.

Prior to, and during the TRMM mission, space-based lightning observations had been provided by the Optical Transient Detector (OTD), launched in April 1995 as a secondary payload on a Pegasus launch vehicle. The OTD mission ended in April 2000.

In a near-polar orbit, OTD detected all types of lightning events, including cloud-to-ground, cloud-to-cloud, and intra-cloud. Considered to be a LIS prototype, OTD data populated a database of global lightning activity to which LIS data are being added.

Suggested Reading

Boccippio, D. J. *et al*., 1998.

Boccippio, D. J. *et al*., 2000.

Boccippio, D. J. *et al*., 2000a,b.

Boccippio, D. J. *et al*., 2002.

Buechler, D. E. *et al*., 2000.

Christian, H. J. *et al*., 1999.

Christian, H. J. *et al*., 2000.

Christian, H. J. *et al*., 2003.

Del Genio, A. D. *et. al*., 2002.

Goodman, S. J. *et al*., 2000.

Koshak, W. J. *et al*., 2000.

Kummerow, C. *et al*., 1998.

Kummerow, C. *et al*., 2000.

Peterson, W. A. *et al*., 2001.

Thomas, R. J. *et al*., 2000.

Toracinta, R. E. *et al*., 2002.

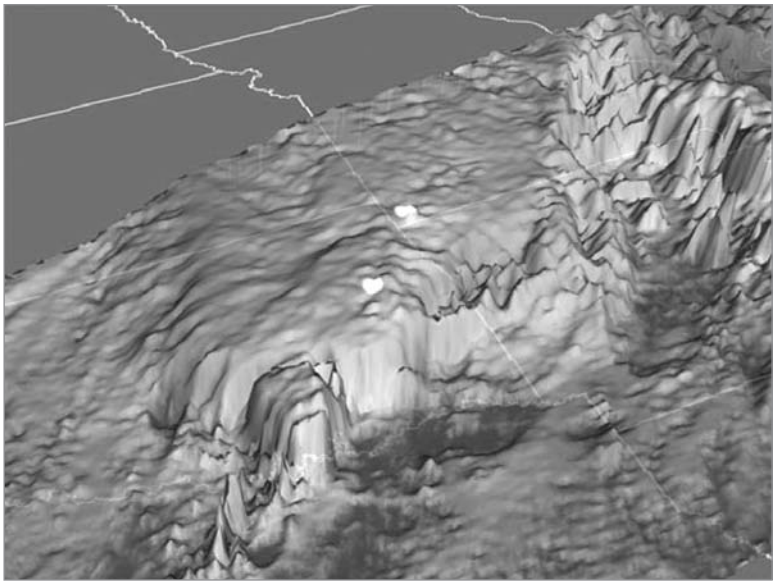

In this image, lightning flashes (bright white spots)—recorded during the NASA Lightning Imaging Sensor's pass over storms moving through Oklahoma in October 1998—are overlaid on high-resolution infrared cloud-top data from the orbiting Tropical Rainfall Measuring Mission (TRMM) satellite. High flash rates visible in the heaviest storm areas may indicate the potential for tornado formation. With an optical sensor locked into geostationary orbit over the Earth, such useful information would be available continuously to meteorologists and other professional stormwatchers. On the internet, visit visibleearth.nasa.gov to view a variety of LIS data images.

Lightning Imaging Sensor Product (LIS02-LIS18)

Product Description

TRMM LIS products of Level 1 and higher are contained in data granules corresponding to individual orbits; segmented at the southernmost nadir point of each orbit. Level 1, 2, and 3 data are included in each granule. Level 2 and higher products primarily consist of aggregation of the primary LIS observable (CCD pixel events) into variables corresponding to lightning strokes, flashes, and thunderstorm cells. Hierarchical links between the levels are included, as well as all data required to recompute Level 2 and 3 products from Level 1 data using alternative algorithms. Data subelements are organized functionally in orbit granules, rather than by processing level (i.e., some data containers may contain more than one level of data).

Level 1 data include events (pixel amplitudes which exceed a threshold for 2 ms), viewtime granules (discretized volumes of x, y, t sampling space denoting actual LIS viewing), navigation data (transform matrices needed to geolocate individual pixel events) and diagnostic data (calibration tables and warning or fatal error flags for a variety of instrument, platform, environmental and processing algorithm conditions). Pixel events are tagged with CCD and geolocated location, amplitude, calibrated radiance, time, applied threshold, and other parameters. Viewtime granules include location on a fixed 0.5° × 0.5° registration grid, start and end viewing times, and adjustments for partial grazing by the LIS FOV. Navigation and diagnostic data are reported every one second.

Level 2 data include groups (adjacent pixel events that are concurrent in time, corresponding to lightning strokes), flashes (spatially and temporally proximate groups, corresponding to true lightning flashes) and areas (spatially proximate flashes, intended to isolate thunderstorm cells from lightning-only data). Each of these products includes links to its subcomponents and its parent under the aggregation algorithms, and includes derived parameters (e.g., net calibrated radiance, total spatial footprint, automated quality/confidence flags, etc.).

Level 3 data include raster browse images and summary vector data, the latter reported in one second intervals and organized in the same data record as navigation and diagnostic data. Level 1 and 2 data are used to produce equal-angle maps of lightning activity, controlled for total and diurnal sampling and cross-calibrated with antecedent and concurrent OTD data.

Granules are organized structurally into orbit summary, point data, and continuous (one-second) data records. Point data include the Level 1 view-time data and all lightning data (Level 1 events and Level 2 groups, flashes, and areas). One-second data include both Level 1 navigation and diagnostic data and Level 3 vector data.

Research and Applications

LIS views a total area exceeding 600 km × 600 km at the cloud top using a 128 × 128 photodiode array. Individual storms and storm systems are monitored for 83 seconds, a period long enough to obtain a measure of the lightning flash rate while the storm is in the field of view of the sensor. This makes it possible to estimate lightning frequency even for storms with flash rates as low as 1-2 discharges per minute. LIS represents a significant advance over any previous satellite-borne lightning detector. Lightning observations from LIS can be readily associated with the thunderstorms that produce them, and the detection of even a single discharge is significant and provides important information (e.g., storm location, precipitation estimates, storm height, the presence of ice, lightning frequency, electrical output, etc.). The earlier satellite-borne lightning instruments provided only a relative global distribution of lightning of a strictly statistical nature; this required collecting data for long periods of time before it could be meaningfully interpreted in terms of global distributions. It was not possible to determine the lightning frequency of a particular storm as compared with the earlier estimates.

Data Set Evolution

NASA U-2 aircraft lightning detection data were collected in order to provide a baseline for future satellite-based lightning instruments. Based on a combination of the results of U-2 data and advances in technology, the OTD has been able to begin establishing a database of lightning observations from a near-polar orbit at a 70° inclination, at an altitude of 740 km, and with a FOV of 1300 km × 1300 km. LIS data sets will further build upon OTD with a FOV of 600 km × 600 km and a storm-scale resolution of 5-10 km.

LIS Product Summary

Coverage: Global, 35°N to 35°S

Spatial/Temporal Characteristics: 4 km × 4 km pixel at nadir, orbit granules, 2 ms resolution; 2.5 × 2.5 monthly, 47-day moving average

Key Science Applications: Thunderstorm distribution and variability, rainfall mapping and thunderstorm analysis

Key Geophysical Parameters: Lightning events, groups, flashes, areas

Processing Level 1B Products:
LIS02 – Image Attributes
LIS03 – Events Statistics
LIS04 – Group Statistics

Processing Level 2 Products:
LIS05 – Flash Statistics
LIS06 – Area Statistics
LIS07 – Flash Density
LIS08 – 2.5° × 2.5° Equal Angle Monthly Grid
LIS09 – 500 km × 500 km Equal Area Monthly Grid

Processing Level 3 Products:
LIS10 – Orbit Attributes
LIS11 – Threshold Attributes
LIS12 – Browse Area
LIS13 – Vector Statistics
LIS14 – Metadata Description
LIS15 – Summary Data
LIS16 – Flash Rate Data
LIS17 – Ephemeris
LIS18 – Event Rate Sets

Product Type: Standard, at-launch

Maximum File Size:
Level 1B Background Data - 5.54 MB
Level 2 Science Data - 1.93 MB
Level 3 Browse and Summary Data - .04 MB

File Frequency: 1/orbit

Primary Data Format: HDF-EOS

Browse Available: Yes (GIF format)

Additional Product Information:
thunder.nsstc.nasa.gov/data/

DAAC: Global Hydrology Resource Center, ghrc.msfc.nasa.gov

Science Team Contacts: H. Christian, S. Goodman, D. Boccippio

Chapter 8

Atmospheric Chemistry

Terra
MOPITT

Atmospheric Chemistry – An Overview

Relationship to Global Change Issues

In recent years, increasing concern has focused on the natural and anthropogenic alteration of the Earth's environment and how these activities impact global change. Human activities are changing the concentrations of trace constituents in the troposphere; these in turn affect the radiative balance, dynamics, and chemistry of the atmosphere. One of the most pressing global change issues facing researchers and policymakers today involves the greenhouse effect and potential global warming. Carbon dioxide, nitrous oxide, methane, and chlorofluorocarbons (CFCs) are the principal anthropogenic greenhouse gases that are responsible for this effect. Of these, carbon dioxide has the highest concentration and plays the most significant role. However, the other gases are more efficient (on a per molecule basis) at trapping infrared radiation, and their combined effects are almost as large as that of carbon dioxide, even though their concentrations are much smaller. Ozone also proves significant, because the catalytic chemical process involved in its breakdown in the stratosphere and its increasing tropospheric concentrations have a multifaceted influence on the Earth's radiative balance.

Within the Terra timeframe, the primary objective of studies in tropospheric chemistry is understanding the interaction with the surface/ocean/biomass systems, atmospheric transports, and the carbon cycle. The particular focus is the time evolution of the distributions of carbon monoxide (CO) and methane (CH_4) in the troposphere. The scientific questions become convoluted when considering the sources, chemistry, and ultimate sinks of minor atmospheric constituents and their interrelationships. The planet's inorganic and organic matter are the sources of many of these gases, increasing the importance of land-surface studies to determine emission rates and locations. Yet, the large-scale and seasonal distribution of these sources remains poorly understood. Space-based remote sensing provides the ideal platform for global monitoring of trace gas sources.

Whether the changes are anthropogenic or naturally occurring, understanding these changes in the trace chemical makeup of the troposphere is a critical component in anticipating global climate change. On Terra, the Measurements of Pollution in The Troposphere (MOPITT) instrument investigates the evolution of tropospheric trace and greenhouse gases and their interaction with the climate and biosphere. Along with trace gas measurements, studies of greenhouse gases also require information from additional disciplines (e.g., ocean color, biomass burning, and land vegetation). Data products associated with those discipline areas are described in other sections of this document. Finally, knowledge is required of the regional increases in tropospheric ozone as well as the decrease in stratospheric ozone.

Product Overview

Key to our understanding of the horizontal and vertical measurements of the troposphere is the measurement of CO and CH_4.

Carbon monoxide possesses a lifetime, on the order of two months, such that the CO is moved around on a regional scale, and thus performs the function of a chemical tracer. In addition to horizontal transport, studies have shown that there is considerable vertical transport of CO, pointing to the use of 3-D measurements, which could be used to study chemical transport processes in the troposphere. MOPITT CO data, along with data from other instruments, are used in modeling efforts by several researchers to advance our understanding of global tropospheric chemistry and its relationship to sources, sinks, and atmospheric transports.

The full range of the effects of the increased concentration of CO are not fully understood at present, but it is believed that CO is photochemically active and plays a major role in the concentration of OH radicals in the troposphere. The OH radical acts as a "cleansing agent" in the troposphere, oxidizing many compounds. Satellite observations may clarify whether CO is increasing or decreasing. Increases in CO are likely to be the result of a rise in human activities. Increases in CO may deplete tropospheric radicals, thereby reducing the yearly removal of many natural and anthropogenic trace species. In particular, this effect may add to the increase of CH_4, which in turn could further reduce OH concentration. Increased CO may also indirectly intensify global warming and perturb stratospheric ozone by increasing the lifetime of other trace greenhouse gases. Greenhouse gases are those chemicals that permit the influx of solar radiation to the surface below, but inhibit to some degree longwave radiation leaving the Earth, producing a net warming effect.

The MOPITT data set also addresses the measurement of CH_4. Methane is the most abundant hydrocarbon in the atmosphere and possesses several infrared absorption bands, including one at approximately 7.7 μm, which lies in an atmospheric

window with no significant absorption by other gases. This wavelength is also close to the peak radiating temperature of terrestrial thermal radiation (about 250 K), making the gas a strong contributor to the so-called "greenhouse effect." Moreover, CH_4 currently appears to be increasing at a rate of one percent per year, but the source of this increase is not certain, and there is evidence that it began decelerating during the 1980s. Improved knowledge of the source strengths and distributions will help to resolve this uncertainty. Knowledge of the global column distribution of CH_4 taken with dynamical data may lead to a better quantitative understanding of its biogeochemical cycles. The Level 2 CH_4 data set may be used to produce Level 3 global grids, which, in turn, may be used to develop regional and seasonal averages and other special products.

Measurements from the Terra platform are useful in observing the distribution and variation of the sources of CH_4. While ground-based observations tend to generate a specified accuracy over time, they cannot observe the spatial and temporal variations of the sources that are of most interest at present. Studies conducted in conjunction with other measurements of meteorological conditions (such as local wind speed and direction) may determine the source magnitude from the atmospheric perturbations to the background amount. The combination of space-based and *in situ* measurements can be synthesized with other databases of gaseous concentrations and emissions into global climate models for a better understanding of the overall problem.

In addition to the MOPITT product, Total Ozone Burden (a parameter in MOD07) measures total column ozone to monitor the potential environmental hazard of anthropogenic ozone depletion, and to help develop and use atmospheric correction models.

Product Interdependency and Continuity with Heritage Data

The MOPITT instrument heritage includes the Nimbus-7 Stratospheric and Mesospheric Sounder (SAMS) instrument and the Improved Stratospheric and Mesospheric Sounder (ISAMS) instrument on UARS, which employed correlation spectroscopy systems similar to that employed by MOPITT. Currently operating stratospheric instruments such as TOMS and others onboard UARS are helping scientists learn about the exchange of trace gases between the stratosphere and troposphere. Prior to the launch of Terra, surface fluxes of some land- and ocean-derived trace gases were estimated using AVHRR and SeaWiFS observations and 4-D data assimilation.

Suggested Reading

Brasseur, G. P., and R. G. Prinn, 1992.

Brenninkmeijer, C. A. M. *et al.*, 1992.

Chicano, R. J., and R. S. Oremland, 1988.

Crutzen, P. J., 1991.

Dickerson, R. R. *et al.*, 1987.

Dlugokencky, E. J. *et al.*, 1994.

Drummond, J. R., 1992.

Novelli, P. C. *et al.*, 1994.

Reichle, Jr., H. G. *et al.*, 1989.

Steele, L. P. *et al.*, 1992.

Wofsy, S. C. *et al.*, 1972.

MOPITT CO Profile, CO Column, and CH_4 Column Data (MOP02)

Product Description

The carbon monoxide (CO) vertical profile and CO column data, along with methane (CH_4) total column, make up the three parameters of the MOPITT Level 2 product. The parameters are retrieved daily over the globe with methane column measurements available only in the sunlit portion. Horizontal resolution is variable from 22 km to ~100 km, depending on cloud clearing and pixel averaging, to maintain high signal to noise. The profile vertical resolution is about 4 km in the troposphere. CO profile and total column precision have been shown to be 10%. Methane column precision is expected to be one percent.

Research and Applications

Global CO measurements are very important because of the role of the gas in the extremely complicated chemical balance of the troposphere. Most of the chemistry in this region of the atmosphere is induced by the chemical activity of the hydroxyl and similar radicals. These agents react rapidly with many trace gases of both natural and anthropogenic origin preventing their buildup in the troposphere through the creation of chemical products that are rained out or lost from the atmosphere by dry deposition. However, the concentrations of these radicals are extremely difficult to measure due to their short lifetimes and low concentrations. The major agents regulating the concentrations of the radicals are carbon monoxide, ozone, and nitrogen oxide. Global CO measurements used in conjunction with atmospheric chemical models therefore provide an important measure of assessing the ability of the atmosphere to "cleanse" itself.

The Level-2 carbon monoxide parameters also are used to produce Level 3 global grids, which in turn may be used to develop regional and seasonal averages and other special products. These data products provide a time evolution of the distribution of CO in the troposphere. From these a better knowledge of the chemical interactions, transports, sources, and sinks is obtained. Understanding their biogeochemical cycles and the intimate interrelation with other gases and the climate will lead to better predictions of possible effects of anthropogenic activities.

Measurements from the Terra platform are extremely useful in resolving the temporal and spatial variations in CH_4 not observable by ground-based networks. Knowledge of the global column distribution of methane taken with dynamical data may lead to a better quantitative understanding of its biogeochemical cycles. The Level 2 methane data set may be used in the future to produce Level 3 global grids, which, in turn, may be used to develop regional and seasonal averages and other special products.

The global distribution of these profiles and column amounts are used in descriptive studies of these gases on a global basis, providing the first detailed information on their horizontal, vertical, and temporal variations, and their relationships to other activities such as biomass burning, industrial activity, thunderstorm venting of the boundary layer, etc. There is also a wide variety of temporal and spatial scales involved. By observing the sources, their magnitudes, and their variation we could learn a considerable amount about the interaction of the surface and the troposphere. By monitoring the magnitude of the sinks, in conjunction with atmospheric chemical models, we learn about the chemistry of the troposphere.

Data Set Evolution

The products are derived from measurements of both thermal upwelling radiation and the attenuation of solar radiation by atmospheric carbon monoxide and methane. Absorption due to CO or CH_4 is discriminated from other gases by means of length modulator cells containing known amounts and pressures of the gases. A fast-forward radiance model is used by the data processing algorithm to compute average and difference signals for known states of the atmosphere. The algorithm adjusts the CO and CH_4 amounts to bring the computed radiances into agreement with the observed. Ancillary data from the National Centers for Environmental Prediction (NCEP) are used to specify the atmospheric temperature and water vapor content in the calculations.

The particular instrument and algorithm configuration described here has not been previously applied. However, the maximum likelihood retrieval scheme has been successfully utilized in several space missions remotely measuring atmospheric chemical species. The use of correlation radiometry to determine concentrations of CO in the mid troposphere has been successfully demonstrated by the Measurement of Air Pollution from Satellites (MAPS) instrument, which has been flown aboard the Space Shuttle several times. The approach of using reflected solar radiation to determine the total column amounts of an atmospheric gas has been successfully used many

times. Perhaps the most notable application has been with NASA's Total Ozone Mapping Spectrometer (TOMS), first deployed on the Nimbus-7 satellite.

Suggested Reading

Brasseur, G. P., and R. G. Prinn, 1992.

Brenninkmeijer, C. A. M. *et al*., 1992.

Cicerone, R. J., and R. S. Oremland, 1988.

Clerbaux, C. *et al*., 2002.

Crutzen, P. J., 1991.

Deeter, M. N. *et al*., 2002.

Deeter, M. N. *et al*., 2003.

Dickerson, R. R. *et al*., 1987.

Dlugokencky, E. J. *et al*., 1994.

Drummond, J. R., 1992.

Drummond, J. R., and G. S. Mand, 1996.

Edwards, D. P. *et al*., 1999.

Edwards, D. P. *et al*., 2003.

Emmons, L. K. *et al*., 2003.

Granier, C. *et al*., 1992.

Lamarque, J. F. *et al*., 2003.

MOPITT Science Team, 1996.

Muller, J. F., and G. P. Brasseur, 1995.

Novelli, P. C. *et al*., 1994.

Pan, L. *et al*., 1995.

Pan, L. *et al*., 1998.

Reichle, Jr., H. G. *et al*., 1989.

Smith, M. W., and S. R. Shertz, 1996.

Steele, L. P. *et al*., 1992.

Wang, J. *et al*., 1999a,b.

Wang, J. *et al*., 2000.

Warner, J. X. *et al*., 2001.

Wofsy, S. C. *et al*., 1972.

Zander, R. P. *et al*., 1989.

MOPITT CO Profile, CO Column and CH_4 Column Data Product Summary

Coverage: Global

Spatial/Temporal Characteristics: CO profiles retrieved daily, day and night; column amounts retrieved daily in sunlit portion of orbits; resolution 22 km with some degradation depending on cloud clearing and pixel averaging

Key Geophysical Parameters: Atmospheric total column carbon monoxide; tropospheric vertical profile of carbon monoxide; atmospheric total column methane

Key Science Applications: Biogeochemical modeling, tropospheric chemical modeling, and greenhouse gas modeling

Processing Level: 2

Product Type: Standard, at-launch

Maximum File Size: 35 MB

File Frequency: 1/day

Primary Data Format: HDF-EOS

Browse Available: Yes

Additional Product Information: www.eos.ucar.edu/mopitt/index.html

www.atmosp.physics.utoronto.ca/MOPITT/home.html

DAAC: Langley Atmospheric Sciences Data Center, eosweb.larc.nasa.gov

Science Team Contact: J. R. Drummond

Chapter 9

Surface Temperatures of Land and Oceans, Fire Occurrence, and Volcanic Effects

Terra
ASTER
MODIS

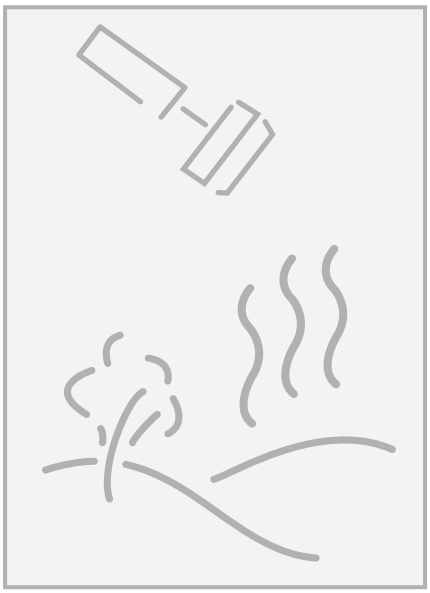

Surface Temperatures of Land and Oceans, Fire Occurrence, and Volcanic Effects – An Overview

Relationship to Global Change Issues

The surface temperature of the land and ocean is a parameter that determines the vigor of biogeochemical activity and the rate of heat flow and water transport between the surface and the atmosphere. These in turn influence global environmental processes. On land, soil and canopy temperature are among the main determinants of the rate of growth of vegetation, and they govern seasonal starting and termination of growth. Hydrologic processes such as evapotranspiration and snow and ice melt are highly sensitive to surface temperature fluctuation. In addition, surface temperature has been shown to be an important discriminating factor in classification of land surface types, which supports the global land cover type product. For the oceans, the surface temperature influences the rate of growth of phytoplankton, the rate of absorption of carbon dioxide and other gases by sea water, and the rate of flow of heat to and from the atmosphere. Thus, temperature products are key inputs to many of the EOS product algorithms as well as providing data for global temperature mapping and change observation.

In the ocean, phytoplankton chemically fix carbon through photosynthesis, which takes in dissolved carbon dioxide in sea water and produces oxygen that enables phytoplankton to grow. This process captures about an equal amount of carbon as does photosynthesis by land vegetation. Changes in the amount of phytoplankton indicate the change in productivity of the oceans and provide a key ocean link for global climate change monitoring. Ocean and land biological productivity, heat exchange, and water exchange processes are tightly coupled; global change models take all interactions into account in global climate change prediction. In addition, these annual productivity products can be used for global- and regional- scale studies of ocean productivity, for comparisons with annual summations of daily analytic algorithms, and for comparison of global biogeochemical models to continually improve the technology for global change analysis.

The need also exists for information on the occurrence of fires on the land surface, since fire changes the surface cover type and releases gases and particulate matter into the atmosphere, affecting ecosystems and atmospheric chemistry on a rapid and intense scale. The burning of oil slicks on water is also a significant, albeit infrequent, intense input into the land and atmosphere systems that are monitored by the fire product.

Monitoring volcanic activity is important because of the disastrous geophysical consequences volcanic eruptions have on the Earth's atmosphere, including increased precipitation, ozone destruction, and the lowering of global temperatures. Moreover, cooling of the middle and upper stratosphere—from the increase in reflectivity caused by aerosols and the reduced absorption of ultraviolet light (because of reduced ozone from volcanoes and other sources)—plays a significant role in climate change.

What Must be Measured?

Surface temperature algorithms require calibrated radiances as a basic input. Since the radiances observed have passed through the atmosphere, corrections must be made for atmospheric attenuation and scattering, hence meteorological data on temperature and water vapor profiles, as well as chemical constituents, are needed. Also, the radiance emitted by the surface is determined by surface emissivity as well as temperature. The land surface pixel can contain a mixture of materials having different emissivity, geometric, and topographic characteristics that must be known before temperature can be computed. Land material emissivity also can have significant variability as a function of wavelength, and for the mid-wave IR bands significant reflectance can exist such that solar reflected energy must be predicted and removed from the observed radiance. The emissivity of the sea surface is assumed to be unity and the sea-surface temperature algorithm in this case produces what is called the brightness temperature. The ancillary information needed is supplied by external sources and precomputed databases keyed on surface material provided by the land-cover-type product and the global ocean masks.

Fire detection and measurement must be implemented with sensor bands that do not saturate at fire temperatures. This requirement is met with MODIS by a special fire channel that saturates at 500 K, which provides sufficient range to segment fire intensity. ASTER temperature data are used in combination with the MODIS global fire data for high-resolution mapping of fires and in the monitoring and analysis of volcanic processes.

Product Overview

The EOS land and ocean surface temperature and fire products are provided by MODIS and ASTER instruments. The MODIS land surface temperature product (MOD11) provides the needed composite temperature of each pixel and the estimated emissivity from database information plus adjustments made possible by the multiwindow algorithm. The accuracy is better than 1 K for materials with known emissivities. The ASTER surface temperature product (AST05, AST08) has high spatial resolution and will be used for comparison and validation of the MODIS temperature products and for the monitoring and analysis of volcanic processes. The sea surface temperature (MOD28) derived from radiance measurements is an estimate of the skin temperature (top millimeter) of the 1-km pixel viewed by MODIS. The algorithm is similar to the land surface temperature algorithm in that it uses multiple atmospheric window techniques to estimate the atmospheric parameters that are required to compensate for absorption and scattering. The bulk temperature of the near-surface ocean is the temperature of the upper 10-20 cm to 1 meter as measured by conventional thermometers on buoys and ships. Extensive analysis has been done of satellite and *in situ* data to enable the algorithm to estimate bulk temperature as well as skin temperature.

The thermal anomaly product (MOD14, MOD40) contains information unique to understanding the characteristics of fires, including energy emitted, brightness temperature, and the ratio of smoldering to flaming area and is available for both day and night periods. The composites produced include a monthly, day and night fire occurrence aggregation and a summary of the number of fires in classes related to the strength of the fire. The ASTER land surface temperature product will provide high resolution mapping of fires as a complement to MODIS global fire data.

Product Interdependency and Continuity with Heritage Data

The land surface temperature product requires MODIS calibrated radiances and the cloud mask product as inputs. Also, atmospheric temperature and water vapor profiles are needed along with a database of emissivities, the use of which is driven by the land cover classification products that enable surface material to be specified for each pixel. The land surface temperature product from ASTER is needed for comparison and spatial variation analysis of the MODIS land surface temperature product over test sites. The land surface temperature product is an input to other land products including vegetation indices, evapotranspiration, and net primary production and as a background temperature estimate for the fire product.

Similarly, the sea surface temperature product uses MODIS calibrated radiances and the cloud mask product, but does not require the complex emissivity estimation databases and algorithms that the land surface temperature product needs. Sun glint is a significant source of error in the mid-wave IR bands, so the mask product is critical to identifying glint pixels as is sea surface wind ancillary data that are used to estimate the magnitude of the glint area radiance.

Existing meteorological stations on land and ship and buoy-based instruments at sea measure surface temperatures at large numbers of worldwide locations; however, these measurements are not adequate in terms of the radiative phenomenon or spatial coverage. Land- and sea-surface temperature data taken by TRMM and Terra add to the valuable input already provided by AVHRR, HIRS, Landsat, CZCS, and SeaWiFS, providing a large, long-term global land and sea surface temperature data set in order that we may more fully understand the effects of the various Earth-system cycles on temperature.

Suggested Reading

Asrar, G., and J. Dozier, 1994.

Becker, F., 1987.

Chahine, M. T., 1980.

Justice, C. O., and S. A. Korontzi, 2001.

Kaufman, Y. J. *et al*., 1991.

Price, J. C., 1983.

Robinson, J. M., 1991.

Running, S. W. *et al*., 1994.

ASTER Surface Emissivity (AST05) and Surface Kinetic Temperature (AST08)

Product Description

This Level 2 product (AST05) contains surface emissivity at 90-m resolution generated only over the land from ASTER's five thermal-IR channels. Surface emissivity is required to derive land-surface temperature (AST08) data, also at a resolution of 90 m. Land surface temperatures are determined from Planck's Law, using the emissivities to scale the measured radiances after correction for atmospheric effects. Pixels classified as "cloud" will have no atmospheric correction due to a lack of knowledge of cloud height, and the cloud temperature will be given as the brightness temperature at sensor.

Research and Applications

The emissivity product is critical for deriving land surface temperatures. It is therefore important in studies of surface energy and water balance. The emissivity product is also useful for mapping geologic and land-cover features. The derived land surface temperature has applications in studies of surface energy and water balance. Temperature data will be used in the monitoring and analysis of volcanic processes; day and night temperature data will be used to estimate thermal inertia; and thermal data will be used for high-resolution mapping of fires as a complement to MODIS global fire data.

Data Set Evolution

Current sensors provided only limited information useful for deriving surface emissivity, and researchers currently are required to use emissivity surrogates such as land-cover type or vegetation index in making rough estimates of emissivity and hence land surface temperatures. The five thermal-IR channels of the ASTER instrument enable direct surface emissivity estimates. Mapping of thermal features from optical sensors such as Landsat and AVHRR has been used for many developmental studies. These instruments, however, lack the spectral coverage, resolution, and radiometric accuracy that will be provided by the ASTER instrument.

Suggested Reading

Dozier, J., and Z. Wan, 1994.

Hook, S. J. *et al*., 1992.

Gillespie, A. *et al*., 1998.

Ogawa, O. *et al*., 2003.

Kahle, A. B., 1986.

ASTER Surface Emissivity and Surface Kinetic Temperature Summary

Coverage: Regional, land surface

Spatial/Temporal Characteristics: 90 m

Key Science Applications: Local heat balance, volcanology, biomass burning, thermal inertia

Key Geophysical Parameters: Surface emissivity, surface temperature

Processing Level: 2

Product Type: Standard, on request

Maximum File Size: 9 MB (Surface Emissivity), 4 MB (Surface Kinetic Energy)

File Frequency: On demand

Primary Data Format: HDF-EOS

Additional Product Information: edcdaac.usgs.gov/aster/asterdataprod.html

DAAC: EDC Land Processes DAAC, edcdaac.usgs.gov

Science Team Contact: A. Gillespie

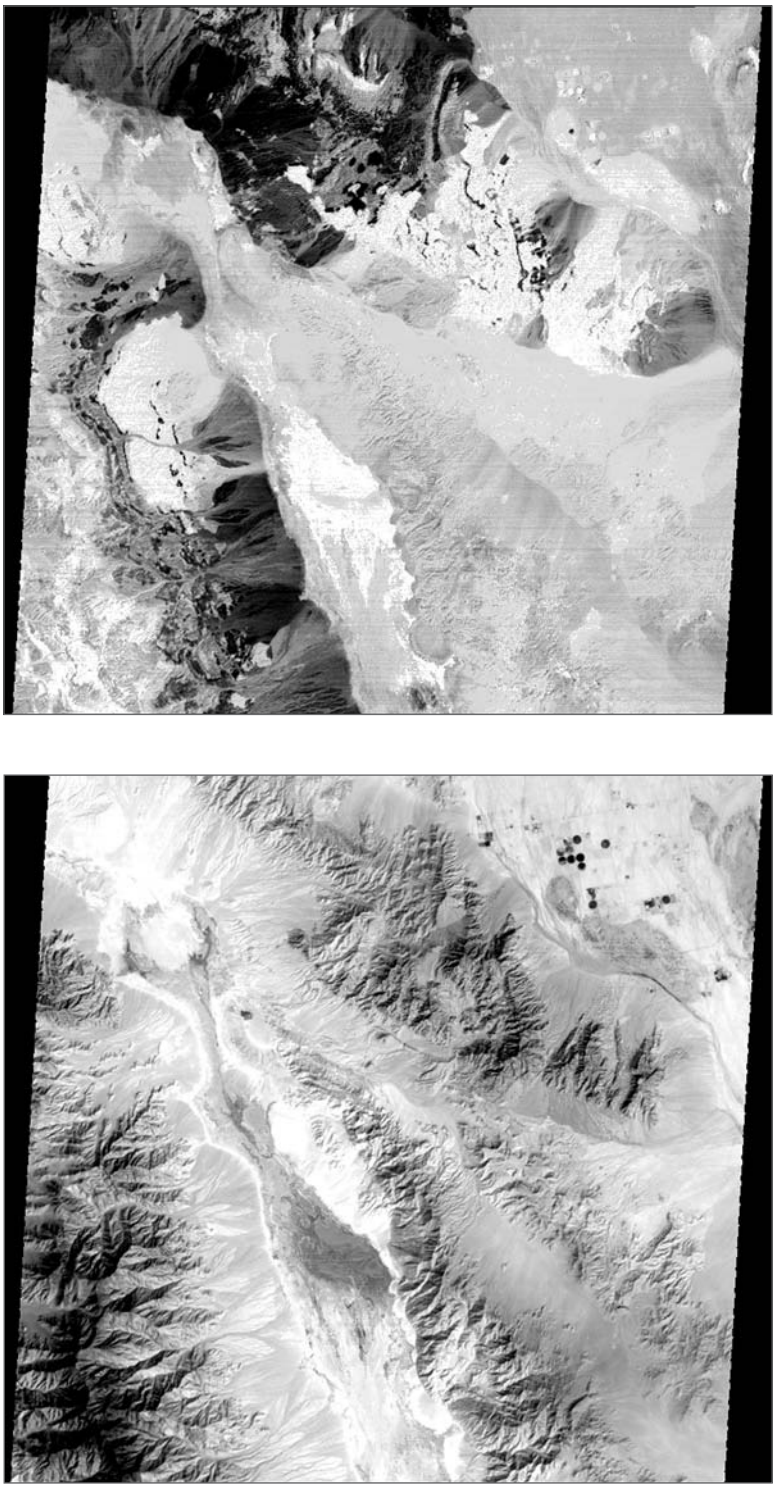

These ASTER images of Death Valley were taken on October 1, 2000. The top image represents Band 10 Emissivity and the lower image shows surface temperature. On the internet, visit visibleearth.nasa.gov to view a variety of ASTER data images.

MODIS Land Surface Temperature (LST) and Emissivity (MOD11)

Product Description

The Terra MOD11 product includes Level 2 and 3 (day and night) LST and emissivity products retrieved from Terra MODIS data over global land surface under clear-sky conditions. The generalized split window LST algorithm is used to retrieve LSTs in the Level-2 product (MOD11_L2) for MODIS pixels with emissivities in bands 31 and 32 estimated from land cover types in the MODIS land-cover and snow products through look-up tables established by thermal infrared (TIR) BRDF and emissivity modeling. The LST and emissivity values of all pixels in MOD11_L2 files are mapped onto 1-km grids in the sinusoidal projection to generate the level-3 1-km LST product (MOD11A1). The physics-based day/night LST algorithm is used to simultaneously retrieve surface band emissivities and temperatures in the level-3 5-km MOD11B1 product from a pair of daytime and nighttime MODIS observations in bands 20, 22, 23, 29, and 31-33. The LST product includes local solar time and viewing angle of the MODIS observation used in LST retrieval, and quality flags for each data set of LST and emissivity. The daily LST products are used to generate global gridded 8-day and monthly LST products (MOD11C2 and MOD11C3) for day and night conditions.

Research and Applications

Land surface temperature is a good indicator of both the energy balance at the Earth's surface and the greenhouse effect because it is one of the key parameters in the physics of the land-surface processes. It is required for a wide variety of climate, hydrological, ecological, and biogeochemical studies. This product is used in generating other MODIS products and in a variety of EOS interdisciplinary studies.

Data Set Evolution

The MODIS LST products build and improve upon the experience of LST retrieval from AVHRR and MODIS Airborne Simulator (MAS) data. The MODIS instrument has been designed to include TIR bands suitable for LST and emissivity retrieval at the global scale. The inputs used in the LST algorithms include calibrated radiance, geolocation, cloudmask, atmospheric temperature and water profile, land-cover, snow, and BRDF data in the MODIS products. The combination of Terra and Aqua provides four observations per day, giving a good sampling of the diurnal cycle of the LST. The accuracy of the LST products has been validated within 1K with *in situ* radiometer measurements at nine validation sites including lakes, playa, grasslands, snow, rice, and soybean fields in wide ranges of the LST and atmospheric conditions.

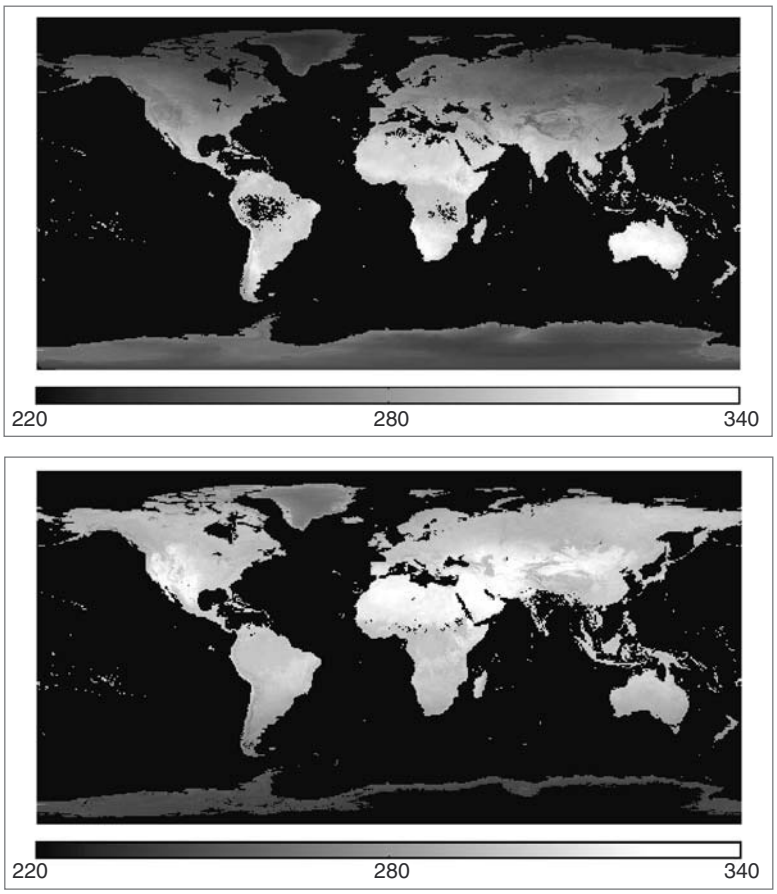

The global monthly daytime LSTs (K) in January (top) and July (bottom) 2001 at equal latitude/longitude grids with a size of 1/4 degree were generated from the daily LST product (MOD11B1). Areas in black are grids in ocean and cloudy conditions. On the internet, visit visibleearth.nasa.gov to view a variety of MODIS data images.

Suggested Reading

Justice, C. *et al*., 1998.

Running, S. W. *et al*., 1994.

Salisbury, J. W., and D. M. D'Aria, 1992.

Snyder, W., and Z. Wan, 1996.

Snyder, W., and Z. Wan, 1998.

Wan, Z., and J. Dozier, 1996.

Wan, Z., and Z.-L. Li, 1997.

Wan, Z. *et al*., 2002.

MODIS Land Surface Temperature and Emissivity Summary

Coverage: Global land surface

Spatial/Temporal Characteristics:
- 1 km/day (MOD11_L2)
- 0.93 km/day (MOD11A1)
- 0.93 km/8-day (MOD11A2)
- 4.64 km/day (MOD11B1)
- 1/20 degree/8-day (MOD11C2)
- 1/20 degree daily and monthly (MOD11C1 and MOD11C3)

Key Science Applications: Inputs to climate, hydrological, ecological modeling

Key Geophysical Parameters: Land-surface temperature, land-surface emissivity

Processing Level: 2 for MOD11_L2; 3 for MOD11A1, MOD11A2, MOD11B1, MOD11C

Product Type: Standard, at-launch and post-launch

Maximum File Size: 26 MB (MOD11_L2), 24 MB (MOD11A1 and MOD11A2), 2 MB (MOD11B1), 441 MB (MOD11C1), 467 MB (MOD11C2), 622 MB (MOD11C3)

File Frequency: 288/day (MOD11_L2), 317/day (MOD11A1 and MOD11B1), 317/8-day (MOD11A2), 1/day (MOD11C1), 1/8-day (MOD11C2), and 1/month (MOD11C3)

Primary Data Format: HDF-EOS

Additional Product Information: modis-land.gsfc.nasa.gov/products/products.asp?ProdFamID=8

DAAC: EDC Land Processes DAAC, edcdaac.usgs.gov

Science Team Contact: Z. Wan

MODIS Thermal Anomalies – Fires (MOD14); MODIS Burn Scars (MOD40)

Product Description

The MODIS Thermal Anomalies product includes fire occurrence (day/night), fire location, the logical criteria used for the fire selection, and an energy calculation for each fire. The product also includes composite 8-day-and-night fire occurrence (full resolution), composite daily day-and-night fire occurrence (full resolution), and a gridded 0.25° summary of fire counts per class (daily/monthly). The Level 2 product includes various fire-related parameters including the occurrence of day and nighttime thermal anomalies, flagged and grouped into different temperature classes with emitted energy from the fire. These parameters are retrieved daily at 1-km resolution. The fire product uses the special fire channel at 3.9 μm that saturates at 500 K and the high-saturation level of the 11-μm channel. The standard products will include the area burned.

Research and Applications

Fire is an important process within a significant number of terrestrial biomes, and the release of gases and particulate matter during biomass burning is an important contributor to the chemical reactions and physical processes taking place in the atmosphere. Fire is a significant and continuous factor in the ecology of savannas, boreal forests, and tundra, and plays a central role in deforestation. Fire information will be used to drive regional emissions models, trace-gas transport models, and mesoscale models of atmospheric chemistry. Important impacts of fires include:

- changes of physical state of vegetation and release of greenhouse gases;
- release of chemically reactive gases during biomass burning;
- release of soot and other particulate matter during fires;
- changes in the exchange of energy and water between land surfaces and the atmosphere; and
- changes in plant community development and soil nutrient, temperature, and moisture, and cloud development and reflectivity.

Data Set Evolution

The MODIS fire products build and improve upon the experience of fire assessment primarily using the NOAA AVHRR and GOES systems. Currently, no one sensing system provides the instrument characteristics needed for an effective global fire-monitoring program. The MODIS sensor has been designed to include characteristics specifically for fire detection and provides a unique capability over existing sensors in terms of fire monitoring. The locational accuracy and improved instrument characterization and calibration will enable unprecedented fire-monitoring data sets. The combination of Terra and Aqua data provides four observations per day, giving a good sampling of the diurnal cycle of fire activity. MODIS will also offer unique spatial and radiometric capabilities for burn-scar detection. Automatic procedures for burn-scar detection are being developed to provide a standard burn-scar product.

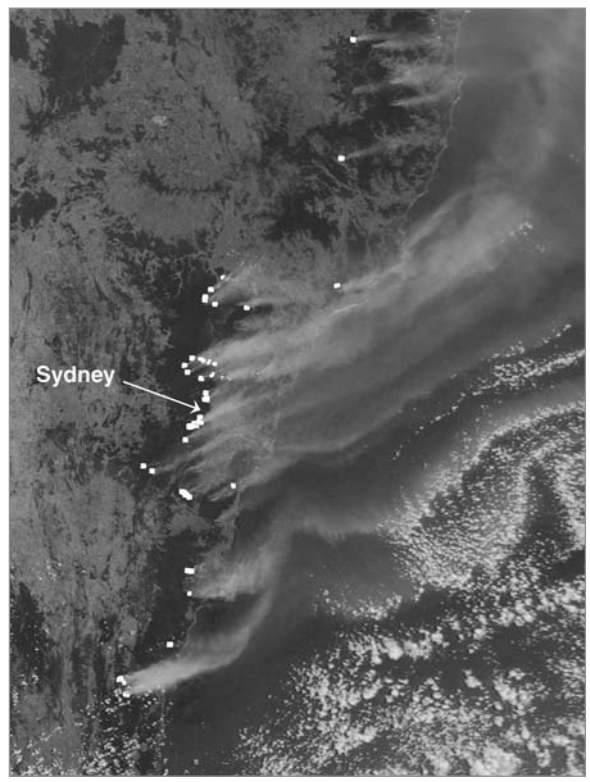

Trail-blazing firefighters and land managers now use NASA satellite data to combat wildfires. This image of the southeastern coast of Australia on January 2, 2002, from MODIS onboard the Terra satellite, shows thick plumes of grayish smoke streaming eastward from more than a dozen active fires. Fires encircle the city of Sydney, which stands out in tan against the surrounding green vegetation. In a collaboration between NASA, the University of Maryland, and the U.S. Department of Agriculture's Forest Service, firefighters receive maps and satellite images of current active fires, and use them for strategic planning. After the fire is controlled, land managers use the satellite images and maps for post-fire rehabilitation and protection of water quality. Image credit: Jacques Descloitres, MODIS Land Rapid Response Team at NASA/GSFC.

Suggested Reading

Ahern, F. *et al*., 2001.

Andreae, M. O. *et al*., 1994.

Giglio L. *et al*., 1999.

Justice C. O. *et al*., 1993.

Justice C. O. *et al*., 1998.

Justice C. O. *et al*., 2002.

Kaufman, Y. J. *et al*., 1990.

Kaufman, Y. J. *et al*., 1998.

Levine, J. S., 1991.

Penner, J. E. *et al*., 1992.

Roy, D. P. *et al*., 2002.

Roy, D. P. *et al*., 1999.

MODIS Thermal Anomalies – Fires and Burn Scars Summary

Coverage: Global, daytime/nighttime

Spatial/Temporal Characteristics: 1 km and 0.25°/1-day (MOD40 only), 8-day, monthly

Key Geophysical Parameters: Fire occurrence and class, fire selection criteria, fire location, smoldering and flaming ratio, burned area

Processing Level: 2, 3 for MOD14; 4 for MOD40

Product Type: Standard, at-launch and post-launch

Maximum File Size: 81 MB (MOD14), 40 MB (MOD40)

File Frequency: 288/day (Level 2), 294/day, 8-day or 16-day (Level 3 and 4)

Primary Data Format: HDF

Additional Product Information: modis-land.gsfc.nasa.gov/products/products.asp?ProdFamID=1

DAAC: EDC Land Processes DAAC, edcdaac.usgs.gov

Science Team Contacts: Y. J. Kaufman, C. O. Justice

MODIS Sea Surface Temperature (SST) (MOD28)

Product Description

This Level 2 and 3 product provides sea surface temperature (SST) at 1-km (Level 2) and 4.6 km, 36 km, and 1° (Level 3) resolutions over the global oceans. This product consists of four global SST fields: daytime (D1) and nighttime (N1) SST derived from the 11-micron channel, and daytime (D2) and nighttime (N2) SST derived from the 4-micron channel. In addition, a quality-assessment parameter is included for each pixel. The Level 2 product is produced daily and used to generate the gridded Level 3 products daily, 8-day weekly, monthly, and yearly for day and night conditions. A quality parameter is provided for each data set.

Research and Applications

The global distribution and variability of sea surface temperature are key inputs to Earth energy and hydrological balance studies and long-term climate change studies. In addition, sea surface temperature is required by a number of MODIS algorithms including those for precipitable water, productivity, oceanic aerosol properties, and temperature and water-vapor profiles. MODIS sea surface temperature retrievals will be incorporated into a match-up database with radiance and buoy sea surface temperature observations (see MOD32). The daytime SST derived from the 4 micron channel (D2) is affected by reflected solar radiation, and therefore the D1 (11 micron) SST is preferable for daytime applications. During the night, the surface ocean is more homogeneously mixed, and thus the skin temperature is more representative of the bulk upper-layer temperature. The N2 has a higher signal-to-noise than N1, but both fields are validated.

Data Set Evolution

Sea surface temperature determination is based on MODIS-calibrated mid-and far-IR radiances (Bands 20, 22, 23, 31, and 32 from MOD02), using an algorithm that exploits the differences in atmospheric transmissivity in the different IR bands to enable highly accurate estimation of the atmospheric effects. A land mask is used to mark nonwater pixels while an ice-extent mask limits polar sea coverage. A sequence of spatial and temporal homogeneity tests is applied

to validate the quality of the cloud-free observations. The AIRS SST estimate is used as a near-real-time quality assessment of skin temperature. Visible and near-IR radiances (Bands 3, 4, 5, 6) are used as a secondary cloud flag when the cloud-screening product is not available.

Suggested Reading

Abbott, M. R., and D. B. Chelton, 1991.

Esaias, W. E. *et al*., 1998.

MODIS Sea Surface Temperature Summary

Coverage: Global ocean surface, clear-sky only

Spatial/Temporal Characteristics: 1 km/daily (Level 2); 4.6 km, 36 km, 1°/daily, 8-day, monthly, yearly (Level 3)

Key Science Applications: Energy and hydrological balance, climate-change models

Key Geophysical Parameters: Sea surface temperature

Processing Level: 2, 3

Product Type: Standard, at-launch

Maximum File Size: 33 MB (Level 2); 640 MB binned, 134 MB mapped (Level 3)

File Frequency: 288/day (Daily Level 2), 4/day (Daily Level 3), 4/8-day (8-day Level 3), 4/month (Monthly Level 3), 4/year (Yearly Level 3)

Primary Data Format: HDF-EOS

Browse Available: 36 km sample imagery available at the GES DAAC (Level 3 only)

Additional Product Information: modis-ocean.gsfc.nasa.gov/dataprod.html

DAAC: Goddard Space Flight Center Earth Sciences DAAC, daac.gsfc.nasa.gov

Science Team Contacts: O. Brown, P. J. Minnett

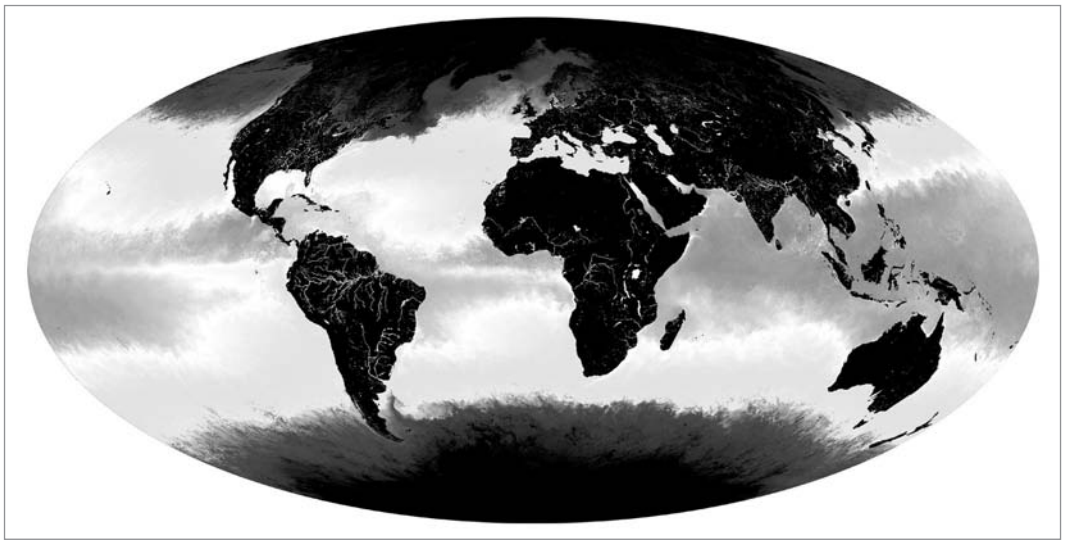

This is a grayscale version of a false-color image that shows a one-month composite for May 2001 developed from MODIS data. The MODIS sea surface temperature product is particularly useful in studies of temperature anomalies, such as El Niño, as well as research into how air-sea interactions drive changes in weather and climate patterns. Image courtesy of the MODIS Ocean Group, NASA GSFC, and the University of Miami. On the internet, visit visibleearth.nasa.gov to view a variety of MODIS data images.

Chapter 10

Vegetation Dynamics, Land Cover, and Land Cover Dynamics

Terra
MODIS

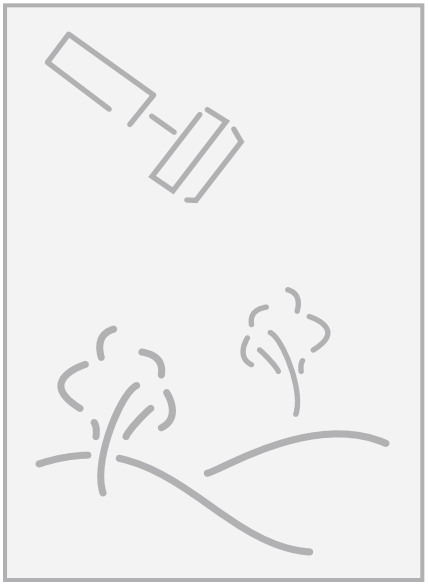

Vegetation Dynamics, Land Cover, and Land Cover Dynamics – An Overview

Relationship to Global Change Issues

About 30% of the Earth's surface is covered by land, and much of this is vegetated, making land surface processes important components of the terrestrial climate system. Vegetation, land cover, and land-use change provide the basis for understanding land and water resource management as well as a range of research and global monitoring objectives, including global carbon modeling, greenhouse gas emission inventories, regional environment and development assessments, and forest resource management. Ecologists and climatologists have developed models that describe the matter and energy exchanges, but lack of long-term global data limits their use in Earth-system models. Additionally, we lack good global data on surface albedoes over land, on the distribution of soils and important properties of vegetation morphology and physiology, and on water storage in soils and snow cover and their relationship to runoff. Incorporation of this information in the land-surface component of climate models will improve estimates of exchanges of water and energy with the atmosphere and lead to more realistic climate simulations

Product Description – Vegetation

The land vegetation products provide information on terrestrial systems which have important links to climate and atmospheric composition that are needed for development and application of models of the Earth's system. These links involve exchanges of energy and moisture, radiatively active trace gases (e.g., carbon dioxide and methane) and photochemically active species such as methane, nitric oxide, and non-methane hydrocarbons that soils, plants, and biomass burning release.

The Terra vegetation products provide the basic measurements of the photosynthetic engines that drive carbon transport on land. For land areas, vegetation density and vegetation canopy factors are produced which are used to generate the land primary productivity, the amount of carbon fixed by vegetation growth per day or longer unit of times such as per year. The MODIS vegetation measurements are provided by the Vegetation Index (MOD13), Leaf Area Index and Fraction of Photosynthetically Active Radiation (FPAR) (MOD15), and Vegetation Cover Conversion (MOD44) products. Vegetation indices are radiometric measures of the amount of vegetation present on the ground in a particular pixel. The indices are obtained from measurements of reflected visible and near-infrared energy from vegetation and are called normalized difference vegetation indices (NDVI). These indices have values between -1 and 1 and increase with increasing amounts of vegetation. Several new indices have been developed that compensate for soil and atmospheric effects, and these are combined into the enhanced vegetation index (EVI), also produced by MODIS. The indices are produced at different resolutions and time-averaging intervals to provide measures of vegetation density and productivity, which are required by global change models.

The Leaf Area Index (LAI) and Fraction of Photosynthetically Active Radiation (FPAR) provide information on green leaf area of Earth's vegetation and how much sunlight the leaves are absorbing. LAI defines an important structural property of a plant canopy, which is the one-sided leaf area per unit ground. FPAR measures the proportion of available radiation in the photosynthetically active wavelengths (0.4 to 0.7 mm) that a canopy absorbs and varies between 0 and 1. These parameters derived from the Surface Reflectance and the Land Cover Type products. A three-dimensional canopy radiation model is used to simulate spectral reflectances of different types and amounts of vegetation. The computer then compares the images collected by MODIS to the simulated images until it finds just the right match. Next it calculates the corresponding leaf area and absorbed radiation. These two products are essential in calculating terrestrial energy, carbon, water cycle processes, and biogeochemistry of vegetation.

Product Description – Land Cover and Land Cover Dynamics

Land Cover Type (MOD12) maps global terrestrial land cover at a 1-km resolution, using five different sets of cover type labels targeted to different applications. The cover type labels indicate broad classes of vegetation distinguished by life-form, leaf type, periodicity, and cover proportion. The land cover dynamics product detects areas of significant inter-annual change, such as flooding, drought, or burning. In addition, it provides the dates of transition for four phenological stages of vegetation for each

pixel during the prior year. Land cover, as well as both human and natural alteration of land cover, plays a major role in global-scale patterns of climate and biogeochemistry.

The primary layer of the land cover product recognizes 17 basic classes of land cover types following the International Geosphere-Biosphere Program (IGBP) scheme. Additional layers of labels include the University of Maryland land cover classes; a set of 6 structural classes used as input to the LAI/FPAR product algorithm; 6 broad biome types for the photosynthesis/net primary productivity algorithm; and a future set of plant functional type labels for use in the NCAR community land model.

The land cover dynamics product will detect and categorize changes in terrestrial features and processes on a global scale. The land-cover dynamics algorithm is independent of the land cover classification algorithm and compares, pixel-by-pixel, the temporal development curve of a set of biophysical and spatial indicators derived from MODIS data to that of the prior year. This product also contains information on the phenology of each pixel, quantifying the dates of onset of greenness, maturity, scenescence, and dormancy as experienced in the prior year. It will be available late in 2002 or early in 2003.

Product Description – MISR Land Surface Data

The MISR instrument provides a variety of information on the Earth's surface. MISR's Aerosol and Surface Products (MIS05, MIS08, MIS09) are included in this chapter.

Product Interdependency and Continuity with Heritage Data

The land products flow in a chain from the Level 2 reflectance and land cover type parameters to the biophysical- and biochemical-derived products that are inputs to the Earth system models.

Specific product dependencies for the land vegetation indices are MODIS radiance and imagery products, including Level 1B calibrated radiance, surface leaving radiance and aerosol optical depth. The Surface Reflectances and Land Cover type are key inputs to Leaf Area Index and FPAR.

Each instrument product set has its own science requirements and objectives and support the generation and validation of other instrument products. Vegetation Index products have been produced for many years from AVHRR and other instrument data and MODIS produces a "continuity" NDVI to maintain the NDVI time series using an algorithm that closely approximates the heritage index. A worldwide database has been created with the data and EOS will continue this series.

References

Asrar, G., and J. Dozier, 1994.

Knyazikhin, Y. *et al.*, 1998.

Li, X. *et al.*, 1995.

Moody, A., and C. E. Woodcock, 1995.

Myneni, R. *et al.*, 2002.

Panferov, O. *et al.*, 2001.

Tian, Y. *et al.*, 2002.

Wang, Y. *et al.*, 2001.

MODIS Surface Reflectance; Atmospheric Correction Algorithm Products (also called Spectral Reflectance) (MOD09)

Product Description

The MODIS Surface-Reflectance Product (MOD09) is computed from the MODIS Level 1B land bands 1, 2, 3, 4, 5, 6, and 7 (centered at 648 nm, 858 nm, 470 nm, 555 nm, 1240 nm, 1640 nm, and 2130 nm, respectively). The product is an estimate of the surface spectral reflectance for each band as it would have been measured at ground level if there were no atmospheric scattering or absorption.

The correction scheme includes corrections for the effect of atmospheric gases, aerosols, and thin cirrus clouds; it is applied to all noncloudy MOD35 Level 1B pixels that pass the Level 1B quality control. The correction uses band 26 to detect cirrus cloud, water vapor from MOD05, aerosol from MOD04, and ozone from MOD07; best-available climatology is used if the MODIS water vapor, aerosol, or ozone products are unavailable. Also, the correction uses MOD43, BRDF without topography, from the previous 16-day time period for the atmosphere-BRDF coupling term.

Research and Applications

The surface-reflectance product is the input for product generation for several land products: Vegetation Indices (VIs), BRDF, thermal anomaly, snow/ice, and Fraction of Photosynthetically Active Radiation/Leaf Area Index (FPAR/LAI). It is, therefore, an important and essential product. The at-launch version is fully operational.

Data Set Evolution

The Aqua MODIS product is based upon the latest version of the Terra MODIS product.

Suggested Reading

Holben B. N. *et al.*, 1998.

Justice C. O. *et al.*, 2002.

Justice, C. O. *et al.*, 2001.

Justice C. O. *et al.*, 2002.

Kaufman Y. J. *et al.*, 1997.

Petitcollin F., and E. F. Vermote, 2002.

Roger J. C., and E. F. Vermote, 1997.

Roger J. C., and E. F. Vermote, 1998.

Vermote E. F. *et al.*, 1997.

Vermote E. F. *et al.*, 1997.

Vermote E. F. *et al.*, 1997.

Vermote E. F. *et al.*, 2001.

Vermote E. F. *et al.*, 2002a,b.

Vermote, E. F., and D. P. Roy, 2002.

Wang Y. J. *et al.*, 2002.

Wang Y. J. *et al.*, 2001.

Wolfe R. E. *et al.*, 1998.

Wolfe R. E. *et al.*, 2002.

MODIS Surface Reflectance; Atmospheric Correction Algorithm Products Summary

Coverage: Global land surface

Spatial/Temporal Characteristics: Bands 1 and 2, 250 m; bands 3-7, 500 m; daily and 8-day

Key Science Applications: Global climate modeling, regional climate modeling, surface-energy-balance modeling, land cover characterization

Key Geophysical Parameters: Surface reflectance

Processing Level: 2, 2G, 3

Product Type: Standard, at-launch

Maximum File Size: 424 MB

File Frequency: 144/day (Level 2) and 294/day or 8-day (Level 2G and 3)

Primary Data Format: HDF-EOS

Additional Product Information: modis-land.gsfc.nasa.gov/mod09/

DAAC: EDC Land Processes DAAC, edcdaac.usgs.gov

Science Team Contact: E. Vermote

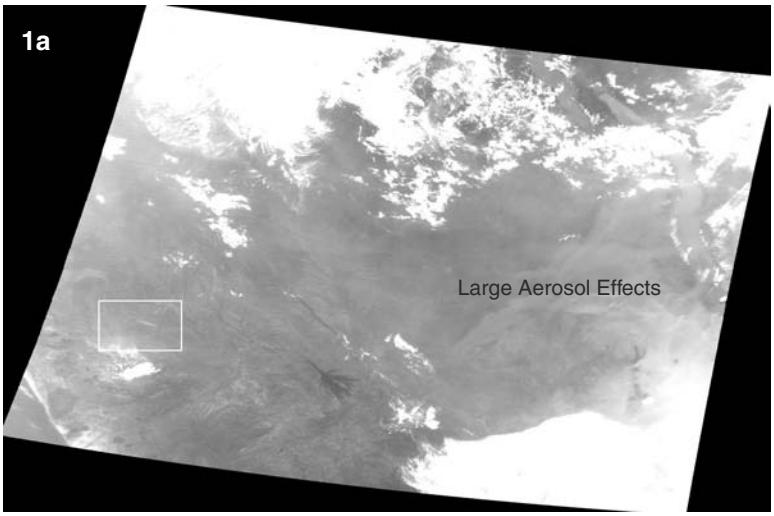

Level 1B granule, band 3 (470nm) gray image over South Africa., the white rectangle delineates the area enlarged in Figures 2.

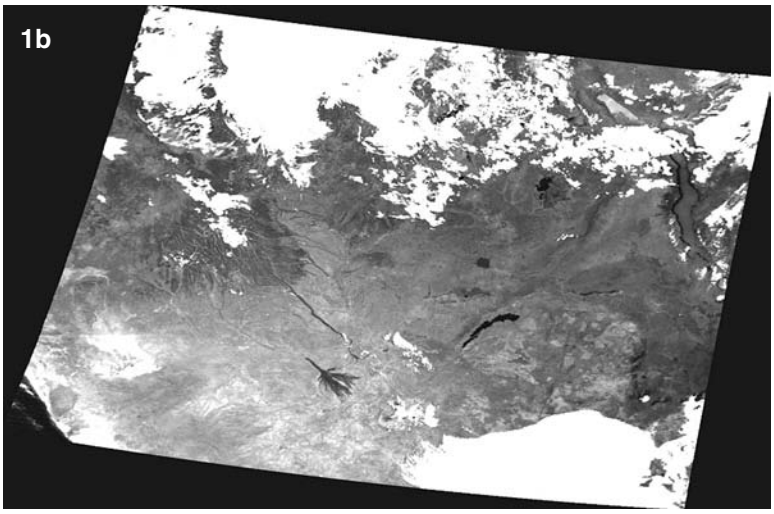

Surface reflectance granule, band 3 (470nm) gray image over South Africa. Land features are clearly enhanced when compared to level 1B. In addition to molecular scattering correction which is important in that band, large aerosol effects have been corrected in the left side of the image where surface features were barely visible in L1B data.

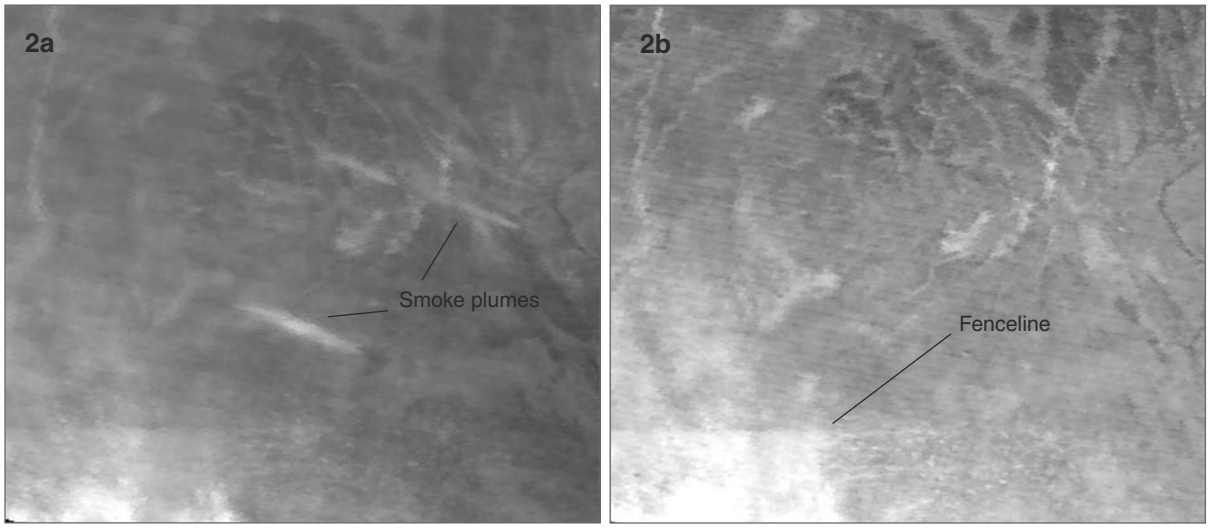

Figure 2a: **L1B, band 3 (470nm), over the subarea deliminited by the black rectangle in Figure 1a (above). Smoke plumes are clearly visible.** ***Figure 2b:*** **Surface reflectance, band 3 (470 nm), over the subarea delimited by the white rectangle in Figure 1a. Smoke plumes (aerosols) have been corrected, the fence line is now visible in the corrected data.**

MODIS Land Cover Type (MOD12)

Product Description

This Level 3 product contains land cover type and land cover dynamics parameters, which are produced at 1-km resolution on a quarterly basis. There are two file types provided. The primary land cover product (MOD12Q1) identifies 17 categories of land cover plus water following the IGBP global vegetation database, which defines nine classes of natural vegetation, three classes of developed lands, two classes of mosaic lands, and three classes of nonvegetated lands (snow/ice, bare soil/rocks, water). In addition, the product provides land cover type labels following the University of Maryland scheme; global structural cover types required for input to the LAI/FPAR algorithm; global biome types for input to the photosynthesis/NPP product; and plant functional types according to the community land model being developed at NCAR for global climate modeling.

The land cover dynamics product (MOD12Q2) quantifies subtle and progressive land-surface transformations as well as major rapid changes. As such, it is not a conventional change product that only compares changes in land cover type at two times but combines analyses of change in multispectral-multitemporal data vectors with models of vegetation-change mechanisms to recognize both the type of change and its intensity. It will highlight interannual variability in particular, distinguishing, for example, regions of flooding, drought, and burning as compared to the prior year. This product also provides phenologic information for each 1-km pixel that quantifies the date of onset of greenup, maturity, senescence, and dormancy each pixel during the prior year. The land cover dynamics product is prepared independently from the 250-m Land Cover Change Product and uses a different algorithm.

In addition to the basic 1-km product, summary products containing proportions of land covers and change characteristics are available at one-quarter, one-half, and 1-degree resolutions.

Research and Applications

This product is used for biophysical and biogeochemical parameterization of land cover for input to global- and regional-scale models of climate, hydrologic processes, and biogeochemical cycling. Examples of such biogeophysical parameters include biomass, cover fraction, and photosynthetic efficiency for carbon balance models, as well as albedo, rough-

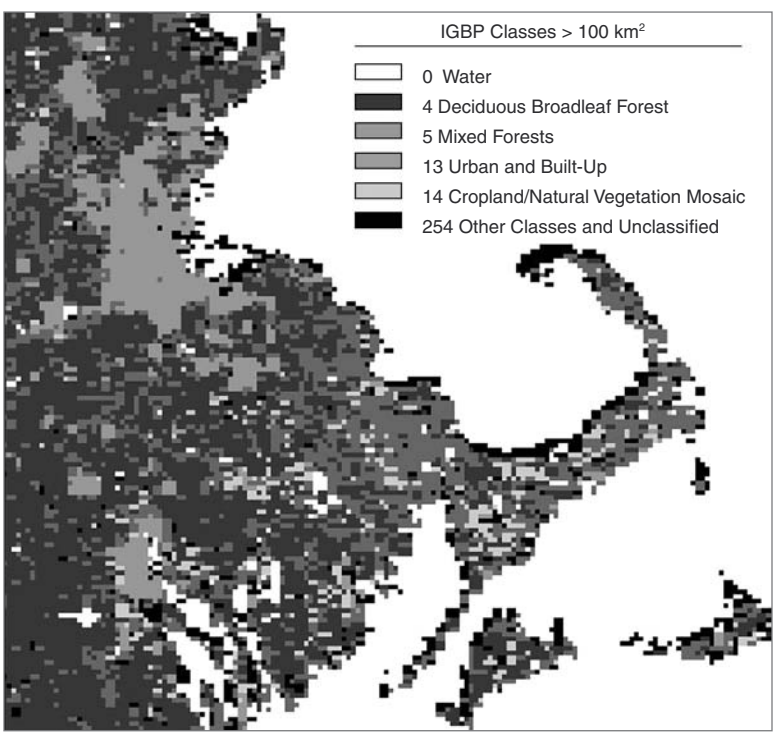

Land Cover Image of Eastern Massachusetts. A close-up view of the global land cover product, made from the first consistent year of MODIS data, for eastern Massachusetts, U.S. Four primary IGBP vegetation classes are represented. Urban areas in the upper left and lower left are Boston and Providence, Rhode Island. Note the general transition from deciduous broadleaf forest on the west to mixed forest in southeastern Massachusetts and the Cape Cod Peninsula, where sandy glacial deposits favor a mix of deciduous trees with evergreen conifers. On the internet, visit visibleearth.nasa.gov to view a variety of MODIS data images.

ness length, and surface resistance for surface energy balance models.

Data Set Evolution

The MODIS land cover type product builds on the heritage of global vegetation cover data sets produced using the coarse spatial resolution and high-temporal-frequency data of the AVHRR instrument aboard the NOAA series of meteorological satellites. With these data, the information source is the annual sequence of composited Normalized Difference Vegetation Index (NDVI) values for each pixel. The NDVI responds to specifically to the proportion of the surface covered by green leaves as well as the thickness of the leaf layer. As such, it does not provide land cover directly. Rather, the timing and intensity of the annual greenup of the surface is the information used to determine land cover type. The MODIS land cover algorithm draws from information domains well beyond those of AVHRR NDVI. These domains include directional surface reflectance in seven spectral bands, near-infrared image texture, enhanced vegetation index, land-surface temperature, and snow/ice cover derived from the MODIS instruments on both Terra and Aqua. They are assembled for a year of observations for each 1-km pixel. The classification algorithm uses a decision-tree classifier trained from a network of 1500 or more training sites. The validation procedure utilizes the training sites and classifier confidence to characterize the accuracy of the product as well as to provide information that can be used in spatial aggregation of land cover data and land cover change data at coarser resolutions.

Suggested Reading

Borak, J. S., and A. H. Strahler, 1999.

Friedl, M. *et al*., 2000.

Friedl, M. A. *et al*., 1999.

Friedl, M. A., and C. E. Brodley, 1998.

Justice, C. *et al*., 1998.

Muchoney, D. *et al*., 1999.

Muchoney, D. *et al*., 1999.

Running, S. W. *et al*., 1994.

Running, S. W. *et al*., 1995.

Salisbury, J. W., and D. M. D'Aria, 1992.

Snyder, W., and Z. Wan, 1996.

Strahler, A. *et al*., 1995.

Wan, Z., and J. Dozier, 1996.

Wan, Z., and Z.-L. Li, 1997.

Zhang, X. *et al*., 2001.

MODIS Land Cover Type Summary

Coverage: Global, clear-sky only

Spatial/Temporal Characteristics: 1 km and 0.05°/annual (produced every 96 days)

Key Science Applications: Biogeochemical cycles, global climate modeling, land cover change

Key Geophysical Parameters: Land cover type, land cover change, vegetation phenology

Processing Level: 3

Product Type: Standard, post-launch

Maximum File Size:
MOD12Q1: 23 MB (1 km)
MOD12Q2: 23 MB (1 km)
Summary Products: 0.92 MB

File Frequency: 317/96 days

Primary Data Format: HDF-EOS

Additional Product Information:
modis-land.gsfc.nasa.gov/products/products.asp?ProdFamID=10

geography.bu.edu/landcover

DAAC: EDC Land Processes DAAC, edcdaac.usgs.gov

Science Team Contact: A. H. Strahler

MODIS Vegetation Indices (MOD13)

Product Description

The MODIS Vegetation-Index (VI) products will provide consistent spatial and temporal comparisons of global vegetation conditions that are used to monitor the Earth's terrestrial photosynthetic vegetation activity in support of change detection and phenologic and biophysical interpretations. Gridded vegetation-index maps depicting spatial and temporal variations in vegetation activity are derived at 16-day and monthly intervals for precise seasonal and interannual monitoring of the Earth's vegetation. The MODIS VI products will improve upon currently available indices and will more accurately monitor and detect changes in the state and condition of the Earth's vegetative cover. The vegetation-index products are made globally robust with enhanced vegetation sensitivity and minimal variations associated with external influences (atmosphere, view and sun angles, clouds) and inherent, non-vegetation influences (canopy background, litter), in order to serve more effectively as a "precise" measure of spatial and temporal vegetation change.

Two vegetation-index (VI) products are produced globally for land. One is the standard normalized difference vegetation index (NDVI), which is referred to as the "continuity index" to the existing NOAA-AVHRR-derived NDVI. The other is an enhanced vegetation index (EVI) with improved sensitivity in high biomass regions and improved vegetation monitoring through a decoupling of the canopy background signal and a reduction in atmosphere influences. The two VIs complement each other in global vegetation studies and improve upon the extraction of canopy biophysical parameters. A new compositing scheme that reduces angular, sun-target-sensor variations is also utilized. The gridded vegetation-index maps use as input MODIS Terra and Aqua surface reflectances, corrected for molecular scattering, ozone absorption, and aerosols. The gridded vegetation indices include quality-assurance (QA) information with statistical data, indicating the quality of the VI product and input data. The MODIS vegetation-index products include:

- 250-m NDVI, EVI, and QA as 16-day products (high resolution);
- 500-m NDVI, EVI, and QA as 16-day products;
- 1-km NDVI, EVI, and QA as 16-day and monthly products (standard resolution); and
- 25-km NDVI, EVI, and QA as 16-day and monthly products (coarse resolution)

Research and Applications

Due to their simplicity, ease of application, and widespread familiarity, vegetation indices are widely used by the broader user community from global circulation climate modelers and EOS instrument teams and interdisciplinary projects in hydrology, ecology, and biogeochemistry to those making regional- and global-based applications involving natural-resource inventories, land-use planning, agricultural monitoring and forecasting, and drought forecasting. Some of the more common applications of the vegetation index concern:

- Global warming/climate
- Global biogeochemical and hydrologic modeling
- Agriculture; precision agriculture; crop stress, crop mapping
- Rangelands; water supply forecasting; grazing capacities; fuel supply
- Forestry, deforestation, and net primary production studies
- Pollution/health issues (Rift valley fever, mosquito-producing rice fields)
- Desertification
- Anthropogenic-change detection and landscape disturbances.

Data Set Evolution

There is a 20+ year NDVI global data set (1981-2002) from the NOAA-AVHRR series, which could be extended by MODIS Terra and Aqua data to provide a long-term data record for use in operational monitoring studies. The MODIS Terra and Aqua data set can readily be composited to provide 16-day, cloud-free time-series maps of vegetation activity. Combined, Terra and Aqua data will provide higher frequency, cloud-free time series data.

Suggested Reading

Cihlar, J. C. *et al*., 1997.

Gao, X. *et al*., 2000.

Gutman, G. G., 1998.

Huete, A. R. *et al*., 1994.

Huete, A. R. *et al*., 1997.

Huete, A. R. *et al*., 1999.

Myneni, R. B. *et al*., 1997a,b.

Pinty, B. *et al*., 1993.

van Leeuwen, W. J. D. *et al*., 1999.

MODIS Vegetation Indices Summary

Coverage: Global land surface

Spatial/Temporal Characteristics: 250-m, 500- m, 1-km, and 0.25°-resolutions/16-day and monthly products for Terra and Aqua data separately.

Key Science Applications: Global vegetation monitoring, biogeochemical and hydrologic modeling, health and food security, range and forestry monitoring, agriculture management

Key Geophysical Parameters: Vegetation indices (NDVI & EVI)

Processing Level: 3

Product Type: Standard, at-launch

Maximum File Size: 277 MB

File Frequency: 286/16-day (16-day), 289/month (Monthly)

Primary Data Format: HDF-EOS

Additional Product Information: modis-land.gsfc.nasa.gov/products/products.asp?ProdFamID=6

DAAC: EDC Land Processes DAAC, edcdaac.usgs.gov

Science Team Contact: A. R. Huete

MODIS Leaf Area Index (LAI) and Fraction of Photosynthetically Active Radiation (FPAR) – Moderate Resolution (MOD15)

Product Description

The MOD15 Leaf Area Index (LAI) and Fraction of Photosynthetically Active Radiation absorbed by vegetation (FPAR) are 1-km at-launch products provided on a daily and 8-day basis. LAI defines an important structural property of a plant canopy, namely the one-sided leaf area per unit ground area. FPAR measures the proportion of available radiation in the photosynthetically active wavelengths (400 to 700 nm) that a canopy absorbs. The LAI product will be a LAI value between 0 and 8 of the global gridded database at the corresponding modified vegetation index (MVI) compositing interval. The FPAR product will be an FPAR value between 0.0 and 1.0 assigned to each 1-km cell of the global gridded database at the corresponding MVI compositing interval.

Research and Applications

LAI and FPAR are biophysical variables that describe canopy structure and are related to functional process rates of energy and mass exchange. Both LAI and FPAR have been used extensively as satellite- derived parameters for calculation of surface photosynthesis, evapotranspiration, and Net Primary Production (NPP). These products are essential in calculating terrestrial energy, carbon, water-cycle processes, and biogeochemistry of vegetation. The LAI product is an input to Biome-BGC (Biogeochemical) models to produce conversion-efficiency coefficients, which are combined with the FPAR product to produce daily terrestrial PSN (photosynthesis) and annual NPP.

Data Set Evolution

This product is derived from the Surface Reflectance Product (MOD09), the Land Cover Type product (MOD12), and ancillary information on surface characteristics such as land cover type and background. The retrievals are performed by comparing observed and modeled surface reflectances for a suite of canopy structures and soil patterns that covers a range of expected natural conditions. All canopy/soil patterns for which the magnitude of the residuals in the comparison does not exceed uncer-

tainties in observed and modeled surface reflectances are treated as acceptable solutions. For each acceptable solution, a value of FPAR is also evaluated. The mean and dispersion values of the LAI solution distribution function are taken as the retrieved LAI accuracy; likewise for FPAR. A three-dimensional formulation of the radiative transfer is used to derive spectral and angular biome-specific signatures of vegetation canopies. Should this main algorithm fail, a back-up algorithm is triggered to estimate LAI and FPAR using a Normalized Difference Vegetation Index (NDVI).

Suggested Reading

Knyazikhin, Y. *et al*., 1998a,b.

Myneni, R. B. *et al*., 1997b.

Tian, Y. *et al*., 2000.

Zhang, Y. *et al*., 2000.

MODIS LAI and FPAR – Moderate Resolution Summary

Coverage: Global

Spatial/Temporal Characteristics: 1 km/daily, 8-day

Key Science Applications: Biogeochemical cycle modeling, NPP estimation

Key Geophysical Parameters: Leaf area index, fraction of photosynthetically active radiation absorbed by vegetation

Processing Level: 4

Product Type: Standard, at-launch

Maximum File Size: 5.8 MB

File Frequency: 286/day (Daily Level 4), 289/8-day (8-day Level 4)

Primary Data Format: HDF-EOS

Additional Product Information: modis-land.gsfc.nasa.gov/products/products.asp?ProdFamID=5

DAAC: EDC Land Processes DAAC, edcdaac.usgs.gov

Science Team Contacts: R. B. Myneni, S. W. Running

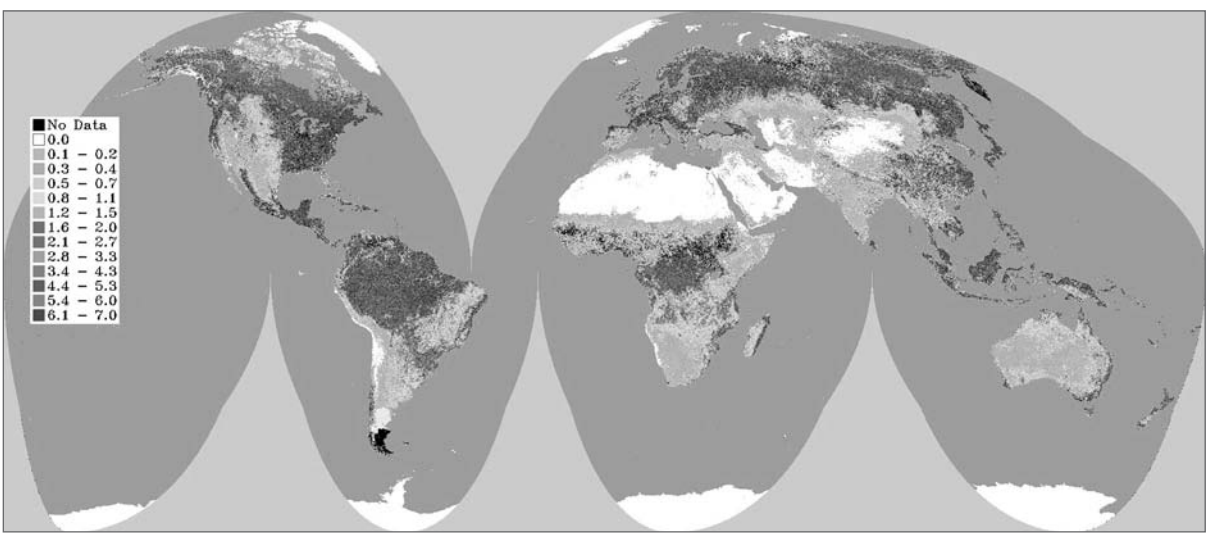

Global Leaf Area Index

MODIS Evapotranspiration (MOD16)

Editor's note: This product is only produced from MODIS on Aqua due to its afternoon equatorial crossing time. It is included in this volume for reference purposes.

Product Description

This Level 4 product is the ratio of evapotranspiration to potential evapotranspiration, expressed as an Evaporative Fraction (EF) to provide compatibility with both energy and hydrologic units. This land EF is an Aqua product that captures sub-optimum conditions produced by soil/atmosphere deficits for vegetation photosynthesis, transpiration and surface energy balances. It has a temporal resolution of 8 days, at 1 km.

Please note this product is only produced from MODIS on Aqua due to its afternoon equatorial crossing time. It is included in this volume for reference purposes.

Research and Applications

This new algorithm infers the fraction of incident solar energy being partitioned into Evaporation, effectively ET/PET. The algorithm's logic is to normalize the observed clear-sky radiometric surface temperature with NDVI. These two parameters are essential to global modeling of climate, water balance, and trace gases. In addition, they are required in estimating photosynthesis, respiration, and net primary production. The Evapotranspiration product is an Aqua (post-launch) research data product intended for real-time implementations. Practical applications of this product are for monitoring wildfire danger and crop/range drought.

Data Set Evolution

The Evapotranspiration product will be calculated using the MODIS Land Surface Temperature (MOD11) and the MODIS modified vegetation index (MOD13), and will be used along with incident radiation for computing the ET.

Suggested Reading

Goward, S. N., and A. S. Hope, 1989.

Nemani, R. R., and S. W. Running, 1989.

Nemani, R. R. *et al.*, 1993.

Running, S. W. *et al.*, 1989.

Running, S. W. *et al.*, 1994.

MODIS Evapotranspiration Summary

Coverage: Global

Spatial/Temporal Characteristics: 1 km/8-day, yearly

Key Science Applications: Global water balance, net primary production

Key Geophysical Parameters: Evaporation, potential evaporation

Processing Level: 4

Product Type: Research, post-launch

Maximum File Size: 5.8 MB

File Frequency: 286/8-day or year

Primary Data Format: HDF-EOS

Additional Product Information: modis-land.gsfc.nasa.gov/products/products.asp?ProdFamID=3

DAAC: EDC Land Processes DAAC, edcdaac.usgs.gov

Science Team Contact: S. W. Running

MODIS Vegetation Production and Net Primary Production (MOD17)

Product Description

MOD17 is a Level 4 product consisting of 8-day Net Photosynthesis (PSN) and Net Primary Production (NPP). Annual NPP is the time integral of the PSN product over a year.

Research and Applications

This product provides an accurate measure of terrestrial vegetation growth and production activity. The theoretical use is to define the seasonally dynamic flux of terrestrial-surface carbon dioxide for climate modeling. Fluxes will be computed specific to each vegetation type. The practical utility is to measure crop yield and forest production and any other socially significant products of vegetation growth. As this global NPP product becomes regularly available, a wide variety of derived products is expected to be developed making regionally specific estimates of crop production. The value of an unbiased, regular source of crop and forest production estimates for global political and economic decision making is immense.

Data Set Evolution

The NPP parameter is the yearly integral of the PSN, which is obtained from the product of PAR (Photosynthetically Active Radiation), FPAR (Fraction of Photosynthetically Active Radiation) and conversion-efficiency coefficients obtained from other MODIS products and other sensors and ancillary data. The algorithms for these products are based on the original logic of Monteith (1972), which relates PSN and NPP to the amount of Absorbed Photosynthetically Active Radiation (APAR). The MODIS modified vegetation indices (MVI) along with climate variables and the land cover product are used to estimate APAR.

Suggested Reading

Field, C. B. *et al*., 1995.

Monteith, J. L., 1972.

Nishida, K. *et al*., 2003.

Prince, S. D., and S. N. Goward, 1995.

Ruimy, A. *et al*., 1994.

Running, S. W., 1990.

Running, S. W. *et al*., 1994.

Running, S. W. *et al*., 2000.

MODIS Vegetation Production and Net Primary Production Summary

Coverage: Global

Spatial/Temporal Characteristics: 0.5, 1, 10 km/8-day, yearly

Key Science Applications: Interannual variability of vegetation

Key Geophysical Parameters: NPP, photosynthesis, respiration

Processing Level: 4

Product Type: Standard, at-launch

Maximum File Size: 4.3 MB

File Frequency: 289/8-day

Primary Data Format: HDF-EOS

Additional Product Information: modis-land.gsfc.nasa.gov/products/products.asp?ProdFamID=3

DAAC: EDC Land Processes DAAC, edcdaac.usgs.gov

Science Team Contact: S. W. Running

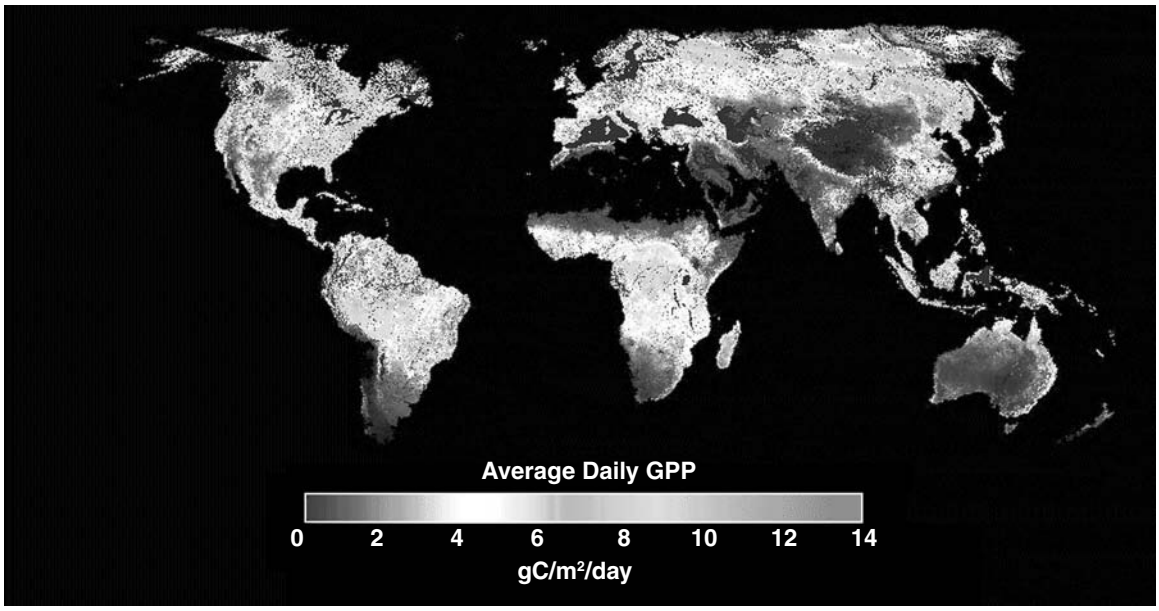

The above image represents Gross Primary Production (GPP) at 1 km resolution from MODIS using data collected from May 31 to June 7, 2001. Image courtesy of the MODIS Land Science Team/University of Montana. On the internet, visit visibleearth.nasa.gov to view a variety of MODIS data images.

MODIS Surface Reflectance BRDF/Albedo Parameter (MOD43)

Product Description

The Bidirectional Reflectance Distribution Function (BRDF)/Albedo product provides coefficients for mathematical functions that describe the BRDF of each pixel in MODIS spectral "Land" bands (1-7), as well as for three broad bands (0.3-0.7, 0.7-5.0, and 0.4-3.0 μm).

These coefficients are then used to provide albedo measures and nadir view-angle corrected surface reflectances resulting in three different file types, each containing global, 1km resolution data and quality assurance information:

- MOD43B1 contains three BRDF/Albedo model parameters and various quality assurance information.
- MOD43B3 contains both the white-sky (wholly diffuse) and black-sky (direct beam at local solar noon) albedo product.
- MOD43B4 contains Nadir BRDF-Adjusted Reflectances (NBAR) at the mean overpass solar angle.

Because deriving BRDF and albedo requires merging multiple looks at each pixel, the BRDF/Albedo products are provided as a 16 day composite. A 16-day summary albedo product at 0.05º spatial resolution is also provided. Both Terra and Aqua data are merged as available.

Research and Applications

The BRDF functions provided by the BRDF/Albedo parameter 1) allow normalization of MODIS data to standard viewing and illumination angles, thus removing geometric effects from multidate images; 2) quantify the directional information in the remotely-sensed signal, which is related to ground-cover type; and 3) provide a surface-radiation-scattering model for boundary-layer parameterization in regional and global climate modeling. The BRDF can also be used in extraction of surface reflectances at Level 2. Two albedo measures are provided: "black-sky" albedo (directional-hemispherical reflectance) and "white-sky" albedo (bihemispherical reflectance). These are intrinsic surface properties, independent of atmospheric state. They describe the upward scattering of the solar beam and of uniform diffuse irradiance, respectively, and may be used as input to global and regional climate models.

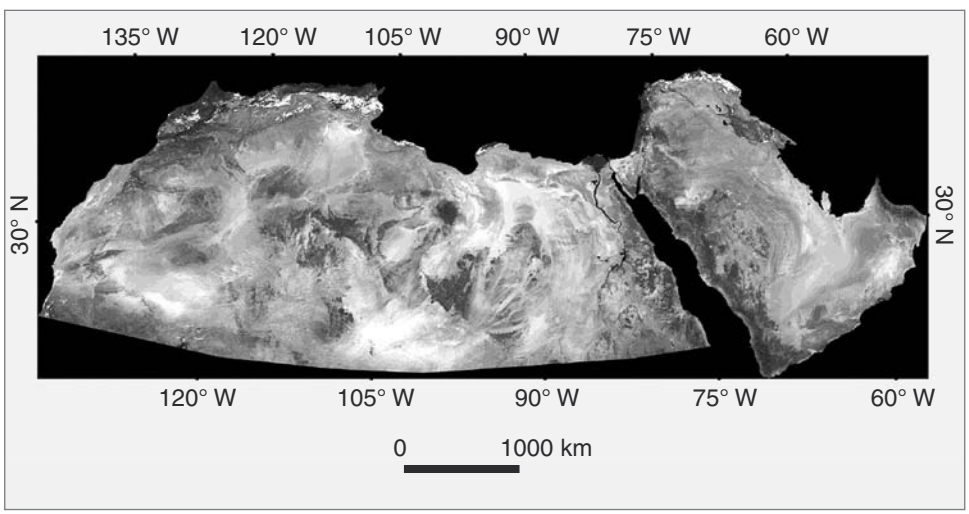

Albedo of the Sahara Desert and Arabian Peninsula. This image, prepared from MODIS data acquired in November 2000, shows the land surface albedo of the Sahara Desert and Arabian Peninsula. While global climate modelers typically assume a fixed albedo for barren deserts, the tonal variation demonstrates that desert albedos are actually quite variable and range from low, in regions of lava flows, to high, in sand sheet and dune fields. On the internet, visit visibleearth.nasa.gov to view a variety of MODIS data images.

Data Set Evolution

The BRDF/Albedo algorithm combines gridded, multidate, multiband surface-reflectance data from EOS MODIS instruments on Terra and Aqua to produce BRDF functions and derived albedo measures. For each grid cell, all cloud-free observations in a 16-day period are assembled and fit to the Ross-Thick/Li-Sparse semiempirical model that describes the BRDF as a linear combination of two basic BRDF shapes and a constant. In addition, the Ross-Thick/Li-Transit model also fitted as a separate parameter. The algorithm outputs include 1) Ross-Thick/Li-Sparse BRDF parameters that best fit the observations, 2) Ross-Thick/Li-Transit parameters, 3) black-sky and white-sky albedos in three broad bands; and 4) nadir BRDF-adjusted reflectances (NBARs).

Suggested Reading

Barnsley, M. J., and J.-P. Muller, 1991.

d'Entremont, R. E. *et al*., 1999.

Gao, F. *et al*., 2001.

Gao, F. *et al*., 2001.

Hu, B. *et al*., 1997.

Hu, B. *et al*., 1999.

Hu, B. *et al*., 2000.

Justice, C. *et al*., 1998.

Li, X. *et al*., 1995.

Li, X. *et al*., 2001.

Liang, S. *et al*., 1999

Lucht, W., 1998.

Lucht, W., and P. Lewis, 2000.

Lucht, W. *et al*., 2000.

Martonchik, J. V. *et al*., 2001.

Strugnell, N., and W. Lucht, 2001.

Strugnell, N. *et al*., 2001.

Wanner, W. *et al*., 1995.

Wanner, W. *et al*., 1997.

MODIS Surface Reflectance BRDF/Albedo Parameter Summary

Coverage: Global land surface

Spatial/Temporal Characteristics: 1 km, 0.05°/16-day

Key Science Applications: Biogeochemical-cycle modeling, net primary productivity estimation, global climate models

Key Geophysical Parameters: Bidirectional reflectance, spectral albedo

Processing Level: 3

Product Type: Standard, at-launch

Maximum File Size (per tile):
MOD43B1: 107 MB
MOD43B3: 66 MB
MOD43B4: 30 MB

File Frequency: 294/16-day

Primary Data Format: HDF-EOS

Additional Product Information:
modis-land.gsfc.nasa.gov/products/products.asp?ProdFamID=2

geography.bu.edu/brdf/

DAAC: EDC Land Processes DAAC, edcdaac.usgs.gov

Science Team Contacts: A. H. Strahler, J.-P. Muller

MODIS Vegetative Cover Conversion and Vegetation Continuous Fields (MOD44)

The MOD44 suite provides two products, which collectively characterize the extent of the Earth's vegetated land cover and changes in same. Both products use the unique combination of temporal and spectral resolution provided by MODIS to monitor the annual phenologic cycle of vegetation and to exploit this information to provide high quality products.

MOD44A: Vegetative Cover Conversion

Product Description

Using MODIS data from the two 250-m bands, the vegetative cover conversion product shows the global distribution of the occurrence of vegetation cover change. Where there is sufficient evidence, the type of change is labeled (e.g., forest conversion to agricultural fields or grassland or bare surface). The distribution of these changes is represented at a spatial resolution of 250 m and a gridded 5-km summary. These are generated at 32-day intervals depicting vegetation change since the corresponding period of the previous year. An enhanced product with a finer temporal resolution is currently being developed. The algorithm is designed as a conservative alarm product, which captures the spatial and temporal distribution of changes at global and regional scales. This information can in turn be used to focus on detected hotspots using finer resolution instruments.

Research and Applications

Vegetation-cover change is an important driver of many important biogeochemical, hydrological, and climate processes. It also represents the integrated response to several biophysical and anthropogenic impacts. Among the important influences of vegetation-cover change are the following:

- It strongly affects changes in many biophysical factors such as surface roughness and albedo;
- It has a major effect on changes in sensible heat flux, because it affects global albedo and surface roughness, which in turn affects atmospheric drag;
- It is of crucial importance for determining the biogeochemical cycling of carbon, nitrogen, and other elements at regional-to-global scales;
- It has a major impact on the runoff characteristics of catchments through its effects on evapotranspiration and partitioning of precipitation into overland flow, interflow, and groundwater accretion;
- It gives a direct insight into ecosystem response related to climate change and anthropogenic influences;
- It affects biodiversity through direct impacts on habitat; and
- It provides increasingly important information for natural-resource managers.

This product can be combined with data obtained from finer spatial resolution data from sensors such as ETM+ on Landsat 7 and ASTER on Terra to assist in the identification of the types of vegetation conversion occurring. The product also provides information to assist the acquisition strategy of finer resolution systems since it helps flag areas where significant changes are likely to be occurring.

Changes of interest include flooding, burning, deforestation, agricultural expansion and urbanization.

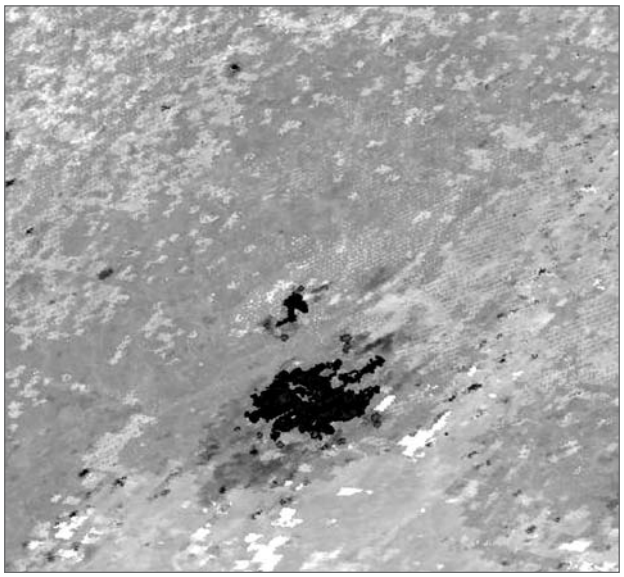

This image shows change as a result of fire in Southern Georgia as detected by the MODIS Vegetation Cover Conversion. The fire occurred in May of 2002 and the changed area is depicted by black in the image. On the internet, visit visibleearth.nasa.gov to view a variety of MODIS data images.

Data Set Evolution

Previous work has shown that data with a resolution of 1 km and coarser are sufficient for the mapping of the distribution of vegetation cover and for the monitoring of those changes in vegetation cover caused by seasonal-to-interannual climate change. However, such relatively coarse resolution data are often inadequate to detect changes caused by anthropogenic factors and heterogeneous change events such as wildfires. Analyses of many types of vegetation-cover change indicate that they are relatively small in size largely due to the inherently local nature of anthropogenic vegetation-cover conversions. Consequently a very large proportion of changes is only detectable at fine spatial resolutions. For this reason it was decided to use the two 250-m bands for the identification and mapping of this type of conversion.

MOD44B: Vegetation Continuous Fields

Product Description

Vegetation Continuous Fields uses an annual database of 8-day surface reflectance observations to derive percent cover estimates at a spatial resolution of 500 m. A gridded 5-km summary product is also available. The variables available include:

- Percent Tree Cover
- Percent Herbaceous Cover
- Percent Bare Cover
- Percent Needleleaf Vegetation
- Percent Broadleaf Vegetation
- Percent Evergreen Vegetation
- Percent Deciduous Vegetation

Continuous training using classified fine resolution data are employed to train the algorithm. A metrics-based approach is employed to capture the annual variation of vegetation characteristics. Example metrics include maximum greenness, minimum temperature, darkest observation and many others. Metrics were chosen based on a analysis to determine the best discriminating factors, which are not autocorrelated.

Research and Applications

The Vegetation Continuous Fields product represents a significant improvement over discrete land cover classifications because no a priori determinations are made as the the definitions of land cover classes. Modelers and resource managers can determine their own thresholds to determine what vegetation composition constitutes a “forest” or “savanna”. For those interested in estimating parameters such as surface roughness, the MOD44B product allows the user to estimate such a variable along a continuum of forest or other cover.

Perhaps the most important application is providing a globally consistent estimate of forest cover which is repeatable and does not rely on the variety of definitions used within different administrative jurisdictions. The data can in turn then be used to

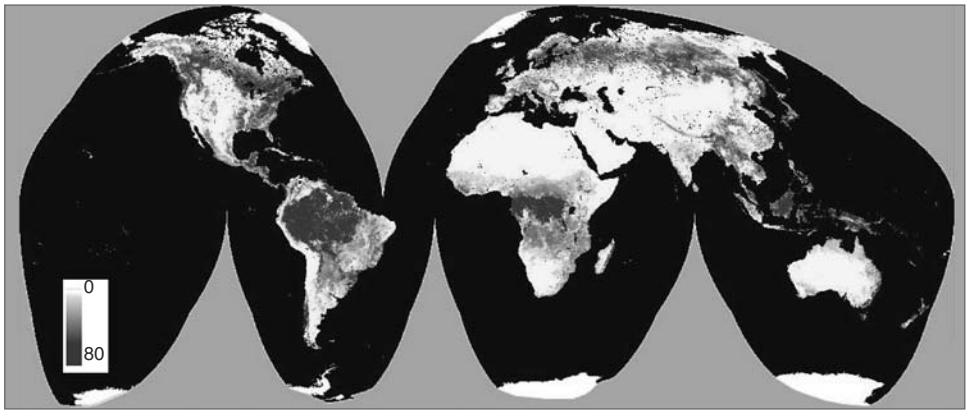

This images represents MODIS Vegetation Continuous Fields tree cover product for 2001 with oceans in black and denser forests depicted in dark grey. On the internet, visit visibleearth.nasa.gov to view a variety of MODIS data images.

estimate stocks of standing carbon. By comparing multiple annual MOD44B data sets it is possible to determine changes in forest extent and carbon inventory over time.

Data Set Evolution

This product has been extensively prototyped using the Advanced Very High Resolution Radiometer at scales of 1 km and 8 km. MODIS derived results show the unique capabilities of the instrument to better depict vegetation extent and characteristics. This is due to the increased spatial and spectral resolution as well as significantly improved calibration and geolocation.

Suggested Reading

DeFries, R. S. *et al*., 2000.

Hansen, M. C. *et al*., 2002.

Townshend, J. R. G., and C. O. Justice, 1988.

Zhan, X. *et al*., 2002.

MODIS Vegetative Cover Conversion and Vegetation Continuous Fields Summary

Coverage: Global, daytime

Spatial/Temporal Characteristics:
MOD44A - 250 m, 5 km/3-month, yearly
MOD44B - 500 m, 5 km/yearly

Key Geophysical Parameters:
MOD44A - Vegetation-cover change occurrence and type
MOD44B - Vegetation-cover extent and composition

Processing Level: 4

Product Type: Research, at-launch and post-launch

Maximum File Size: 1 GB/tile (land tiles only)

File Frequency: 294 files/32-day

Primary Data Format: HDF-EOS

Browse Available:
modis.umiacs.umd.edu

Additional Product Information:
modis.umiacs.umd.edu

DAAC: EDC Land Processes DAAC, edcdaac.usgs.gov

Science Team Contact: J. R. G. Townshend

Chapter 11

Ocean Primary Productivity, Phytoplankton and Organic Matter

Terra
MODIS

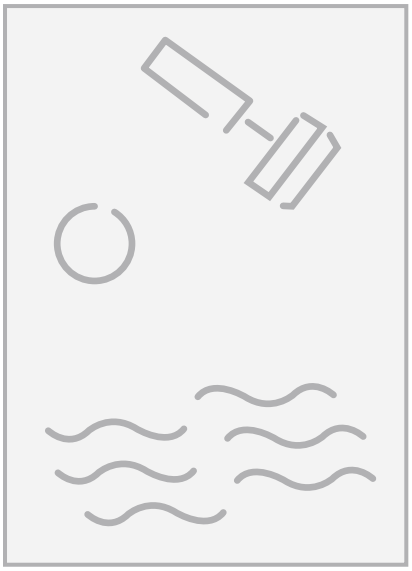

Ocean Primary Productivity, Phytoplankton and Organic Matter – An Overview

Relationship to Global Change Issues

The global oceans, covering approximately 70% of the Earth's surface and extending in some locations to depths exceeding 10 km, contain a varied abundance of life forms; and central to the ocean ecosystem are the unicellular plants called phytoplankton. Phytoplankton take dissolved carbon dioxide from sea water and use it for photosynthesis, enabling phytoplankton growth and releasing oxygen. This process captures approximately the same amount of carbon as does photosynthesis by land vegetation. The amount and distribution of carbon dioxide consumed by the phytoplankton depends heavily on ocean circulation, which supplies nutrients to the upper layers of the ocean where sunlight is abundant. Some fraction of carbon produced by the phytoplankton sinks to the ocean floor—a long-term sink for atmospheric carbon dioxide. The fraction is not well known and is a source of a large uncertainty in the global carbon budget.

Changes in the amount of phytoplankton indicate changes in productivity of the oceans and provide a key ocean link for the monitoring of global climate change. Ocean and land biological productivity, heat-exchange processes, and water-exchange processes are tightly coupled, and it is important for global change models to take such interactions into account in global climate-change prediction. The hope is that the phytoplankton and organic matter data products will help scientists to determine whether ocean productivity is changing and, if so, how such changes relate to the global carbon cycle and other global changes.

Product Overview

The ten products discussed in this chapter are all from the MODIS instruments on the Terra and Aqua satellites, and include 25 different variables (sometimes called "parameters") related to ocean biology and biogeochemistry. The products are grouped according to the Science Team members responsible for the algorithms.

Phytoplankton pigment or chlorophyll concentration has historically been the most widely used ocean color product. MODIS provides three Chlorophyll Concentration products, and two additional Pigment Concentration products. Several of these are based on heritage algorithms to provide continuity with the CZCS and SeaWiFS data sets. Others differ with respect to whether they are for open ocean (Case 1) or coastal (Case 2) waters, and whether the algorithms are empirical or semi-analytical. The Pigment Concentration products (MOD19) and two associated products, Suspended Solids Concentration (MOD23) and Ocean Water Attenuation Coefficient (MOD26), are all based on empirical algorithms. Total Absorption Coefficients (MOD36), Dissolved Organic Matter Absorption (MOD24), and the phytoplankton absorption coefficient at 675 nm are derived by inverting a radiance model, and a chlorophyll concentration (semi-analytic, MOD21) is then derived from the absorption at 675 nm. This relationship depends on the amount of chlorophyll per cell, which is related to the nutrient status (replete vs. deplete) as inferred from the SST (MOD28).

The Ocean Primary Productivity product (MOD27) provides the rate of net photosynthetic carbon fixation, a process that influences CO_2 in the atmosphere and ultimately global climate. Estimates are provided for the daily rate integrated over the euphotic zone and the mixed layer, averaged over 8-day periods, and an empirically derived estimate of annual euphotic production based on the mean annual chlorophyll concentration. MOD27 is a Level 4 product that is analogous to the Net Primary Production (NPP) product over land (MOD04).

MODIS introduces three products that have never been produced before from space. The Coccolith Concentration product (MOD25) describes the concentration of calcium carbonate scales produced by the phytoplankton group named coccolithophores. These scales (called coccoliths) eventually sink to the ocean floor, accounting for about 75% of the deposition of carbon on the sea floor (Holligan *et al.*, 1993; Archer and Maier-Reimer, 1994). Chlorophyll Fluorescence (MOD20) provides another measure of the chlorophyll concentration, but the fluorescence per unit of chlorophyll depends on the health of the phytoplankton. Thus the ratio of chlorophyll fluorescence (MOD20) to chlorophyll (MOD21) provides information that is useful in modeling primary productivity. Finally, Phycoerythrin Concentration (MOD31) provides information about the abundance of species containing phycoerythrin. Among these are certain species of cyanobacteria which have the

ability to convert nitrogen (N_2) into organic nitrogen, thus playing an important role in the global nitrogen cycle (Capone *et al*., 1997).

Product Interdependency and Continuity with Heritage Data

All of the products described in this chapter require accurate water-leaving radiances (MOD18), which in turn require match-up data (MOD32) to provide coincident remote sensing and *in situ* radiance measurements. Some individual products require additional parameters. For example, the semi-analytic chlorophyll product (MOD21) uses SST (MOD28), and the primary productivity product requires chlorophyll (MOD21) and SST (MOD28). The Chlorophyll Fluorescence (MOD20) is normalized to the absorbed radiation by phytoplankton (MOD22) to obtain a fluorescence efficiency. The MODIS Pigment Concentration (MOD19) includes a CZCS-analog pigment concentration to provide a direct link to the series of measurements made by CZCS over the period from 1978 to 1986. Likewise, a SeaWiFS-analog chlorophyll concentration (MOD21) provides continuity with the SeaWiFS chlorophyll product. NASA's Sensor Intercomparison and Merger for Biological and Interdisciplinary Oceanic Studies (SIMBIOS) Project is developing methods for merging MODIS data with data from the heritage ocean color missions and data from contemporary international space missions (e.g., MERIS and GLI).

Suggested Reading

Archer, A., and E. Maier-Reimer, 1994.

Capone, D. G. *et al*., 1997

Esaias, W. E. *et al*., 1999.

Gordon, H. R., 1978.

Gordon, H. R., 1997.

Goyet, C., and P. G. Brewer, 1993.

Holligan, P. M. *et al*., 1993.

Iverson, R. L. *et al*., 2000.

Letelier, R. M. *et al*., 1997.

Sikes, S., and V. Fabry, 1994.

Yoder, J. A. *et al*., 1993.

MODIS Pigment Concentration (MOD19), Suspended Solids Concentration (MOD23), and Ocean Water Attenuation Coefficient (MOD26)

Product Description

This set of products provides estimates of the concentration of phytoplankton pigments and other particulate matter, as well as a measure of light attenuation which is governed by these materials. The Pigment Concentration product (MOD19) provides three derived fields: a Coastal Zone Color Scanner (CZCS)-analog pigment concentration based on fluorometric measurements of chlorophyll *a* plus phaepigment; chlorophyll concentration based on high-pressure liquid chromatography (HPLC); and the total pigment concentration, also based on HPLC. Two additional products derived by empirical algorithms are the Total Suspended Matter (MOD23), and the Diffuse Attenuation Coefficient at 490 nm (MOD26). Level 2 products are generated daily and used to create Level 3 daily, 8-day weekly, monthly, and yearly products.

Research and Applications

Optical properties of the open ocean are predominantly governed by phytoplankton, specifically by pigments contained in living cells and by organic materials generated by the phytoplankton. Where this is true, the waters are called Case 1 waters. In Case 2 waters, generally found in coastal regions, optical properties are affected by substances that do not covary with phytoplankton, such as suspended sediments and dissolved organic matter derived from the land. The suite of materials found in Case 1 waters tend to covary systematically. Consequently, the concentration of these substances can be derived empirically from the spectral reflectance or "color" of the water. Likewise, the penetration depth of incoming solar radiation is influenced by the concentration of these materials. The Diffuse Attenuation Coefficient at 490 nm (the wavelength of maximum light penetration in the open ocean) is inversely related to the optical (or e-folding) depth of light at this wavelength. Ninety percent of the water-leaving radiance originates from the upper optical depth, and the euphotic depth is ~4.6 times the optical depth.

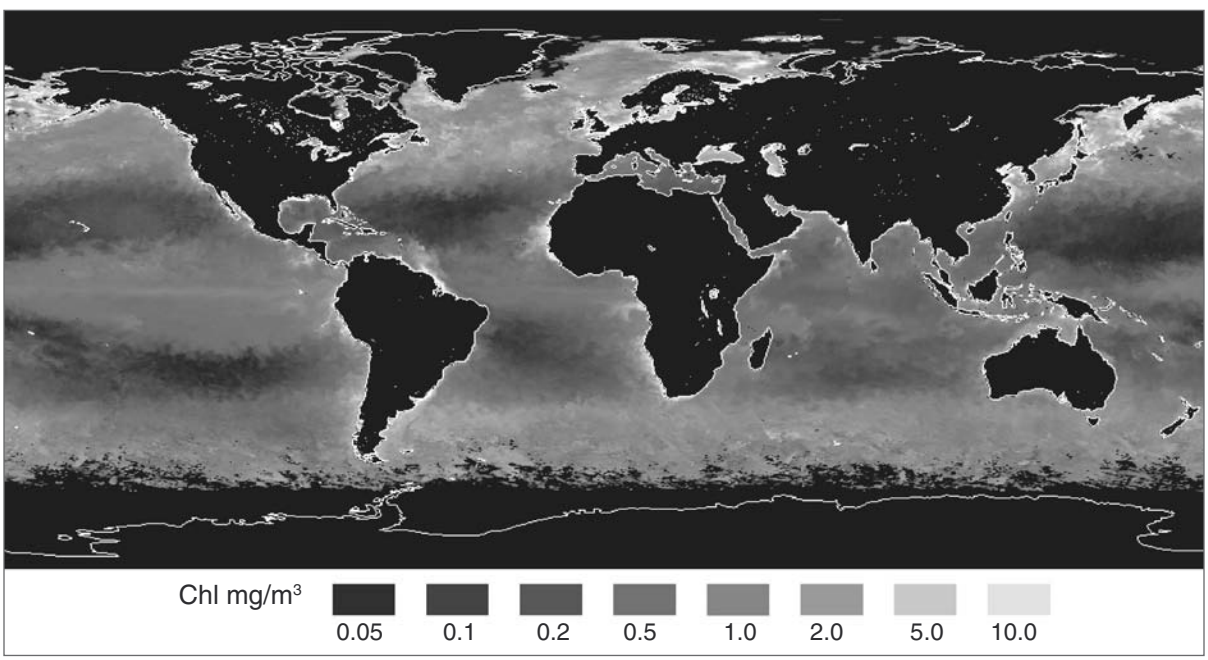

Global image of Chlor_MODIS (MOD19) for May 2001 revealing the concentration of phytoplankton chlorophyll *a*. The algorithm used for Chlor_MODIS is based on high-pressure liquid chromatography (HPLC) measurements. On the internet, visit visibleearth.nasa.gov to view a variety of MODIS data images.

Data Set Evolution

The algorithms used to generate these products are based on empirical relationships, derived according to methods developed for the CZCS mission as described by Gordon and Clark (1980). The algorithms have been refined and adapted to the MODIS bands. In addition, several of the algorithms are now based on HPLC pigment measurements rather than the fluorometric measurements used during the CZCS era. The Diffuse Attenuation Coefficient at 490 (called K490) has historically been a standard product provided by the CZCS and SeaWiFS missions.

Suggested Reading

Esaias, W. E. *et al*., 1998.

Gordon, H. R., and D. K. Clark, 1980.

Gordon, H. R. *et al*., 1980.

Gordon, H. R., and A. Y. Morel, 1983.

Lorenzen, C. J., and S. W. Jeffrey, 1980.

Smith, R. C., and K. S. Baker, 1977.

MODIS Pigment Concentration, Suspended Solids Concentration, and Ocean Water Attenuation Coefficient Product Summary

Coverage: Global ocean surface, clear-sky only

Spatial/Temporal Characteristics: 1 km/daily (Level 2); 4.6 km, 36 km, 1°/daily, 8-day, monthly, yearly (Level 3)

Key Science Applications: Ocean productivity, biogeochemical models

Key Geophysical Parameters: Phytoplankton pigment concentration, total suspended matter concentration, light attenuation

Processing Level: 2, 3

Product Type: Standard, at-launch

Maximum File Size:
MOD19: 102 MB (Level 2); 620 MB (Level 3)

MOD23: 102 MB (Level 2); 640 MB binned, 134 MB mapped (Level 3)

MOD26: 102 MB (Level 2); 640 MB binned, 134 MB mapped (Level 3)

File Frequency:
MOD19: 144/day (Daily Level 2); 3/day (Daily Level 3), 3/8-day (8-day Level 3), 3/month (Monthly Level 3), 3/year (Yearly Level 3)

MOD23, MOD26: 144/day (Daily Level 2); 1/day (Daily Level 3), 1/8-day (8-day Level 3), 1/month (Monthly Level 3), 1/year (Yearly Level 3)

Primary Data Format: HDF-EOS

Browse Available: 36-km sample imagery available at the GES DAAC (Level 3 only)

Additional Product Information:
modis-ocean.gsfc.nasa.gov/dataprod.html

DAAC: Goddard Space Flight Center Earth Sciences DAAC, daac.gsfc.nasa.gov

Science Team Contact: D. Clark

MODIS Chlorophyll Fluorescence (MOD20)

Product Description

This product contains three parameters describing ocean chlorophyll fluorescence properties. Fluorescence Line Height is a relative measure of the amount of radiance leaving the sea surface at the fluorescence wavelength of 683 nm. Fluorescence Efficiency provides a relative measure of the absorption of PAR and its emission as chlorophyll fluorescence. Fluorescence Baseline is the level above which the Line Height is calculated, determined by interpolating between adjacent MODIS bands. The Level 2 product is produced daily at 1 km spatial resolution, and Level 3 is gridded and produced daily, 8-day weekly, monthly, and yearly.

Research and Applications

Solar-stimulated chlorophyll fluorescence is a measure of the current photophysiology of phytoplankton, in contrast to the biomass estimate provided by chlorophyll. The product quantifies the level of photosynthesis by phytoplankton in the ocean. Historically, the coupling between fluorescence and chlorophyll has been studied extensively, and recent research has focused on the use of Sun-stimulated fluorescence to estimate primary productivity (Kiefer and Reynolds, 1992). Basic fluorometric measurements are made using an instrument described by Holm-Hansen *et al*. (1965) that uses blue-light stimulation; this method has been used unchanged for 30 years. Gower and Borstad (1990) were among the first to attempt to use solar-stimulated fluorescence at 683 nm to estimate chlorophyll concentrations from aircraft and satellites.

Data Set Evolution

Inputs to the algorithm are Water-Leaving Radiance (MOD18) in MODIS bands 13 (667 nm), 14 (678 nm), and 15 (748 nm), and the Absorbed Radiation by Phytoplankton (ARP) (MOD22). The algorithm is applied to the daily input standard-product data sets and is remapped into standard Level 3 grids. The validation approach is to compare the fluorescence results with other MODIS data products (e.g., Chlorophyll *a* concentration), with surface measurements, and with other satellite-based estimates of the same products. The products are produced only for non-cloud, glint-free ocean pixels during daylight hours.

Suggested Reading

Abbott, M. R. *et al*., 1982.

Abbott, M. R., and R. M. Letelier, 1998.

Chamberlin, W. S., and J. Marra, 1992.

Esaias, W. E. *et al*., 1998.

Gower, F. J. R., and G. A. Borstad, 1990.

Hoge, F. E. *et al*., 2003.

Holm-Hansen, O. *et al*., 1965.

Kiefer, D. A., and R. A. Reynolds, 1992.

Letelier, R. M. *et al*., 1997.

Topliss, B. J., and T. Platt, 1986.

MODIS Chlorophyll Fluorescence Summary

Coverage: Global ocean surface, clear-sky only

Spatial/Temporal Characteristics: 1 km for chlorophyll levels greater than 2.0 mg/m^3/daily, (Level 2); 4.6 km, 36 km, 1°/8-day, monthly, yearly (Level 3)

Key Science Applications: Ocean chlorophyll, ocean productivity

Key Geophysical Parameters: Chlorophyll fluorescence (fluorescence line height, fluorescence efficiency, fluorescence line curvature)

Processing Level: 2, 3

Product Type: Standard, at-launch

Maximum File Size: 102 MB (Level 2); 640 MB binned, 134 MB mapped (Level 3)

File Frequency: 144/day (Daily Level 2); 3/day (Daily Level 3), 3/week (Weekly Level 3), 3/month (Monthly Level 3), 3/year (Yearly Level 3)

Primary Data Format: HDF-EOS

Additional Product Information: modis-ocean.gsfc.nasa.gov/dataprod.html

DAAC: Goddard Space Flight Center Earth Sciences DAAC, daac.gsfc.nasa.gov

Science Team Contacts: M. Abbott, R. Letelier

Chlorophyll *a* (Chl)

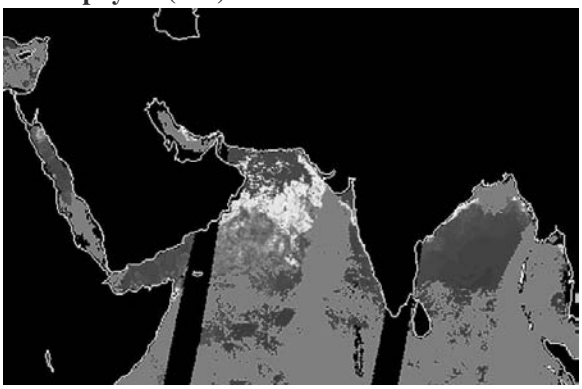

Chlorophyll *a* Concentrations (MOD21) as measured by MODIS in the Indian Ocean on March 1, 2000. Chlorophyll, the green pigment in plants and phytoplankton, absorbs sunlight for use in photosynthesis. Note the high concentrations (light grays) in the Arabian Sea and relatively low concentrations (dark grays) in the Bay of Bengal. The black color in the image represents land areas and gaps between successive satellite orbits, and the gray "stripes" indicate where clouds or sun glint prevented accurate measurements.

Fluorescence Line Height (FLH)

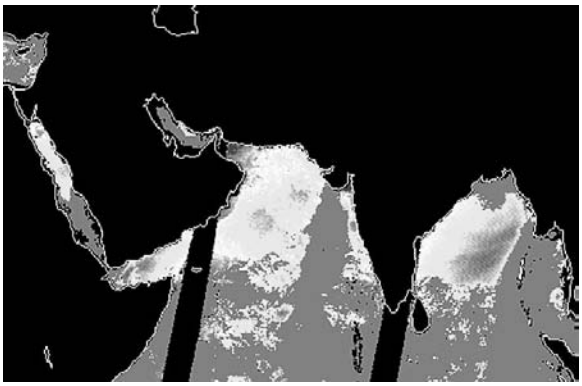

Chlorophyll Fluorescence (MOD20) as measured from the Terra MODIS instrument on March 1, 2000. Phytoplankton re-emit some of the light that is captured by chlorophyll as fluorescence. The amount of fluorescence is roughly proportional to the amount of chlorophyll, so in this image, for example, high fluorescence can be found in the Arabian Sea.

FLH/Chl Ratio

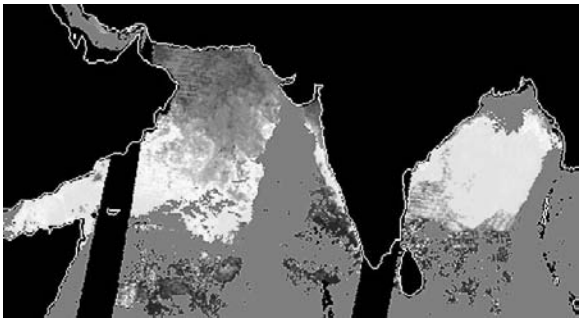

Ratio of Chlorophyll Fluorescence (MOD20) to Chlorophyll *a* Concentration (MOD21), illustrating the considerable variability in the amount of fluorescence per unit of chlorophyll. This variability is largely a function of the health of the phytoplankton. A high ratio implies lower growth rates, as the light captured by phytoplankton is being re-emitted as fluorescence rather than being used for photosynthesis. Phytoplankton in the Arabian Sea are probably growing more rapidly than elsewhere, perhaps in response to dust inputs (which are rich in iron) from the Arabian Peninsula.

MODIS Chlorophyll *a* Pigment Concentration (MOD21), Organic Matter Concentration (MOD24), and Absorption Coefficients (MOD36)

Product Description

The MODIS Chlorophyll *a* Pigment Concentration product (MOD21) provides two estimates of the concentration of chlorophyll *a*: Chlor_a_2 and Chlor_a_3. Chlor_a_2 is a SeaWiFS analog derived according to the OC3M algorithm as documented by O'Reilly *et al*., 2000. This is based on an empirical algorithm, and is intended to provide continuity with the SeaWiFS chlorophyll product. Chlor_a_3 is derived from a semi-analytic algorithm for Case 1 and Case 2 waters. This involves the inversion of a radiance model to determine the absorption coefficient due to phytoplankton at 675 nm, and the absorption coefficient of chromophoric dissolved organic matter (CDOM, also called yellow substance or gelbstoff) at 400 nm. Absorption coefficients generated by this algorithm are also provided. The Absorption Coefficient product (MOD36) includes phytoplankton absorption at 675 nm, and total absorption at 412, 443, 488, 532, and 551 nm. The CDOM absorption at 400 nm is MOD24. The Level 2 products are produced daily at 1-km resolution, and then remapped to derive Level 3 products for daily, 8-day weekly, monthly, and yearly periods. Valid data exist only for cloud-free ocean pixels. The weekly and longer term composites are the average of cloud-free acquisitions for each ocean pixel.

Research and Applications

Chlorophyll *a* is the light-harvesting pigment found in all photosynthetic plants. Its concentration is widely used as an index of phytoplankton biomass and, as such, is a key input to primary productivity models. When converted to carbon or nitrogen, it is used in modeling biogeochemical cycles. On short time scales, chlorophyll can be used to trace oceanographic currents, jets, and plumes. The 1-km resolution and nearly daily coverage of the MODIS data thus allows the observation of meso-scale oceanographic features in coastal and estuarine environments, which are of increasing importance in marine science studies (Liu *et al*., 2002). Absorption coefficients can be used to estimate the solar heating rate of the upper ocean mixed layer, and to study the variability of this rate attributable to variations in phytoplankton absorption. The importance of CDOM as another constituent absorbing radiant energy is a topic ongoing research (Garver and Siegel, 1997).

Data Set Evolution

The Chlor_a_2 algorithm (OC3M) was parameterized using the same data set used to parameterize the SeaWiFS chlorophyll algorithm (OC4.v4). It consists of over 2,800 *in situ* measurements of reflectance and chlorophyll in Case 1 waters worldwide. The empirical OC3M algorithm depends on a predictable relationship between the water's optical variability and its chlorophyll concentration. Thus it is suitable only for Case 1 waters. To derive the chlorophyll concentration in Case 2 waters, one must simultaneously solve for the effects of substances (e.g., CDOM) which do not covary with chlorophyll (for definitions of Case 1 and Case 2, see MOD19 product description). This is the rationale for developing semi-analytic algorithms such as that used by Chlor_a_3.

Chlor_a_3 requires Water-Leaving Radiance (MOD18) and SST (MOD28) as input, and the Absorption Coefficients (MOD36) generated as an intermediate product. The relationship between absorption and the concentration of chlorophyll depends on the amount of "packaging" of chlorophyll in the cells. Packaging is affected by species composition (and size), exposure to light, nutrient conditions, and other factors. The SST (MOD28) is used to determine the relationship between the chlorophyll concentration and the absorption at 670 nm. This algorithm has been thoroughly tested using SeaWiFS data, and post-launch validation has been conducted using data from validation cruises. In addition, the algorithm has been tested using the same data used to parameterize the SeaWiFS at-launch chlorophyll algorithm (OC2). Chlor_a_3 is a principal input to the Ocean Primary Productivity product (MOD27).

Suggested Reading

Austin, R. W., 1974.

Carder, K. L. *et al*., 1986.

Carder, K. L. *et al*., 1991a,b.

Carder, K. L. *et al*., 1999.

Carder, K. L. *et al*., 2003.

Esaias, W. E. *et al*., 1998.

Holm-Hansen, O., and B. Riemann, 1978.

Lee, Z. P. *et al*., 1996.

O'Reilly, J. J. *et al*., 2000.

Smith, R. C., and K. S. Baker, 1982.

MODIS Chlorophyll a Pigment Concentration, Organic Matter Concentration, and Absorption Product Summary

Coverage: Global ocean surface, clear-sky only

Spatial/Temporal Characteristics: 1 km/daily (Level 2); 4.6 km, 36 km, 1°/daily, 8-day, monthly, yearly (Level 3)

Key Science Applications: Ocean productivity, bio-optical properties

Key Geophysical Parameters: Case 1 and 2 chlorophyll a concentration, absorption coefficients

Processing Level: 2, 3

Product Type: Standard, at-launch

Maximum File Size:
MOD21: 83 MB (Level 2); 640 MB binned, 134 MB mapped (Level 3)

MOD24: 83 MB (Level 2); 640 MB binned, 134 MB mapped (Level 3)

MOD36: 102 MB (Level 2); 865 MB binned, 134 MB mapped (Level 3)

File Frequency:
MOD21 and MOD36: 144/day (Daily Level 2); 2/day (Daily Level 3), 2/8-day (8-day Level 3), 2/month (Monthly Level 3), 2/year (Yearly Level 3)

MOD24: 144/day (Daily Level 2); 1/day (Daily Level 3), 1/8-day (8-day Level 3), 1/month (Monthly Level 3), 1/year (Yearly Level 3)

Primary Data Format: HDF-EOS

Browse Available: 36 km sample imagery available at the GES DAAC (Level 3 only)

Additional Product Information:
modis-ocean.gsfc.nasa.gov/dataprod.html

DAAC: Goddard Space Flight Center Earth Sciences DAAC, daac.gsfc.nasa.gov

Science Team Contacts: K. Carder, J. Campbell

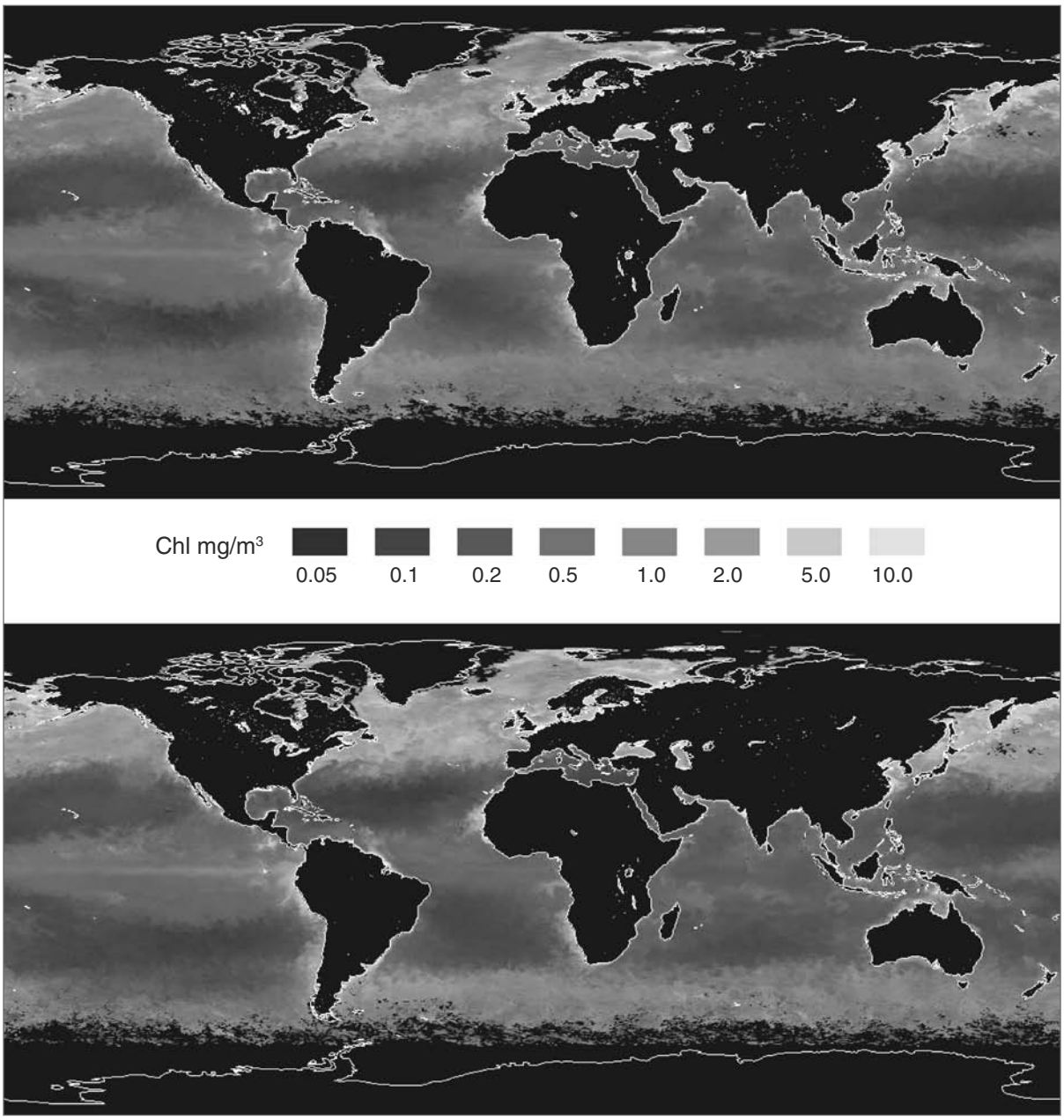

Global images of chlorophyll concentration for May 2001 derived from MODIS Terra data (MOD21). The Chlor_a_2 product (top) is based on an empirical band-ratio algorithm (OC3M) designed to be consistent with the SeaWiFS chlorophyll algorithm (OC4). The Chlor_a_3 chlorophyll concentration (bottom) is derived from a semi-analytic algorithm which accounts for the effects of pigment packaging. This effect is especially pronounced in the Southern Ocean where Chlor_a_3 indicates higher chlorophyll levels than the empirical (ratio) algorithms used by SeaWiFS and Chlor_a_2. Chlor_a_3 is used in deriving primary productivity (MOD27). On the internet, visit visibleearth.nasa.gov to view a variety of MODIS data images.

MODIS Coccolith Concentration (MOD25)

Product Description

This Level 2 and 3 product provides five parameters describing the concentration of coccoliths in sea water: the detached coccolith concentration in number/m^3; the estimated calcite concentration due to the coccoliths in mg-$CaCO_3$/m^3; the pigment concentration in the coccolithophore biomass; a descriptor for the particular look-up table used; and a quality measure. The product is produced at 1-km spatial resolution daily for Level 2 and at 4.6-km, 36-km, and 1° resolution daily, 8-day weekly, monthly, and yearly for Level 3.

Research and Applications

Coccolithophores are small marine phytoplankton, which form external calcium carbonate ($CaCO_3$) scales (called coccoliths) having diameters of a few mm and a thickness of 250 to 750 nm. Coccolithophores are the largest source of calcium carbonate on Earth. Thus, coccolith production is an important part of the biogenic carbon cycle. The observed characteristics of coccolithophores, including their ubiquitous nature, possible role in climate, and intense scattering property, make a global-scale study of their distribution an important application for MODIS imagery. Specifically, it is important to estimate the rate at which $CaCO_3$ is formed by phytoplankton and to look for long-term changes in that rate.

Data Set Evolution

The algorithm for extracting the detached coccolith concentration from surface waters is based on the semianalytic model of ocean color of Gordon (1988). The model relates the normalized water-leaving radiance to the absorption and scattering properties of the constituents of the water using radiative-transfer theory. The absorption and scattering properties are then related to the constituent concentrations through statistical analysis of direct measurements. The model is validated by comparison with a set of water-leaving radiances independent of the measurements used to establish the statistical relationships between constituents and optical properties.

Suggested Reading

Balch, W. M. *et al.*, 1991.

Balch, W. M. *et al.*, 1996a,b.

Balch, W. M. *et al.*, 1999.

Balch, W. M. *et al.*, 2001.

Gordon, H. R. *et al.*, 1988.

Holligan, P. M. *et al.*, 1983.

Sarmiento, J. L. *et al.*, 1988.

Sikes, S., and V. Fabry, 1994.

MODIS Coccolith Concentration Summary

Coverage: Global ocean surface, clear-sky only

Spatial/Temporal Characteristics: 1 km/daily (Level 2); 4.6 km, 36 km, 1°/daily, 8-day, monthly, yearly (Level 3)

Key Science Applications: Input to global biogeochemical cycle models

Key Geophysical Parameters: Coccolith and calcite concentration, pigment concentration in coccolithophore blooms

Processing Level: 2, 3

Product Type: Standard, at-launch

Maximum File Size: 102 MB (Level 2); 640 MB binned, 134 MB mapped (Level 3)

File Frequency: 144/day (Daily Level 2); 3/day (Daily Level 3), 3/8-day (8-day Level 3), 3/month (Monthly Level 3), 3/year (Yearly Level 3)

Primary Data Format: HDF-EOS

Browse Available: 36 km sample imagery available at the GES DAAC (Level 3 only)

Additional Product Information: modis-ocean.gsfc.nasa.gov/dataprod.html

DAAC: Goddard Space Flight Center Earth Sciences DAAC, daac.gsfc.nasa.gov

Science Team Contacts: H. R. Gordon, W. B. Balch

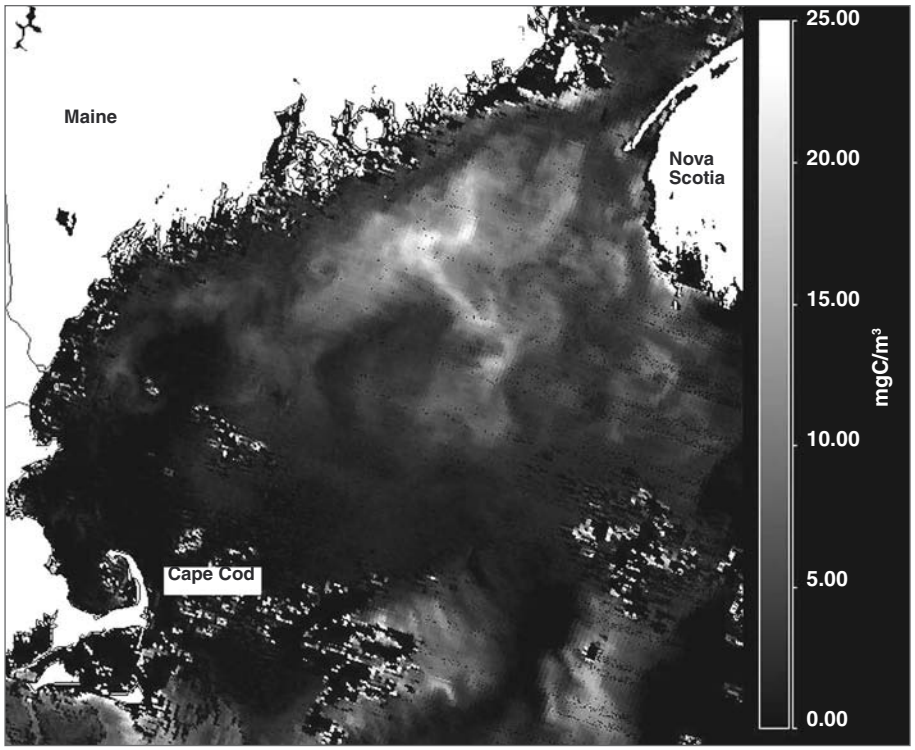

Calcite concentration image of the Gulf of Maine on July 11, 2002. Satellite ocean-color imagery, in addition to allowing the concentration of phytoplankton pigments to be measured remotely, permits the detection and identification of certain algal blooms. The white-to-light-grey waters over the deep basins in the Gulf of Maine are elevated levels of calcite produced by a single type of algae (called coccolithophores), that affects regional climate and fisheries. The apparent high calcite levels over Georges Bank (lower right) are artifacts that occur over shallow regions that are high in suspended sediment. On the internet, visit visibleearth.nasa.gov to view a variety of MODIS data images.

MODIS Ocean Primary Productivity (MOD27)

Product Description

This Level 4 product provides estimates of the Ocean Primary Productivity on an 8-day and an annual basis at spatial resolutions of 4.6 km and 36 km. There are two 8-day productivity estimates in units of gC/m^2d: One (P1) is based on the Behrenfeld and Falkowski (1997a) model which provides primary productivity within the euphotic zone (above the 1% light depth), and the other (P2) is based on the model of Howard and Yoder (1997), which represents productivity within the upper mixed layer. The annual primary productivity, in units of gC/m^2y, is derived using an empirical algorithm based on the annual mean chlorophyll concentration as described in Iverson *et al*. (2000).

Research and Applications

The objective of the product is to quantify the magnitude and interannual variability (for decadal trends) in the oceanic primary productivity and phytoplankton carbon fixation. Primary productivity is the time rate of change of phytoplankton biomass, and, with allowance for excreted soluble carbon compounds, reflects the daily integrated photosynthesis within the water column. The integral of the values over the year is the annual primary productivity. The annual productivity product will be used for global-and regional-scale studies of interannual variability of ocean productivity, for comparisons with annual summations of short-term (8-day) analytical estimates, and for comparison with global biogeochemical models (Esaias *et al*., 1999). Cloudiness prevents deriving chlorophyll *a* concentrations over about 50% of the ocean on a daily basis, excluding that already lost due to high sun glint. Chlorophyll *a* concentrations derived from all available sensors, including the Terra and Aqua MODIS instruments, will be used to increase sampling frequency since these plankton processes vary rapidly over time and space.

Data Set Evolution

Ocean primary productivity algorithms fall into two general classes, termed empirical and analytical. The empirical approach is based on a simple linear correlation between time-averaged in situ estimates of productivity and satellite-derived estimates of surface chlorophyll concentration in regions of the ocean where there are seasonal phytoplankton blooms. The analytical approach is based on models of the general photosynthetic response of the algal biomass as a function of major environmental variables such as light, temperature, and nutrient concentration. The overall methodologies differ significantly in the way various parameters are estimated and in the way they are assigned spatially and temporally across ocean basins (Behrenfeld and Falkowski, 1997b). The approach taken for the MODIS algorithm was to implement the annual empirical algorithm, and two analytical algorithms which were selected as part of a primary productivity algorithm round robin (PPARR) experiment (Campbell *et al*., 2002).

The PPARR experiment involved the comparison of 12 algorithms developed by 10 teams. It was undertaken with the goal of developing a consensus analytical algorithm for short-term (daily to weekly) global productivity. The two analytical algorithms used for this MODIS product were among the best performing algorithms. When compared with *in situ* data at 89 globally distributed stations, their retrievals were within a factor of two of the depth-integrated primary productivity estimated using ^{14}C incubation techniques. Temporally and areally integrated production is expected to reduce the standard error, according to statistical principles, but this cannot be tested because the only means of obtaining basin- or global-scale estimates of oceanic productivity is by satellite observations.

This Level 4 product uses the Chlor_a_3 chlorophyll concentration from MOD21 and the D1 sea surface temperature from MOD28. The photosynthetically available radiation (PAR) is obtained from the GSFC Data Assimilation Office (DAO) by the GES DAAC, and mixed layer depth (MLD) is obtained from the Navy's Fleet Numerical Monterey Oceanographic Center via NOAA NESDIS. These ancillary data fields used in the calculations for primary productivity are provided with the MOD27 product and are also archived and available from the GES DAAC.

Suggested Reading

Behrenfeld, M. J., and P. G. Falkowski, 1997a,b.

Campbell, J. W. *et al*., 2002.

Eppley, R. W. *et al*., 1985.

Esaias, W. E. *et al*., 1998.

Esaias, W. E. *et al*., 1999.

Falkowski, P. G., and J. A. Raven, 1997.

Fitzwater, S. E. *et al*., 1982.

Iverson, R. L. *et al*., 2000.

Morel, A., and J. M. Andre, 1991.

Platt, T. C. *et al*., 1991.

MODIS Ocean Primary Productivity Summary

Coverage: Global ocean surface, clear-sky only

Spatial/Temporal Characteristics: 4.6 km and 36 km/8-day and a running annual average

Key Science Applications: Ocean productivity, biogeochemical models

Key Geophysical Parameters: Annual and weekly ocean productivity

Processing Level: 4

Product Type: Standard, at-launch

Maximum File Size: 1200 MB binned (8-day), 1360 MB binned (Yearly); 32 MB mapped (8-day and Yearly)

File Frequency: 4/8-day

Primary Data Format: HDF-EOS

Additional Product Information: modis-ocean.gsfc.nasa.gov/dataprod.html

DAAC: Goddard Space Flight Center Earth Sciences DAAC, daac.gsfc.nasa.gov

Science Team Contact: W. Esaias

MODIS Phycoerythrin Concentration (MOD31)

Product Description

This product consists of two parameters which give the concentration of one of the major algal pigment groups in ocean water, Phycoerythrin. The two parameters are Phycoerythrobilin Concentration and Phycourobilin Concentration. These quantities are provided for Level 2 at 1-km spatial resolution daily and for Level 3 daily, 8-day weekly, monthly, and yearly at 4.6-km, 36-km, and 1° resolution. The product is valid only for clear-sky ocean pixels.

Research and Applications

One of the intended uses of the phycoerythrin data product is to allow scientific investigators to study the global distributions of the phycoerythrin pigment and, in so doing, to allow definition of the diversity of phycoerythrin-bearing species such as cyanobacteria. Phycoerythrin is one of three major algal pigment groups found in marine phytoplankton and bacteria (Bidigare *et al*., 1990). The phycoerythrins are subdivided into phycourobilin-rich (PUB) and phycoerythrobilin-rich (PEB) phycoerythrins. This algorithm retrieves both PUB- and PEB-rich cases. Phycoerythrin is a chlorophyll accessory pigment and serves to receive photosynthetically usable light in the 480-505 nm and 540-560 nm ranges. It is used to infer the global extent of phycoerythrin-bearing phytoplankton such as cyanobacteria, some of which are nitrogen-fixing and thus provide information on the nitrogen cycle. Used in conjunction with phytoplankton chlorophyll *a* and coccolithophore distributions, the apparent species diversity of the oceans can be inferred.

Data Set Evolution

The phycoerythrin retrieval algorithm requires water-leaving radiances (MOD18) and involves the inversion of a semi-analytical radiance model. In the forward direction, the model (Gordon *et al*., 1988) predicts the radiance from the incident solar irradiance, the total backscatter, and the total absorption of sea water. The PUB and PEB parameters are retrieved by inverting the model using a sequential-convergent-iteration method applied to the first five MODIS ocean bands (bands 8-12). MODIS band 10

(488 nm) and band 12 (551 nm) correspond to the peaks of the PUB and PEB phycoerythrins. The major assumption for the algorithm is that the pigment-specific absorption-coefficient spectral model used is applicable for the oceanic province where the satellite image was acquired. The algorithm will be validated by ship and airborne laser-induced and water Raman-normalized fluorescence measurements.

Suggested Reading

Bidigare, R. R. *et al*., 1990.

Culver, M. E., and M. J. Perry, 1994.

Esaias, W. E. *et al*., 1998.

Gordon, H. R. *et al*., 1988.

Hoge, F. E., and R. N. Swift, 1986.

Hoge, F. E., and R. N. Swift, 1990.

Hoge, F. E. *et al*., 1999a,b.

MODIS Phycoerythrin Concentration Summary

Coverage: Global ocean surface, clear-sky only

Spatial/Temporal Characteristics: 1 km/daily (Level 2); 4.6 km, 36 km, 1°/daily, 8-day, monthly, yearly (Level 3)

Key Science Applications: Global phytoplankton species studies, ocean productivity models

Key Geophysical Parameters: Phycoerythrobilin-rich (PEB) and phycourobulin-rich (PUB) phycoerythrins

Processing Level: 2, 3

Product Type: Research, at-launch

Maximum File Size: 102 MB (Level 2); 640 MB binned, 134 MB mapped (Level 3)

File Frequency: 144/day (Daily Level 2); 2/day (Daily Level 3), 2/8-day (8-day Level 3), 2/month (Monthly Level 3), 2/year (Yearly Level 3)

Primary Data Format: HDF-EOS

Browse Available: 36-km sample imagery available at the GES DAAC (Level 3 only)

Additional Product Information: modis-ocean.gsfc.nasa.gov/dataprod.html

DAAC: Goddard Space Flight Center Earth Sciences DAAC, daac.gsfc.nasa.gov

Science Team Contact: F. E. Hoge

Chapter 12

Snow and Ice Cover

Terra
MODIS

Snow and Ice Cover – An Overview

Relationship to Global Change Issues

Snow and ice cover dramatically influence surface albedo, hydrologic processes, the interactions between the atmosphere and the Earth's surface, and regulation of ecosystem biological activity. For instance, when sea ice is formed in the ocean or snow is deposited on land, there is a dramatic increase in the surface reflectance, and a decrease in the amount of solar energy which is absorbed, hence affecting the Earth's radiation balance and, in turn, its climate. Furthermore, both snow and ice are highly variable components of the climate system, changing dramatically from summer to winter, and, to a lesser extent, from year to year and thus dramatically influence the Earth's energy balance. Two key sensors that provide enhanced global sea ice and snow measurements to supplement existing data sets are the AMSR-E on Aqua and MODIS. The MODIS is onboard both the Terra and Aqua satellites. Both instruments provide information to be used in the development of more accurate models to help understand and predict Earth's climate. MODIS has been providing daily, global coverage of sea ice and snow under clear-sky conditions, and sea ice extent and ice-surface temperature (IST) during both daylight and darkness. Sea ice and snow maps are used for climate research. By extending the existing time series of sea ice and snow cover, which currently spans over 20 years, scientists expect to obtain a better understanding of global, hemispheric, and regional variables on seasonal, interannual, and decadal time scales. Monthly special products are used in general circulation modeling (GCM) for validation of their models.

Sea ice is present over approximately 7% of the Earth's ocean surface (Washington and Parkinson, 1986). Snow-covered sea ice, with its high albedo, is a key parameter of the global energy balance, reflecting much of the incident solar radiation back to space. Additionally, sea ice cover is an insulating layer between the ocean and atmosphere; heat loss through open water is up to 100 times greater than heat loss through thick sea ice. As a consequence, leads and polynyas (linear and nonlinear openings in the sea ice, respectively) are significant to the energy budget of the ice-covered ocean and to local and regional climatology. Such open-water areas and areas of reduced ice concentration are also important for shipping in ice-covered oceans.

In addition to the importance of snow and ice maps in the GCMs, well-validated snow and ice maps are necessary for flood and drought (water quantity) prediction. And sea ice maps are needed for navigation and for energy-balance studies. MODIS snow and ice products can contribute to these efforts.

In many regions, particularly in mountainous areas such as the western United States, knowledge of the amount of snow cover is critical in successfully predicting water supply, planning for agricultural and industrial developments, anticipating flooding, forecasting crop yield, and estimating freeze damage.

Product Overview

Global snow extent has been mapped by MODIS since shortly after the launch of the Terra satellite. The MODIS snow cover products are provided daily and as 8-day composites at 500-m resolution over the Earth's land surfaces, using an algorithm based on the normalized difference of a visible and a shortwave-infrared band. In addition, daily and 8-day composite climate-modeling grid (CMG) maps are provided at 0.05° resolution. The sea ice products derived from MODIS include sea ice extent and temperature, both during the day and at night. Products are provided at 1-km resolution. The MODIS sea ice product is based on the normalized difference between a visible and a shortwave-infrared band. Global sea ice extent and ice-surface temperature (IST) are also mapped daily and as 8-day composite maps. The algorithm to map sea ice is similar to that used to map snow cover, but in addition, a split-window technique using two thermal bands calculates IST.

Product Interdependency and Continuity with Heritage Data

There have been several different satellite instruments that have collected snow and ice data for many years. Snow and ice are among the variables included in NASA's Pathfinder Program, which is providing research-quality data sets on global change from past and current satellite instruments. The heritage of the MODIS instrument is strong. Data sets from MODIS are extending those from historical and current sensors and providing the continuity needed for long-term global climate-change studies. The first detailed data sets of snow cover and sea ice cover came from the NOAA GOES, VHRR, and AVHRR instruments on polar-orbiting platforms. The Landsat Thematic Mapper (TM) was useful in developing

the snow/cloud discrimination ability of the present MODIS snow and sea ice algorithms.

Suggested Reading

Ackerman, S. A. *et al*., 1998.

Armstrong, R. L., and M. J. Brodzik, 2002.

Carroll, T. R., 1995.

Cavalieri, D. J. *et al*., 2002.

Chang, A. T. C. *et al*., 1997.

Chang, A. T. C. *et al*., 2002.

Foster, J. L. *et al*., 1984.

Hall, D. K. *et al*., 1995.

Hall, D. K. *et al*., 2002a,b.

Key, J. R., and J. B. Collins, 1997.

Klein, A. G. *et al*., 1998.

Klein, A. G., and J. Stroeve, 2002.

Magnuson, J. J. *et al*., 2000.

Parkinson, C. L., 2002.

Ramsay, B., 1998.

Riggs, G. A. *et al*., 1999.

Riggs, G. A. *et al*., 2002a,b.

Riggs, G. A., and D. K. Hall, 2002.

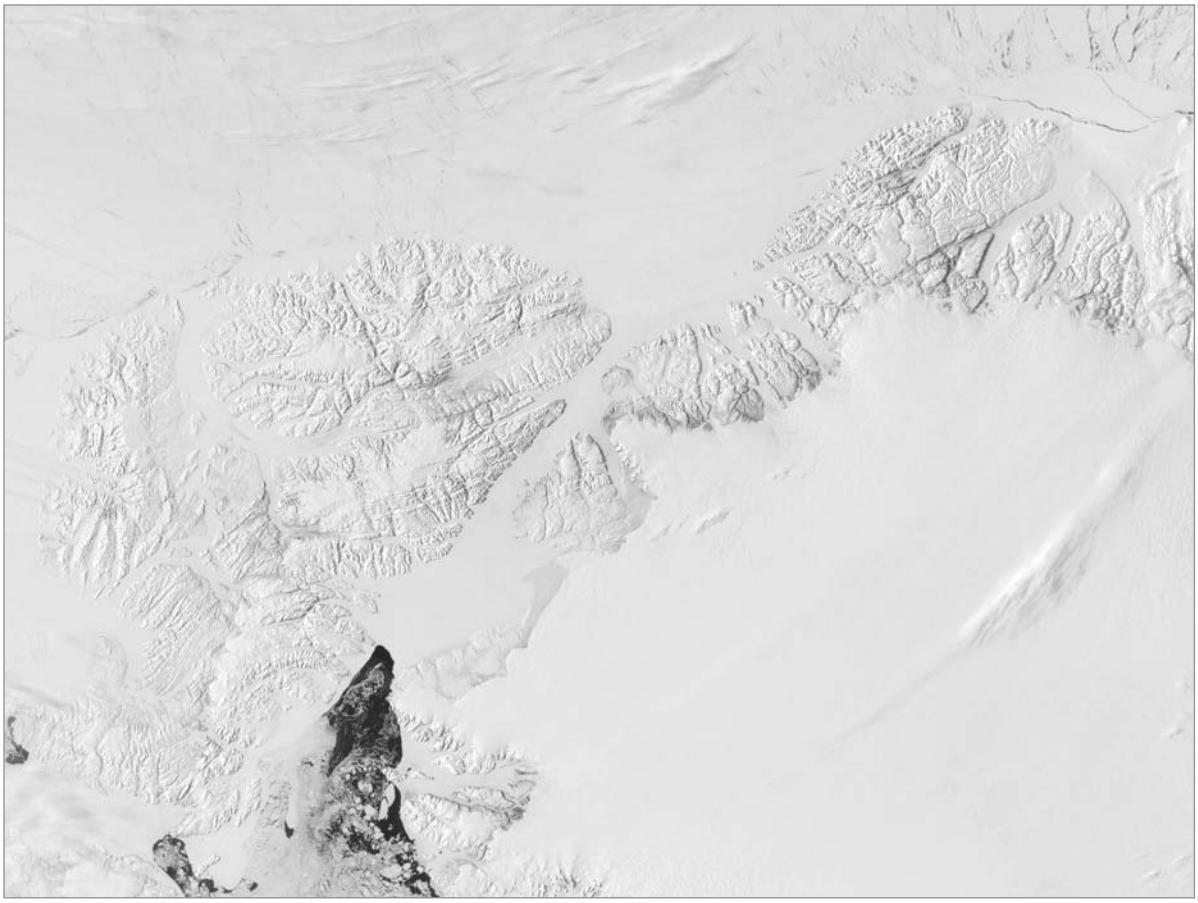

The warmth of spring is reaching the northernmost waters of Baffin Bay between Greenland (right) and Canada's Ellesmere Islands (left). This MODIS image from May 1, 2002 shows that the area of relatively open water is approaching Nares Strait (center), the last narrow passage way that connects the Atlantic Ocean to the Arctic. Image credit: Jacques Descloitres, MODIS Land Rapid Response Team, NASA/Goddard Space Flight Center. On the internet, visit visibleearth.nasa.gov to view a variety of MODIS data images.

MODIS Snow Cover (MOD10)

Product Description

Global snow cover (including ice cover on large, inland water bodies) is mapped daily and as 8-day composites over the Earth's land surfaces at 500-m resolution. A global, daily snow-cover map has been produced since late February 2000. Snow cover, with its high albedo, is a key parameter of the global energy balance, reflecting much of the incident solar radiation back to space. Snow cover of the Northern Hemisphere is currently mapped by NOAA on a daily basis using their Interactive Multisensor Snow and Ice Mapping System (IMS) product (Ramsay, 1998). Another NOAA operational product, from the National Hydrologic Remote Sensing Center (NOHRSC) provides maps of most of the United States and parts of southern Canada, on nearly a daily basis during the Northern Hemisphere snow season (Carroll, 1995). The MODIS snow maps have been compared with the IMS and NOHRSC products. Though none of the snow maps has been determined to be the "gold standard," the maps are shown to be in good agreement under most circumstances (Hall *et al*., 2002). However the maps are of different spatial resolutions and are intended for different purposes.

A daily 500-m snow albedo product is also produced as part of the MODIS snow cover product (MOD10) (Klein and Stroeve, 2002). Once a pixel has been identified as being clear using the MODIS cloud mask (MOD35) and as snow covered using the MODIS snow mapping algorithm, both spectral and broadband albedos are computed using MODIS atmospherically-corrected surface reflectances (MOD09). For surfaces determined to be non-forested by the MODIS land-cover product (MOD12), angular reflection effects are considered using a snow bi-directional reflectance function (BRDF) calculated with a discrete-ordinate radiative transfer model (Disort) and snowpack optical properties. Validation of the snow albedo began in 2002-2003 winter.

The MODIS cloud mask (MOD35) (Ackerman *et al*., 1998) is used to mask clouds on the snow products. Two different versions of the cloud mask are used. A more liberal cloud mask is used for the swath-level products (MOD10_L2) and a conservative cloud mask is used for the tile (MOD10_A1 and MOD10_A2) and climate-modeling grid (CMG) (MOD10_C1 and MOD10_C2) products (Riggs and Hall).

Research and Applications

Large, inland water bodies such as the Great Lakes, are often ice covered during the winter months, and navigation during part of the winter is a significant problem. NOAA data are currently used to map ice cover on the Great Lakes, but discrimination between snow/ice and cloud is a problem. Additionally, ice cover on lakes can be an important climatic indicator, as the dates of freeze-up and break-up are influenced by meteorological conditions. A trend toward earlier break-up, for example, could signify a warming as has been observed in the Northern Hemisphere over the last 150 years (e.g. Magnuson *et al*., 2000). Thus, it is important to measure ice conditions on large lakes over an extended period of time in order to detect trends as well as for operational uses over the short term.

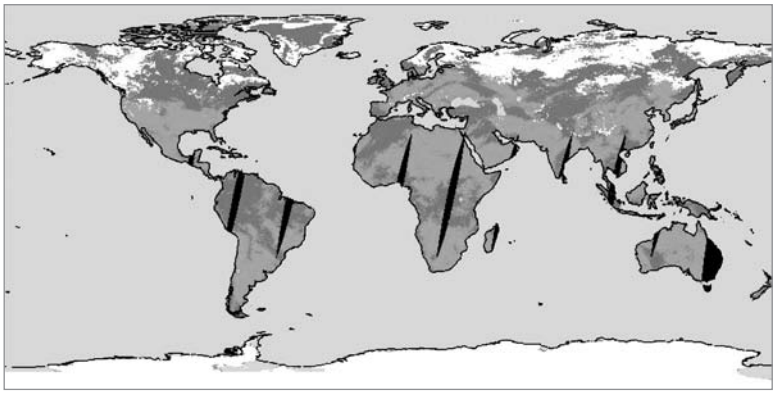

Daily MODIS Climate Modeling Grid (CMG) map at 0.05° resolution. Fractional snow cover in each pixel is also available. The darker gray over land represents cloud cover, lighter gray depicts snow-free areas, and white represents snow cover. On the internet, visit visibleearth.nasa.gov to view a variety of MODIS data images.

Data Set Evolution

The snow-mapping algorithm that is used to produce the MODIS snow maps has a considerable heritage. It is based on the normalized difference of a visible and a shortwave-infrared band. This technique has been used, since at least 1978, to map snow from aircraft, and later from satellites (Kyle *et al*., 1978; Bunting and d'Entremont, 1982; Dozier, 1984). Since the mid-1980s, it has been used to map snow using Landsat data on the drainage-basin scale. The algorithm has been enhanced by incorporating the normalized difference vegetation index (NDVI) (Tucker, 1979), to map the snow cover in denser forests than was possible with the original algorithm (Klein *et al*., 1998). Other threshold tests are employed as well (Riggs *et al*., 2002a).

Global snow cover has also been mapped using passive-microwave data at a resolution of about 50 km. While these data allow snow mapping through cloud cover, passive-microwave data have not provided a resolution that is suitable for detailed snow mapping at the basin scale. With the launch of the Advanced Microwave Scanning Radiometer (AMSR) on the Aqua satellite, snow maps may now be produced at a resolution of up to ~15 km (Chang *et al*., 2002). The expected use of passive-microwave and MODIS snow-cover data, together, should yield information on snow extent and snow-water equivalent (Armstrong and Brodzik, 2002).

Suggested Reading

Carroll, T. R. 1995.

Chang, A. T. C. *et al*., 2002.

Foster, J. L., and A. T. C. Chang, 1993.

Hall, D. K. *et al*., 1995.

Hall, D. K. *et al*., 2002a,b.

Klein *et al*., 1998.

Klein A. G., and J. Stroeve, 2002.

Ramsay, B., 1998.

Riggs, G. A. *et al*., 2002a,b.

Riggs, G. A., and D. K. Hall, 2002.

Salomonson, V. V. *et al*., 1995.

MODIS Snow Cover Summary

Coverage: Global, daytime

Products Available:
MOD10_L2 (swath 500-m resolution),
MOD10_A1 (tile 500-m resolution, daily),
MOD10_A2 (tile 500-m resolution, 8-day composite),
MOD10_C1 (CMG 0.05° resolution, daily),
MOD10_C2 (CMG 0.05° resolution, 8-day composite)

Spatial/Temporal Characteristics: 500 m/daily; 500 m/8-day composite; 0.05° daily and 8-day composites

Key Geophysical Parameters: Snow cover, snow albedo, lake ice cover

Processing Level: 2, 3 (mapped)

Product Type: Standard

Maximum File Size: 34 MB (MOD10_L2); 12 MB (MOD10A1); 12 MB (MOD10A2); 104 MB (MOD10C1); 105 MB (MOD10C2)

File Frequency: 288/day (MOD10_L2); 333/day (MOD10A1), 333/8 day period (MOD10A2), 1/day (MOD10C1), 1/8 day period (MOD10C2)

Primary Data Format: HDF-EOS

Additional Product Information: modis-snow-ice.gsfc.nasa.gov

DAAC: National Snow and Ice Data Center, nsidc.org/daac/

Science Team Contact: D. Hall

MODIS Sea Ice Cover and Ice Surface Temperature (MOD29)

Product Description

Global sea ice cover has been mapped daily and as 8-day composites at 1-km resolution since shortly after the December 1999 launch of the Terra satellite. The MODIS sea ice cover products are based on an algorithm that utilizes the normalized difference snow index (NDSI). In addition, daily and 8-day composite climate-modeling grid (CMG) maps are produced at 0.05º resolution. MODIS sea ice cover maps will complement passive-microwave-derived maps and maps produced using imaging radar. MODIS-derived ice-surface temperature (IST) maps at 1-km resolution, complement IST maps derived from the AMSR instrument, at 25-km resolution.

Research and Applications

Sea ice cover is currently mapped by NOAA visible and near-infrared sensors, and by microwave sensors, both passive and active. Snow/cloud discrimination is a major hindrance in mapping sea ice using visible and near-infrared sensors, while microwave sensors, such as AMSR-E on the Aqua satellite (Cavalieri *et al*., in press), can map sea ice through cloud cover, but at a relatively low resolution. However, passive-microwave sensors can map sea ice type (e.g., first year versus multiyear) (Zwally *et al*., 1983) and sea ice concentration (Parkinson, 2002).

One advantage of using MODIS for mapping sea ice is its relatively high spatial resolution, and the fact that snow/cloud discrimination is possible using the normalized difference snow index (NDSI). Although there is still some ice/cloud confusion, it is possible to map sea ice cover and ice-surface temperature (IST) at a resolution of 1 km (Riggs *et al*., 1999). Thus the visible/near-IR and IR sensors such as MODIS and AVHRR are complementary to the passive-microwave sensors such as the AMSR, and the MODIS maps, when not precluded by clouds, provide a higher-resolution view of sea ice than is obtainable using passive-microwave data.

Data Set Evolution

The sea-ice mapping algorithm has a considerable heritage. It is based on the NDSI and has been shown to be effective for mapping sea ice as well as snow cover (Riggs *et al*., 1999 and 2002b). Additionally, IST is derived using a split-window technique based on the work of Key and Collins (1997) which has been used to map IST with AVHRR data.

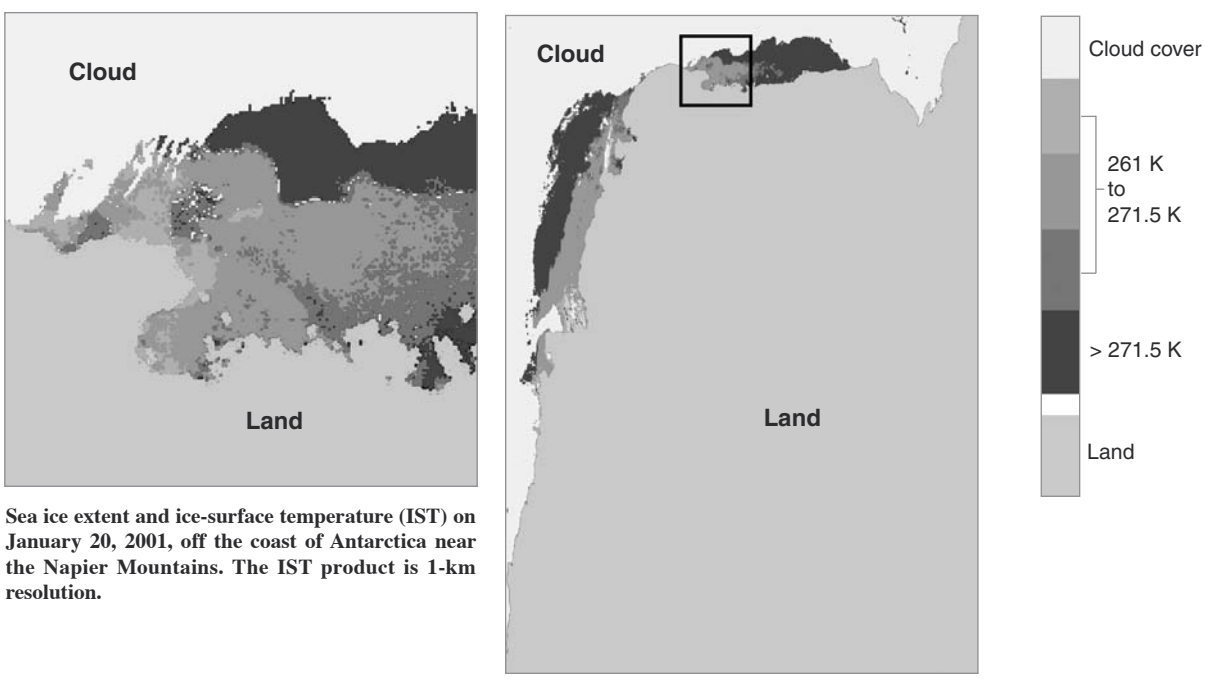

Sea ice extent and ice-surface temperature (IST) on January 20, 2001, off the coast of Antarctica near the Napier Mountains. The IST product is 1-km resolution.

Suggested Reading

Cavalieri, D. J. *et al*., 2002.

Hall, D. K. *et al*., 1995.

Kyle, H. L. *et al*., 1978.

Magnuson, J. J. *et al*., 2000.

Parkinson, C. L., 1997.

Ramsay, B., 1998.

MODIS Sea Ice Cover and Ice Surface Temperature Summary

Coverage: Global, daytime and nighttime over nonequatorial ocean

Products Available: MOD29 (sea ice extent and IST, 1-km resolution); MOD29P1D (sea ice extent and IST, 1-km resolution, daily daytime); MOD29P1N (IST 1-km resolution, daily nighttime)

Spatial/Temporal Characteristics: 1 km/daily; 1 km 8-day composite; 0.05° daily and 8-day composite

Key Geophysical Parameters: Sea ice cover, sea ice surface temperature

Processing Level: 2, 3 (mapped)

Product Type: Standard

Maximum File Size:
MOD29: 20 MB
MOD29P1D: 6 MB
MOD29P1N: 4 MB
MOD29P2D and MOD29P2N: 12 MB (8 day Level 3)

File Frequency:
MOD29: 288/day;
MOD29P1D, MOD29P1N, MOD29P2D and MOD29P2N: 378/day

Primary Data Format: HDF-EOS

Browse Available: No

Additional Product Information: modis-snow-ice.gsfc.nasa.gov

DAAC: National Snow and Ice Data Center, nsidc.org/daac/

Science Team Contact: D. Hall

Chapter 13

Data Assimilation System

Data Assimilation Office/Data Assimilation System – An Overview

The Data Assimilation Office (DAO) develops research-quality 4-dimensional atmosphere-ocean-land data assimilation products for EOS. The data assimilation combines all available data into a dynamically consistent depiction of the Earth-atmosphere system, and has the unique ability to produce estimates of unobserved quantities.

Data assimilation approaches are used throughout science and engineering. Most simply, data assimilation is the use of a mathematical-physical model to analyze observations, while at the same time quantifying the shortcomings of the model formulation.

In Earth science, a data assimilation system is effectively an Earth-system model constrained by Earth-system observations. The data assimilation system: 1) organizes the observations from many diverse instrument sources and measurement times into a single useful data product; 2) complements the observations by propagation of information from observed into unobserved regions and times; 3) provides estimates of expected values of the observations with which to assess data and instrument quality; 4) provides superior products for environmental assessment studies; and 5) supplements the observations by providing estimates of quantities that are difficult or impossible to observe.

The Goddard EOS Data Assimilation System (GEOS DAS) provides Level 4 products of land-surface and atmospheric quantities. GEOS DAS operates on a 6-hour cycle; data are gathered over a 6-hour window, and combined with a General Circulation Model (GCM) background estimate using an objective analysis system at a time in the middle of the 6-hour window. The output from the analysis is then used in the GCM to generate a forecast to provide the background fields in the middle of the next 6-hour assimilation window. The data flow into and out of the DAS is summarized in the Operational Data Flow Diagram, presented in this section.

The GCM used in GEOS DAS uses a physical space discretization with a horizontal resolution of 1° in latitude and 1.25° longitude. The GCM has a vertical discretization using approximately 55 layers with computational top near 0.01 hPa; this combi-

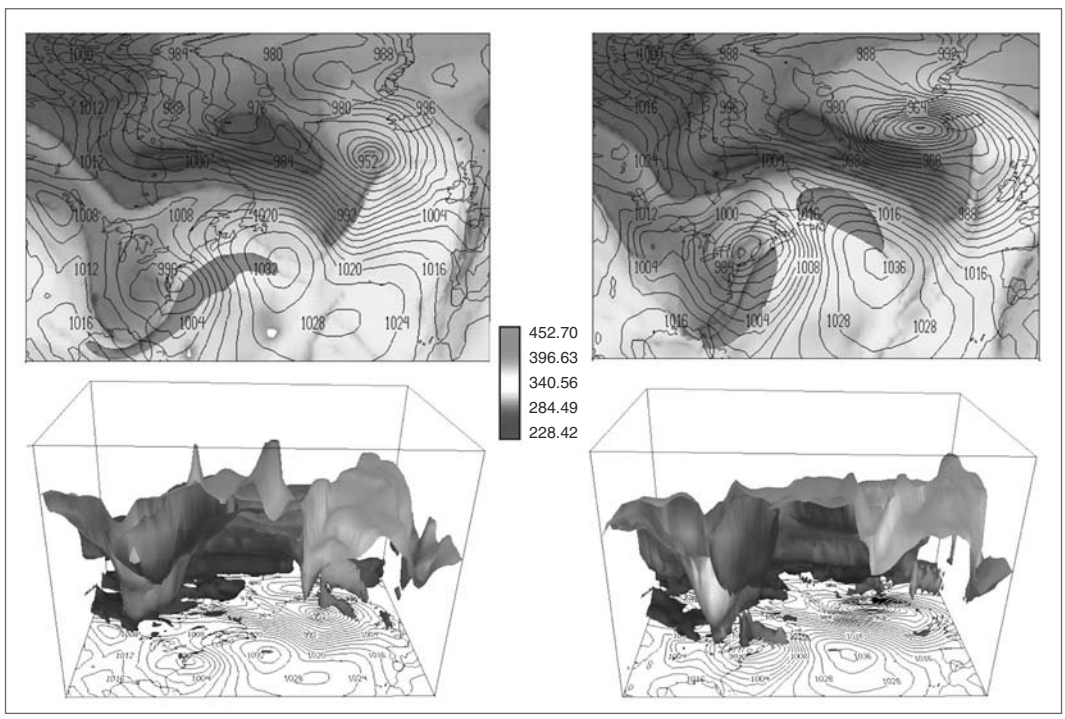

The above image displays variables from the D4FAXMIS/D4LAXMIS and D4FAPMIS/D4LAPMIS products. The ability to determine the location and topography of the tropopause is of interest for a number of applications, including stratospheric chemistry. Top panels: sea level pressure (contours in 4 hPa intervals), jet stream wind speed (60 m/s), and tropopause potential temperature (shaded according to legend). Lower panels: three-dimensional perspective from a southern viewpoint of the above mentioned variables and the dynamic tropopause (1.5PVU surface) with tropopause potential temperature shaded according to legend (slp, uwnd, vwnd, tmpu).

nation allows the GCM to have a fully-resolved stratosphere.

The objective analysis used in GEOS DAS is the Physical-space Statistical Analysis System (PSAS). This is a full 3-dimensional variational analysis system which seeks to produce an optimal combination of disparate data with a 6-h GCM forecast estimate such that the resulting analysis errors are minimized.

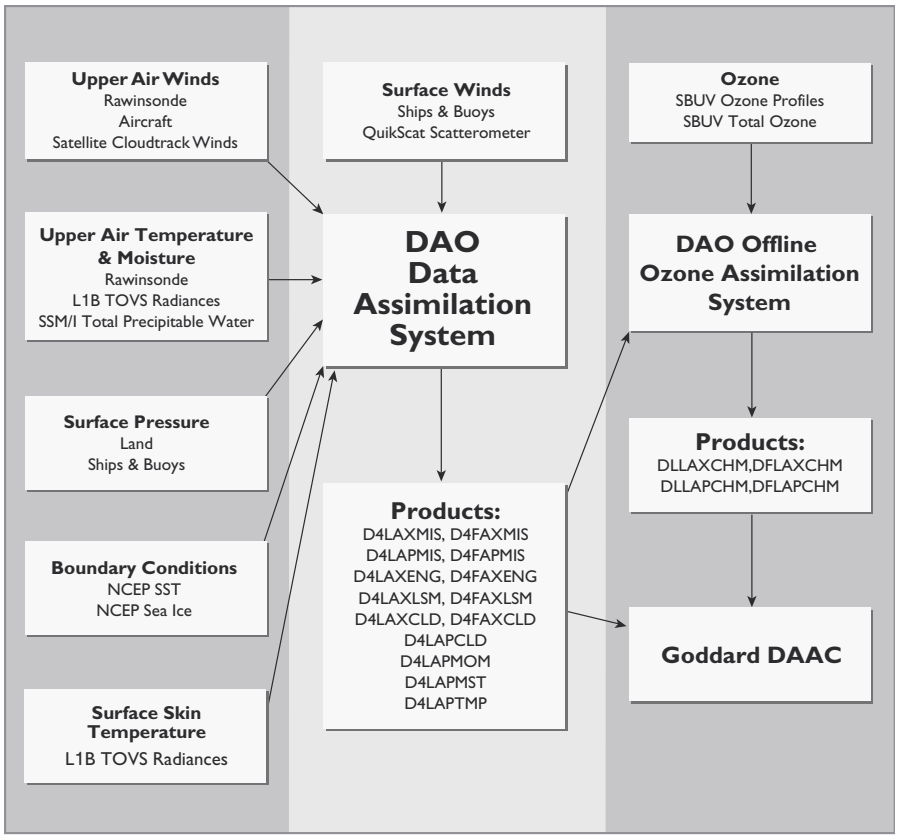

Support for EOS Science Goals

The goals of the DAO during the EOS timeframe are to produce assimilation analyses to ensure that the maximum information is gained from EOS and other observations, and to set the foundation for future Earth system models. Continual research into numerical and theoretical techniques and associated Earth science process studies ensures that the developed system meets the needs of EOS. Analyzing historical and new data sets available in the pre-launch phase of EOS serves as the basis to confront Earth system problems, and the successes and failures of these diagnostic and interpretive studies will define the evolution of the data assimilation system. The assimilated data produced in the pre-launch period were made available to the broad science community to assure infusion of relevant diverse applications into the development process. A commitment is made to continued reanalysis of these data sets to minimize the impact of algorithm changes on interannual signals.

Operational Product Generation

DAO products are produced in two modes, a near-real-time mode called "first-look" and a delayed mode called "late-look." Both modes of operation use the same GEOS-DAS algorithm, but late-look uses higher quality observational inputs. Typically, a larger number of observations are available for late-look, and there is less chance of missing data due to problems with networks or data providers. Due to the accelerated nature of first-look processing, only a subset of DAO products is produced. First-look product IDs begin with "D4F" and late-look product IDs begin with "D4L".

Each DAO product is packaged in an HDF-EOS formatted data set spanning a single day. Some products are time-averaged, and others are instantaneous. This is discussed in the product description section of this chapter and in the File Specification documentation found at dao.gsfc.nasa.gov/Operations/.

Data products are transferred from DAO systems to the Goddard DAAC, from where they are distributed to subscribed customers. The nominal delivery time at the DAAC for first-look products valid for a given day is 11:00 GMT of the following day. The ozone products (D4FAXCHM, D4LAPCHM) are exceptions as they are delivered around 22:00 GMT of the following day. Late-look products are delivered to the DAAC with a 14-to-21 day delay.

GEOS-3 Products

The discussion in this document refers to GEOS-4 data. Version 4 of the GEOS-DAS became operational on October 1, 2002. Prior to this date, the DAO generated GEOS-3 first-look and late-look products that are stored at the GES DAAC under a different set of Earth Science Data Types (EDSTs). The products are very similar to GEOS-4, but there are some differences. For more information, see the GEOS-3 File Specification on the DAO Operations web page (dao.gsfc.nasa.gov/Operations). Note that the period from January 1, 2000 through October 1, 2002 will be re-processed using GEOS-4.

DAO-DAS Time-Averaged Single Level Cloud Quantities (D4FAXCLD, D4LAXCLD)

Product Description

This Level 4 product consists of a collection of time-averaged cloudiness and other cloud-related quantities produced by the DAO Data Assimilation System (DAS). These are typically saved every three hours, averaged for the three hours previous to the time stamp. This includes the total and clear sky outgoing long-and shortwave radiation, total cloud fraction, the low, middle, and high cloud fraction and optical depth, and cloud top temperature and pressure. Products are produced in both a near-real-time "first look" mode and a delayed or "late look" mode, which is described in the overview section of this chapter.

Research and Applications

The cloudiness fields are useful for a wide range of weather and climate studies.

Data Set Evolution

The data are the output of an assimilation process that combines various observations with a short-term forecast (or first guess) provided by the assimilation model. Details of the assimilation process for the current version of the DAO-DAS can be found in the DAO ATBD, located at dao.gsfc.nasa.gov. It is important to know that the quality of each DAS product depends on a number of factors including the quality and density of the relevant input observations, the ability of the forecast model to provide a reasonable first guess for the quantity of interest, and the degree to which the observations constrain that quantity.

It is advisable to refer to the DAO-DAS data flow diagram for the input observations relevant to each of the quantities in this collection of DAS products. All quantities in this collection are diagnostic quantities generated by the model that should be used with caution. Clouds are not directly constrained by observations in the current DAO-DAS, and may be substantially impacted by model bias.

The operational status of first-look and late-look product generation can be found on the DAO web page: dao.gsfc.nasa.gov/Operations/

Suggested Reading

DAO ATBD, available on the DAO home page, dao.gsfc.nasa.gov

File Specification for GEOS-DAS Gridded Output, available at dao.gsfc.nasa.gov/Operations/

DAO-DAS Time-Averaged Single Level Cloud Quantities Product Summary

Coverage: Global

Spatial/Temporal Characteristics: 1.25° × 1° lon-lat grid (288 × 181 grid points), 8 times/file: 01.30, 04.30, 07.30, 10.30, 13.30, 16.30, 19.30, and 22.30 UTC; three-hour average centered on timestamp

Key Geophysical Parameters: Clouds, radiation, optical depth

Processing Level: 4

Product Type: Standard, post-launch, late-look and first-look

Approximate File Size: 15 MB

File Frequency: 1/day

Primary Data Format: HDF-EOS

Additional Product Information: dao.gsfc.nasa.gov/Operations/

Science Team Contact: R. Atlas

DAO-DAS Time-Averaged Near Surface and Vertically-Integrated Quantities (D4FAXENG, D4LAXENG)

Product Description

This Level 4 product consists of a collection of time-averaged near surface, vertically-integrated, and other single-level atmospheric and land quantities produced by the DAO Data Assimilation System (DAS). These are saved every three hours, averaged for the three hours centered on the time stamp. This includes the total precipitation, convective precipitation, surface evaporation, surface sensible heat flux, the ground (skin) temperature, the temperature and specific humidity at 2 and 10 meters, net radiation at the ground, albedo, and vertically-integrated moisture and heat fluxes, specific humidity, and analysis increments. Products are produced in both a near-real time "first look" mode and a delayed or "late look" mode, which is described in the overview section of this chapter. Note that over the ocean the ground temperature is the NCEP sea surface temperature (SST) product specified as a boundary condition in the DAS.

Research and Applications

The surface/near surface fields provide valuable information for a wide variety of land and ocean, and weather and climate studies. The vertically-averaged fields are convenient for studies of various atmospheric budgets and other diagnostic calculations. The vertically-integrated analysis increments are included to close the budget equations.

Data Set Evolution

The data are the output of an assimilation process that combines various observations with a short term forecast (or first guess) provided by the assimilation model. Details of the assimilation process for the current version of the DAO-DAS can be found in the DAO ATBD, located at dao.gsfc.nasa.gov. It is important to know that the quality of each DAS product depends on a number of factors including the quality and density of the relevant input observations, the ability of the forecast model to provide a reasonable first guess for the quantity of interest, and the degree to which the observations constrain that quantity.

It is advisable to check the DAO-DAS data flow diagram for the input observations relevant to each of the quantities in this collection of DAS products. This collection includes a number of diagnostic quantities generated by the model that should be used with caution. These fields, which include the precipitation, surface fluxes, and albedo, are not directly constrained by observations in the current DAO-DAS, and may be substantially impacted by model bias. Over land, the ground temperature, and the two-meter temperature and moisture are also only weakly constrained by the observations since the current version of the DAO-DAS does not assimilate surface/near surface temperature and moisture observations (see above for information about the ground temperature over the oceans).

The operational status of first-look and late-look product generation can be found on the DAO web page: dao.gsfc.nasa.gov/Operations/

Suggested Reading

DAO ATBD, available on the DAO home page, dao.gsfc.nasa.gov

File Specification for GEOS-DAS Gridded Output, available at dao.gsfc.nasa.gov/Operations/

DAO-DAS Time-Averaged Near Surface and Vertically-Integrated Quantities Product Summary

Coverage: Global

Spatial/Temporal Characteristics: 1.25° × 1° lon-lat grid (288 × 181 grid points), 8 times/file: 01.30, 04.30, 07.30, 10.30, 13.30, 16.30, 19.30, and 22.30 UTC; three-hour average centered on timestamp

Key Geophysical Parameters: Precipitation, temperature, moisture, albedo, radiation

Processing Level: 4

Product Type: Standard, post-launch, late-look and first-look

Approximate File Size: 52 MB

File Frequency: 1/day

Primary Data Format: HDF-EOS

Additional Product Information: dao.gsfc.nasa.gov/Operations/

Science Team Contact: R. Atlas

DAO-DAS Time-Averaged 2-Dimensional Surface Data (D4FAXLSM, D4LAXLSM)

Product Description

This Level 4 product consists of 2-dimensional time-averaged surface data produced by the DAO Data Assimilation System (DAS). These are saved every three hours, averaged for the three hours centered on the time stamp. This includes the components of the total precipitation, components of the longwave radiation, components of the photosynthetically active radiation, snow cover, vegetation characteristics and diagnostics of the temperature prediction. The product is gridded, and has one level equivalent to the model surface. Products are produced in both a near-real-time "first look" mode and a delayed or "late look" mode, which is described in the overview section of this chapter.

Research and Applications

The product has 3-hourly intervals to represent the diurnal cycle of the precipitation and energy budget terms. The precipitation is divided into convective, large-scale and frozen components. Both upwelling and downwelling longwave radiation fluxes at the model surface are provided. Leaf area index and greenness are generally prescribed quantities.

Data Set Evolution

In general, the variables in this product are based on model quantities. However, the user should confirm which data are being assimilated for any given data set. For example, precipitation and land data assimilation techniques are under development, and may be implemented, if the appropriate data are available. Likewise, the source of data to prescribe leaf area index and greenness should be confirmed. Furthermore, the parameterization of the land surface is actively developing, and may be updated or changed more frequently than this document. The DAO provides comprehensive descriptions of system updates as they are made.

The operational status of first-look and late-look product generation can be found on the DAO web page: dao.gsfc.nasa.gov/Operations/

Suggested Reading

DAO ATBD, available on the DAO home page, dao.gsfc.nasa.gov

File Specification for GEOS-DAS Gridded Output, available at dao.gsfc.nasa.gov/Operations/

DAO-DAS Time-Averaged 2-Dimensional Surface Data Product Summary

Coverage: Global

Spatial/Temporal Characteristics: 1.25° × 1° lon-lat grid (288 × 181 grid points), 8 times/file: 01.30, 04.30, 07.30, 10.30, 13.30, 16.30, 19.30, and 22.30 UTC; three-hour average centered on timestamp

Key Geophysical Parameters: Precipitation, radiation, temperature, vegetation

Processing Level: 4

Product Type: Standard, post-launch, late-look and first-look

Approximate File Size: 12 MB

File Frequency: 1/day

Primary Data Format: HDF-EOS

Additional Product Information: dao.gsfc.nasa.gov/Operations/

Science Team Contact: R. Atlas

DAO-DAS Time-Averaged Surface and Top-of-the-Atmosphere Stresses (D4FAXSTR, D4LAXSTR)

Product Description

This Level 4 product consists of time-averaged surface frictional stresses and surface and top of the atmosphere stresses due to gravity-wave drag produced by the DAO Data Assimilation System (DAS). These are typically saved every three hours, averaged for the three hours centered on the time stamp. Also included in this collection of quantities are the surface drag coefficient, friction velocity, surface roughness, and the estimated height of the planetary boundary layer (PBL). Products are produced in both a near-real-time "first look" mode and a delayed or "late look" mode, which is described in the overview section of this chapter.

Research and Applications

The surface stress fields are useful for a wide variety of weather and climate studies, particularly those focused on atmosphere-ocean interaction.

Data Set Evolution

The data are the output of an assimilation process that combines various observations with a short term forecast (or first guess) provided by the assimilation model. Details of the assimilation process for the current version of the DAO-DAS can be found in the DAO ATBD, located at dao.gsfc.nasa.gov. It is important to know that the quality of each DAS product depends on a number of factors, including the quality and density of the relevant input observations, the ability of the forecast model to provide a reasonable first guess for the quantity of interest, and the degree to which the observations constrain that quantity.

It is advisable to refer to the DAO-DAS data flow diagram for the input observations relevant for each of the quantities in this collection of DAS products. The surface stress fields in this collection are strongly tied to the analyzed surface winds that, over the oceans, are well constrained by various surface wind observations (e.g., SSM/I winds speed, QuikScat etc., see Atlas *et al.*). The gravity wave stresses should be used with caution since they are sensitive to errors in the model's gravity wave drag parameterization. Similarly, quantities such as the surface drag coefficient, surface roughness, and PBL height are model diagnostic fields that are not directly constrained by the observations.

Suggested Reading

Atlas, R. *et al.*, in press.

DAO ATBD, available on the DAO home page, dao.gsfc.nasa.gov

File Specification for GEOS-DAS Gridded Output, available at dao.gsfc.nasa.gov/Operations/

DAO-DAS Time-Averaged Surface and Top-of-the-Atmosphere Stresses Product Summary

Coverage: Global

Spatial/Temporal Characteristics: 1.25° × 1° lon-lat grid (288 × 181 grid points), 8 times/file: 01.30, 04.30, 07.30, 10.30, 13.30, 16.30, 19.30, and 22.30 UTC; three-hour average centered on timestamp

Key Geophysical Parameters: Pressure, surface stress

Processing Level: 4

Product Type: Standard, post-launch, late-look and first-look

Approximate File Size: 22 MB

File Frequency: 1/day

Primary Data Format: HDF-EOS

Additional Product Information: dao.gsfc.nasa.gov/Operations/

Science Team Contact: R. Atlas

DAO-DAS Time-Averaged 3-Dimensional Cloud Quantities (D4LAPCLD)

Product Description

This Level 4 product consists of a collection of time-averaged 3-dimensional cloud-related quantities produced by the DAO Data Assimilation System (DAS). These are typically saved every six hours, averaged for the three hours previous to and the three hours following the time stamp. This includes the cloud optical depth, the total cloud fraction, and the convective cloud fraction. These products are produced only in a delayed or "late look" mode, which is described in the overview section of this chapter. The fields are gridded and provided on pressure levels as documented in the GEOS-DAS File Specification.

Research and Applications

The cloudiness fields are useful for a wide range of weather and climate studies.

Data Set Evolution

The data are the output of an assimilation process that combines various observations with a short-term forecast (or first guess) provided by the assimilation model. Details of the assimilation process for the current version of the DAO-DAS can be found in the DAO ATBD, located at dao.gsfc.nasa.gov. It is important to know that the quality of each DAS product depends on a number of factors including the quality and density of the relevant input observations, the ability of the forecast model to provide a reasonable first guess for the quantity of interest, and the degree to which the observations constrain that quantity.

It is advisable to refer to the DAO-DAS data flow diagram for the input observations relevant for each of the quantities in this collection of DAS products. All quantities in this collection are diagnostic quantities generated by the model that should be used with caution. Clouds are not directly constrained by observations in the current DAO-DAS, and may be substantially impacted by model bias.

The operational status of first-look and late-look product generation can be found on the DAO web page: dao.gsfc.nasa.gov/Operations/

Suggested Reading

DAO ATBD, available on the DAO home page, dao.gsfc.nasa.gov

File Specification for GEOS-DAS Gridded Output, available at dao.gsfc.nasa.gov/Operations/

DAO-DAS Time-Averaged 3-Dimensional Cloud Quantities Product Summary

Coverage: Global

Spatial/Temporal Characteristics: 1.25° × 1° lon-lat grid, 36 pressure levels in the vertical (360 × 181 × 36 grid points), 4 times/file: 03, 09, 15, and 21 UTC; data are 6-hour time averages centered at the timestamp

Key Geophysical Parameters: Clouds, radiation

Processing Level: 4

Product Type: Standard, post-launch, late-look

Approximate File Size: 90 MB

File Frequency: 1/day

Primary Data Format: HDF-EOS

Additional Product Information: dao.gsfc.nasa.gov/Operations/

Science Team Contact: R. Atlas

DAO-DAS Time-Averaged 3-Dimensional Wind Tendency Fields (D4LAPMOM)

Product Description

This Level 4 product consists of a collection of time-averaged 3-dimensional wind forcing fields produced by the DAO Data Assimilation System (DAS). These are typically saved every six hours, averaged for the three hours previous to and the three hours following the time stamp. This includes the wind forcing due to turbulence, gravity-wave drag, Rayleigh friction, and the analysis increments. These products are produced only in a delayed or "late look" mode, which is described in the overview section of this chapter. The fields are gridded and provided on pressure levels as documented in the GEOS-DAS File Specification.

Research and Applications

The wind forcing fields are useful for a wide range of weather and climate budget and diagnostic studies. The analysis increments are included to close the momentum budgets.

Data Set Evolution

The data are the output of an assimilation process that combines various observations with a short-term forecast (or first guess) provided by the assimilation model. Details of the assimilation process for the current version of the DAO-DAS can be found in the DAO ATBD, located at dao.gsfc.nasa.gov. It is important to know that the quality of each DAS product depends on a number of factors including the quality and density of the relevant input observations, the ability of the forecast model to provide a reasonable first guess for the quantity of interest, and the degree to which the observations constrain that quantity.

It is advisable to refer to the DAO-DAS data flow diagram for the input observations relevant for each of the quantities in this collection of DAS products. All quantities in this collection are diagnostic quantities generated by the model that should be used with caution. The forcing fields are produced by the model parameterizations and are not directly constrained by observations in the current DAO-DAS. They may be substantially impacted by model bias.

The operational status of first-look and late-look product generation can be found on the DAO web page: dao.gsfc.nasa.gov/Operations/

Suggested Reading

DAO ATBD, available on the DAO home page, dao.gsfc.nasa.gov

File Specification for GEOS-DAS Gridded Output, available at dao.gsfc.nasa.gov/Operations/

DAO-DAS Time-Averaged 3-Dimensional Wind Tendency Fields Product Summary

Coverage: Global

Spatial/Temporal Characteristics: 1.25° × 1° lon-lat grid, 36 pressure levels in the vertical (360 × 181 × 36 grid points), 4 times/file: 03, 09, 15, and 21 UTC; data are 6-hour time averages centered at the timestamp

Key Geophysical Parameters: Wind tendencies

Processing Level: 4

Product Type: Standard, post-launch, late-look

Approximate File Size: 150 MB

File Frequency: 1/day

Primary Data Format: HDF-EOS

Additional Product Information: dao.gsfc.nasa.gov/Operations/

Science Team Contact: R. Atlas

DAO-DAS Time-Averaged 3-Dimensional Moisture Tendency Fields (D4LAPMST)

Product Description

This Level 4 product consists of a collection of time-averaged 3-dimensional moisture tendency fields produced by the DAO Data Assimilation System (DAS). These are typically saved every six hours, averaged for the three hours previous to and the three hours following the time stamp. This includes the moisture tendency due to turbulence, moist processes, and the analysis increments. These products are produced only in a delayed or "late look" mode, which is described in the overview section of this chapter. The fields are gridded and provided on pressure levels as documented in the GEOS-DAS File Specification.

Research and Applications

The moisture tendency fields are useful for a wide range of weather and climate budget and diagnostic studies. The analysis increments and moisture filling are included to close the moisture budget.

Data Set Evolution

The data are the output of an assimilation process that combines various observations with a short term forecast (or first guess) provided by the assimilation model. Details of the assimilation process for the current version of the DAO-DAS can be found in the DAO ATBD, located at dao.gsfc.nasa.gov. It is important to know that the quality of each DAS product depends on a number of factors including the quality and density of the relevant input observations, the ability of the forecast model to provide a reasonable first guess for the quantity of interest, and the degree to which the observations constrain that quantity.

It is advisable to refer to the DAO-DAS data flow diagram for the input observations relevant for each of the quantities in this collection of DAS products. All quantities in this collection are diagnostic quantities generated by the model that should be used with caution. The tendency fields are produced by the model parameterizations and are not directly constrained by observations in the current DAO-DAS. They may be substantially impacted by model bias.

The operational status of first-look and late-look product generation can be found on the DAO web page: dao.gsfc.nasa.gov/Operations/

Suggested Reading

DAO ATBD, available on the DAO home page, dao.gsfc.nasa.gov

File Specification for GEOS-DAS Gridded Output, available at dao.gsfc.nasa.gov/Operations/

DAO-DAS Time-Averaged 3-Dimensional Moisture Tendency Fields Product Summary

Coverage: Global

Spatial/Temporal Characteristics: 1.25° × 1° lon-lat grid, 36 pressure levels in the vertical (360 × 181 × 36 grid points), 4 times/file: 03, 09, 15, and 21 UTC; data are 6-hour time averages centered at the timestamp

Key Geophysical Parameters: Transport parameters

Processing Level: 4

Product Type: Standard, post-launch, late-look

Approximate File Size: 60 MB

File Frequency: 1/day

Primary Data Format: HDF-EOS

Additional Product Information: dao.gsfc.nasa.gov/Operations/

Science Team Contact: R. Atlas

DAO-DAS Total Column Ozone (D4FAXCHM, D4LAXCHM)

Product Description

This Level 4 product contains instantaneous vertically integrated atmospheric ozone columns produced by the DAO's ozone data assimilation system (Stajner *et al.*, 2001). It is produced in both near-real-time "first look" mode and in a delayed "late look" mode, which is described in the overview section of this chapter. The fields are two-dimensional and gridded.

Research and Applications

Global total column ozone distribution is needed in climate and weather studies. These global vertically integrated ozone columns are convenient for studies of ozone budget. Total column ozone is a key factor determining the amount of ultraviolet radiation reaching the Earth's surface. Total column ozone amounts are needed in retrievals of geophysical fields from satellite instrument measurements.

Data Set Evolution

Total column ozone and stratospheric ozone profile observations are assimilated into an off-line ozone transport model in repeating assimilation cycles. In one assimilation cycle, an ozone analysis from the previous assimilation cycle is advected to produce a short-term ozone forecast. The advection is done using an off-line transport (forecast) model driven by assimilated winds from the meteorological DAO data assimilation system. The time step of this transport model is 15 minutes, and the observations are introduced to the model after every transport time step. The ozone forecast and observations are combined in a statistical analysis according to specifications of their respective error statistics. A global physical space-based statistical analysis scheme is used. Another assimilation cycle is started from the resulting analyzed ozone field. The three-dimensional analyzed ozone field is vertically integrated to provide analyzed total column ozone every three hours.

Suggested Reading

Stajner, I. *et al.*, 2001.

DAO ATBD, available on the DAO home page, dao.gsfc.nasa.gov

File Specification for GEOS-DAS Gridded Output, available at dao.gsfc.nasa.gov/Operations/

DAO-DAS Total Column Ozone Product Summary

Coverage: Global

Spatial/Temporal Characteristics: 2.5° × 2.0° lon-lat grid, (144 × 91 grid points), 8 times/file: 00, 03, 06, 09, 12, 15, 18 and 21 UTC; data are instantaneous, valid at the timestamp

Key Geophysical Parameters: Total ozone

Processing Level: 4

Product Type: Standard, post-launch, late-look and first-look

Approximate File Size: 0.5 MB

File Frequency: 1/day

Primary Data Format: HDF-EOS

Additional Product Information: dao.gsfc.nasa.gov/Operations/

Science Team Contact: R. Atlas

DAO-DAS Instantaneous Near Surface and Vertically-Integrated State Variables (D4FAXMIS, D4LAXMIS)

Product Description

This Level 4 product consists of a collection of instantaneous near surface, vertically-integrated, and other single-level atmospheric and land quantities produced by the DAO Data Assimilation System (DAS). This includes winds, temperature, and moisture at two and ten meters; ground temperature; vertically-averaged winds, temperature and moisture; sea level pressure; and tropopause temperature and pressure. Products are produced in both a near-real-time "first look" mode and a delayed or "late look" mode, which is described in the overview section of this chapter. Note that over the ocean the ground temperature is the NCEP sea surface temperature (SST) product specified as a boundary condition in the DAS. Other useful quantities included in this collection are the geopotential height and pressure at the Earth's surface at the resolution of the assimilating model, as well as the distribution of the surface types used by the model.

Research and Applications

The near surface fields provide valuable information for a wide variety of land and ocean, and weather and climate studies. The vertically-averaged fields are convenient for studies of various atmospheric budgets and other diagnostic calculations. The tropopause information is provided to aid in the investigation of tropospheric/stratospheric exchange and related studies.

Data Set Evolution

The data are the output of an assimilation process that combines various observations with a short-term forecast (or first guess) provided by the assimilation model. Details of the assimilation process for the current version of the DAO-DAS can be found in the DAO ATBD, located at dao.gsfc.nasa.gov. It is important to know that the quality of each DAS product depends on a number of factors including the quality and density of the relevant input observations, the ability of the forecast model to provide a reasonable first guess for the quantity of interest, and the degree to which the observations constrain that quantity.

It is advisable to refer to the DAO-DAS data flow diagram for the input observations relevant for each of the quantities in this collection of DAS products. In the current version of the DAO-DAS, the surface winds over the ocean are strongly constrained by wind estimates provided by a number satellites (SSM/I, NSCAT, QuikScat, see Atlas *et al.*). Total moisture is well constrained by SSM/I estimates of total precipitable water (see Hou *et al.*). The vertically-integrated temperature and winds are also well-constrained by both satellite and conventional observations. The near surface temperature, humidity, and winds over land should be used with caution since they are weakly constrained by observations and sensitive to model bias.

The operational status of first-look and late-look product generation can be found on the DAO web page: dao.gsfc.nasa.gov/Operations/

Suggested Reading

Atlas, R. *et al.*, in press.

Hou, A. *et al.*, 2000.

DAO ATBD, available on the DAO home page, dao.gsfc.nasa.gov

File Specification for GEOS-DAS Gridded Output, available at dao.gsfc.nasa.gov/Operations/

DAO-DAS Instantaneous Near Surface and Vertically-Integrated State Variables Product Summary

Coverage: Global

Spatial/Temporal Characteristics: 1.25° × 1° lon-lat grid, (360 × 181), 8 times/file: 00, 03, 06, 09, 12, 15, 18, and 21 UTC; data are instantaneous, valid at the timestamp

Key Geophysical Parameters: Sea-level and surface pressure, surface moisture, temperature and winds, tropopause temperature and pressure, and vertically averaged temperature and winds

Processing Level: 4

Product Type: Standard, post-launch, late-look and first-look

Approximate File Size: 32 MB

File Frequency: 1/day

Primary Data Format: HDF-EOS

Additional Product Information: dao.gsfc.nasa.gov/Operations/

Science Team Contact: R. Atlas

DAO-DAS Ozone Mixing Ratio (D4FAPCHM, D4LAPCHM)

Product Description

This Level 4 product contains instantaneous three-dimensional ozone fields produced by the DAO's ozone data assimilation system. It is produced in both near-real-time "first look" mode and in a delayed "late look" mode, which is described in the overview section of this chapter. The fields are gridded and provided on pressure levels as documented in the GEOS-DAS File Specification.

Note that the ozone mixing ratio fields at the following levels: 1000, 975, 950, 925, 900, and 875 hPa are provided at the request of users. No geophysical significance should be attributed to ozone distribution at these levels. The ozone values provided at these levels are extrapolated from the values at 850 hPa. Ozone data are assimilated between 850 and 0.2 hPa.

Research and Applications

Global three-dimensional ozone distribution is needed in climate and weather studies, in determining the amount of ultraviolet radiation reaching the Earth's surface, and in retrievals of geophysical fields from satellite instrument measurements. The ozone profiles can be used as first guess fields in an under-determined problem of ozone retrievals from satellite instrument measurements. They can be used in validation or monitoring of independent ozone measurements. Ozone distribution is also needed in radiative transfer calculations in general circulation models.

Data Set Evolution

Total column ozone and stratospheric ozone profile observations are assimilated into an off-line ozone transport model in repeating assimilation cycles. In one assimilation cycle, an ozone analysis from the previous assimilation cycle is advected to produce short-term ozone forecast. The advection is done using an off-line transport (forecast) model driven by assimilated winds from the meteorological DAO data assimilation system. The time step of this transport model is 15 minutes, and the observations are introduced to the model after every transport time step. The ozone forecast and observations are combined in a statistical analysis according to specifications of their respective error statistics. A global physical space-based statistical analysis scheme is used. Another assimilation cycle is started from the resulting analyzed ozone field. The analyzed three-dimensional ozone field on model levels is interpolated to 36 constant pressure surfaces and saved every 6 hours.

The operational status of first-look and late-look product generation can be found on the DAO web page: dao.gsfc.nasa.gov/Operations/

Suggested Reading

Stajner, I. *et al.*, 2001.

DAO ATBD, available on the DAO home page, dao.gsfc.nasa.gov

File Specification for GEOS-DAS Gridded Output, available at dao.gsfc.nasa.gov/Operations/

DAO-DAS Ozone Mixing Ratio Product Summary

Coverage: Global

Spatial/Temporal Characteristics: 2.5° × 2.0° lon-lat grid, 36 pressure levels in the vertical (144 × 91 × 36 grid points), 4 times/file: 00, 06, 12, and 18 UTC; data are instantaneous, valid at the timestamp

Key Geophysical Parameters: Ozone

Processing Level: 4

Product Type: Standard, post-launch, late-look and first-look

Approximate File Size: 9 MB

File Frequency: 1/day

Primary Data Format: HDF-EOS

Additional Product Information: dao.gsfc.nasa.gov/Operations/

Science Team Contact: R. Atlas

DAO-DAS Instantaneous 3-Dimensional State Variables (D4FAPMIS, D4LAPMIS)

Product Description

This Level 4 product consists of a collection of instantaneous 3-dimensional fields of atmospheric state and other atmospheric variables produced by the DAO Data Assimilation System (DAS). This includes the horizontal winds, temperature, moisture, geopotential height and vertical motion fields. Products are produced in both a near-real-time "first look" mode and a delayed or "late look" mode, which is described in the overview section of this chapter. The fields are gridded and provided on pressure levels as documented in the GEOS-DAS File Specification.

Research and Applications

The 3-dimensional atmospheric state and other fields included in this collection are critical for a wide variety of weather and climate studies. They provide basic information about the dynamics and thermodynamics of the atmosphere, including aspects of the atmospheric component of the hydrological cycle (e.g., atmospheric moisture content, atmospheric moisture flux).

Data Set Evolution

The data are the output of an assimilation process that combines various observations with a short-term forecast (or first guess) provided by the assimilation model. Details of the assimilation process for the current version of the DAO-DAS can be found in the DAO ATBD, located at dao.gsfc.nasa.gov. It is important to know that the quality of each DAS product depends on a number of factors including the quality and density of the relevant input observations, the ability of the forecast model to provide a reasonable first guess for the quantity of interest, and the degree to which the observations constrain that quantity.

It is advisable to refer to the DAO-DAS data flow diagram for the input observations relevant for each of the quantities in this collection of DAS products. In the current version of the DAO-DAS, the winds, temperature, and geopotential height are well-constrained by a combination of *in situ* and satellite observations (radiosonde, cloud track winds, TOVS, SSM/I TPW, etc.). The moisture field is reasonably well constrained by observations (TOVS, SSM/I TPW, limited radiosonde), though values near the surface and in the upper troposphere and stratosphere must be used with caution (see Wu *et al.*). The vertical velocity is not observed. It is produced by the model, though it is of course consistent with the available other observations (horizontal winds, temperature, etc.). Turbulent kinetic energy is also a model-derived field: it is not directly constrained by observations. It should be considered an experimental product.

The operational status of first-look and late-look product generation can be found on the DAO web page: dao.gsfc.nasa.gov/Operations/

Suggested Reading

Wu, M. L. *et al.*, 2001.

DAO ATBD, available on the DAO home page, dao.gsfc.nasa.gov

File Specification for GEOS-DAS Gridded Output, available at dao.gsfc.nasa.gov/Operations/

DAO-DAS Instantaneous 3-Dimensional State Variables Product Summary

Coverage: Global

Spatial/Temporal Characteristics: 1.25° × 1° lon-lat grid, 36 pressure levels in the vertical (288 × 181 × 36 grid points), 4 times/file: 00, 06, 12, and 18 UTC; data are instantaneous, valid at the timestamp

Key Geophysical Parameters: Winds, temperature, geopotential heights, moisture, and kenetic energy

Processing Level: 4

Product Type: Standard, post-launch, late-look and first-look

Approximate File Size: 180 MB

File Frequency: 1/day

Primary Data Format: HDF-EOS

Additional Product Information: dao.gsfc.nasa.gov/Operations/

Science Team Contact: R. Atlas

DAO-DAS Time-Averaged 3-Dimensional Temperature Tendency Fields (D4LAPTMP)

Product Description

This level-4 product consists of a collection of time-averaged 3-dimensional temperature tendency fields produced by the DAO Data Assimilation System (DAS). These are typically saved every six hours, averaged for the three hours previous to and the three hours following the time stamp. This includes the temperature tendency due to turbulence, moist processes, radiative heating/cooling, Rayleigh friction, gravity wave drag, and the analysis increments. These products are produced only in a delayed or "late look" mode, which is described in the overview. The fields are gridded and provided on pressure levels as documented in the GEOS-DAS File Specification.

Research and Applications

The temperature tendency fields are useful for a wide range of weather and climate budget and diagnostic studies. The analysis increments are included to close the moisture budget.

Data Set Evolution

The data are the output of an assimilation process that combines various observations with a short term forecast (or first guess) provided by the assimilation model. The basic data flow for the DAO DAS is illustrated in the overview. Details of the assimilation process for the current version of the DAO-DAS may be found in DAO ATBD. It is important to know that the quality of each DAS product depends on a number of factors including the quality and density of the relevant input observations, the ability of the forecast model to provide a reasonable first guess for the quantity of interest, and the degree to which the observations constrain that quantity.

It is advisable to check the DAO-DAS data flow diagram to check on the input observations relevant for each of the quantities in this collection of DAS products. All quantities in this collection are diagnostic quantities generated by the model that should be used with caution. The tendency fields are produced by the model parameterizations and are not directly constrained by observations in the current DAO-DAS. They may be substantially impacted by model bias.

The operational status of first-look and late-look product generation can be found on the DAO web page: dao.gsfc.nasa.gov/Operations/

Suggested Reading

DAO ATBD, available on the DAO home page, dao.gsfc.nasa.gov

File Specification for GEOS-DAS Gridded Output, available at dao.gsfc.nasa.gov/Operations/

DAO-DAS Time-Averaged 3-Dimensional Temperature Tendency Fields Product Summary

Coverage: Global

Spatial/Temporal Characteristics: 1.25° × 1° lon-lat grid, 36 pressure levels in the vertical (288 × 181 × 36 grid points), 4 times/file: 03, 09, 15, and 21 UTC; data are 6 hour time-averages centered at the timestamp

Key Geophysical Parameters: Temperature tendencies

Processing Level: 4

Product Type: Standard, post-launch, late-look

Approximate File Size: 150 MB

File Frequency: 1/day

Primary Data Format: HDF-EOS

Additional Product Information: dao.gsfc.nasa.gov/Operations/

Science Team Contact: R. Atlas

DAO-DAS Time-Averaged 3-Dimensional Eddy-Diffusivity and Cloud Mass Flux Fields (D4LAPTRP)

Product Description

This level-4 product consists of time-averaged 3-dimensional Eddy-Diffusivity and Cloud Mass Flux Fields produced by the DAO Data Assimilation System (DAS). These are typically saved every six hours, averaged for the three hours previous to and the three hours following the time stamp. This includes the eddy diffusivity for scalers and momentum, the cloud mass flux, and the detrainment cloud mass flux. These products are produced only in a delayed or "late look" mode, which is described in the overview.

Research and Applications

These fields are useful for various off-line transport calculations.

Data Set Evolution

The data are the output of an assimilation process that combines various observations with a short term forecast (or first guess) provided by the assimilation model. The basic data flow for the DAO DAS is illustrated in this chapter's overview. Details of the assimilation process for the current version of the DAO-DAS may be found in the DAO ATBD. It is important to know that the quality of each DAS product depends on a number of factors including the quality and density of the relevant input observations, the ability of the forecast model to provide a reasonable first guess for the quantity of interest, and the degree to which the observations constrain that quantity.

It is advisable to refer to the DAO-DAS data flow diagram for the input observations relevant to each of the quantities in this collection of DAS products. All quantities in this collection are diagnostic quantities generated by the model that should be used with caution. The eddy diffusivity and mass flux fields are a product of the model parameterizations and are not directly constrained by observations in the current DAO-DAS. They may be substantially impacted by model bias.

The operational status of first-look and late-look product generation can be found on the DAO web page: dao.gsfc.nasa.gov/Operations/

Suggested Reading

DAO ATBD, available on the DAO home page, dao.gsfc.nasa.gov

File Specification for GEOS-DAS Gridded Output, available at dao.gsfc.nasa.gov/Operations/

DAO-DAS Time-Averaged 3-Dimensional Eddy-Diffusivity and Cloud Mass Flux Fields Product Summary

Coverage: Global

Spatial/Temporal Characteristics: 1.25° × 1° lon-lat grid, 36 pressure levels in the vertical (288 × 181 × 36 grid points), 4 times/file: 03, 09, 15, and 21 UTC; data are 6 hour time-averages centered at the timestamp

Key Geophysical Parameters: Transport parameters

Processing Level: 4

Product Type: Standard, post-launch, late-look

Approximate File Size: 150 MB

File Frequency: 1/day

Primary Data Format: HDF-EOS

Additional Product Information: dao.gsfc.nasa.gov/Operations/

Science Team Contact: R. Atlas

Appendix A: EOS Distributed Active Archive Centers (DAACs) Contact Information

DAAC & Discipline	Address	User Support Office Contact Information
Alaska SAR Facility (ASF) Sea Ice, Polar Processes, Synthetic Aperture Radar (SAR) Imagery	Alaska SAR Facility, User Services PO Box 757320 University of Alaska Fairbanks, AK 99775-7320	*Email:* asf@eos.nasa.gov, uso@asf.alaska.edu *Phone:* 907-474-6166 *Fax:* 907-474-5195 *URL:* www.asf.alaska.edu/
Land Processes (LP) DAAC Land Processes	United States Geological Survey EROS Data Center Sioux Falls, SD 57198	*Email:* edc@eos.nasa.gov *Phone:* 605-594-6116 *Fax:* 605-594-6963 *URL:* edcdaac.usgs.gov
GSFC Earth Sciences (GES) DAAC Upper Atmosphere, Global Biosphere, Atmospheric Dynamics	NASA/Goddard Space Flight Center Code 902.2 Greenbelt, MD 20771	*Email:* gsfc@eos.nasa.gov *Phone:* 301-614-5224 *Fax:* 301-614-5268 *URL:* daac.gsfc.nasa.gov/
Physical Oceanography (PO) DAAC Physical Oceanography	Physical Oceanography DAAC M/S Raytheon-299 4800 Oak Grove Drive Pasadena, CA 91109	*Email:* jpl@eos.nasa.gov, podaac@podaac.jpl.nasa.gov *Phone:* 626-744-5508 *Fax:* 626-744-5506 *URL:* podaac.jpl.nasa.gov/
Langley Research Center (LaRC) Radiation Budget, Clouds, Aerosols, Tropospheric Chemistry	NASA/Langley Research Center Mail Stop 157D 2 South Wright Street Hampton, VA 23681-2199	*Email:* larc@eos.nasa.gov *Phone:* 757-864-8656 *Fax:* 757-864-8807 *URL:* eosweb.larc.nasa.gov/
Natoinal Snow and Ice Data Center (NSIDC) Snow and Ice, Cryosphere and Climate	University of Colorado Campus Box 449 Boulder, CO 80309-0449	*Email:* nsidc@eos.nasa.gov, nsidc@kryos.colorado.edu *Phone:* 303-492-6199 *Fax:* 303-492-2468 *URL:* www-nsidc.colorado.edu
Oak Ridge National Laboratory (ORNL) Biogeochemical Dynamics	Oak Ridge National Laboratory Environmental Sciences Division PO Box 2008, MS 6407, Bldg. 1507 Oak Ridge, TN 37831-6407	*Email:* ornl@eos.nasa.gov, ornldaac@ornl.gov *Phone:* 423-241-3952 *Fax:* 423-574-4665 *URL:* www-eosdis.ornl.gov
Socioeconomic Data and Applications Center (EDAC) Human Impact on Global Change	Socioeconomic Data and Applications Center Columbia Univ./Lamont-Doherty Earth Observatory P.O. Box 1000, 61 Rt. 9W Palisades, NY 10964	*Email:* ciesin.info@ceisin.columbia.edu *Phone:* 845-365-8920 *Fax:* 845-365-8922 *URL:* sedac.ciesin.org, www.ciesin.org
Global Hydrology Resource Center (GHRC) Lightning, Hydrologic Processes	National Space Science and Technology Center 320 Sparkman Drive Huntsville, AL 35805	*Email:* ghrc@eos.nasa.gov *Phone:* 256-961-7932 *Fax:* 256-961-7859 *URL:* ghrc.msfc.nasa.gov/

Appendix B: Points of Contact

ASTER

Michael Abrams
Mail Stop 183-501
NASA/Jet Propulsion Laboratory
4800 Oak Grove Drive
Pasadena, CA 91109
Phone: 818-354-0937
Fax: 818-354-0966
Email: michael.abrams@jpl.nasa.gov

Ronald Alley
Mail Stop 183-501
NASA/Jet Propulsion Laboratory
4800 Oak Grove Drive
Pasadena, CA 91109
Phone: 818-354-0751
Fax: 818-354-0966
Email: ron.alley@jpl.nasa.gov

Alan Gillespie
University of Washington
Department of Earth and Space Sciences
Campus Box 35-1310
Seattle, WA 98195-1310
Phone: 206-685-8265
Fax: 206-685-2379
Email: alan@oz.geology.washington.edu

Frank Palluconi
Mail Stop 183-501
NASA/Jet Propulsion Laboratory
4800 Oak Grove Drive
Pasadena, CA 91109
Phone: 818-354-8362
Fax: 818-354-0966
Email: frank.d.palluconi@jpl.nasa.gov

Kurt Thome
University of Arizona
Optical Sciences Center
Meinel Building
P.O. Box 210094
Tucson, AZ 85721
Phone: 520-621-4535
Fax: 520-621-8292
Email: kurt.thome@opt-sci.arizona.edu

Hiroshi Wantanabe
ERSDAC
Forefront Tower
3-12-1-Kachidoki
Chuo-ku Tokyo 104-0054 Japan
Phone: 011-81-33-533-9380
Fax: 011-81-33-533-9383
Email: wantanabe@ersdac.or.jp

Ronald Welch
South Dakota School of Mines and Technology
Institute of Atmospheric Science
Rapid City, SD 57701
Phone: 605-394-2291
Fax: 605-394-6061
Email: welch@cloud.ias.sdsmt.edu

CERES

Bruce R. Barkstrom
Mail Stop 420
NASA/Langley Research Center
Hampton, VA 23681
Phone: 757-864-5676
Fax: 757-864-7996
Email: Bruce.R.Barkstrom@nasa.gov

Thomas P. Charlock
Mail Stop 420
NASA/Langley Research Center
Hampton, VA 23681
Phone: 757-864-5687
Fax: 757-864-7996
Email: Thomas.P.Charlock@nasa.gov

David P. Kratz
Mail Stop 420
NASA/Langley Research Center
Hampton, VA 23681
Phone: 757-864-5669
Fax: 757-864-7996
Email: David.P.Kratz@nasa.gov

Robert B. Lee III
Mail Stop 420
NASA/Langley Research Center
Hampton, VA 23681
Phone: 757-864-5679
Fax: 757-864-7996
Email: Robert.B.Lee@nasa.gov

Norman G. Loeb
Mail Stop 420
NASA/Langley Research Center
Hampton, VA 23681
Phone: 757-864-5688
Fax: 757-864-7996
Email: n.g.loeb@larc.nasa.gov

Patrick Minnis
Mail Stop 420
NASA/Langley Research Center
Hampton, VA 23681
Phone: 757-864-5671
Fax: 757-864-7996
Email: Patrick.Minnis-1@nasa.gov

Kory J. Priestley
Mail Stop 420
NASA/Langley Research Center
Hampton, VA 23681
Phone: 757-864-8147
Fax: 757-864-7996
Email: Kory.J.Priestley@nasa.gov

David F. Young
Mail Stop 420
NASA/Langley Research Center
Hampton, VA 23681
Phone: 757-864-5740
Fax: 757-864-7996
Email: David.F.Young@nasa.gov

Bruce A. Wielicki
Mail Stop 420
NASA/Langley Research Center
Hampton, VA 23681
Phone: 757-864-5683
Fax: 757-864-7996
Email: Bruce.A.Wielicki@nasa.gov

Takmeng Wong
Mail Stop 420
NASA/Langley Research Center
Hampton, VA 23681
Phone: 757-864-5607
Fax: 757-864-7996
Email: Takmeng.Wong@nasa.gov

DAS

Robert M. Atlas
Code 910.3
NASA/Goddard Space Flight Center
Greenbelt, MD 20771
Phone: 301-614-6140
Fax: 301-614-6297
Email: Robert.M.Atlas@nasa.gov

LIS

Dennis Boccippio
Code SD60
NASA/Marshall Space Flight Center
320 Sparkman Dr.
Huntsville, AL 35805
Phone: 256-961-7909
Fax: 256-961-7979
Email: dennis.J.boccippio@nasa.gov

Hugh Christian
Code SD60
NASA/Marshall Space Flight Center
320 Sparkman Dr.
Huntsville, AL 35805
Phone: 256-961-7828
Fax: 256-961-7979
Email: Hugh.J.Christian@nasa.gov

Steven Goodman
Code SD60
NASA/Marshall Space Flight Center
320 Sparkman Dr.
Huntsville, AL 35805
Phone: 256-961-7891
Fax: 256-961-7979
Email: Steven.J.Goodman@nasa.gov

MISR

Carol Bruegge
Mail Stop 169-237
NASA/Jet Propulsion Laboratory
4800 Oak Grove Drive
Pasadena, CA 91109-8099
Phone: 818-354-4956
Fax: 818-393-4619
Email: carol.j.bruegge@jpl.nasa.gov

Roger Davies
Mail Stop 169-237
NASA/Jet Propulsion Laboratory
4800 Oak Grove Drive
Pasadena, CA 91109-8099
Phone: 818-393-7236
Fax: 818-393-4619
Email: roger.davies@jpl.nasa.gov

David Diner
Mail Stop 169-237
NASA/Jet Propulsion Laboratory
4800 Oak Grove Drive
Pasadena, CA 91109-8099
Phone: 818-354-6319
Fax: 818-393-4619
Email: david.j.diner@jpl.nasa.gov

Ralph Kahn
Mail Stop 169-237
NASA/Jet Propulsion Laboratory
4800 Oak Grove Drive
Pasadena, CA 91109-8099
Phone: 818-354-9024
Email: ralph.kahn@jpl.nasa.gov
Fax: 818-393-4619

John Martonchik
Mail Stop 169-237
NASA/Jet Propulsion Laboratory
4800 Oak Grove Drive
Pasadena, CA 91109-8099
Phone: 818-354-2207
Fax: 818-393-4619
Email: john.v.martonchik@jpl.nasa.gov

MODIS

Mark Abbott
College of Oceanic & Atmospheric Sciences
Oceanography Administration Building 104
Oregon State University
Corvallis, OR 97331-5503
Phone: 541-737-4045
Fax: 541-737-2064
Email: mark@oce.orst.edu

Steven A. Ackerman
Department of Atmospheric & Oceanic Sciences
University of Wisconsin Madison
1225 W. Dayton Street
Madison, WI 53706
Phone: 608-263-3647
Fax: 608-262-5974
Email: stevea@ssec.wisc.edu

William B. Balch
Bigelow Laboratory
McKown Point
W. Boothbay Harbor, ME 04575
Phone: 207-633-9600
Fax: 207-633-9641
Email: bbalch@bigelow.org

William L. Barnes
Code 970
NASA/Goddard Space Flight Center
Greenbelt, MD 20771
Phone: 301-614-5672
Fax: 301-614-5666
Email: William.L.Barnes@nasa.gov

Otis Brown
RSMAS/MPO
University of Miami
4600 Rickenbacker Causeway
Miami, FL 33149-1098
Phone: 305-361-4000
Fax: 305-361-4622
Email: obrown@rsmas.miami.edu

Janet W. Campbell
Ocean Process Analysis Laboratory
Institute for the Study of Earth, Ocean, and Space
University of New Hampshire
Durham, NH 03824-2535
Phone: 603-862-1070
Fax: 603-862-0243
Email: janet.campbell@unh.edu

Kendall Carder
Department of Marine Science
University of South Florida
140 Seventh Avenue South
St. Petersburg, FL 33701-5016
Phone: 727-553-3952
Fax: 727-553-3918
Email: kcarder@monty.marine.usf.edu

Dennis Clark
Code E/RA28
NOAA/NESDIS
5200 Auth Road, Room 105
Camp Springs, MD 20746-4304
Phone: 301-763-8102
Fax: 301-763-8020
Email: dennis.k.clark@noaa.gov

Wayne Esaias
Code 971
NASA/Goddard Space Flight Center
Greenbelt, MD 20771
Phone: 301-614-5709
Fax: 301-614-5644
Email: Wayne.E.Esaias@nasa.gov

Robert H. Evans
RSMAS/MPO
University of Miami
Meteorology & Physical Oceanography
4600 Rickenbacker Causeway
Miami, FL 33149-1098
Phone: 305-361-4799
Fax: 305-361-4622
Email: bob@rrsl.rsmas.miami.edu

Albert J. Fleig
Code 922.0
NASA/Goddard Space Flight Center
Greenbelt, MD 20771
Phone: 301-614-5498
Fax: 301-614-5269
Email: Albert.J.Fleig.1@gsfc.nasa.gov

Bo-Cai Gao
Remote Sensing Division, Code 7212
Naval Research Laboratory
4555 Overlook Drive, SW
Washington, DC 20375-5320
Phone: 202-767-8252
Fax: 202-404-8894
Email: bo-cai.gao@nrl.navy.mil

Howard R. Gordon
Department of Physics
University of Miami
Coral Cables, FL 33124
Phone: 305-284-2323
Fax: 305-284-4845
Email: gordon@phyvax.ir.miami.edu

Dorothy Hall
Code 974
NASA/Goddard Space Flight Center
Greenbelt, MD 20771
Phone: 301-614-5771
Fax: 301-614-5808
Email: Dorothy.K.Hall@nasa.gov

Frank E. Hoge
Building N-159 (West)
NASA/Wallops Flight Facility
Wallops Island, VA 23337
Phone: 757-824-1567
Fax: 757-824-1036
Email: Frank.E.Hoge@nasa.gov

Alfredo R. Huete
Department of Soil, Water, and Environmental Sciences
University of Arizona
1200 E South Campus Drive
Shantz Building #38
Tuscon, AZ 85721-0038
Phone: 520-621-3228
Fax: 520-621-1647
Email: ahuete@ag.arizona.edu

Christopher O. Justice
Department of Geography
University of Maryland
College Park, MD 20742
Phone: 301-405-1600
Fax: 301-314-6503
Email: justice@hermes.geog.umd.edu

Yoram J. Kaufman
Code 913
NASA/Goddard Space Flight Center
Greenbelt, MD 20771
Phone: 301-614-6189
Fax: 301-614-6307
Email: Yoram.J.Kaufman@nasa.gov

Michael D. King
Code 900
NASA/Goddard Space Flight Center
Greenbelt, MD 20771
Phone: 301-614-5636
Fax: 301-614-5620
Email: Michael.D.King@nasa.gov

Ricardo Letelier
College of Oceanic & Atmospheric Sciences
Oregon State University
104 Ocean Admin Bldg
Corvallis, OR 97331-5503
Phone: 541-737-3890
Fax: 541-737-2064
Email: letelier@coas.oregonstate.edu

Edward J. Masuoka
Code 922
NASA/Goddard Space Flight Center
Greenbelt, MD 20771
Phone: 301-614-5515
Fax: 301-614-5269
Email: Edward.J.Masuoka@nasa.gov

W. Paul Menzel
NOAA/NESDIS
University of Wisconsin Madison
1225 W. Dayton Street
Madison, WI 53706
Phone: 608-264-5325
Fax: 608-262-5974
Email: paulm@ssec.wisc.edu

Peter J. Minnett
RSMAS/MPO
University of Miami
4600 Rickenbacker Causeway
Miami, FL 33149-1098
Phone: 305-361-4104
Fax: 305-361-4622
Email: pminnett@papaya.rsmas.miami.edu

Jan-Peter Muller
Department of Geomatic Engineering
University College London
Gower Street
London WC1E 6BT
United Kingdom
Phone: 44-20-7679-7227
Fax: 44-20-7380-0453
Email: jpmuller@ge.ucl.ac.uk

Ranga B. Myneni
Department of Geography
Boston University
Center for Remote Sensing
675 Commonwealth Avenue
Boston, MA 02215
Phone: 617-353-5742
Fax: 617-353-8399
Email: rmyneni@crsa.bu.edu

Steven Platnick
Code 913
NASA/Goddard Space Flight Center
Greenbelt, MD 20771
Phone: 301-614-6243
Fax: 301-614-6307
Email: steven.platnick@nasa.gov

Lorraine A. Remer
Code 913
NASA/Goddard Space Flight Center
Greenbelt, MD 20771
Phone: 301-614-6194
Fax: 301-614-6307
Email: Lorraine.A.Remer@nasa.gov

Steven W. Running
University of Montana
School of Forestry
Missoula, MT 59812
Phone: 406-243-6311
Fax: 406-243-4510
Email: swr@ntsg.umt.edu

Vincent V. Salomonson
Code 974
NASA/Goddard Space Flight Center
Greenbelt, MD 20771
Phone: 301-614-5631
Fax: 301-614-5808
Email: Vincent.V.Salomonson@nasa.gov

Alan H. Strahler
Department of Geography
Center for Remote Sensing
Boston University
725 Commonwealth Avenue
Boston, MA 02215
Phone: 617-353-5984
Fax: 617-353-8399
Email: alan@bu.edu

Didier Tanré
Laboratoire d' Optique Atmosphérique
Université des Sciences et Techniques de Lille
Bat P5
F-59655 Villeneuve d'Ascq Cedex
France
Phone: 33-3-20-33-70-33
Fax: 33-3-20-43-43-42
Email: tanre@loa.univ-lille1.fr

Kurtis Thome
Remote Sensing Group/OCS
University of Arizona
1630 E. University Blvd
Tucson, AZ 85721-0094
Phone: 520-621-4535
Fax: 520-621-8292
Email: kurt.thome@opt-sci.arizona.edu

John R. G. Townshend
Department of Geography
University of Maryland at College Park
2181 LeFrak Hall
College Park, MD 20742-8225
Phone: 301-405-4050
Fax: 301-314-9299
Email: jt59@umail.umd.edu

Eric Vermote
Code 922
NASA/Goddard Space Flight Center
Greenbelt, MD 20771
Phone: 301-614-5521
Fax: 301-614-5269
Email: eric@kratmos.gsfc.nasa.gov

Kenneth Voss
Department of Physics
University of Miami
Coral Cables, FL 33124
Phone: 305-284-2323
Fax: 305-284-4222
Email: voss@phyvax.physics.miami.edu

Zhengming Wan
Institute for Computational Earth Systems Science
University of California
Santa Barbara, CA 93106-3060
Phone: 805-893-4541
Fax: 805-893-2578
Email: wan@icess.ucsb.edu

Robert E. Wolfe
Code 922.0
NASA/Goddard Space Flight Center
Greenbelt, MD 20771
Phone: 301-614-5508
Fax: 301-614-5269
Email: Robert.E.Wolfe.1@gsfc.nasa.gov

Xiaoxiong (Jack) Xiong
Code 920
NASA/Goddard Space Flight Center
Greenbelt, MD 20771
Phone: 301-867-2179
Fax: 301-614-6015
Email: Xiaoxiong.Xiong-1@nasa.gov

MOPITT

James Drummond
University of Toronto
Department of Physics
60 St. George Street
Toronto, Ontario M5S 1A7
Canada
Phone: 416-978-4723
Fax: 416-978-8905
Email: jim@atmosp.physics.utoronto.ca

David Edwards
National Center for Atmospheric Research
P.O. Box 3000
Boulder, CO 80307
Phone: 303-497-1857
Fax: 303-497-1492
Email: edwards@ucar.edu

John Gille
National Center for Atmospheric Research
P.O. Box 3000
Boulder, CO 80307
Phone: 303-497-8062
Fax: 303-497-2920
Email: gille@ucar.edu

TRMM

Robert Adler
Code 912
NASA/Goddard Space Flight Center
Greenbelt, MD 20771
Phone: 301-286-9086
Fax: 301-286-1762
Email: Robert.F.Adler@nasa.gov

William L. Barnes
Code 970
NASA/Goddard Space Flight Center
Greenbelt, MD 20771
Phone: 301-614-5672
Fax: 301-614-5666
Email: William.L.Barnes@nasa.gov

Alfred Chang
Code 974
NASA/Goddard Space Flight Center
Greenbelt, MD 20771
Phone: 301-286-8997
Fax: 301-286-1758
Email: Alfred.T.Chang@nasa.gov

Robert Houze
Department of Atmospheric Sciences
University of Washington
ATG Bldg., Rm. 608, Code AK-40
Seattle, WA 98195
Phone: 206-543-6922
Fax: 206-543-0308
Email: houze@atmos.washington.edu

Christian Kummerow
Department of Atmospheric Science
Colorado State University
Ft. Collins, CO 80523
Phone: 970-491-7473
Fax: 970-491-8449
Email: kummerow@atmos.colostate.edu

Ken'ichi Okamoto
Director, Global Environment Division
Communications Research Laboratory
4-2-1 Nukui-Kita
Konegai, Tokyo 184
Japan
Phone: 0423-27-7541
Fax: 0423-27-6665
Email: okamoto@crl.go.jp

James Shiue
Code 975
NASA/Goddard Space Flight Center
Greenbelt, MD 20771
Phone: 301-286-6716
Fax: 301-286-1762
Email: James.C.Shiue@nasa.gov

Eric Smith
Code 912.1
NASA/Goddard Space Flight Center
Greenbelt, MD 20771
Phone: 301-286-5770
Fax: 301-286-1626
Email: Eric.A.Smith@nasa.gov

William L. Teng
Code 902
NASA/Goddard Space Flight Center
Greenbelt, MD 20771
Phone: 301-614-5164
Fax: 301-614-5268
Email: teng@daac.gsfc.nasa.gov

Appendix C: References

Abbott, M. R., P. J. Richerson, and T. M. Powell, 1982: *In situ* response of phytoplankton fluorescence to rapid variations in light. *Limn. Oceanog.*, **27**, 218-225.

Abbott, M. R., and R. M. Letelier, 1998: Decorrelation scales of chlorophyll as observed from bio-optical drifters in the California Current. *Deep-Sea Res.*, **45**, 1639-1668.

Abrams, M., 2000: The Advanced Spaceborne Thermal Emission and Reflection Radiometer (ASTER): data products for the high spatial resolution imager on NASA's Terra platform. *Int. J. Remote Sens.*, **21**(5), 847-859.

Abrams, M., S. Hook, and B. Ramachandran, 2002: *ASTER User Handbook, Version 2*. NASA Jet Propulsion Laboratory, 135 pp. Available at: asterweb.jpl.nasa.gov/

Ackerman, S. A., K. I. Strabala, W. P. Menzel, R. A. Frey, C. C. Moeller, and L. E. Gumley, 1998: Discriminating clear sky from clouds with MODIS. *J. Geophys. Res.*, **103**, 32,141-32,157.

Adler, R. F., G. J. Huffman, D. T. Bolvin, S. Curtis, and E. J. Nelkin, 2000: Tropical rainfall distributions determined using TRMM combined with other satellite and rain gauge information. *J. Appl. Meteor.*, **39**, 2007-2023.

Adler, R. F., G. J. Huffman, P. R. Keehn, and A. J. Negri, 1994: Global tropical rain estimates from microwave-adjusted geosynchronous IR data. *Remote Sens. Rev.*, **11**, 125-152.

Ahern, F., G. Goldammer, and C. O. Justice, Eds., 2001: *Global and Regional Vegetation Fire Monitoring From Space: Planning a Coordinated International Effort*. SPB Academic Publishing, The Hague, The Netherlands.

Andreae, M. O., J. Fishman, M. Garstang, J. G. Goldammer, C. O. Justice, J. S. Levine, R. J. Sholes, B. J. Stocke, A. M. Thompson, B. VanWilgen, and STARE/TRACE-A SAFARI-92 Science Team, 1994: Biomass burning in the global environment. *Global Atmospheric-Biospheric Chemistry*, ed. by R. G. Prinn, Plenum Press, New York, 83-101.

Archer D., and E. Maier-Reimer, 1994: Effect of deep-sea sedimentary calcite preservation on atmospheric CO_2 concentration. *Nature*, **367**, 260-263.

Armstrong, R. L., and M. J. Brodzik, 2002: Hemispheric–scale comparison and evaluation of passive-microwave snow algorithms. *Ann. Glaciol.*, **34**, 38-44.

Asrar, G., and J. Dozier, 1994: *Science Strategy for the Earth Observing System*. American Institute of Physics Press, Woodbury, New York, 119 pp.

Asrar, G., and R. Greenstone, eds., 1995: *MTPE/EOS Reference Handbook*. NASA Pub. NP-215, National Aeronautics and Space Administration, Washington, D.C., 276 pp.

Asrar, G., J. F. Creedon, R. S. Estes, A. V. Diaz, H. McDonald, K. Pedersen, and E. Stone, Eds., 2001: *Earth Science Enterprise Strategic Plan*. NASA Headquarters.

Atlas, D., D. Rosenfeld, and D. A. Short, 1990: The estimation of convective rainfall by area integrals, Part 1 the theoretical and empirical basis. *J. Geophys. Res.*, **95**, 2153-2160.

Atlas, R., R. N. Hoffman, S. M. Leidner, J. Sienkiewicz, T.-W. Yu, S. C. Bloom, E. Brin, J. Ardizzone, J. Terry, D. Bungato, and J. C. Jusem, 2001: The effects of marine winds from scatterometer data on weather analysis and forecasting. *Bull. Amer. Meteor. Soc.*, **82**, 1965-1990.

Austin, R. W., 1974: Inherent spectral radiance signals of the ocean surface. In *Ocean Color Analysis*, SIO ref. 74-10, Scripps Inst. Oceanog., La Jolla, CA, 2.1-2.20.

Avis, L. M., R. N. Green, J. T. Suttles, and S. K. Gupta, 1984: A robust pseudoinverse spectral filter applied to the Earth Radiation Budget Experiment (ERBE) scanning channels. *NASA Tech. Memo.* TM-85781, 33 pp.

Awaka, J., T. Iguchi, and K. Okamoto, 1998: Early results on rain type classification by the Tropical Rainfall Measuring Mission (TRMM) precipitation radar. *Proc. 8th URSI Commission F Open Symp.*, Aveiro, Portugal, 143-146.

Balch, W. M., P. M. Holligan, S. G. Ackleson, and K. J. Voss, 1991: Biological and optical properties of mesoscale coccolithophore blooms in the Gulf of Maine. *Limn. Oceanog.*, **34**, 629-643.

Balch, W. M., K. A. Kilpatrick, P. M. Holligan, and C. Trees., 1996a: The 1991 coccolithophore bloom in the central north Atlantic. I. Optical properties and factors affecting their distribution. *Limnol. Oceanogr.*, **41**, 1669-1683.

Balch, W. M., D. Drapeau, J. Fritz, B. Bowler, and J. Nolan, 2001: Optical backscattering in the Arabian Sea-continuous underway measurements of particulate inorganic and organic carbon. *Deep-Sea Res.*, **I48**, 2423-2452.

Balch, W. M., D. T. Drapeau, T. L. Cucci, R. D. Vaillancourt, K. A. Kilpatrick, and J. J. Fritz., 1999: Optical backscattering by calcifying algae—Separating the contribution by particulate inorganic and organic carbon fractions. *J. Geophys. Res.*, **104**, 1541-1558.

Balch, W. M., K. Kilpatrick, P. M. Holligan, D. Harbour, and E. Fernandez., 1996b: The 1991 coccolithophore bloom in the central north Atlantic. II. Relating optics to coccolith concentration. *Limnol. Oceanogr.*, **41**, 1684-1696.

Barkstrom, B. R., and G. L. Smith, 1986: The Earth radiation budget experiment: Science and implementation. *Rev. Geophys.*, **24**, 379-390.

Barkstrom, B. R., and B. A. Wielicki, 1995: Clouds and the Earth's Radiant Energy System (CERES) Algorithm Theoretical Basis Document. Volume I - Overviews, Subsystem 0 - CERES Data Processing System Objectives and Architecture, NASA Ref. Pub. 1376, vol. I, 21-97.

Barnes, R. A., W. L. Barnes, C. Lyu, and J. M. Gales, 2000: An overview of the visible and infrared scanner radiometric calibration algorithm. *J. Atmos. Oceanic Technol.*, **17**, 395-405.

Barnes, W. L., T. S. Pagano, and V. V. Salomonson, 1998: Prelaunch characteristics of the Moderate Resolution Imaging Spectroradiometer (MODIS) on EOS-AM1. *IEEE Trans. Geosci. Remote Sens.*, **36**, 1088.

Barnsley, M. J., and J.-P. Muller, 1991: Measurement, simulation and analysis of directional reflectance properties of Earth surface materials. ESA SP-319, 375-382.

Barry, R. G., and A. L. Varani, eds., 1995: *Earth Observing Science: Highlights 1994*, NSIDC Distributed Active Archive Center, Boulder, CO.

Becker, F., 1987: The impact of spectral emissivity on the measurement of land surface temperature from a satellite. *Int. J. Remote Sens.*, **8**(10), 1509-1522.

Behrenfeld, M. J., and P. G. Falkowski, 1997a: Photosynthetic rates derived from satellite-based chlorophyll concentration. *Limnol. Oceanogr.*, **42**, 1-20.

Behrenfeld, M. J., and P. G. Falkowski, 1997b: A consumer's guide to phytoplankton primary productivity models. *Limnol. Oceanogr.*, **42**, 1479-1491.

Bidigare, R. R., M. E. Ondrusek, J. H. Morrow, and D. A. Kiefer, 1990: In vivo absorption properties of algal pigments. SPIE Vol. 1302, Ocean Optics X, 290-302.

Boccippio, D. J., K. T. Driscoll, J. M. Hall, and D. E. Buechler, 1998: LIS/OTD Software Guide, available at thunder.nssta.nasa.gov/data.html.

Boccippio, D. J., K. T. Driscoll, W. J. Koshak, R. J. Blakeslee, W. L. Boeck, D. A. Mach, D. E. Buechler, H. J. Christian, and S. J. Goodman, 2000: The Optical Transient Detector (OTD): Instrument characteristics and cross-sensor validation. *J. Atmos. Oceanic Technol.*, **17**, 441-458.

Boccippio, D. J., S. J. Goodman, and S. Heckman, 2000: Regional differences in tropical lightning distributions. *J. Appl. Meteor.*, **39**, 2231-2248.

Boccippio, D. J., W. J. Koshak, and R. J. Blakeslee, 2002: Performance assessment of the Optical Transient Detector and Lightning Imaging Sensor:1. Predicted diurnal variability. *J. Atmos. Oceanic Technol.*, **19**, 1318-1332.

Boccippio, D. J., and coauthors, 2000b: The Optical Transient Detector (OTD): Instrument characteristics and cross-sensor validation. *J. Atmos. Oceanic Technol.*, **17**, 441-458.

Bohme, R., 1991-1993: *Inventory of world topographic mapping*. In three volumes on behalf of the International Cartographic Association, Elsevior Applied Science Publishers, New York, 1070 pp.

Borak, J. S., and A. H. Strahler, 1999: Feature selection and land cover classification of a MODIS-like data set for a semiarid environment. *Int. J. Remote Sens.*, **20**, 919-938.

Bothwell, G. W., E. G. Hansen, R. E. Vargo, and K. C. Miller, 2002: The Multi-angle Imaging SpectroRadiometer science data system, its products, tools, and performance. *IEEE Trans. Geosci. Remote Sens.*, **40**, 1467-1476.

Brasseur, G. P., and R. G. Prinn, 1992: Biogenic and anthropogenic trace gases in the atmosphere. *The Use of EOS for Studies of Atmospheric Physics*, ed. by J. C. Gille and G. Visconti, North Holland, Amsterdam, 45-64.

Breigleb, B. P., and V. Ramanathan, 1982: Spectral and diurnal variations in clear-sky planetary albedo. *J. Climate Appl. Meteor.*, **21**, 1168-1171.

Brenninkmeijer, C. A. M., M. R. Manning, D. C. Lowe, G. Wallace, R. J. Sparks, and A. Volz-Thomas, 1992: Interhemispheric asymmetry in OH abundance inferred from measurements of atmospheric CO. *Nature*, **356**, 50-52.

Brest, C. L., and S. N. Goward, 1987: Deriving surface albedo measurements from narrow band satellite data. *Int. J. Remote Sens.*, **8**, 351-367.

Brooks, D. R., E. F. Harrison, P. Minnis, J. T. Suttles, and R. S. Kandel, 1986: Development of algorithms for understanding the temporal and spatial variability of the Earth's radiation balance. *Rev. Geophys.*, **24**, 422-438.

Brown, O., R. Evans, P. Minnett, E. Kearns, and K. Kilpatrick, 2002: Sea Surface Temperature measured by the Moderate Resolution Imaging Spectroradiometer (MODIS) (PowerPoint presentation), EOS IWG, Ellicott City, MD.

Bruegge, C. J., N. L. Chrien, R. R. Ando, D. J. Diner, W. A. Abdou, M. C. Helmlinger, S. H. Pilorz, and K. J. Thome, 2002: Early validation of the Multi-angle Imaging SpectroRadiometer (MISR) radiometric scale. *IEEE Trans. Geosci. Remote Sens.*, **40**, 1477-1492.

Bruegge, C. J., V. G. Duval, N. L. Chrien, R. P. Korechoff, B. J. Gaitley, and E. B. Hochberg, 1998. MISR prelaunch instrument calibration and characterization results. *IEEE Trans. Geosci. Remote Sens.* **36**, 1186-1198.

Buechler, D. E., K. T. Driscoll, S. J. Goodman, and H. J. Christian, 2000: Lightning activity within a tornadic thunderstorm observed by the Optical Transient Detector (OTD). *Geophys. Res. Lett.*, **27**, 2253-2256.

Campbell, J. W., D. Antoine, R. Armstrong, K. Arrigo, W. Balch, R. Barber, M. Behrenfeld, R. Bidigare, J. Bishop, M.-E. Carr, W. Esaias, P. Falkowski, N. Hoepffner, R. Iverson, D. Kiefer, S. Lohrenz, J. Marra, A. Morel, J. Ryan, V. Vedernikov, K. Waters, C. Yentsch, and J. Yoder, 2002: Comparison of algorithms for estimating ocean primary productivity from surface chlorophyll, temperature, and irradiance. *Global Biogeochem. Cycles*, in press.

Capone, D. G., J. P. Zehr, H. W. Paerl, B. Bergman, and E. J. Carpenter, 1997: Trichodesmium: A globally significant marine cyanobacterium. *Science*, **276**, 1221-1229.

Carder, K., 2001: Chrlorophyll *a* (Semi-Analytic), PAR, total Absobption Coefficient, MOD 21, 22, 36, 39 Status. Powerpoint Presentation, MODIS Science Team Meeting, BWI Marriott, December 17-19, 2001. modis-ocean.gsfc.nasa.gov/refs.html

Carder, K., 2002: Performance of MODIS Semi-analytic Ocean Color Algorithms: Chlorophyll *a*, Absorption Coefficients, and Absorbed Radiation by Phytoplankton, Powerpoint Presentation, MODIS Science Team Meeting, Greenbelt, MD, July 22-24, 2002. modis-ocean.gsfc.nasa.gov/refs.html.

Carder, K. L., F. R. Chen, J. P. Cannizzaro, J. W. Campbell, and B. G. Mitchell, 2003: Performance of the MODIS semi-analytical ocean color algorithm for chlorophyll-*a*. *Adv. Space Res.*, in press.

Carder, K. L, F. R. Chen, Z. P. Lee, S. K. Hawes, and D. Kamykowski, 1999: Semianalytic Moderate-Resolution Imaging Spectrometer algorithms for chlorophyll *a* and absorption with bio-optical domains based on nitrate-depletion temperatures. *J. Geophys. Res.*, **104**(C3), 5403-5421.

Carder, K. L., R. G. Steward, J. H. Paul, and G. A. Vargo, 1986: Relationship between chlorophyll and ocean color constituents as they affect remote-sensing reflectance models. *Limn. Oceanog.*, **31**, 403-413.

Carder, K. L., S. K. Hawes, K. A. Baker, R. C. Smith, R. G. Steward, and B. G. Mitchell, 1991a: Reflectance model for quantifying chlorophyll *a* in the presence of productivity degradation products. *J. Geophys. Res.*, **96**, 599-611.

Carder, K. L., W. W. Greg, D. K. Costello, K. Haddad, and J. M. Prospero, 1991b: Determination of Saharan dust radiance and chlorophyll from CZCS imagery. *J. Geophys. Res.*, **96**, 5369-5378.

Carroll, T. R., 1995: Remote sensing of snow in the cold regions. *Proceedings of the First Moderate Resolution Imaging Spectroradiometer (MODIS) Snow and Ice Workshop*, 13-14 September, 1995, Greenbelt, MD, NASA Conf. Pub. 3318, 3-14.

Cavalieri, D. J., J. Maslanik, T. Markus, J. Stroeve, M. Sturm, J. Heinrichs, E. Kim, A. J. Gasiewski, and J. C. Comiso, 2002: EOS Aqua AMSR-E Arctic sea ice validation program. *Proceedings of the International Society for Optical Engineering, Symposium on Remote Sensing of the Atmosphere, Ocean, Environment, and Space*, 23-27 October 2002, Hangzhou, China.

Caylor I. J., G. M. Heymsfield, R. Meneghini, and L. S. Miller, 1997: Correction of sampling errors in ocean surface cross-sectional estimates from nadir-looking weather radar. *J. Atmos. Oceanic Technol.*, **14**, 203-210.

Cess, R., E. Dutton, J. DeLuisi, and F. Jiang, 1991: Determining surface solar absorption from broadband satellite measurements for clear skies: Comparisons with surface measurements. *J. Climatol.*, **4**, 236-247.

Chahine, M. T., 1980: Infrared remote sensing of sea surface temperature. In *Remote Sensing of Atmospheres and Oceans*, ed. by A. Deepak, Academic Press, New York, 411-435.

Chambers, L. H., B. Lin, and D. F. Young, 2002: Examination of new CERES data for evidence of tropical Iris feedback. *J. Climate*, **15**, 3719-3726.

Chamberlin, W. S., and J. Marra, 1992: Estimation of photosynthetic rate from measurements of natural fluorescence: Analysis of the effects of light and temperature. *Deep-Sea Res.*, **39**, 1695-1706.

Chang, A. T. C., L. S. Chiu, C. Kummerow, and J. Meng, 1999a: First results of the TRMM Microwave Imager (TMI) monthly oceanic rain rate: Comparison with SSM/I. *Geophys. Res. Lett.*, **26**, 2379-2382.

Chang, A. T. C., L. S. Chiu, 1999b: Nonsystematic Errors of Monthly Oceanic Rainfall Derived from SSM/I. *Mon. Wea. Rev.*, **127**, 1630–1638.

Chang, A. T. C., R. E. J. Kelly, J. L. Foster, and D.K. Hall, 2002: Estimation of global snow cover using passive microwave data. *Proceedings of the International Society for Optical Engineering, Symposium on Remote Sensing of the Atmosphere, Ocean, Environment, and Space*, 23-27 October 2002, Hangzhou, China.

Charlock, T. P., and T. L. Alberta, 1996: The CERES/ARM/GEWEX Experiment (CAGEX) for the retrieval of radiative fluxes with satellite data. *Bull. Amer. Meteor. Soc.*, **77**, 2673-2683.

Charlock, T. P., F. Rose, S.-K Yang, T. Alberta, and G. Smith, 1993: An observation study of the interaction of clouds, radiation, and the general circulation. *Proceedings of the IRS '92: Current Problems in Atmospheric Radiation*. Tallinn (3-8 August 1992), A. Deepak Publishing, 151-154.

Charlock, T. P., D. Rutan, G. L. Smith, F. G. Rose, T. L. Alberta, N. Manalo-Smith, L. H. Coleman, D. P. Kratz, T. D. Bess, and K. A. Bush, 1995: Clouds and the Earth's Radiant Energy System (CERES) Algorithm Theoretical Basis Document. Volume IV - Determination of Surface and Atmosphere Fluxes and Temporally and Spatially Averaged Products (Subsystems 5-12), Subsystem 5.0 - Compute Surface and Atmospheric Fluxes, NASA Ref. Pub. 1376, Vol. IV, 1-52.

Chen, Y., S. Sun-Mack, P. Minnis, D. F. Young, and W. L. Smith, Jr., 2002: Surface spectral emissivity derived from MODIS data. *Proc. SPIE 3rd Intl. Asia-Pacific Environ. Remote Sens. Symp. 2002: Remote Sensing of Atmosphere, Ocean, Environment, and Space*, Hangzhou, China, October 23-27.

Chicano, R. J., and R. S. Oremland, 1988: Biogeochemical aspects of atmospheric methane. *Global Biogeochem. Cycles*, **2**, 299-327.

Chiu, L. S., 1988: Rain estimation from space observations: Areal rainfall-rain area relationship. Paper presented at the Third Conference on Satellite Meteorology and Oceanography of the American Meteorological Society, Feb. 1-5, 1988, Anaheim, CA. Preprint Volume, pp. 3663-3668.

Chiu, L. S., A. Chang, J. Janowiak, 1993: Comparison of Monthly Rain Rates Derived from GPI and SSM/I Using Probability Distribution Functions. *J. Appl. Meteor.*, **32**, 323-334.

Chomko, R., and H. R. Gordon, 1998: Atmospheric correction of ocean color imagery: Use of the Junge power-law aerosol size distribution with variable refractive index to handle aerosol absorption. *Appl. Opt.*, **37**, 5560-5572.

Christian, H. J., R. J. Blakeslee, D. J. Boccippio, W. L. Boeck, D. E. Buechler, K. T. Driscoll, S. J. Goodman, J. M. Hall, W. J. Koshak, D. M. Mach, and M. F. Stewart, 2003: Global frequency and distribution of lightning as observed by the Optical Transient Detector. *J. Geophys. Res.*, **108**(D1), 4004, doi: 10.1029/2002JD002347.

Christian, H. J., R. J. Blakeslee, S. J. Goodman, D. A. Mach, M. F. Stewart, D. E. Buechler, W. J. Koshak, J. M. Hall, K. T. Driscoll, and D. J. Boccippio, 1999: *The Lightning Imaging Sensor*, poster presented at Proc. 11th International Conference on Atmospheric Electricity (NASA), Guntersville, AL, 7-11 June, 746-749.

Christian, H. J., R. J. Blakeslee, and S. J. Goodman, 1989: The detection of lightning from geostationary orbit. *J. Geophys. Res.*, **94**, 13,329-13,337.

Christian, H. J., R. J. Blakeslee, S. J. Goodman, and D. M. Mach, eds., 2000: Algorithm Theoretical Basis Document (ATBD) for the Lightning Imaging Sensor, 53 pp.

Chu, D. A., Y. J. Kaufman, C. Ichoku, L. A. Remer, D. Tanré, and B. N. Holben, 2002: Validation of MODIS aerosol optical depth retrieval over land. *Geophys. Res. Lett.*, **29**(12), doi: 10.1029/2001GL013205.

Chu, D. A., Y. J. Kaufman, L. A. Remer, and B. N. Holben, 1998: Remote sensing of smoke from MODIS airborne simulator during the SCAR-B experiment. *J. Geophys. Res.*, **103**(D24), 31,979-31,987.

Churchill, D. D., and R. A. Houze, Jr., 1984: Development and structure of winter monsoon cloud clusters on 10 December 1978. *J. Atmos. Sci.*, **41**, 933-960.

Cicerone, R. J., and R. S. Oremland, 1988: Biogeochemical aspects of atmospheric methane. *Global Biogeochem. Cycles*, **2**, 299-327.

Cihlar, J. C., H. Ly, Z. Li, J. Chen, H. Pokrant, and F. Huang, 1997: Mult-temporal, multichannel AVHRR data sets for land biosphere studies—Artifacts and corrections. *Remote Sens. Environ.*, **60**, 35-57.

Cohen, W. B., and C. O. Justice, Eds. 1999: Validating MODIS terrestrial ecology products: linking *in situ* and satellite measurements. Special Edition, *Remote Sens. Environ.*, **70**, 1-3.

Crutzen, P. J., 1991: Methane's sinks and sources. *Nature*, **350**, 380-381.

Culver, M. E., and M. J. Perry, 1994: Detection of phycoerythrin fluorescence in upwelling irradiance spectra. *Eos, Trans. Amer. Geophys. Union*, **75**, 233.

d'Entremont, R. E., C. L. Barker Schaaf, W. Lucht, and A. H. Strahler, 1999: Retrieval of red spectral albedo and bidirectional reflectance using AVHRR HRPT and GOES satellite observations of the New England region. *J. Geophys. Res.*, **D-104**, 6229-6239.

De Abreu, R. A., J. Key, J. A. Maslanik, M. C. Serreze, and E. F. LeDrew, 1994: Comparison of in situ and AVHRR-derived broadband albedo over Arctic sea ice. *Arctic*, **47**(3), 288-297.

Deeter, M. N., G. L. Francis, D. P. Edwards, J. C. Gille, E. McKernan, and J. R. Drummond, 2002: Operational validation of the MOPITT instrument optical filters. *J. Atmos. Oceanic Tech.*, **19**(11), 1772-1782.

DeFries, R. S., M. C. Hansen, J. R. G. Townshend, and A. C. Janetos, 2000: A new global 1-km dataset for percentage tree cover derived from remote sensing. *Global Change Biology*, **6**, 247-254.

Del Genio, A. D., and W. Kovari, 2002: Climatic properties of tropical precipitating convection under varying environmental conditions. *J. Climate*, **15**, 2597-2615.

Deschamps, P. Y., M. Herman, and D. Tanré, 1983: Modeling of the atmospheric effects and its application to the remote sensing of ocean color. *Appl. Opt.*, **22**, 3751-3758.

Deschamps, P. Y., and T. Phulpin, 1980: Atmospheric correction of infrared measurements of sea surface temperature using channels at 3.7, 11, and 12 μm. *Bound.-Layer Meteor.*, **18**, 131-143.

Di Girolamo, L., and R. Davies, 1994: A band-differenced angular signature technique for cirrus cloud detection. *IEEE Trans. Geosci. Remote Sens.*, **36**, 890-896.

Dickerson, R. R., G. J. Huffman, W. T. Luke, L. J. Nunnermacker, K. E. Pickering, A. C. D. Leslie, C. G. Lindsey, W. G. N. Slinn, T. J. Kelly, P. H. Daum, A. C. Delany, J. P. Greenberg, P. R. Zimmerman, J. F. Boatmen, J. D. Ray, and D. H. Stedman, 1987: Thunderstorms: an important mechanism in the transport of air pollutants. *Science*, **235**, 460.

Diner, D. J., W. A. Abdou, C. J. Bruegge, J. E. Conel, K. A. Crean, B. J. Gaitley, M. C. Helmlinger, R. A. Kahn, J. V. Martonchik, S. H. Pilorz, and B.N. Holben, 2001: MISR aerosol optical depth retrievals over southern Africa during the SAFARI-2000 dry season campaign. *Geophys. Res. Lett.*, **28**, 3127-3130.

Diner, D. J., G. P. Asner, R. Davies, Y. Knyazikhin, J-P. Muller, A. W. Nolin, B. Pinty, C. B. Schaaf, and J. Stroeve, 1999: New directions in Earth observing: Scientific applications of multiangle remote sensing. *Bull. Amer. Meteor. Soc.*, **80**, 2209-2228.

Diner, D. J., J. C. Beckert, G. W. Bothwell, and J. I. Rodriguez, 2002: Performance of the MISR instrument during its first 20 months in Earth orbit. *IEEE Trans. Geosci. Remote Sens.*, **40**, 1449-1466.

Diner, D. J., J. C. Beckert, T. H. Reilly, C. J. Bruegge, J. E. Conel, R. A. Kahn, J. V. Martonchik, T. P. Ackerman, R. Davies, S. A. W. Gerstl, H. R. Gordon, J -P. Muller, R. B. Myneni, P. J. Sellers, B. Pinty, and M. M. Verstraete, 1998: Multi-angle Imaging SpectroRadiometer (MISR) instrument description and experiment overview. *IEEE Trans. Geosci. Remote Sens.*, **36**, 1072-1087.

Dlugokencky, E. J., L. P. Steele, P. M. Lang, and K. A. Masarie, 1994: The growth rate and distribution of atmospheric methane. *J. Geophys. Res.*, **99**, 17,021-17,043.

Dong, X., P. Minnis, G. G. Mace, E. E. Clothiaux, C. Long, and S. Sun-Mack, 1999: Validation of CERES/VIRS cloud properties using ground-based measurements obtained at the DOE ARM sites. *Proc. AMS 10th Conf. Atmos. Rad.*, Madison, WI, June 28-July 2, 29-32.

Dozier, J., and Z. Wan, 1994: Development of practical multiband algorithms for estimating land-surface temperature from EOS-MODIS data. *Adv. Space Res.*, **13**(3), 81-90.

Drummond, J. R., 1992: Measurements of pollution in the troposphere (MOPITT). *The Use of EOS for Studies of Atmospheric Physics*, ed. by J.C. Gille and G. Visconti, North Holland, Amsterdam, pp. 77-101.

Drummond, J. R. and G. S. Mand, 1996: The Measurements of Pollution in the Troposphere (MOPITT) Instrument: Overall Performance and Calibration Requirements. *J. Atmos. Oceanic Technol.*, **13**, 314.

Dubovik, O., B. N. Holben, T. F. Eck, A. Smirnov, Y. J. Kaufman, M. D. King, D. Tanré, and I. Slutsker, 2002: Variability of absorption and optical properties of key aerosol types observed in worldwide locations. *J. Atmos. Sci.*, **59**, 590-608.

Ebert, E., 1987: A pattern recognition technique for distinguishing surface and cloud types in the polar regions. *J. Climate Appl. Meteor.*, **26**, 1412- 1427.

Edwards, D. P., C. M. Halvorson, and J. C. Gille, 1999: Radiative transfer modeling for the EOS Terra satellite Measurement of Pollution in the Troposphere (MOPITT) instrument. *J. Geophys. Res.*, **104**, 16755.

Edwards, D. P., 2002: The MOPITT Instrument on Terra: Mission and Data Processing Status, SWAMP, Nov. 2002 (presentation), www.eos.ucar.edu/mopitt/pubs/index.html.

Eppley, R. W., E. Stewart, M. R. Abbott, and U. Heyman, 1985: Estimating ocean primary production from satellite chlorophyll: Introduction to regional differences and statistics for the Southern California Bight. *J. Plank. Res.*, **7**, 57-70.

Esaias, W. E., M. R. Abbott, I. Barton, O. B. Brown, J. W. Campbell, K. L. Carder, D. K. Clark, R. H. Evans, F. E. Hoge, H. R. Gordon, W. M. Balch, R. Letelier, and P. J. Minnett, 1998: An overview of MODIS capabilities for ocean science observations. *IEEE Trans. Geosci. Remote Sens.*, **36**(4), 1250-1265.

Esaias, W. E., R. L. Iverson, and K. Turpie, 1999: Ocean province classification using ocean colour data: Observing biological signatures of variations in physical dynamics. *Global Change Biology*, **5**, 1-17.

Evans, R. H., and H. R. Gordon, 1994: CZCS System Calibration: A retrospective examination. *J. Geophys. Res.*, **99C**, 7293-7307.

Falkowski, P. G., and J. A. Raven, 1997: *Aquatic Photosynthesis*, Blackwell Science, Malden, MA., 375 pp.

Field, C. B., J. T. Randerson, and C. M. Malstrom, 1995: Global net primary production: Combining ecology and remote sensing. *Remote Sens. Environ.*, **51**, 74-88.

Fitzwater, S. E., G. A. Knauer, and J. H. Martin, 1982: Metal contamination and its effect on primary production measurements. *Limn. Oceanog.*, **27**, 544-551.

Friedl, M. A., and C. E. Brodley, 1998: Decision tree classification of land cover from remotely sensed data. *Remote Sens. Environ.*, **61**, 399-409.

Friedl, M. A., C. E. Brodley, and A. H. Strahler, 1999: Maximizing land cover classification accuracies produced by decision trees at continental to global scales. *IEEE Trans. Geosci. Remote Sens.*, **37**, 969-977.

Friedl, M., D. Muchoney, D. McIver, F. Gao, J. Hodges, and A. Strahler, 2000: Characterization of North American Land Cover from NOAA-AVHRR Data Using the EOS-MODIS Land Cover Classification Algorithm. *Geophys. Res. Lett.*, **27**, 977-980.

Fu, Q., and K. Liou, 1993: Parameterization of the radiative properties of cirrus clouds. *J. Atmos. Sci.*, **50**, 2008-2025.

Fujisada, H., 1994: Overview of ASTER Instruments on EOS-AM1 Platform. *Proc. SPIE*, **2268**, 14-36.

Fujisada, H., 1998: ASTER Level-1 Processing Algorithm. *IEEE Trans. Geosci. Remote Sens.*, **36**, 1101-1112.

Furuhama, Y., T. Ihara, M. Fujita, T. Shinozuka, K. Nakamura, and J. Awaka, 1982: Propagation characteristics of millimeter and centimeter waves of ETS-II classified by rainfall types. *Annales des Telecom.*, **36**, 24-32.

Gao, B. C., and A. F. H. Goetz, 1990: Column atmospheric water vapor and vegetation liquid water retrievals from airborne imaging spectrometer data. *J. Geophys. Res.*, **95**, 3549-3564.

Gao, B. C., A. F. H. Goetz, and W. J. Wiscombe, 1993a: Cirrus cloud detection from airborne imaging spectrometer data using the 1.38 micron water vapor band. *Geophys. Res. Lett.*, **4**, 301-304.

Gao, B. C., K. D. Heidebrecht, and A. F. H. Goetz, 1993b: Derivation of scaled surface reflectances from AVIRIS data. *Remote Sens. Environ.*, **44**, 165-178.

Gao, B. C., and Y. J. Kaufman, 2003: Water vapor retrievals from images of MODIS near-IR channels. *J. Geophys. Res.*, **108**(D13), 4389.

Gao, B. C., Y. J. Kaufman, W. Han, and W. J. Wiscombe, 1998: Correction of thin cirrus path radiance in the 0.4-1.0 μm spectral region using the sensitive 1.375-μm cirrus detecting channel. *J. Geophys. Res.*, **103**, 32,169-32,176.

Gao, B. C., Y. J. Kaufman, D. Tanré, and R.-R. Li, 2002b: Distinguishing tropospheric aerosols from thin cirrus clouds for improved aerosol retrievals using the ratio of 1.38-mm and 1.24-mm channels. *Geophys. Res. Lett.*, **29**, 1890, 10.1029/2002GL015475.

Gao, B. C., P. Yang, W. Han, R.-R. Li, and W. J. Wiscombe, 2002a: An algorithm using visible and 1.38-μm channels to retrieve cirrus cloud reflectances from aircraft and satellite data. *IEEE Trans. Geosci. Remote Sens.*, **40**, 1659-1668.

Gao, B. C., P. Yang, R.-R. Li, S. K. Park, and W. J. Wiscombe, 2003: Detection of high clouds in polar regions during the daytime using the MODIS 1.375-micron channel. *IEEE Trans. Geosci. Remote Sens.*, **41**(2), 474-481.

Gao, F., C. Schaaf, A. H. Strahler, and W. Lucht, 2001: Using a multi-kernel least variance approach to retrieve and evaluate albedo from limited BRDF observations. *Remote Sens. Environ.*, **76**, 57-66.

Gao, F., X. Li, A. H. Strahler, and C. Schaaf, 2001: Evaluation of the LiTransit Kernel for BRDF Modeling. *Remote Sens. Rev.*, **19**, 205-224.

Gao, X., A. R. Huete, W. Ni, and T, Miura, 2000: Optical-biophysical relationships of vegetation spectra without background contamination. *Remote Sens. Environ.,* **74**, 609-620.

Garver, S. A., and D. A. Siegel, 1997: Inherent optical property inversion of ocean color spectra and its biogeochemical interpretation. 1. Time series from the Sargasso Sea. *J. Geophys. Res.*, **102**, 18,607-18,625.

Giglio L., J. D. Kendall, and C. O. Justice, 1999: Evaluation of global fire detection algorithms using simulated AVHRR infrared data. *Int. J. Remote Sens.*, **20**, 1947-1985.

Gillespie, A. R., A. B. Kahle, and R. E. Walker, 1986: Color enhancement of highly correlated images. I. Decorrelation and HSI contrast stretches. *Remote Sens. Environ.*, **20**, 209-235.

Gillespie, A., S. Rokugawa, T. Matsunaga, J. S. Cothern, S. Hook, and A. B. Kahle, 1998: A temperature and emissivity separation algorithm for Advanced Spaceborne Thermal Emission and Reflection Radiometer (ASTER) images. *IEEE Trans. Geosci. Remote Sens.*, **36**(4), 1113-1126.

Goodman, A. H., and A. Henderson-Sellers, 1988: Cloud detection analysis: A review of recent progress. *Atmos. Res.*, **21**, 203.

Goodman, S. J., D. E. Buechler, K. Knupp, K. T. Driscoll, and E. W. McCaul, 2000: The 1997-98 El Niño event and related wintertime lightning variations in the Southeastern United States. *Geophys. Res. Lett.*, **27**, 541-544.

Gordon, H. R., 1978: Removal of atmospheric effects from satellite imagery of the oceans. *Appl. Opt.*, **17**, 1631-1636.

Gordon, H. R., 1987: Calibration requirements and methodology for remote sensors viewing the oceans in the visible. *Remote Sens. Environ.*, **22**, 103-126.

Gordon, H. R., 1997: Atmospheric correction of ocean color imagery in the Earth Observing System era. *J. Geophys. Res.*, **102D**, 17,081-17,106.

Gordon, H. R., and A. Y. Morel, 1983: *Remote Assessment of Ocean Color for Interpretation of Satellite Visible Imagery: A Review*, Springer-Verlag, New York, 114 pp.

Gordon, H. R., and D. K. Clark, 1981: Clear water radiances for atmospheric correction of coastal zone color scanner imagery. *Appl. Opt.*, **20**(24), 4175-4180.

Gordon, H. R., O. B. Brown, R. H. Evans, J. W. Brown, R. C. Smith, K. S. Baker, and D. K. Clark, 1988: A semi-analytic radiance model of ocean color. *J. Geophys. Res.*, **93**, 10,909-10,924.

Gordon, H. R., and M. Wang, 1994: Retrieval of water-leaving radiance and aerosol optical thickness over the oceans with SeaWiFS: A preliminary algorithm. *Appl. Opt.*, **33**, 443-452.

Gordon, H. R., T. Du, and T. Zhang, 1997: Remote sensing ocean color and aerosol properties: Resolving the issue of aerosol absorption. *Appl. Opt.*, **36**, 8670-8684.

Goward, S. N., and A. S. Hope., 1989: Evapotranspiration from combined reflected solar and emitted terrestrial radiation: Preliminary FIFE results from AVHRR data. *Adv. Space Res.*, **9**(7), 239-249.

Goyet, C., and P. G. Brewer, 1993: Biochemical properties of the oceanic cycle. In *Modeling Oceanic Climate Interactions*, ed. by J. Willebrand, NATO Advanced Study Institute, **I11**, 271-297.

Green, R. N., and B. A. Wielicki, 1995: Convolution of imager cloud properties with CERES footprint point spread function (Subsystem 4.4). *Clouds and the Earth's Radiant Energy System (CERES) Algorithm Theoretical Basis Document, Volume III: Cloud Analyses and Radiance Inversions (Subsystem 4)*, NASA Ref. Pub. 1376, Vol. III, ed. by the CERES Science Team, 177-194.

Green, R. N., B. A. Wielicki, J. A. Coakley, L. L. Stowe, and P. O'R. Hinton, 1995: CERES inversion to instantaneous TOA fluxes (Subsystem 4.5). *Clouds and the Earth's Radiant Energy System (CERES) Algorithm Theoretical Basis Document, Volume III: Cloud Analyses and Radiance Inversions (Subsystem 4)*, NASA Ref. Pub. 1376, Vol. III, ed. by the CERES Science Team, 195-206.

Green, R. O., and J. E. Conel, 1995: Movement of water vapor in the atmosphere measured by an imaging spectrometer at Rogers Dry Lake, CA. *Proc. Summaries of the Fifth Annual JPL Airborne Earth Science Workshop*, JPL Pub. 95-1, 1, 79–83.

Greenstone, R., and M. D. King, 1999: *EOS Science Plan Executive Summary: The State of Science in the EOS Program*, NASA Goddard Space Flight Center, Greenbelt, MD, 64 pp.

Gregg, W. W., and K. L. Carder, 1990: A simple solar irradiance model for cloudless maritime atmospheres. *Limn. Oceanog.*, **35**(8), 1657-1675.

Groom, S. B., and P. M. Holligan, 1987: Remote sensing of coccolithophore blooms. *Adv. Space Res.*, **7**, 73-78.

Guenther, B., G. D. Godden, X. Xiong, E. J. Knight, S. Y. Qiu, H. Montgomery, M. M. Hopkins, M. G. Khayat, and Z. Hao, 1998: Prelaunch algorithm and data format for the Level 1B calibration products for the EOS AM-1 Moderate Resolution Imaging Spectroradiometer (MODIS). *IEEE Trans. Geosci. Remote Sens.*, **36**, 1142.

Guenther, B., X. Xiong, V. V. Salomonson, W. L. Barnes, and J. Young, 2002: On-orbit performance of the Earth Observing System Moderate Resolution Imaging Spectroradiometer; first year of data. *Remote Sens. Environ.*, **83**, 16-30.

Gustafson, G. B., R. G. Isaacs, R. P. d'Entremont, J. M. Sparrow, T. M. Hamill, C. Grassotti, D. W. Johnson, C. P. Sarkisian, D. C. Peduzzi, B. T. Pearson, V. D. Jakabhazy, J. S. Belfiore, and A. S. Lisa, 1994: Support of Environmental Requirements for Cloud Analysis and Archive (SERCAA): Algorithm descriptions. Phillips Laboratory Scientific Report No. 2, Hanscom Air Force Base, MA, 100 pp.

Gutman, G. G., 1998: On the use of long-term global data of land reflectances and vegetation. *J. Geophys. Res.*, **104**(D6), 6241-6256.

Haddad, Z., E. A. Smith, C. Kummerow, T. Iguchi, M. R. Farrar, S. L. Durden, M. Alves, and W. S. Olsen, 1997a: The TRMM "day-1" radar/radiometer combined rain-profiling algorithm. *J. Meteor. Soc. Japan,* **75**, 799-809.

Haddad, Z. S., D. A. Short, S. L. Durden, E. Im, S. Hensley, M. B. Grable and R. A. Black, 1997b: A New Parametrization of the Rain Drop Size Distribution. *IEEE Trans. Geosci. Rem. Sens.*, **35**, 532-539.

Hall, D. K., R. E. J. Kelly, G. A. Riggs, A. T. C. Chang, and J. L. Foster, 2002: Assessment of the relative accuracy of hemispheric scale snow-cover maps. *Ann. Glaciol.*, **34**, 24-30.

Hall, D. K., G. A. Riggs, and V. V. Salomonson, 1995: Development of methods for mapping global snow cover using Moderate Resolution Imaging Spectroradiometer (MODIS) data. *Remote Sens. Environ.,* **54**, 127-140.

Hall, D. K., G. A. Riggs, V. V. Salomonson, N. DiGirolamo, and K. Bayr, 2002a: MODIS Snow Products. *Remote Sens. Environ.*, **83**(1-2), 181-194.

Hansen, M. C., R. S. DeFries, J. R. G. Townshend, R. A. Sohlberg, C. Dimiceli, and M. Carroll, 2002b: Towards an operational MODIS continuous field of percent tree cover algorithm: Examples using AVHRR and MODIS data. *Remote Sens. Environ.*, **83**(1-2), 303-319.

Harrison, E. F., D. R. Brooks, P. Minnis, B. A. Wielicki, W. F. Staylor, G. G. Gibson, D. F. Young, F. M. Denn, and the ERBE Science Team, 1988: First estimates of the diurnal variation of longwave radiation from the multiple-satellite Earth Radiation Budget Experiment (ERBE). *Bull. Amer. Meteor. Soc.*, **69**, 1144-1151.

Harrison, E. F., P. Minnis, B. R. Barkstrom, B. A., Wielicki, G. G. Gibson, F. M. Denn, and D. F. Young, 1990a: Seasonal variation of the diurnal cycles of Earth's radiation budget determined from ERBE. *AMS 7th Conf. on Atmos. Radiation*, San Francisco, CA, July 23-27, 87-91.

Harrison, E. F., P. Minnis, B. R. Barkstrom, V. Ramanathan, R. D. Cess, and G. G. Gibson, 1990b: Seasonal variation of cloud radiative forcing derived from the Earth Radiation Budget Experiment. *J. Geophys. Res.*, **95**, 18,687-18,703.

Harrison, E. F., D. F. Young, P. Minnis, G. G. Gibson, R. D. Cess, V. Ramanathan, T. D. Murray, and D. J. Travers, 1995: Clouds and the Earth's Radiant Energy System (CERES) Algorithm Theoretical Basis Document. Volume IV - Determination of Surface and Atmosphere Fluxes and Temporally and Spatially Averaged Products (Subsystems 5-12), Subsystem 10.0 - Monthly Regional TOA and Surface Radiation Budget, NASA Ref. Pub. 1376, Vol. IV, 139-156.

Hayden, C. M., 1988: GOES-VAS simultaneous temperature-moisture retrieval algorithm. *J. Appl. Meteor.*, **27**, 705-733.

Hilland, J. E., D. B. Chelton, and E. G. Njoku, 1985: Production of global sea surface temperature fields for the Jet Propulsion Laboratory workshop comparisons. *J. Geophys. Res.*, **90**(C6), 11,642-11,650.

Hirano, A, R. Welch, and H. Lang, 2003: Mapping from ASTER stereo image data: DEM validation and accuracy assessment. *ISPRS J. Photogram. Remote Sens.*, **57**(5-6), 356-370.

Hobish, M. K., Ardanuy, P. E., and V. V. Salomonson, 1994: Surface imaging technologies for NASA's Earth Observing System. *J. Imaging Science Tech.*, **38**, 301-310.

Hoffman, L. H., W. L. Weaver, and J. F. Kibler, 1987: Calculation and accuracy of ERBE scanner measurement locations. NASA Tech. Paper 2670.

Hoge, F. E., and R. N. Swift, 1986: Chlorophyll pigment concentration using spectral curvature algorithms: An evaluation of present and proposed satellite ocean color sensor bands. *Appl. Opt.*, **25**, 3677-3682.

Hoge, F. E., and R. N. Swift, 1990: Photosynthetic accessory pigments: Evidence for the influence of phycoerythrin on the submarine light field. *Remote Sens. Environ.*, **34**, 19-35.

Hoge, F. E., C. W. Wright, P. E. Lyon, R. N. Swift, and J. K. Yungel, 1999a: Satellite retrieval of inherent optical properties by inversion of an oceanic radiance model: A preliminary algorithm. *Appl. Opt.*, **38**, 495-504.

Hoge, F. E., C. W. Wright, P. E. Lyon, R. N. Swift, and J. K. Yungel, 1999b: Satellite retrieval of the absorption coefficient of phytoplankton phycoerythrin pigment: Theory and feasibility status. *Appl. Opt.*, **38**, 7431-7441.

Hoge, F. E., P. E. Lyon, R. N. Swift, J. K. Yungel, M. R. Abbott, R. M. Letelier, W. E Esaias, 2003: Validation of Terra-MODIS phytoplankton chlorophyll fluorescence line height. I. Initial airborne lidar results. *Appl. Opt.*, **42**(15), 2767-2771.

Holben, B. N., T. F. Eck, I. Slutsker, D. Tanré, J. P. Buis, A. Setzer, E. Vermote, J. A. Reagan, Y. J. Kaufman, T. Nakajima, F. Lavenu, I. Jankowiak, and A. Smirnov, 1998: AERONET-A federated instrument network and data archive for aerosol characterization. *Remote Sens. Environ.*, **66**(1), 1-16.

Holligan, P. M., E. Fernandez, J. Aiken, W. M. Balch, P. Boyd, P. H. Burkhill, M. Finch, S. B. Groom, G. Malin, K. Muller, D. A. Purdie, C. Robinson, C. C. Trees, S. M. Turner, and P. van der Wal, 1993: A biogeochemical study of the coccolithophore Emiliania huxleyi in the north Atlantic. *Global Biogeochem. Cycles*, **7**, 879-900.

Holligan, P. M., M. Viollier, D. S. Harbour, P. Camus, and M. Champagne-Philippe, 1983: Satellite and ship studies of coccolithophore production along the continental shelf edge. *Nature*, **304**, 339-342.

Holm-Hansen, O., and B. Riemann, 1978: Chlorophyll *a* determination: Improvements in methodology. *Oikos*, **30**, 438-477.

Holm-Hansen, O., C. J. Lorenzen, R. W. Holmes, and J. D. H. Strickland, 1965: Fluorometric determination of chlorophyll. *J. Cons. Int. Explor. Mer.*, **30**, 3-15.

Hong, Y., C. Kummerow, and W. S. Olson, 1999: Separation of Convective and Stratiform Precipitation Using Microwave Brightness Temperature. *J. Appl. Meteor.*, **38**(8), 1195-1213.

Hook, S. J., A. R. Gabell, A. A. Green, and P. S. Kealy, 1992: A comparison of techniques for extracting emissivity information from thermal infrared data for geological studies. *Remote Sens. Environ.*, **42**, 123-135.

Horvath, A., and R. Davies, 2001: Feasibility and error analysis of cloud motion wind extraction from near simultaneous multiangle MISR measurements. *J. Atmos. Oceanic Technol.*, **18**, 591-608.

Horvath, A., and R. Davies, 2001: Simultaneous retrieval of cloud motion and height from polar-orbiter multiangle measurements. *Geophys. Res. Lett.*, **28**, 2915-2918.

Hou, A. Y., D. V. Ledvina, A. M. Da Silva, S. Q. Zhang, J. Joiner, R. M. Atlas, G. J. Huffman, and C. Kummerow, 2000: Assimilation of SSM/I-derived surface rainfall and total precipitable water for improving the GEOS analysis for climate studies. *Mon. Wea. Rev.*, **128**, 509-537.

Houze, R. A. Jr., 1989: Observed structure of mesoscale convective systems and implications for large-scale heating. *Quart. J. Roy. Meteor. Soc.*, **115**, 425-461.

Howard, K. L., and J. A. Yoder, 1997: Contribution of the subtropical ocean to global primary primary production. In *Space Remote Sensing of the Subtropical Oceans*, ed. by C. -T. Liu, Pergamon Press, New York, 157-168.

Hu, B., W. Lucht, and A. H. Strahler, 1999: The interrelationship of atmospheric correction of reflectances and surface BRDF retrieval: A sensitivity study. *IEEE Trans. Geosci. Remote Sens.*, **37**, 724-738.

Hu, B., W. Lucht, X. Li, and A. H. Strahler, 1997: Validation of kernel-driven models for global modeling of bidirectional reflectance. *Remote Sens. Environ.*, **62**, 201-214.

Hu, B., W. Lucht, A. Strahler, C. Schaaf, and M. Smith, 2000: Surface albedos and angle-corrected NDVI from AVHRR observations over South America. *Remote Sens. Environ.*, **71**, 119-132.

Huete, A. R., K. Didan, T. Miura, and E. Rodriguez, 2002: Overview of the Radiometric and Biophysical Performance of the MODIS Vegetation Indices. *Remote Sens. Environ.*, **83**(1-2), 195-213..

Huete, A. R., C. O. Justice, and W. van Leeuwen, 1999: MODIS Vegetation Index (MOD 13) Algorithm Theoretical Basis Document (ATBD-MOD-13), version 3, available at eospso.gsfc.nasa.gov/atbd/modistables.html.

Huete, A. R., C. Justice, and H. Liu, 1994: Development of vegetation and soil indices for MODIS-EOS. *Remote Sens. Environ.*, **49**, 224- 234.

Huete, A. R., H. Q. Liu, K. Batchily, and W. van Leeuwen, 1997: A comparison of vegetation indices over a global set of TM images for EOS-MODIS. *Remote Sens. Environ.*, **59**, 440-451.

Huffman, G. J., R. F. Adler, B. Rudolf, U. Schneider, and P. R. Keehn, 1995: A technique for combining satellite data, raingauge analysis and model precipitation information into global precipitation estimates. *J. Climate*, **8**(5), 1284-1295.

Huffman, G. J., 1997a: Estimates of Root-Mean-Square Random Error for Finite Samples of Estimated Precipitation. *J. Appl. Meteor.*, **36**(9), 1191-1201.

Huffman, G. J., R. F. Adler, P. Arkin, A. Chang, R. Ferraro, A. Gruber, J. Janowiak, A. McNab, B. Rudolph, and U. Schneider, 1997b: The Global Precipitation Climatology Project (GPCP) Combined Precipitation Dataset. Bul. *Amer. Meteor. Soc.*, **78**(1), 5-20.

Ichoku, C., D. A. Chu, S. Mattoo, Y. J. Kaufman, L. A. Remer, D. Tanré, I. Slutsker, and B. N. Holben, 2002: A spatio-temporal approach for global validation and analysis of MODIS aerosol products. *Geophys. Res. Lett.*, **29**(12), 10.1029/2001GL013206.

Iguchi, T., T. Kozu, R. Meneghini, J. Awaka, and K. Okamoto, 1998: Preliminary results of rain profiling with TRMM Precipitation Radar. *Proc. of URSI-F International Triennial Open Symposium on Wave Propagation and Remote Sensing*, Aveiro, Portugal, 147-150.

Iguchi, T., T. Kozu, R. Meneghini, J. Awaka, and K. Okamoto, 2000: Rain-profiling algorithm for the TRMM Precipitation Radar. *J. Appl. Meteor.*, **39**, 2038-2052.

Iguchi, T., and R. Meneghini, 1994: Intercomparison of single frequency methods for retrieving a vertical rain profile from airborne or spaceborne data. *J. Atmos. Oceanic Technol.*, **11**, 1507-1516.

Iguchi, T., T. Kozu, R. Meneghini, J. Awaka, and K. Okamoto, 2000: Rain profiling algorithm for the TRMM Precipitation Radar. *J. Appl. Meteor.*, **39**, 2038-2052.

Inamdar, A. K., and V. Ramanathan, 1994: Physics of greenhouse effect and convection in warm oceans. *J. Climate*, **7**, 715-731.

Inamdar, A. K., and V. Ramanathan, 1995: Clouds and the Earth's Radiant Energy System (CERES) Algorithm Theoretical Basis Document. Volume III - Cloud Analyses and Determination of Improved Top of Atmosphere Fluxes (Subsystem 4), Subsystem 4.6.2 - Estimation of Longwave Surface Radiation Budget From CERES, NASA Ref. Pub. 1376, Vol. III, 217-234.

Inoue, T., 1987: An instantaneous delineation of convective rainfall areas using split window data of NOAA-7 AVHRR. *J. Meteor. Res. Japan*, **65**, 469-481.

Iqbal, M., 1983: *An Introduction to Solar Radiation*. Academic Press, Toronto and New York, 390 pp.

Iverson, R. L., W. E. Esaias, and K. R. Turpie, 2000: Ocean annual phytoplankton carbons and new production, and annual export production estimated with empirical equations and CZCS data. *Global Change Biol.*, **6**, 57-72.

Iwasaki, A., H. Fujisada, H. Akao, O. Shindou, and S. Akagi, 2002: Proc. Enhancement of spectral separation performance for ASTER/SWIR. In *Infrared Spaceborne Remote Sensing IX*, ed. by M. Strojnik and B. F. Andresen, SPIE Vol. 4486, 42-50.

Jarecke, P. J., M. A. Folkman, and L. A. Darnton, 1991: Radiometric calibration plan for the clouds and the Earth's radiant energy system instruments. *Proc. SPIE*, **1493**, 244-254.

Jovanovic, V. M., M. A. Bull, M. M. Smyth, and J. Zong, 2002: MISR in-flight camera geometric model calibration and georectification performance. *IEEE Trans. Geosci. Remote Sens.*, **40**, 1512-1519.

Jovanovic, V. M., M. M. Smyth, J. Zong, R. Ando, and G.W. Bothwell, 1998: MISR photogrammetric data reduction for geophysical retrievals. *IEEE Trans. Geosci. Remote Sens.*, **36**, 1290-1301.

Justice C. O., A. Belward, J. Morisette, P. Lewis, J. Privette, and F. Baret, 2000: Developments in the 'validation' of satellite sensor products for the study of the land surface. *Int. J. Remote Sens.*, **21**, 3383-3390.

Justice C. O., and S. A. Korontzi, 2001: A review of satellite fire monitoring and the requirements for global environmental change research. In *Global and Regional Vegetation Fire Monitoring From Space: Planning a Coordinated International Effort*, ed. by F. Ahern, G. Goldammer, C. O. Justice, SPB Academic Publishing, The Hague, The Netherlands, 1-18.

Justice C. O., L. Giglio, S. Korontzi, J. Owens, J. T. Morisette, D. Roy, J. Descloitres, S. Alleaume, F. Petitcolin, and Y. Kaufman, 2002: The MODIS Fire Products. *Remote Sens. Environ.*, **83**(1-2) 244-262.

Justice, C. O., J. P. Malingreau, and A. Setzer 1993: Satellite remote sensing of fires: potential and limitation. In *Fire in the Environment: The ecological, atmospheric, and climatic importance of vegetation fires*, ed. by P. J. Crutzen and J. G. Goldammer, John Wiley & Sons, Chichester, 77-88.

Justice, C. O., E. Vermote, J. R. G. Townshend, R. DeFries, D. P. Roy, D. K. Hall, V. V. Salomonson, J. L. Privette, G. Riggs, A. Strahler, W. Lucht, R. B. Myneni, Y. Knyazikhin, S. W. Running, R. R. Nemani, Z. Wan, A. R. Huete, W. van Leeuwen, R. E. Wolfe, L. Giglio, J.-P. Muller, P. Lewis, and M. J. Barnsley, 1998: The Moderate Resolution Imaging Spectroradiometer (MODIS): Land remote sensing for global change research. *IEEE Trans. Geosci. Remote Sens.*, **36**, 1228-1249.

Justice, C. O., R. Wolfe, N. El-Saleous, J. Descloitres, E. Vermote, D. Roy, J. Owens, E. Masuoka, and the MODIS Land Science Team (MODLAND), 2001: The Availability and Status of MODIS Land Data Products. *The Earth Observer*, **13**, 16-17.

Justice C. O., J. R. G. Townshend, E. F. Vermote, E. Masuoka, R. E. Wolfe, N. El Saleous, D. P. Roy, and J. T. Morisette, 2002: An overview of MODIS Land data processing and product status. *Remote Sens. Environ.*, **83**(1-2), 3-15.

Kaab, A., 2002: Monitoring high-mountain terrain deformation from repeated air- and spaceborne optical data: examples using digital aerial imagery and ASTER data. *ISPRS J. Photogram. Remote Sens.*, **57**(1-2), 39-52.

Kahle, A. B., 1986: Surface emittance, temperature, and thermal inertia derived from Thermal Infrared Multispectral Scanner (TIMS) data for Death Valley, California. *Geophysicas*, **52**(7), 858-874.

Kahle, A., F. Palluconi, S. Hook, V. J. Realmuto, and G. Bothwell, 1991: The Advanced Spaceborne Thermal Emission and Reflectance Radiometer (ASTER). *Int. J. Imaging Syst. Technol.*, **3**, 144-156.

Kahn, R., P. Banerjee, and D. McDonald, 2001: Sensitivity of multi-angle imaging to natural mixtures of aerosols over ocean. *J. Geophys. Res.*, **106**, 18,219-18,238.

Kahn, R., P. Banerjee, D. McDonald, and D. J. Diner, 1998: Sensitivity of multi-angle imaging to aerosol optical depth and to pure-particle size distribution and compositon over ocean. *J. Geophys. Res.*, **103**, 32,195-32,213.

Kahn, R., P. Banerjee, D. McDonald, and J. Martonchik, 2001: Aerosol Properties Derived from Aircraft Multi-angle Imaging Over Monterey Bay. *J. Geophys. Res.,* **106**, 11,977-11,995.

Kahn, R., R. West, D. McDonald, B. Rheingans, and M. I. Mishchenko, 1997: Sensitivity of multi-angle remote sensing observations to aerosol sphericity. *J. Geophys. Res.*, **102**, 16,861-16,870.

Kaufman, Y. J., R. S. Fraser, and R. L. Mahoney, 1991: Fossil fuel and biomass burning effects on climate-heating or cooling? *J. Climate*, **4**, 578-588.

Kaufman, Y. J., and B. C. Gao, 1992: Remote sensing of water vapor in the near IR from EOS/MODIS. *IEEE Trans. Geosci. Remote Sens.*, **30**, 871–884.

Kaufman, Y. J., C. O. Justice, L. P. Flynn, J. D. Kendall, E. M. Prins, L. Giglio, D. E. Ward, P. Menzel, and A. W. Setzer, 1998: Potential global fire monitoring from EOS-MODIS. *J. Geophys. Res.*, **103**, 31,955, 32,215-32,238.

Kaufman, Y. J., and L. A. Remer, 1994: Remote sensing of vegetation in the mid-IR: The 3.75 μm channels. *IEEE Trans. Geosci. Remote Sens.*, **32**, 672–683.

Kaufman, Y. J., D. Tanré, and O. Boucher, 2002: A satellite view of aerosols in the climate system. *Nature*, **419**, 215-223.

Kaufman, Y. J., D. Tanré, H. R. Gordon, T. Nakajima, J. Lenoble, R. Frouin, H. Grassl, B. M. Herman, M. D. King, and P. M. Teillet, 1997a: Passive remote sensing of tropospheric aerosol and atmospheric correction for the aerosol effect. *J. Geophys. Res.*, **102**(D14)**,** 16,815-16,830.

Kaufman, Y. J., D. Tanré, L. Remer, E. Vermote, A. Chu, and B. N. Holben, 1997b: Operational remote sensing of tropospheric aerosol over land from EOS-moderate resolution imaging spectroradiometer. *J. Geophys. Res.*, **102**(D14), 17,051-17,068.

Kaufman, Y. J., C. J. Tucker, and I. Fung, 1990: Remote sensing of biomass burning in the tropics. *J. Geophys. Res.*, **95**(D7), 9927-9939.

Kearns, E., J. A. Hanafin, R. H. Evans, P. J. Minnett, and O. B. Brown, 2000: An Independent Assessment of Pathfinder AVHRR Sea Surface Temperature Accuracy Using the Marine Atmosphere Enitted Radiance Interferomter (MAERI). *Bull. Amer. Meteor. Soc.*, **81**(7), 1525-1536.

Kedem, B., L. S. Chiu, G. R. North, 1990: Estimation of mean rate—Application to satellite-observations. *J. Geophys. Res.*, **95**(D2), 1965-1972.

Keenan, T. D., G. J. Holland, M. J. Manton, and J. Simpson, 1988: TRMM ground truth in a monsoon environment: Darwin, Australia. *Aust. Meteor. Mag.*, **36**, 81-90.

Key, J. R., and J. B. Collins, 1997: High-latitude surface temperature estimates from thermal satellite data. *Remote Sens. Environ.*, **61**, 302-309.

Kiefer, D. A., and R. A. Reynolds, 1992: Advances in understanding phytoplankton fluorescence and photosynthesis. In *Primary Productivity and Biogeochemical Cycles in the Sea*, ed. by P. G. Falkowski and A. D. Woodhead, Plenum, New York, 155-174.

Kilpatrick, K. A., G. P. Podesta, and R. H. Evans, 2001: Overview of the NOAA/NASA Pathfinder Algorithm for Sea Surface Temperature and Associated Matchup Database. *J. Geophys. Res.*, **106**, 9179-9198.

King, M. D., ed., 1999: *EOS Science Plan: The State of Science in the EOS Program*, NASA Goddard Space Flight Center, Greenbelt, MD, 397 pp.

King, M. D., and R. Greenstone, 1999: *1999 EOS Reference Handbook: A Guide to NASA's Earth Science Enterprise and the Earth Observing System*, NASA Goddard Space Flight Center, Greenbelt, MD, 361 pp.

King, M. D., Y. J. Kaufman, W. P. Menzel, and D. Tanré, 1992: Remote sensing of cloud, aerosol, and water vapor properties from the Moderate Resolution Imaging Spectroradiometer (MODIS). *IEEE Trans. Geosci. Remote Sens.*, **30**, 2-27.

King, M. D., W. P. Menzel, P. S. Grant, J. S. Myers, G. T. Arnold, S. E. Platnick, L. E. Gumley, S. C. Tsay, C. C. Moeller, M. Fitzgerald, K. S. Brown, and F. G. Osterwisch, 1996: Airborne scanning spectrometer for remote sensing of cloud, aerosol, water vapor and surface properties. *J. Atmos. Oceanic Technol.*, **13**, 777-794.

King, M. D., W. P. Menzel, Y. J. Kaufman, D. Tanré, B. C. Gao, S. Platnick, S. A. Ackerman, L. A. Remer, R. Pincus, and P. A. Hubanks, 2003: Cloud and aerosol properties, precipitable water, and profiles of temperature and humidity from MODIS. *IEEE Trans. Geosci. Remote Sens.*, **41**(2), 442-458.

King, M. D., S. C. Tsay, S. A. Ackerman, and N. F. Larsen, 1998: Discriminating heavy aerosol, clouds, and fires during SCAR-B: Application of airborne multispectral MAS data. *J. Geophys. Res.*, **103**, 31,989-32,000.

King, M. D., Y. J. Kaufman, D. Tanré, and T. Nakajima, 1999: Remote sensing of tropospheric aerosols from space: Past, present, and future. *Bull. Amer. Meteor. Soc.*, **80**, 2229-2260.

Kleepsies, T. J., and L. M. McMillan, 1984: Physical retrieval of precipitable water using the split window technique. *Proc. Conf. on Satellite Meteorology/ Remote Sensing and Applications*, Amer. Meteor. Soc., Boston, MA, 55-57.

Klein, A. G., D. K. Hall, and G. A. Riggs, 1998: Improving snow-cover mapping in forests through the use of a canopy reflectance model. *Hydrological Processes*, **12**, 1723-1744.

Klein, A. G., and D. K. Hall, 2000: Snow albedo determination using the NASA MODIS instrument. *Proc. 56th Annual Eastern Snow Conference*, 2-4 June 1999, Fredericton, New Brunswick, Canada, 77-85.

Klein, A. G., and J. Stroeve, 2002: Development and validation of a snow albedo algorithm for the MODIS instrument. *Annal. Glaciol.*, **34**, 45-52.

Knap, W. H., and J. Oerlemans, 1996: The surface albedo of the Greenland ice sheet: satellite-derived and in situ measurements in the Søndre Strømfjord area during the 1991 melt season. *J. Glaciol.*, **42**(141), 364-374.

Knyazikhin, Y., J. V. Martonchik, D. J. Diner, R. B. Myneni, M. M. Verstraete, B. Pinty, and N. Gobron, 1998: Estimation of vegetation canopy leaf area index and fraction of absorbed photosynthetically active radiation from atmosphere-corrected MISR data. *J. Geophys. Res.*, **103**, 32,239-32,256.

Knyazikhin, Y., J. V., Martonchik, R. B. Myneni, D. J. Diner, and S. W. Running, 1998: Synergistic algorithm for estimating vegetation canopy leaf area index and fraction of absorbed photosynthetically active radiation from MODIS and MISR data. *J. Geophys. Res.*, **103**, 32,257-32,276.

Koshak, W. J., J. W. Bergstrom, M. F. Stewart, H. J. Christian, J. M. Hall, and R. J. Solakiewicz, 2000: Laboratory calibration of the Optical Transient Detector and Lightning Imaging Sensor. *J. Atmos. Oceanic Technol.*, **17**, 905-915.

Kozu, T., K. Nakamura, R. Meneghini, and W. C. Boncyk, 1991: Dual-parameter radar rainfall measurement from space: A test result from an aircraft experiment. *IEEE Trans. Geosci. Remote Sens.*, **29**, 690-703.

Kozu T., T. Kawanishi, H. Kuroiwa, M. Kojima, K. Oikawa, H. Kumagai, K. Okamoto, M. Okumura, H. Nakatsuka and K. Nishikawa, 2001: Development of precipitation radar onboard the tropical rainfall measuring mission satellite. *IEEE Geosci. Remote Sens.*, **39**(1), 102-116.

Kozu, T., 1995: A generalized surface echo radar equation for down-looking pencil beam radar. *IE-ICE Trans. Commun.*, **E78-B**, 1245-1248.

Kozu, T., and T. Iguchi, 1996: A preliminary study of non-uniform beam filling correction for space-borne radar rainfall measurement. *IEICE Trans. Commun.*, **E79-B**, 763-769.

Krajewski, W. F., 1987: Co-kriging of radar-rainfall and rain gage data. *J. Geophys. Res.*, **92**(D8), 9571-9580.

Kratz, D. P., and Z. Li, 1995: Clouds and the Earth's Radiant Energy System (CERES) Algorithm Theoretical Basis Document. Volume III - Cloud Analyses and Determination of Improved Top of Atmosphere Fluxes (Subsystem 4), Subsystem 4.6.1 - Estimation of Longwave Surface Radiation Budget from CERES, NASA Ref. Pub. 1376, Vol. III, 213-216.

Kummerow, C., W. S. Olson and L. Giglio. 1996: A Simplified Scheme for Obtaining Precipitation and Vertical Hydrometeor Profiles from Passive Microwave Sensors. *IEEE Trans. on Geosci. and Remote Sens.*, **34**, 1213-1232.

Kummerow, C., W. Barnes, T. Kozu, J. Shiue, and J. Simpson, 1998: The Tropical Rainfall Measuring Mission (TRMM) sensor package. *J. Atmos. Oceanic Technol.*, **15**, 809-816.

Kummerow, C., and L. Giglio, 1994: A passive microwave technique for estimating rainfall and vertical structure information from space, Part I: Algorithm description. *J. Appl. Meteor.*, **33**, 3-18.

Kummerow, C., Y. Hong, W. S. Olson, S. Yang, R. F. Adler, J. McCollum, R. Ferraro, G. Petty, D. B. Shin, and T. T. Wilheit, 2001: The evolution of the Goddard Profiling algorithm (GPROF) for rainfall estimation from passive microwave sensors. *J. Appl. Meteor.*, **40**, 1801-1820.

Kummerow, C., J. Simpson, O. Thiele, W. Barnes, A. T. C. Chang, E. Stocker, R. F. Adler, A. Hou, R. Kakar, F. Wentz, P. Ashcroft, T. Kozu, Y. Hong, K. Okamoto, T. Iguchi, H. Kuroiwa, E. Im, Z. Haddad, G. Huffman, B. Ferrier, W. S. Olson, E. Zipser, E. A. Smith, T. T. Wilheit, G. North, T. Krishnamurti, and K. Nakamura, 2000: The status of the Tropical Rainfall Measuring Mission (TRMM) after two years in orbit. *J. Appl. Meteor.*, **39**, 1965-1982.

Lee, Z. P., K. L. Carder, T. G. Peacock, C. O. Davis, and J. L. Mueller, 1996: Method to derive ocean absorption coefficients from remote sensing reflectance. *Appl. Opt.*, **35**(3), 453-462.

Lee III, R. B., B. R. Barkstrom, G. L. Smith, J. E. Cooper, L. P. Kopia, and R. W. Lawrence, 1996: The Clouds and Earth's Radiant Energy System (CERES) sensors and preflight calibration plans. *J. Atmos. Oceanic Technol.*, **12**, 300-313.

Letelier, R. M., M. R. Abbott, and D. M. Karl, 1997: Chlorophyll natural fluorescence response to upwelling events in the Southern Ocean. *Geophys. Res. Lett.*, **24**, 409-412.

Levine, J. S., ed., 1991: *Global Biomass Burning*, MIT Press, Cambridge, MA, 569 pp.

Li, J., and H.-L. Huang, 1999: Retrieval of atmospheric profiles from satellite sounder measurements by use of the discrepancy principle. *Appl. Opt.*, **38**(6), 916-923.

Li, J., and K. Nakamura, 2002: Characteristics of the mirror image of precipitation observed by the TRMM Precipitation Radar. *J. Atmos. Oceanic Technol.*, **19**, 145-158.

Li, J., W. Wolf, W. P. Menzel, W. Zhang, H.-L. Huang, and T. H. Achtor, 2000: Global soundings of the atmosphere from ATOVS measurements: The algorithm and validation. *J. Appl. Meteorol.*, **39**, 1248-1268.

Li, J., C. C. Schmidt, J. P. Nelson, T. J. Schmit, and W. P. Menzel, 2001: Estimation of total ozone from GOES sounder radiances with high temporal resolution. *J. Atmos. Oceanic Technol.*, 157-168.

Li, X., A. H. Strahler, and C. E. Woodcock, 1995: A hybrid geometric optical-radiative transfer approach for modeling albedo and directional reflectance of discontinuous canopies. *IEEE Trans. Geosci. Remote Sens.,* **33**, 466-480.

Li, X., F. Gao, J. Wang, and A. H. Strahler, 2001: A priori knowledge accumulation and its application to linear BRDF model inversions. *J. Geophys. Res.*, **D106**, 11,925-11,935.

Li, Z., and H. Leighton, 1993: Global climatologies of solar radiation budgets at the surface and in the atmosphere from 5 years of ERBE data. *J. Geophys. Res.*, **98**, 4919-4930.

Liao, L., R. Meneghini, and T. Iguchi, 2001: Comparison of rain rate and reflectivity factor derived from the TRMM Precipitation Radar and the WSR-88D over the Melbourne, FL Site. *J. Atmos. Oceanic Technol.*, **18**, 1959-1974.

Liang, S., A. H. Strahler, and C. W. Walthall, 1999: Retrieval of land surface albedo from satellite observations: A simulation study. *J. Appl. Meteorol.*, **38**, 712-725.

Liou, K.-N., 1992: *Radiation and Cloud Processes in the Atmosphere*, Oxford University Press, Oxford, UK, 487 pp.

Liu, A. K., Y. Zhao, W. E. Esaias, J. W. Campbell, and T. S. Moore, 2002: Ocean surface layer drift revealed by satellite data. *Eos Trans. Amer. Geophys. Union*, **83**(7), 61-64.

Loeb, N. G., and R. Davies,1997: Angular dependence of observed reflectances: a comparison with plane parallel theory. *J. Geophys. Res.*, **102**, 6865-6881.

Loeb, N. G., S. Seiji Kato, and B. A. Wielicki: 2002: Defining top-of-the-atmosphere flux reference level for Earth radiation budget studies. *J. Climate*, **15**(22), 3301-3309.

Loeb, N. G, N. Manalo-Smith, S. Kato, W. F. Miller, S. K. Gupta, P. Minnis, and B. A. Wielicki, 2003: Angular distribution models for top-of-atmosphere radiative flux estimation from the CERES instrument on the TRMM satellite. Part I:Methodology. *J. Appl. Meteor.*, **42**, 240-265.

Lorenzen, C. J., and S. W. Jeffrey, 1980: Determination of chlorophyll in sea water, UNESCO Tech. Paper. *Marine Science*, No. 35, 20 pp.

Lucht, W., 1998: Expected retrieval accuracies of bidirectional reflectance and albedo from EOS-MODIS and MISR angular sampling. *J. Geophys. Res.*, **103**, 8763-8778.

Lucht, W., and P. Lewis, 2000: Theoretical noise sensitivity of BRDF and albedo retrieval from the EOS-MODIS and MISR sensors with respect to angular sampling. *Int. J. Remote Sens.*, **21**(1), 81-98.

Lucht, W., C. B. Schaaf, and A. H. Strahler, 2000: An algorithm for the retrieval of albedo from space using semiempirical BRDF models. *IEEE Trans. Geosci. Remote Sens.*, **38**(2), 977-998.

Lyu, C., and W. Barnes, 2003: Four Years of TRMM/VIRS On-Orbit Calibration and Performance Using Lunar Models and Data from Terra/MODIS. *J. Atmos. Oceanic Technol.*, **20**(3), 333-347.

Lyu, C., W. L. Barnes, and R. A. Barnes, 2000: First results from the on-orbit calibration of the visible and infrared scanner for the tropical rainfall measuring mission. *J. Atmos. Oceanic Technol.*, **17**, 385-394.

Lyu, C., and W. Barnes, 2003: Four Years of TRMM/VIRS On-Orbit Calibration and Performance Using Lunar Models and Data from Terra/MODIS. *J. Atmos. Oceanic Technol.*, **20**(3), 333-347.

Magnuson, J. J., D. M. Robertson, B. J. Benson, and 11 other authors, 2000: Historical trends in lake and river ice cover in the Northern Hemisphere. *Science*, **289**, 1743-1746.

Martins, J. V., D. Tanré, L. A. Remer, Y. J. Kaufman, S. Mattoo, and R. Levy, 2002: MODIS Cloud screening for remote sensing of aerosol over oceans using spatial variability. *Geophys. Res. Lett.*, **29**(12), 10.1029/2001GL013252.

Martonchik, J. V., C. J. Bruegge, and A. H. Strahler, 2001: A review of reflectance nomenclature used in remote sensing. *Remote Sens. Rev.*, **19**, 9-20.

Martonchik, J. V., D. J. Diner, R. Kahn, M. M. Verstraete, B. Pinty, H. R. Gordon, and T. P. Ackerman, 1998: Techniques for the retrieval of aerosol properties over land and ocean using multiangle imaging. *IEEE Trans. Geosci. Remote Sens.*, **36**, 1212-1227.

Martonchik, J. V., D. J. Diner, K. A. Crean, and M. A. Bull, 2002: Regional aerosol retrieval results from MISR. *IEEE Trans. Geosci. Remote Sens.*, **40**, 1520-1531.

Martonchik, J. V., D. J. Diner, B. Pinty, M. M. Verstraete, R. B Myneni, Y. Knyazikhin, and H. R. Gordon, 1998: Determination of land and ocean reflective, radiative, and biophysical properties using multiangle imaging. *IEEE Trans. Geosci. Remote Sens.*, **36**, 1266-1281.

Marzoug, M., and P. Amayenc, 1994: A class of single- and dual-frequency algorithms for rain rate profiling from a spaceborne radar. Part I: Principle and tests from numerical simulations. *J. Atmos. Oceanic Technol.*, **11**, 1480-1506.

Mather, P. M., 1999: *Computer Processing of Remotely-Sensed Images, an Introduction, Second Edition*. New York: John Wiley & Sons, 137-138.

Meneghini, R., and K. Nakamura, 1990: Range profiling of the rain rate by an airborne weather radar. *Remote Sens. Environ.*, **31**, 193-209.

Meneghini, R., T. Iguchi, T. Kozu, L. Liao, K. Okamoto, J. A. Jones, and J. Kwiatkowski, 2000: Use of the surface reference technique for path attenuation estimates from the TRMM Precipitation Radar. *J. Appl. Meteor.*, **39**, 2053-2070.

Meneghini, R., and J. A. Jones, 1993: An approach to estimate areal rain-rate distribution from spaceborne radar by the use of multiple thresholds. *J. Appl. Meteor.*, **32**, 386-398.

Meneghini, R., J. A. Jones, T. Iguchi, K. Okamoto, and J. Kwiatkowski, 2001: Statistical Methods of Estimating Average Rainfall over Large Space–Timescales Using Data from the TRMM Precipitation Radar. *J. Appl. Meteor.*, **40**(3), 568–585.

Meneghini. R., and T. Kozu, 1990: *Spaceborne Weather Radar*, Artech House, Boston, MA, 197 pp.

Meneghini, R., 1998: Application of a Threshold Method to Airborne–Spaceborne Attenuating-Wavelength Radars for the Estimation of Space–Time Rain-Rate Statistics. *J. Appl. Meteor.*, **37**(9), 924–938.

Minnis, P., and E. F. Harrison, 1984: Diurnal variability of regional cloud and clear-sky radiative parameters derived from GOES data, Part III: November 1978 radiative parameters. *J. Climate Appl. Meteor.*, **23**, 1033-1051.

Minnis, P., D. P. Kratz, J. A. Coakley, Jr., M. D. King, R. Arduini, D. P. Garber, P. W. Heck, S. Mayor, W. L. Smith, Jr., and D. F. Young, 1995: Cloud optical property retrieval (Subsystem 4.3). *Clouds and the Earth's Radiant Energy System (CERES) Algorithm Theoretical Basis Document, Volume III: Cloud Analyses and Radiance Inversions (Subsystem 4)*, NASA Ref. Pub. 1376, Vol. III, ed. by the CERES Science Team, 135-176.

Minnis, P., D. P. Garber, D. F. Young, R. F. Arduini, and Y. Takano, 1998: Parameterization of reflectance and effective emittance for satellite remote sensing of cloud properties. *J. Atmos. Sci.*, **55**, 3313-3339.

Minnis, P., D. F. Young, B. A. Wielicki, P. W. Heck, S. Sun-Mack, and T. D. Murray, 1999: Cloud properties Derived from VIRS for CERES. *Proc. AMS 10th Conf. Atmos. Rad.*, Madison, WI, June 28-July 2, 21-24.

Minnis, P., D. F. Young, B. A. Weilicki, S. Sun-Mack, Q. Z. Trepte, Y. Chen, P. W. Heck, and X. Dong, 2002: A global cloud database from VIRS and MODIS for CERES. *Proc. SPIE 3rd Intl. Asia-Pacific Environ. Remote Sens. Symp. 2002: Remote Sens. of Atmosphere, Ocean, Environment, and Space*, Hangzhou, China, October 23-27.

Monteith, J. L., 1972: Solar radiation and productivity in tropical ecosystems. *J. Appl. Ecology*, **9**, 747-766.

Moody, A., and C. E. Woodcock, 1995: The influence of scale and the spatial characteristics of landscapes on land-cover mapping using remote sensing. *Landscape Ecology*, **10**, 363-379.

MOPITT Science Team, 1996: MOPITT Algorithm Theoretical Basis Document: Conversion of MOPITT Digital Counts into Calibrated Radiances in Carbon Monoxide and Methane Absorption Bands (Level 0 to Level 1), available at eospso.gsfc.nasa.gov/atbd/mopittables.html.

MOPITT Science Team, 1996: MOPITT Algorithm Theoretical Basis Document: Retrieval of Carbon Monoxide Profiles and Column Amounts of Carbon Monoxide and Methane from MOPITT Radiances (Level 1 to Level 2), available at eospso.gsfc.nasa.gov/atbd/mopittables.html.

Morel, A., and J. M. Andre, 1991: Pigment distribution and primary production in the Western Mediterranean as derived and modeled from Coastal Zone Color Scanner observations. *J. Geophys. Res.*, **96**, 12,685-12,698.

Morel, A., and B. Gentili, 1991: Diffuse reflectance of oceanic waters: its dependence on Sun angle as influenced by the molecular scattering contribution. *Applied Opt.*, **30**, 4427-4438.

Morel, A., and B. Gentili, 1993: Diffuse reflectance of oceanic waters: II Bidirectional aspects. *Applied Opt.*, **32**, 6864-6879.

Morel, A., and B. Gentili, 1996: Diffuse reflectance of oceanic waters: III. Implication of bidirectionality for the remote sensing problem. *Applied Opt.*, **35**, 4850-4862.

Morel, A., K. J. Voss, and B. Gentili, 1995: Bidirectional reflectance of oceanic waters: A comparison of modeled and measured upward radiance fields. *J. Geophys. Res.*, **100C**, 13,143-13,150.

Moroney, C., R. Davies, and J-P. Muller, 2002: Operational retrieval of cloud-top heights using MISR data. *IEEE Trans. Geosci. Remote Sens.*, **40**, 1532-1540.

Muchoney. D., J. Borak, H. Chi, M. Friedl, J. Hodges, N. Morrow, and A. Strahler, 1999: Application of the MODIS global supervised classification model to vegetation and land cover mapping of Central America. *Int. J. Remote Sens.*, **21**, 1115-1138.

Muchoney, D., A. Strahler, J. Hodges, and J. LoCastro, 1999: The IGBP DISCover Confidence Sites and the System for Terrestrial Ecosystem Parameterization: Tools for Validating Global Land Cover Data. *Photogrammetric Engineering Remote Sens.*, **65**, 1061-1067.

Mugnai, A., E. A. Smith, and G. J. Tripoli, 1993: Foundations for physical-statistical precipitation retrieval from passive microwave satellite measurements. Part II: Emission source and generalized weighting function propertiesof a time dependent cloud-radiation model. *J. Appl. Meteor.*, **32**, 17-39.

Muller, J. F., and G. P. Brasseur, 1995: IMAGES: A three-dimensional chemical transport model of the global troposphere. *J. Geophys. Res.*, **100**, 16,445-16,490.

Myneni, R. B., S. Hoffman, Y. Knyazikhin, J. L. Privette, J. Glassy, Y. Tian, Y. Wang, X. Song,Y. Zhang, G. R. Smith, A. Lotsch, M. Friedl, J. T. Morisette, P. Votava, R. R. Nemani, and S. W. Running, 2002: Global products of vegetation leaf area and fraction absorbed PAR from year one of MODIS data. *Remote Sens. Environ.*, **83**(1-2), 214-231.

Myneni, R. B., C. D. Keeling, C. J. Tucker, G. Asrar, and R. R. Nemani, 1997a: Increased plant growth in the northern high latitudes from 1981 to 1991. *Nature*, **386**, 698-702.

Myneni, R. B., R. R. Nemani, and S. W. Running, 1997b: Estimation of global leaf area index and absorbed PAR using radiative transfer model. *IEEE Trans. Geosci. Remote Sens.*, **35**, 1380-1393.

Nakajima, T. Y., and T. Nakajima, 1995: Wide-area determination of cloud microphysical properties from NOAA AVHRR measurements for FIRE and ASTEX regions. *J. Atmos. Sci.*, **52**, 4043-4059.

Nemani, R. R., L. Pierce, S. Running, and S. Goward, 1993: Developing satellite-derived estimates of surface moisture status. *J. Appl. Meteor.*, **32**(3), 548-557.

Nemani, R. R., and S. W. Running, 1989: Estimation of regional surface resistance to evapotranspiration from NDVI and thermal-IR AVHRR data. *J. Appl. Meteor.*, **28**(4), 276-284.

Nemani, R. R., and S. W. Running, 1995: Satellite monitoring of global land-cover changes and their impact on climate. *Climatic Change*, **31**, 395-413.

Neckel, H., and D. Labs, 1984: The solar radiation between 3300 and 12500 A. *Solar Phys.*, **90**, 205-258.

Nishida, K., R. R. Nemani, S. W. Running, and J. M. Glassy, 2003: An operational remote sensing algorithm of land surface evaporation. *J. Geophys. Res.-Atmos.*, **108**(D9), 4270.

Novelli, P. C., K. A. Masarie, P. P. Tans, and P. M. Lang, 1994: Recent changes in atmospheric carbon monoxide. *Science*, **263**, 1587-1589.

Ogawa, K., T. Schmugge, F. Jacob, and A. French, 2003: Estimation of land surface window (8-12 mμm) emissivity from multispectral thermal infrared remote sensing—A case study in a part of Sahara Desert. *Geophys, Res. Lett.*, **30**(2), 1067.

Olson, W. S., C. D. Kummerow, Y. Hong, and W. Tao, 1999: Atmospheric Latent Heating Distributions in the Tropics Derived from Satellite Passive Microwave Radiometer Measurements. *J. Appl. Meteor.*, **38**(6), 633–664.

O'Neill, M. A., and I. J. Dowman, 1993: A simulation study of the ASTER sensor using versatile general purpose rigid sensor modeling systems. *Int. J. Remote Sens.*, **14**, 565-585.

O'Reilly, J. J. and 21 co-authors, 2000: Ocean color chlorophyll *a* algorithms for SeaWiFS, OC2 and OC4: Version 4. Chapter 2 in SeaWiFS Post-launch Calibration and Validation Analyses, Part 3, SeaWiFS *Post-launch Technical Memorandum Series*, Vol. 11, NASA.

Pan, L., D. Edwards, J. Gille, M. W. Smith, and J. R. Drummond, 1995: Satellite remote sensing of tropospheric CO and CH_4: Forward model studies of the MOPITT instrument. *Appl. Opt.*, **34**, 6976-6988.

Pan, L., J. C. Gille, D. P. Edwards, P. L. Bailey, and C. D. Rodgers, 1998: Retrieval of tropospheric carbon monoxide for the MOPITT experiment. *J. Geophys. Res.*, **103**(32), 277-290.

Panferov, O., Y. Knyazikhin, R. B. Myneni, J. Szarzynski, S. Engwald, K. G. Schnitzler, and G. Gravenhorst, 2001: The role of canopy structure in the spectral variation of transmission and absorption of solar radiation in vegetation canopies. *IEEE Trans. Geosci. Remote Sens.*, **39**(2), 241-253.

Parkinson, C. L., 1997: *Earth from Above: Using Color-Coded Satellite Images to Examine the Global Environment*, University Science Books, Sausalito, California, 176 pp.

Parkinson, C. L., 2002: Trends in the length of the Southern Ocean sea-ice season, 1979-99. *Annal. Glaciol.*, **34**, 435-440.

Penner, J. E., R. E. Dickinson, and C. A. O'Neill, 1992: Effects of aerosol from biomass burning on the global radiation budget. *Science*, **256**, 1432-1434.

Petersen, W. A., and S. A. Rutledge, 2001: Regional variability in tropical convection: observations from TRMM. *J. Climate*, **14**, 3566-3586.

Petitcollin F., and E. F. Vermote, 2002: Land surface reflectance, emissivity and temperature from MODIS middle and thermal infrared data. *Remote Sens. Environ.*, **83**(1-2), 112-134.

Pfaendtner, J., S. Bloom, D. Lamich, M. Seablom, M. Sienkiewicz, J. Stobie, and A. da Silva, 1995: *Documentation of the Goddard Earth Observing System (GEOS) Data Assimilation System—Version 1*. NASA Tech Memo. 104606, Vol. 4, NASA Goddard Space Flight Center, Greenbelt, MD, 44 pp.

Pinty, B., C. Leprieur, and M. M. Verstraete, 1993: Towards a quantitative interpretation of vegetation indices, part1: biophysical canopy properties and classical indices. *Remote Sens. Environ.*, **7**, 127-150.

Platnick, S., P. A. Durkee, K. Nielson, J. P. Taylor, S. C. Tsay, M. D. King, R. J. Ferek, P. V. Hobbs, and J. W. Rottman, 2000: The role of background cloud microphysics in the radiative formation of ship tracks. *J. Atmos. Sci.*, **57**, 2607-2624.

Platnick, S., M. D. King, S. A. Ackerman, W. P. Menzel, B. A. Baum, J. C. Riédi, and R. A. Frey, 2003: The MODIS cloud products: Algorithms and examples from Terra. *IEEE Trans. Geosci. Remote Sens.*, **41**(2), 459-473.

Platt, T. C., C. Caverhill, and S. Sathyendranath, 1991: Basin scale estimates of oceanic primary production by remote sensing: The North Atlantic. *J. Geophys. Res.*, **96**(15), 147-149.

Prabhakara, C., B. J. Conrath, and R. A. Hanel, 1970: Remote sensing of atmospheric ozone using the 9.6 micron band. *J. Atmos. Sci.*, **26**, 689-697.

Priestley, K. J., B. R. Barkstrom, R. B. Lee III, R. N. Green, S. Thomas, R. S. Wilson, P. L. Spence, J. Paden, D. K. Pandey, and A. Al-Hajjah, 2000: Post-launch radiometric validation of the Clouds and the Earth's Radiant Energy System (CERES) proto-flight model on the Tropical Rainfall Measuring Mission (TRMM) spacecraft through 1999. *J. Appl. Meteor.*, **39**, 2249-2258.

Priestley, K. J., B. A. Wielicki, R. N. Green, M. P. A. Haeffelin, R. B. Lee and N. G. Loeb, 2002: Early radiometric validation results of the CERES flight model 1 and 2 instruments onboard NASA's Terra spacecraft. *Adv. Space Res.*, **30**(11), 2371-2376.

Price, J. C., 1983: Estimating surface temperature from satellite thermal infrared data—a simple formulation for the atmospheric effect. *Remote Sens. Environ.*, **13**, 353-361.

Price, J. C., 1984: Land surface temperature measurements from the split window channels of the NOAA 7 Advanced Very High Resolution Radiometer. *J. Geophys. Res.*, **89**, 7231-7237.

Prince, S. D., and S. N. Goward, 1995: Global primary production: A remote sensing approach. *J. Biogeography*, **22**, 815-835.

Ramanathan V., R. D. Cess, E. F. Harrison, P. Minnis, B. R. Barkstrom, E. Ahmad, and D. Hartmann, 1989: Cloud-radiative forcing and climate: Results for the Earth Radiation Budget Experiment. *Science*, **243**, 57-63.

Ramsay, B., 1998: The interactive multisensor snow and ice mapping system. *Hydrological Processes*, **12**, 1537-1546.

Rao, C. R .N., L. L. Stowe, and E. P. McClain, 1989: Remote sensing of aerosols over the oceans using AVHRR data: Theory, practice, and applications. *Int. J. Remote Sens.*, **10**, 743-749.

Rasmusson, E. M., 1985: El Niño and variations in climate. *Amer. Sci.*, **73**, 168-178.

Reichle, Jr., H. G., H. A. Wallio, and B. E. Gormsen, 1989: Feasibility of determining the vertical profile of carbon monoxide from a space platform. *Appl. Opt.*, **28**, 2104-2110.

Remer, L. A., Y. J. Kaufman, and B. N. Holben, 1996: The size distribution of ambient aerosol particles: Smoke vs. urban/industrial aerosol. In *Global Biomass Burning*, ed. by J. S. Levine, The MIT Press, Cambridge, MA, 519-530.

Remer, L. A., D. Tanré, Y. J. Kaufman, C. Ichoku, S. Mattoo, R. Levy, D. A. Chu, B. N. Holben, O. Dubovik, A. Smirnov, J. V. Martins, R.-R. Li, and Z. Ahmad, 2002: Validation of MODIS aerosol retrieval over ocean. *Geophys. Res. Lett.*, **29**(12), doi: 10.1029/2001GL013204.

Riggs, G. A., and D. K. Hall, 2002: *Proceedings of the 59th Eastern Snow Conference*, 6-7 June 2002, Stowe, VT.

Riggs, G. A., D. K. Hall, and S. A. Ackerman, 1999: Sea Ice Extent and Classification Mapping with the Moderate Resolution Imaging Spectroradiometer Airborne Simulator. *Remote Sens. Environ.*, **68**, 152-163.

Riggs, G. A., D. K. Hall, and V. V. Salomonson, 2002a: MODIS Snow Products User's Guide, modis-snow-ice.gsfc.nasa.gov/siugkc.html.

Riggs, G. A., D. K. Hall, and V.V. Salomonson, 2002b: MODIS Sea Ice Products User's Guide, modis-snow-ice.gsfc.nasa.gov/siugkc.html.

Robert III, L. B., B. R. Barkstrom, H. Bitting, D. A. H. Crommelynck, J. Paden, D. K. Pandey, K. J. Priestley, G. L. Smith, S. Thomas, K. L. Thornhill, and R. S. Wilson, 1998: Pre-Launch Calibrations of the CERES Tropical Rainfall Measuring Mission (TRMM) and Earth Observing System (EOS) Morning (AM-1) Spacecraft Thermistor Bolometers. *IEEE Trans. Geosci. Remote Sens.*, **36**(4), 1173-1185.

Robinson, J. M., 1991: Fire from space: Global fire evaluation using infrared remote sensing. *Int. J. Remote Sens.*, **12**(1), 3-24.

Roger J. C., and E. F. Vermote, 1997: Computation and use of the reflectivity at 3.75mm from AVHRR thermal channels. *Remote Sens. Rev.*, **15**, 75-98.

Roger J. C., and E. F. Vermote, 1998: A method to Retrieve the Reflectivity Signature at 3.75mm from AVHRR data. *Remote Sens. Environ.*, **64**, 103-114.

Rosenfeld, D., D. B. Wolff, and E. Amitai, 1994: The window probability matching method for rainfall measurements with radar. *J. Appl. Meteor.*, **33**, 682-693.

Rossow, W. B., and L. C. Garder, 1993: Cloud detection using satellite measurements of infrared and visible radiances for ISCCP. *J. Climate*, **6**, 2341-2369.

Rothery, D. A., 1987: Decorrelation stretching as an aid to image interpretation. *Int. J. Remote Sens.*, **8**, 1253-1254.

Roy, D. P., P. E. Lewis, and C. O. Justice, 2002: Burned area mapping using multi-temporal moderate spatial resolution data–a bi-directional reflectance model-based expectation approach. *Remote Sens. Environ.*, **83**(1-2), 263-286.

Roy, D. P., L. Giglio, J. K. Kendall, and C. Justice, 1999: Multi-temporal active-fire based burn scar detection algorithm. *Int. J. Remote Sens.*, **20**(5), 1031-1038.

Ruimy, A., B. Saugier, and G. Dedieu, 1994: Methodology for the estimation of terrestrial net primary production from remotely sensed data. *J. Geophys. Res.*, **99**(D3), 5263-5283.

Running, S. W., 1990: Estimating terrestrial primary productivity by combining remote sensing and ecosystem simulation. In *Remote Sensing of Biosphere Functioning*, ed. by R. Hobbs and H. Mooney, New York: Springer-Verlag, 65-86.

Running, S. W., C. Justice, V. Salmonson, D. Hall, J. Barker, Y. Kaufmann, A. Strahler, A. Huete, J.-P. Muller, V. Vanderbilt, Z. Wan, P. Teillet, and D. Carneggie, 1994: Terrestrial remote sensing science and algorithms planned for EOS/MODIS. *Int. J. Remote Sens.*, **15**, 3587-3620.

Running, S. W., T. R. Loveland, L. L. Pierce, R. R. Nemani, and E. R. Hunt, 1995: A remote sensing based vegetation classification logic for global land cover analysis. *Remote Sens. Environ.*, **51**, 39-48.

Running, S. W., R. R. Nemani, D. L. Peterson, L. E. Band, D. F. Potts, L. L. Pierce, and M. A. Spanner, 1989: Mapping regional forest evapotranspiration and photosynthesis by coupling satellite data with ecosystem simulation. *Ecology*, **70**, 1090-1101.

Running, S. W., P. E. Thornton, R. R. Nemani, and J. M. Glassy, 2000: Global terrestrial gross and net primary productivity from the earth observing system. pp. 44-57. In *Methods in Ecosystem Science*, ed. by O. Sala, R. Jackson, and H. Mooney, Springer-Verlag, New York.

Salisbury, J. W., and D. M. D'Aria, 1992: Emissivity of terrestrial materials in the 8-14 mm atmospheric window. *Remote Sens. Environ.*, **42**, 83-106.

Sarmiento, J. L., J. R. Toggweiler, and R. Najjar, 1988: Ocean carbon-cycle dynamics and atmospheric CO_2. *Philos. Trans. Roy. Soc. London*, **325**, 3-21.

Saunders, R. W., and K. T. Kriebel, 1988: An improved method for detecting clear-sky and cloud radiances for AVHRR data. *Int. J. Remote Sens.*, **9**, 123-150.

Schols, J. L., and J. A. Weinman, 1994: Retrieval of hydrometeor distributions over the ocean from airborne single-frequency radar and multifrequency radiometric measurements. *Atmos. Res.*, **34**, 329-346.

Schubert, S. D., R. B. Rood, and J. Pfaendtner, 1993: An assimilated dataset for earth science applications. *Bull. Amer. Meteor. Soc.*, **74**, 2331-2342.

Sellers, P. J., 1987: Canopy reflectance, photosynthesis and transpiration. *Int. J. Remote Sens.*, **6**, 1335-1372.

Seemann, S. W., J. Li, W. P. Menzel, and L. E. Gumley, 2003: Operational retrieval of atmospheric temperature, moisture and ozone from MODIS infrared radiances. *J. Appl. Meteor.*, **42**(8), 1072-1091.

Shapiro, M. A., A. J. Krueger, and P. J. Kennedy, 1982: Nowcasting the position and intensity of jet streams using a satellite borne total ozone mapping spectrometer. In *Nowcasting*, ed. by K. A. Browning, Academic Press, London, UK, 137-145.

Short, D. A., K. Shimizu, and B. Kedem, 1993: Optimal Thresholds for the Estimation of Area Rain-Rate Moments by the Threshold Method. *J. Appl. Meteor.*, **32**(2), 182–192.

Simpson, J., C. Kummerow, W.-K. Tao, and R. F. Adler, 1996: On the Tropical Rainfall Measuring Mission (TRMM). *Meteorol. Atmos. Phys.*, **60**, 19-36.

Slater, P. N., S. F. Biggar, R. G. Holm, R. D. Jackson, Y. Mao, M. S. Moran, J. M. Palmer, and B. Yuan, 1987: Reflectance-based and radiance-based methods for the in-flight absolute calibration of multi-spectral sensors. *Remote Sens. Environ.*, **22**, 11-37.

Smith, E. A., and T. D. Hollis, 2003: Performance evaluation of Level 2 TRMM Rain Profile algorithms by intercomparison and hypothesis testing. AMS Meteorological Monographs, Symposium in Cloud Systems, Hurricanes and TRMM (Special Issue for Joanne Simpson), in press.

Smith, E. A., C. Kummerow, and A. Mugnai: 1994a: The emergence of inversion-type profile algorithms for estimation of precipitation from satellite passive microwave measurements. *Remote Sens. Rev.*, **11**, 211-242.

Smith, E. A., J. Turk, M. Farrar, A. Mugnai, and X. Xieng, 1997: Estimating 13.8 GHz path integrated attenuation from 10.7 GHz brightness temperatures for TRMM Combined PR-TMI Precipitation Algorithm. *J. Appl. Meteor.*, **36**, 365-388.

Smith, E. A., X. Xiang, A. Mugnai, and G. J. Tripoli, 1994b: Design of an inversion-based precipitation profile retrieval algorithm using an explicit cloud model for initial guess microphysics. *Meteor. Atmos. Phys.*, **54**.

Smith, G. L., K. A. Bush, F. E. Martino, III, R. Hazra, N. Manalo-Smith, and D. Rutan, 1995: Clouds and the Earth's Radiant Energy System (CERES) Algorithm Theoretical Basis Document. Volume IV - Determination of Surface and Atmosphere Fluxes and Temporally and Spatially Averaged Products (Subsystems 5-12), Subsystem 9.0—Grid TOA and Surface Fluxes for Instantaneous Surface Product, NASA Ref. Pub. 1376, Vol. IV, 129-138.

Smith, G. L., R. N. Green, E. Raschke, L. M. Avis, J. T. Suttles, B. A. Wielicki, and R. Daview, 1986: Inversion methods for satellite studies of the Earth's radiation budget: Development of algorithms for the ERBE mission. *Rev. Geophys.*, **24**, 407-421.

Smith, M. W., and S. R. Shertz, 1996: Current plans and status of MOPITT algorithm test radiometer (MATR), in Earth Observing System , W. L. Barnes, ed., *Proc. SPIE*, **2820**, 78-86.

Smith, R. C., and K. S. Baker, 1977: The bio-optical state of ocean waters and remote sensing. Scripps Institution of Oceanography, Ref. 77-2, 36 pp.

Smith, R. C., and K. S. Baker, 1982: Oceanic chlorophyll concentrations as determined by satellite (Nimbus-7 Coastal Zone Color Scanner). *Marine Biology*, **66**, 269-279.

Smith, W. L., H. M. Woolf, and A. J. Schreiner, 1985: Simultaneous retrieval of surface and atmospheric parameters: A physical and analytically direct approach. In *Advances in Remote Sensing Retrieval Methods*, ed. by A. Deepak, H.E. Fleming, and M.T. Chahine, A. Deepak Publishing, Hampton, VA, 221-232.

Smith, W. L., and F. X. Zhou, 1982: Rapid extraction of layer relative humidity, geopotential thickness and atmospheric stability from satellite sounding radiometer data. *Appl. Opt.*, **21**, 924-928.

Snyder, W., and Z. Wan, 1996: Surface temperature correction for active infrared reflectance measurements of natural materials. *Appl. Opt.*, **35**(13), 2216-2220.

Snyder, W., and Z. Wan, 1998: BRDF models to predict spectral reflectance and emissivity in the thermal infrared. *IEEE Trans. Geosci. Remote Sens.*, **36**, 214-225.

Stajner, I., L. P. Riishojgaard, and R. B. Rood, 2001: The GEOS ozone data assimilation system: specification of error statistics. *Quart. J. Roy. Meteor. Soc.*, **127**, 1069-1094.

Steele, L. P., E. J. Dlugokencky, P. M. Lang, P. P. Tans, R. C. Martin, and K. A. Masarie, 1992: Slowing down of the global accumulation of atmospheric methane during the 1980s. *Nature*, **358**, 313-316.

Steiner, M., R. A. Houze, Jr., and S. E. Yuter, 1995: Climatological characterization of three-dimensional storm structure from operational radar and rain gauge data. *J. Appl. Meteor.*, **34**, 1978-2007.

Stowe, L. L., P. Ardanuy, R. Hucek, P. Abel, and H. Jacobowitz, 1993: Evaluating the design of an earth radiation budget instrument with system simulations. Part I: Instantaneous estimates. *J. Atmos. Oceanic Tech.*, **10**, 809-826.

Stowe, L. L., E. P. McClain, R. Carey, P. Pellegrino, G. Gutman, P. Davis, C. Long, and S. Hart, 1991: Global distribution of cloud cover derived from NOAA/AVHRR operational satellite data. *Adv. Space Res.,* **11**, 51-54.

Strabala, K. I., S. A. Ackerman, and W. P. Menzel, 1994: Cloud properties inferred from 8-12 micron data. *J. Appl. Meteor.*, **33**, 212-229.

Strahler, A., A. Moody, and E. Lambin, 1995: Land cover and land-cover change from MODIS. *Proc. 15th Int. Geosci. and Remote Sens. Symp.*, Florence, Italy, July 10-14, 1995, vol. 2, 1535-1537.

Stroeve, J., A. Nolin, and K. Steffen, 1997: Comparison of AVHRR-derived and in situ surface albedo over the Greenland Ice Sheet. *Remote Sens. Environ.*, **62**, 262-276.

Strugnell, N., and W. Lucht, 2001: Continental-scale albedo inferred from AVHRR data, land cover class and field observations of typical BRDFs. *J. Climate*, **14**, 1360-1376.

Strugnell, N., W. Lucht, and C. Schaaf, 2001: A global albedo data set derived from AVHRR data for use in climate simulations. *Geophys. Res. Lett.*, **28**, 191-194.

Sullivan, J., L. Gandin, A. Gruber, and W. Baker, 1993: Observation error statistics for NOAA-10 temperature and height retrievals. *Mon. Wea. Rev.*, **121**, 2578-2587.

Sun-Mack, S., Y. Chen, T. D. Murray, P. Minnis, and D. F. Young, 1999: Visible clear-sky and near-infrared surface albedos derived from VIRS for CERES. *Proc. AMS 10th Conf. Atmos. Rad.*, Madison, WI, June 28-July 2, 422-425.

Suttles, J. T., and G. Ohring, 1986: Surface radiation budget for climate applications. NASA Ref. Pub. 1169, Washington, DC, 136 pp.

Takacs, L. L., A. Molod, and T. Wang, 1994: *Documentation of the Goddard Earth Observing System (GEOS) General Circulation Model—Version 1*. NASA Tech. Memo. 104606, Vol. 1, NASA Goddard Space Flight Center, Greenbelt, MD, 100 pp.

Tanré, D., F. M. Bréon, J. L. Deuzé, M. Herman, P. Goloub, F. Nadal, and A. Marchand, 2001: Global observation of anthropogenic aerosols from satellite. *Geophys. Res. Lett.*, **28**(24), 4555.

Tanré D., M. Herman, and Y. J. Kaufman, 1996: Information on the aerosol size distribution contained in the solar reflected spectral radiances. *J. Geophys. Res.*, **101**, 19,043-19,060.

Tanré, D., Y. J. Kaufman, M. Herman, and S. Mattoo, 1997: Remote sensing of aerosol properties over oceans using the MODIS/EOS spectral radiances. *J. Geophys. Res.*, **102**(D14), 16,971-16,988.

Tao, W.-K., S. Land, W. S. Olsen, S. Yang, R. Meneghini, J. Simpson, C. Kummerow, E. Smith, and J. Halverson, 2001: Retrieved vertical profiles of latent heating release using TRMM product for February 1998. *J. Appl. Meteor.*, **40**, 957-982.

Taylor, J. P., M. D. Glew, J. A. Coakley Jr., W. R. Tahnk, S. Platnick, P. V. Hobbs, and R. J. Ferek, 2000: Effects of aerosols on the radiative properties of clouds. *J. Atmos. Sci.*, **57**(16), 2656-2670.

Theon, J. S., T. Matsuno, T. Sakata, and N. Fugono, Eds., 1992: *The Global Role of Tropical Rainfall*, A. Deepak Publishing, Hampton, VA, 280 pp.

Thomas, D., R. Vogel, W. E. Esaias, K. Turpie, and A. Bahatti, 2002: Status of MODIS Ocean Data. Powerpoint poster, EOS IWG meeting, Ellicott City, MD, November 18-20, 2002.
modis-ocean.gsfc.nasa.gov/refs.html

Thomas, R. J., P. R. Krehbiel, W. Rison, T. Hamlin, D. J. Boccippio, S. J. Goodman, and H. J. Christian, 2000: Comparison of ground-based 3-dimensional lightning mapping observations with satellite-based LIS observations in Oklahoma. *Geophys. Res. Lett.*, **27**, 1703-1706.

Thome, K., P. Slater, S. Arai, S. Hook, H. Lang, F. Palluconi, H. Kieffer, T. Matsunaga, A. Ono, and H. Sakuma, 1998a: ASTER preflight and inflight calibration and the validation of Level 2 products. *IEEE Trans. Geosci. Remote Sens.*, **36**(4), 1161-1172.

Thome, K., F. Palluconi, T. Takashima, and K. Masuda, 1998b: Atmospheric correction of ASTER. *IEEE Trans. Geosci. Remote Sens.*, **36**(4), 1199-1211.

Tian, B., and V. Ramanathan, 2002: Role of tropical clouds in surface and atmospheric energy budget. *J. Climate*, **15**(3), 296-305.

Tian, Y., Y. Wang, Y. Zhang, Y. Knyazikhin, J. Bogaert, and R. Myneni, 2003: Radiative transfer based scaling of LAI retrievals from reflectance data of different resolutions. *Remote Sens. Environ.*, **84**(1), 143-159.

Tian, Y., Y. Zhang, Y. Knyazikhin, R. B. Myneni, J. M. Glassy, D. Dedieu, and S. W. Running, 2000: Prototyping of MODIS LAI and FPAR algorithm with LASUR and LANDSAT data. *IEEE Trans. Geosci. Remote Sens.*, **38**, 2387-2401.

Topliss, B. J., and T. Platt, 1986: Passive fluorescence and photosynthesis in the ocean: Implications for remote sensing. *Deep Sea Res.*, **33**, 849-864.

Toracinta, R. E., D. J. Cecil, E. J. Zipser, and S. W. Nesbitt, 2002: Radar, passive microwave, and lightning characteristics of precipitating systems in the Tropics. *Mon. Wea. Rev.*, **130**, 802-824.

Toutin, T., 2002: Three-dimensional topographic mapping with ASTER stereo data in rugged topography. *IEEE Trans. Geosci. Remote Sens.*, **40**(10), 2241-2247.

Tovinkere, V. R., M. Penaloza, A. Logar, J. Lee, R. C. Weger, T. A. Berendes, and R. M. Welch, 1993: An intercomparison of artificial intelligence approaches for polar scene identification. *J. Geophys. Res.*, **98**, 5001-5016.

Townshend, J. R. G., and C. O. Justice, 1988: Selecting the spatial resolution of satellite sensors required for global monitoring of land transformations. *Int. J. Remote Sens.*, **9**, 187-236.

Townshend, J. R. G., C. O. Justice, W. Li, C. Gurney, and J. McManus, 1991: Global land cover classification by remote sensing: Present capabilities and future possibilities. *Remote Sens. Environ.*, **35**, 243-256.

Trepte, Q., Y. Chen, S. Sun-Mack, P. Minnis, D. F. Young, B. A. Baum, and P. W. Heck, 1999: Scene identification for the CERES cloud analysis subsystem. *Proc. AMS 10th Conf. Atmos. Rad.*, Madison, WI, June 28-July 2, 169-172.

van Leeuwen, W. J. D., A. R. Huete, and T. W. Laing, 1999: MODIS vegetation index compositing approach: A prototype with AVHRR data. *Remote Sens. Environ.*, **69**, 264-280.

Vermote E. F., C. O. Justice, J. Descloitres, N. El Saleous, J. Ray, D. Roy, B. Margerin, and L. Gonzalez, 2001: A global monthly coarse resolution reflectance data set from SeaWiFS for use in Land, Ocean and Atmosphere applications. *Int. J. Remote Sens.*, **22**(6), 1151-1158.

Vermote, E. F., and D. P. Roy, 2002: Land Surface Hot-Spot observed by MODIS over Central Africa. *Int. J. Remote Sens.*, **Cover Letter** (11), 2141-2143.

Vermote E. F., N. El Saleous, and C. O. Justice, 2002: Atmospheric correction of the MODIS data in the visible to middle infrared: First results. *Remote Sens. Environ.*, **83**(1-2), 97-111.

Vermote, E. F., N. El Saleous, C. O. Justice, Y. J. Kaufman, J. L. Privette, L. Remer, J. C. Roger, and D. Tanré, 1997: Atmospheric correction of visible to middle-infrared EOS-MODIS data over land surfaces: Background, operational algorithm and validation. *J. Geophys. Res.*, **102**(D14), 17,131-17,141.

Vermote E. F., N. El Saleous, Y. J. Kaufman, and E. Dutton, 1997: Stratospheric aerosol perturbing effect on the remote sensing of vegetation: Correction method for the composite NDVI after the Pinatubo eruption. *Remote Sens. Rev.*, **15**, 7-21.

Vermote E. F., D. Tanré, J. L. Deuzé, M. Herman, and J. J. Morcrette, 1997: Second simulation of the satellite signal in the solar spectrum: an overview. *IEEE Trans. Geosci. Remote Sens.*, **35**, 3,675-3,686.

Wan, Z., and J. Dozier, 1996: A generalized split-window algorithm for retrieving land-surface temperature from space. *IEEE Trans. Geosci. Remote Sens.*, **34**(4), 892-905.

Wan, Z., and Z.-L. Li, 1997: A physics-based algorithm for retrieving land-surface emissivity and temperature from EOS/MODIS data. *IEEE Trans. Geosci. Remote Sens.*, **35**, 980-996.

Wan, Z., Y. Zhang, Z.-L. Li, R. Wang, V. V. Salomonson, A. Yves, R. Bosseno, and J. F. Hanocq, 2002: Preliminary estimate of calibration of the Moderate Resolution Imaging Spectroradiometer (MODIS) thermal infrared data using Lake Titicaca. *Remote Sens. Environ.*, **80**, 497-515.

Wan, Z., Y. Zhang, Q. Zhang, and Z.-L. Li, 2002: Validation of the land-surface temperature products retrieved from Terra Moderate Resolution Imaging Spectroradiometer data. *Remote Sens. Environ.*, **83**, 163-180.

Wang, Y., Y. Tian, Y. Zhang, N. El-Saleous, Y Knyazikhin, E. Vermote, and R. Myneni, 2001: Investigation of Product Accuracy as a Function of Input and Model Uncertainties: Case Study with SeaWIFS and MODIS LAI/FPAR Algorithm. *Remote Sens. Environ.*, **78**, 296-311.

Wang, J., J. C. Gille, P. L. Bailey, J. R. Drummond, and L. Pan, 1999: Instrument Sensitivity and Error Analysis for the Remote Sensing of Tropospheric Carbon Monoxide by MOPITT. *J. Atmos. Oceanic Technol.*, **16**, 465.

Wang, J., J. C. Gille, P. L. Bailey, L. Pan, D. Edwards, and J. R. Drummond, 1999: Retrieval of Tropospheric Carbon Monoxide Profiles from High-Resolution Interferometer Observations: A New Digital Gas Correlation (DGC) Method and Applications. *J. Atmos. Sci.*, 56, 219.

Wang, J., J. C. Gille, and V. P. Walden, 2000: Validation Study of the MOPITT Retrieval Algorithm: Carbon Monoxide Retrieval from IMG Observations during WINCE. *J. Atmos. Oceanic Technol.*, **17**, 1285.

Wanner, W., X. Li, and A. H. Strahler, 1995: On the derivation of kernels for kernel-driven models of bidirectional reflectance. *J. Geophys. Res.*, **100**, 21,077-21,090.

Wanner, W., A. H. Strahler, B. Hu, X. Li, C. L. Barker Schaaf, P. Lewis, J.-P. Muller, and M. J. Barnsley, 1997: Global retrieval of bidirectional reflectance and albedo over land from EOS MODIS and MISR data: Theory and algorithm. *J. Geophys. Res.*, **102**, 17,143-17,162.

Washington, W., and C. Parkinson, 1986: An Introduction to Three-Dimensional Climate Modeling. University Science Books, 422 pp.

Welch, R. M., K. S. Kuo, and S. L. Sengupta, 1990: Cloud and surface textural features in polar regions. *IEEE Trans. Geosci. Remote Sens.*, **28**, 520-528.

Welch, R. M., and H. Lang, 1994: ASTER as a source of global topographic data in the late 1990s. *Int. Arch. Photogram. Remote Sens.*, **30**, 222-224.

Welch, R. M., S. K. Sengupta, and D. W. Chen, 1988: Cloud field classification based upon high spatial resolution textural features. 1. Gray level co-occurrence matrix approach. *J. Geophys Res.*, **93**, 12,663-12,681.

Whitlock, C. H., T. P. Charlock, W. F. Staylor, R. T. Pinker, I. Laszlo, A. Ohmura, H. Gilgen, T. Konzelman, R. C. DiPasquale, C. D. Moats, S. R. LeCroy, and N. A. Ritchey, 1995: First global WCRP shortwave surface radiation budget dataset. *Bull. Amer. Meteor. Soc.*, **76**, 905-922.

Wielicki, B. A., B. R. Barkstrom, E. F. Harrison, R. B. Lee III, G. L. Smith, and J. E. Cooper, 1996: Clouds and the Earth's Radiant Energy System (CERES): An Earth Observing System Experiment. *Bull. Amer. Met. Soc.*, **77**, 853-868.

Wielicki, B. A., B. R. Barkstrom, and 21 others, 1998: Clouds and the Earth's Radiant Energy System (CERES): Algorithm overview. *IEEE Trans. Geosci. Remote Sens.*, **36**, 1127-1141.

Wielicki, B. A., R. D. Cess, M. D. King, D. A. Randall, and E. F. Harrison, 1995: Mission to Planet Earth: Role of clouds and radiation in climate. *Bull. Amer. Meteor. Soc.*, **76**, 2125-2153.

Wilheit, T. T., A. T. C. Chang, and L. S. Chiu, 1991: Retrieval of monthly rainfall indices from microwave radiometric measurements using probability distribution functions. *J. Atmos. Oceanic Technol.*, **8**, 118-136.

Wofsy, S. C., J. C. McConnell, and M. B. McElroy, 1972: Atmospheric CH_4, CO and CO_2. *J. Geophys. Res.*, **77**, 4477-4493.

Wolfe R. E., M. Nishihama, A. J. Fleig, J. R. Kuyper, D. P. Roy, J. C. Storey, and F. S. Patt, 2002: Achieving sub-pixel geolocation accuracy in support of MODIS land science. *Remote Sens. Environ.*, **83**(1-2), 31-49.

Wolfe, R. E., D. P. Roy, and E. F. Vermote, 1998: MODIS land data storage, gridding and compositing methodology: Level 2 grid. *IEEE Trans. Geosci. Remote Sens.*, **36**(4), 1324-1338.

Wong, T., D. Young, M. Haeffelin, and S. Weckman, 2000: Validation of the CERES/TRMM ERBE-like monthly mean clear-sky longwave dataset and the effects of the 1998 ENSO event. *J. Climate*, **13**(24), 4256-4267.

Wu, M., and L.-P. Chang, 1992: Longwave radiation budget parameters computed from ISCCP and HIRS2/MSU products. *J. Geophy. Res.*, **97**, 1083-1101.

Wu, M. L. C., S. Schubert, C.-I Lin, and I. Stajner, 2001: A method for assessing the quality of model-based estimates of ground temperature and atmospheric moisture using satellite data. *J. Geophys. Res.*, **106**, 10,129-10,144.

Wu, R., J. A. Weinman, and R. T. Chin, 1985: Determination of rainfall rates from GOES satellite images by a pattern recognition technique. *J. Atmos. Oceanic Technol.*, **2**, 314-330.

Wylie, D. P., and W. P. Menzel, 1998: Eight years of global high cloud statistics using HIRS. *J. Climate*, **12**, 170-184.

Yamaguchi, Y., H. Fujisada, A. B. Kahle, H. Tsu, M. Kato, H. Watanabe, I. Sato and M. Kudoh, 2001: ASTER instrument performance, operation status, and application to Earth sciences. *IGARSS 2001, IEEE 2001 International Geoscience and Remote Sensing Symposium*, Volume 3, 9-13 July 2001, Sydney, Australia, pp. 1215-1216.

Yamaguchi, Y., A. Kahle, H. Tsu, T. Kawakami, and M. Pniel, 1998: Overview of ASTER. *IEEE Trans. Geosci. Remote Sens.*, **36**, 1062–1071.

Yamaguchi, Y., H. Tsu, and H. Fujisada, 1993: Scientific Basis of ASTER Instrument Design. *Proc. SPIE*, **1939**, 150-160.

Yamaguchi, Y., A. Tsu, A. Kahle, and D. A. Nochols, 1994: ASTER Instrument design and science Objectives. American Institute of Aeronomy and Astronomy, 7, paper 94-0597.

Yamaguchi, Y., H. Fujisada, H. Tsu, I. Sato, H. Watanabe, M. Kato, M. Kudoh, A. B. Kahle, and M. Pniel, 2001: ASTER early image evaluation —calibration and characterization of satellite sensors and accuracy of derived physical parameters. *Adv. Space Res.*, **28**(1), 69-76.

Yoder, J. A., C. R. McClain, G. C. Feldman, and W. E. Esaias, 1993: Annual cycles of phytoplankton chlorophyll concentrations in the global ocean, A satellite view. *Global Biogeochem. Cycles*, **7**, 181-193.

Young, D. F., E. F. Harrison, B. A. Wielicki, P. Minnis, G. G. Gibson, B. R. Barkstrom, T. P. Charlock, D. R. Doelling, A. J. Miller, O. C. Smith, and J. C. Stassi, 1995a: Clouds and the Earth's Radiant Energy System (CERES) Algorithm Theoretical Basis Document. Volume IV - Determination of Surface and Atmosphere Fluxes and Temporally and Spatially Averaged Products (Subsystems 5-12), Subsystem 7.0 - Time Interpolation and Synoptic Flux Computation for Single and Multiple Satellites, NASA Ref. Pub. 1376, Vol. IV, 69-108.

Young, D. F., E. F. Harrison, and E. Singh, 1995b: Clouds and the Earth's Radiant Energy System (CERES) Algorithm Theoretical Basis Document. Volume IV - Determination of Surface and Atmosphere Fluxes and Temporally and Spatially Averaged Products (Subsystems 5-12), Subsystem 8.0 - Monthly Regional, Zonal, and Global Radiation Fluxes and Cloud Properties, NASA Ref. Pub. 1376, Vol. IV, 109-128.

Young, D. F., P. Minnis, D. Baumgardner, and H. Gerber, 1998: Comparison of in situ and satellite-derived cloud properties during SUCCESS. *Geophys. Res. Lett.*, **25**, 1125-1128.

Yuter, S. E., and R. A. Houze, Jr. 1995: Three-dimensional kinematic and microphysical evolution of Florida cumulonimbus. Part II: Frequency distributions of vertical velocity, reflectivity and differential reflectivity. *Mon. Wea. Rev.*, **123**, 1941-1963.

Zander, R. P., Demoulin, D. H. Ehhalt, U. Schmidt, and C. P. Rinsland, 1989: Secular increase of the total vertical column abundance of carbon monoxide above central Europe since 1950. *J. Geophy. Res.*, **94**, 11,021.

Zhan, X., R. DeFries, M. Hansen, C. DiMiceli, R. Sohlberg, and C. Huang. 1999: Algorithm Theoretical Basis Document of the MODIS Enhanced Land Cover and Land Cover Change Product (MOD 29), update available at eospso.gsfc.nasa.gov/atbd/modistables.html.

Zhan, X., R. DeFries, J. R. G. Townshend, C. DiMiceli, M. Hansen, C. Huang, and R. Sohlberg, 2000: The 250m global land cover change product from the Moderate Resolution Imaging Spectroradiometer of NASA's Earth Observing System. *Int. J. Remote Sens.*, **21**, 1433-1460.

Zhan, X., R. A. Sohlberg, J. R. G. Townshend, C. DiMiceli, M. L. Carroll, J. C. Eastman, M. C. Hansen, and R. S. DeFries, 2002: Detection of land cover changes using MODIS 250 m data. *Remote Sens. Environ.*, **83**(1-2), 336-350.

Zhang, X., J. C. F. Hodges, C. Schaaf, M. A. Friedl, A. H. Strahler, and F. Gao, 2001: Global Vegetation Phenology from AVHRR and MODIS Data. *Proc. 2001 Int. Geosci. Remote Sens. Symp.*, Sydney, 2001.

Zhang, Y., Y. Tian, Y. Knyazikhin, J. V. Martonchik, D. J. Diner, M. Leroy, and R. B. Myneni, 2000: Prototyping of MODIS LAI and FPAR algorithm with POLDER data over Africa. *IEEE Trans. Geosci. Remote Sens.*, **38**, 2402-2418.

Appendix D: Acronyms and Abbreviations

A

ACRIM	Active Cavity Radiometer Irradiance Monitor
ACRIMSAT	ACRIM Satellite
ACP	Aerosol Climatology Project
ADEOS	Advanced Earth Observing Satellite
ADM	Angular Distribution Model
AEM	Applications Explorer Mission
AERONET	Aerosol Robotic Network
AGC	Automatic Gain Control
AGP	Ancillary Geographic Product
AIRS	Atmospheric Infrared Sounder
ALI	Advanced Land Instrument
AMI	Active Microwave Instrument
AMS	American Meteorological Society
AMSR	Advanced Microwave Scanning Radiometer
AMSR-E	Advanced Microwave Scanning Radiometer for EOS
AMSU	Advanced Microwave Sounding Unit
AOD	Aerosol Optical Depth
APAR	Absorbed Photosynthetically Active Radiation
APOLLO	AVHRR Processing scheme Over Cloud Land and Ocean
AREAS	Altimeter Return Echo Analysis System
ARM	Atmospheric Radiation Measurement
ARMAR	Airborne Rain Mapping Radar
ARP	Absorbed Radiation by Phytoplankton
ARP	Ancillary Radiometric Product (MISR)
ASAS	Advanced Solid-state Array Spectroradiometer
ASF	Alaska SAR Facility
ASTER	Advanced Spaceborne Thermal Emission and Reflection Radiometer
ASTEX	Atlantic Stratocumulus Transition Experiment
ATBD	Algorithm Theoretical Basis Document
ATMS	Advanced Technology Microwave Sounder
ATSR	Along Track Scanning Radiometer
AVG	Name used for the CERES average Monthly Regional Radiative Fluxes and Cloud product
AVHRR	Advanced Very High Resolution Radiometer
AVIRIS	Airborne Visible-Infrared Imaging Spectrometer

B

BDS	Bi-Directional Scan
BGC	Biogeochemical
BIOME	Biogeochemical Information Ordering Management Environment
BOREAS	Boreal Ecosystems Atmosphere Study
BRDF	Bidirectional Reflectance Distribution Function
BUAN	Baseline Upper Air Network

C

CO	Carbon monoxide
CAGEX	CERES/ARM/GEWEX Experiment
CART	Cloud and Radiation Testbed
CCD	Charge-Coupled Device
CCN	Cloud Condensation Nuclei
CDDIS	Crustal Dynamics Data Information System
CDOM	Colored (or Chromomorphic) Dissolved Organic Matter
CEES	Committee on Earth and Environmental Sciences
CERES	Clouds and the Earth's Radiant Energy System
CFAD	Contoured Frequency by Altitude Diagram
CFC	Chlorofluorocarbon
CH_4	Methane
CHEM-1	Chemistry Mission-1 (now Aura)

CrIS	Cross-track Infrared Sounder
CLAVR	Cloud Advanced Very high resolution Radiometer
ClO_x	Oxides of chlorine
CNES	Centre National d'Etudes Spatiales (France)
CO	Carbon monoxide
CPF	Calibration Parameter File
CRS	Clouds and Radiative Swath
CZCS	Coastal Zone Color Scanner

D

DAAC	Distributed Active Archive Center
DAO	Data Assimilation Office
DAS	Data Assimilation System
DEM	Digital Elevation Model
DIS	Data and Information System
DMSP	Defense Meteorological Satellite Program
DoE	Department of Energy
DOM	Dissolved Organic Matter
DORIS	Doppler Orbitography and Radiopositioning Integrated by Satellite
DPH	Data Products Handbook
DTED	Digital Terrain Elevation Data

E

EASE	Equal-Area Scalable Earth, a grid for data mapping
ECMWF	European Centre for Medium-Range Weather Forecasts
ECS	EOSDIS Core System
EDC	EROS Data Center
EDST	Earth Science Data Type
ENSO	El Niño-Southern Oscillation
ENVISAT	Environmental Satellite, ESA
EO-1	Earth Observing 1
EOS	Earth Observing System
EOS PM	EOS afternoon-crossing satellite (now Aqua)
EOSDIS	EOS Data and Information System
EOSPSO	EOS Project Science Office
EP	Earth Probe
EPGN	EOS Polar Ground Network
ERB	Earth Radiation Budget
ERBE	Earth Radiation Budget Experiment
ERBS	Earth Radiation Budget Satellite
EROS	Earth Resources Observation System
ERS	European Remote Sensing Satellite
ERS-1	European Remote Sensing Satellite-1
ERTS	Earth Resources Technology Satellite
ES	EOS Science, a product identification code for CERES data products
ESA	European Space Agency
ESDIS	Earth Science Data and Information System
ESDT	Earth Science Data Type
ESE	Earth Science Enterprise
ESMR	Electrically Scanning Microwave Radiometer
ESSP	Earth System Sciences Pathfinder
ET	Evapotranspiration
ETM	Enhanced Thematic Mapper
ETM+	Enhanced Thematic Mapper Plus
EVI	Enhanced Vegetation Index

F

FACE	Florida Area Cumulus Experiment
FIFE	First ISLSCP Field Experiment
FIRE	First ISCCP Regional Experiment
FOV	Field of View
FPAR	Fraction of Photosynthetically Active Radiation
FSW	Name used for the CERES Monthly Gridded Radiative Fluxes and Clouds product
FTP	File Transfer Protocol

G

GARP	Global Atmospheric Research Program
GATE	GARP Atlantic Tropical Experiment
GCM	General Circulation Model (also Global Climate Model)
GDR	Geophysical Data Record
GEOS	Goddard Earth Observing System
GEOS DAS	Goddard Earth Observing System Data Assimilation System
GEOSAT	Geodetic Satellite
GES DAAC	Goddard Space Flight Center Earth Sciences Distributed Active Archive Center

GEWEX	Global Energy and Water cycle Experiment
GHRC	Global Hydrology Resource Center
GOES	Geostationary Operational Environmental Satellite
GPCP	Global Precipitation Climatology Project
GPS	Global Positioning System
GRACE	Gravity Recovery And Climate Experiment
GRP	Geo-rectified Radiance (product)
G/S	Ground Station
GSFC	Goddard Space Flight Center

H

HDF	Hierarchical Data Format
HIRDLS	High-Resolution Dynamics Limb Sounder
HIRS	High-Resolution Infrared Radiation Sounder
HO_x	Hydrogen oxides
HRPT	High-Resolution Picture Transmission
HSB	Humidity Sounder for Brazil

I

ICEMAP	Ice-Mapping Algorithm
ICESat	Ice, Clouds, and Land Elevation Satellite
ID	Identification
IEOS	International Earth Observing System
IES	Instrument Earth Scans
IFOV	Instantaneous Field of View
IfSAR	Interferometric Synthetic Aperture Radar
IGBP	International Geosphere-Biosphere Programme
IGDR	Interim Geophysical Data Record
IGS	International Ground Station
IPAR	Instantaneous Photosynthetically-Active Radiation
IPCC	Intergovernmental Panel on Climate Change
IR	Infrared
IR/MW	Infrared/microwave
ISAMS	Improved Stratospheric And Mesospheric Sounder
ISCCP	International Satellite Cloud Climatology Project
ISLSCP	International Satellite Land Surface Climatology Project
ITPP	International TOVS Processing Package

J

JERS-1 OPS	Japanese Earth Resources Satellite Optical Sensor
JMR	Jason-1 Microwave Radiometer
JPL	Jet Propulsion Laboratory

K

Kbps	Kilobits per second

L

LAI	Leaf Area Index
Landsat	Land Remote Sensing Satellite
LaRC	Langley Research Center
LASE	Laser Atmospheric Sensing Experiment
LI	Lifted Index
LIS	Lightning Imaging Sensor
LMC	Length Modulation Cells
LP	Level Processors
LST	Land Surface Temperature
Ltyp	Spectral radiance at typical conditions
LVIS	Laser Vegetation Imaging Sensor
LW	Longwave

M

MAPS	Measurement of Air Pollution from Satellites
MAS	MODIS Airborne Simulator
MB	Megabyte
MBLA	Multi-Beam Laser Altimeter
MERIS	Medium Resolution Imaging Spectrometer
Met. data	Meteorological data
METEOSAT	Meteorology Satellite (an ESA geosynchronous satellite)
METI	Ministry of Economy, Trade and Industry

MISR	Multi-angle Imaging SpectroRadiometer
MIT	Massachusetts Institute of Technology
MLR	Multiple Linear Regression
MLS	Microwave Limb Sounder
MMS	Multi-mission Modular Spacecraft
MOA	Meteorological Ozone and Aerosol
MOBY	Marine Optical Buoy
MODIS	Moderate Resolution Imaging Spectroradiometer
MODLAND	MODIS Land science team
MOLA	Mars Orbiter Laser Altimeter
MOPITT	Measurements of Pollution in the Troposphere
MSE	Mean squared error
MSFC	Marshall Space Flight Center
MSS	Multispectral Scanner
MSU	Microwave Sounding Unit
MVI	Modified Vegetation Index
MW	Microwave
MW/IR	Microwave/infrared
MWP	Microwave Water Path

N

N/A	Not Applicable
NASA	National Aeronautics and Space Administration
NASDA	National Space Development Agency (Japan)
NBAR	Nadir BRDF-Adjusted Reflectance
NCEP	National Centers for Environmental Prediction
NCSA	National Center for Supercomputing Applications (at the University of Illinois)
NDVI	Normalized Difference Vegetation Index
NE	Noise Equivalent
NESDIS	National Environmental Satellite, Data, and Information Service
NGDC	National Geophysical Data Center
NIR	Near Infrared
NISN	NASA Integrated Services Network
NMC	National Meteorological Center
NMP	New Millennium Program
NOAA	National Oceanic and Atmospheric Administration
NOHRSC	National Operational Hydrologic Remote Sensing Center
NORAD	North American Aerospace Defense Command
NO_X	Nitrogen oxides (NO, NO_2, NO_3)
NPOESS	National Polar-orbiting Operational Environmental Satellite System
NPP	Net Primary Production
NSCAT	NASA Scatterometer
NSIDC	National Snow and Ice Data Center
NWS	National Weather Service

O

OBC	On-Board Calibrator
OClO	Chlorine dioxide
OI	Optimum Interpolation
OLR	Outgoing Longwave Radiation
OLS	Optical Linescan System
OMI	Ozone Monitoring Instrument
ORNL	Oak Ridge National Laboratory
OSDR	Operational Sensor Data Record
OTD	Optical Transient Detector
O_X	Oxides

P

PAR	Photosynthetically-Active Radiation
PDF	Portable Document Format
pdf	Probability density function
PEB	Phycoerythrobilin
PGE	Product Generation Executive
PICASSO	Pathfinder Instruments for Cloud and Aerosol Spaceborne Observations
PICASSO-CENA	Pathfinder Instruments for Cloud and Aerosol Spaceborne Observations-Climatologie Etendue des Nuages et des Aerosols
PMC	Pressure Modulation Cells
POCC	Project Operation Control Center
PO.DAAC	Physical Oceanography Distributed Active Archive Center (at the Jet Propulsion Laboratory)
POES	Polar Orbiting Environmental Satellite
POLDER	Polarization and Directionality of the Earth's Reflectance
PP	Pre-Processor
ppm	Parts per million
ppmv	Parts per million by volume
PR	Precipitation Radar
PSC	Polar Stratospheric Cloud
PSF	Point Spread Functions

PSN	Photosynthesis
PUB	Phycourobilin

Q

QA	Quality Assurance
QuikScat	Quick Scatterometer
QuikTOMS	Quick Total Ozone Mapping Spectrometer

R

RAOBS	Radiosonde Observations
RLRA	Reflecting Level Reference Altitude
RMS	Root Mean Square
RSMAS	Rosenstiel School of Marine and Atmospheric Science, University of Miami
RSS	Root Sum Square

S

SAGE	Stratospheric Aerosol and Gas Experiment
SAM	Stratospheric Aerosol Measurement
SAMS	Stratospheric And Mesospheric Sounder
SAR	Synthetic Aperture Radar
SARB	Surface and Atmospheric Radiation Budget
SASS	SEASAT-A Satellite Scatterometer
SBRS	Santa Barbara Remote Sensing
S/C	Spacecraft
SCAR-B	Smoke, Cloud, and Radiation-Brazil
SCF	Science Computing Facility
SEASAT	Sea Satellite
SeaWiFS	Sea-viewing Wide Field-of-view Sensor
SEDAC	Socioeconomic Data and Applications Center
SERCAA	Support of Environmental Requirements for Cloud Analysis and Archive
SFC	Surface Fluxes and Clouds
SGDR	Sensor Geophysical Data Record
SGP	Southern Great Plains
SI	Systeme Internationale
SIM	Spectral Irradiance Monitor
SIPS	Science Investigator-led Processing System
SLA	Shuttle Laser Altimeter
SLR	Satellite Laser Ranging
SMM	Solar Maximum Mission
SMMR	Scanning Multichannel Microwave Radiometer
SNOMAP	Snow-Mapping Algorithm
SNR	Signal-to-Noise Ratio
SOHO	Solar Heliospheric Observatory
SOM	Space-Oblique Mercator
SORCE	Solar Radiation and Cloud Experiment
SPOT	Systeme Pour l'Observation de la Terre
SPOT-2	Systeme Pour l'Observation de la Terre-2
SRB	Surface Radiation Budget
SRBAVG	Name for CERES Monthly TOA/Surface Averages product
SRTM	Shuttle Radar Topography Mission
SSALTO	Segment Sol Multimission Altimetry and Orbitography
SSF	Single Scanner Footprint*
SSM/I	Special Sensor Microwave/Imager
SST	Sea Surface Temperature
SW	Shortwave
SWE	Snow Water Equivalent
SWH	Significant Wave Height
SWIR	Shortwave Infrared
SWS	SeaWinds Standard
SYN	Name for CERES Synoptic Radiative Fluxes and Clouds product

T

TARFOX	Tropospheric Aerosol Radiative Forcing Observational Experiment
Tb	Brightness temperature
TCP	Topographic Control Points
TEC	Total Electron Content
TES	Tropospheric Emission Spectrometer
TIM	Total Irradiance Monitor
TIMED	Thermosphere, Ionosphere, Mesosphere, Energetics, and Dynamics
TIMS	Thermal Infrared Multispectral Scanner
TIR	Thermal Infrared
TLSCF	Team Leader Science Computing Facility
TM	Thematic Mapper
TMI	TRMM Microwave Imager
TMR	TOPEX Microwave Radiometer
TOA	Top Of the Atmosphere

*SSF is also used in the Product ID for the CERES Single Scanner TOA/Surface Fluxes and Clouds product

TOGA	Tropical Ocean Global Atmosphere
TOMS	Total Ozone Mapping Spectrometer
TOPEX	Ocean Topography Experiment
TOPEX/ Poseidon	Ocean Topography Experiment/ Poseidon (U.S.-France)
TOVS	TIROS Operational Vertical Sounder
T/P	TOPEX/Poseidon
TRMM	Tropical Rainfall Measuring Mission
T_s	Sea surface temperature
TSDIS	TRMM Science Data and Information System
TSI	Total Solar Irradiance
TSIM	Total Solar Irradiance Mission
TT	Total Totals
Ttyp	Temperature at typical conditions

U

UARS	Upper Atmosphere Research Satellite
UMD	University of Maryland
UNESCO	United Nations Educational, Scientific, and Cultural Organization
USGS	United States Geological Survey
USNO	United States Naval Observatory
UT	Universal Time
UTC	Universal Time Coordinate
UV	Ultraviolet

V

VCL	Vegetation Canopy Lidar
VDC	VCL Data Center
VDIS	Vertical Distribution of Intercepted Surfaces
VI	Vegetation Index
VIIRS	Visible Infrared Imaging Radiometer Suite
VIRGO	Variability of solar Irradiance and Gravity Oscillations
VIRS	Visible Infrared Scanner
VIS	Visible
VISSR	Visible Infrared Spin-Scan Radiometer
VNIR	Visible and Near Infrared
VPGS	VCL Precision Geolocation System

W

WCRP	World Climate Research Program
WINCE	Winter Cloud Experiment
WMO	World Meteorological Organization
WN	Window

Z

ZAVG	Name for CERES Monthly Zonal and Global Radiative Fluxes and Clouds product

Appendix E: Data Products Index

ASTER (on Terra)

ASTER Brightness Temperature at Sensor *55*
ASTER Browse Data-Decorrelation Stretch Product *56*
ASTER Digital Elevation Models (DEMs) *59*
ASTER Polar Surface and Cloud Classification Product *105*
ASTER Reconstructed, Unprocessed Instrument Data *54*
ASTER Registered Radiance at Sensor *55*
ASTER Surface Emissivity and Surface Kinetic Temperature *152*
ASTER Surface Reflectance and Surface Radiance *57*

CERES (on Terra)

CERES Bi-Directional Scans Product *61*
CERES Clouds and Radiative Swath *111*
CERES ERBE-like Instantaneous TOA Estimates *106*
CERES ERBE-like Monthly Regional Averages and ERBE-like Monthly Geographical Averages *107*
CERES Monthly Gridded Radiative Fluxes and Clouds *112*
CERES Monthly Gridded TOA/Surface Fluxes and Clouds *116*
CERES Monthly Regional Radiative Fluxes and Clouds and Monthly Zonal and Global Radiative Fluxes and Clouds *115*
CERES Monthly TOA/Surface Averages *118*
CERES Single Scanner TOA/ Surface Fluxes and Clouds *109*
CERES Synoptic Radiative Fluxes and Clouds *114*

Data Assimilation System

DAS Instantaneous Near Surface and Vertically-Integrated State Variables *213*
DAS Instantaneous 3-Dimensional State Variables *216*
DAS Ozone Mixing Ratio *215*
DAS Time-Averaged 3-Dimensional Temperature Tendency Fields System *217*
DAS Time-Averaged 3-Dimensional Eddy-Diffusivity and Cloud Mass Flux Fields *218*
DAS Time-Averaged Single Level Cloud Quantities *205*
DAS Time-Averaged Near Surface and Vertically-Integrated Quantities *206*
DAS Time-Averaged 2-Dimensional Surface Data *207*
DAS Time-Averaged Surface and Top-of-the-Atmosphere Stresses *208*
DAS Time-Averaged Surface 3-Dimensional Cloud Quantities *209*
DAS Time-Averaged 3-Dimensional Wind Tendency Fields *210*
DAS Time-Averaged 3-Dimensional Moisture Tendency Fields *211*
DAS Total Column Ozone *212*

LIS (on TRMM)

LIS 2.5° × 2.5° Equal Angle Monthly Grid *140*
LIS 500 km × 500 km Equal Area Monthly Grid *140*
LIS Area Statistics *140*
LIS Background Product *50*
LIS Browse Area *140*
LIS Ephemeris Data *140*
LIS Event Rate Sets *140*
LIS Events Statistics *140*
LIS Flash Density *140*
LIS Flash Rate Data *140*
LIS Flash Statistics *140*
LIS Group Statistics *140*
LIS Image Attributes *140*
LIS Metadata Description *140*
LIS Orbit Attributes *140*
LIS Summary Data *140*
LIS Threshold Attributes *140*
LIS Vector Statistics *140*

MISR (on Terra)

MISR Aerosol and Surface Product *122*
MISR Aerosol Climatology Product *123*
MISR Ancillary Geographic Product *66*
MISR Ancillary Radiometric Product *66*
MISR Geo-rectified Radiance Product *65*
MISR Radiometric Product *64*
MISR Reformatted Annotated Product *63*
MISR Top-of-Atmosphere (TOA)/Cloud Product *120*

MODIS (on Terra)

MODIS Absorption Coefficients *184*

MODIS Aerosol Optical Depth *69*

MODIS Aerosol Product *124*

MODIS Atmospheric Profiles *98*

MODIS Burn Scars *156*

MODIS Chlorophyll *a* Pigment Concentration *184*

MODIS Chlorophyll Fluorescence *182*

MODIS Clear-Water Epsilon *73*

MODIS Cloud Mask *134*

MODIS Cloud Product *127*

MODIS Coccolith Concentration *187*

MODIS Evapotranspiration *169*

MODIS Geolocation Data Set *68*

MODIS Land Cover Type *164*

MODIS Land Surface Temperature and Emissivity *154*

MODIS Leaf Area Index and Fraction of Photosynthetically Active Radiation - Moderate Resolution *167*

MODIS Level 1A Radiance Counts *67*

MODIS Level 1B Calibrated, Geolocated Radiances *67*

MODIS Level 3 Atmosphere Products *130*

MODIS Normalized Water-Leaving Radiance *69*

MODIS Ocean Primary Productivity *189*

MODIS Ocean Water Attenuation Coefficient *180*

MODIS Organic Matter Concentration *184*

MODIS Photosynthetically Active Radiation *70*

MODIS Phycoerythrin Concentration *190*

MODIS Pigment Concentration *180*

MODIS Processing Framework and Match-up Database *72*

MODIS Sea Ice Cover and Ice Surface Temperature *198*

MODIS Sea Surface Temperature *157*

MODIS Snow Cover *196*

MODIS Surface Reflectance; Atmospheric Correction Algorithm Products *162*

MODIS Surface Reflectance BRDF/ Albedo Parameter *172*

MODIS Suspended Solids Concentration *180*

MODIS Thermal Anomalies – Fires *156*

MODIS Total Precipitable Water *95*

MODIS Vegetative Cover Conversion and Vegetation Continuous Fields *174*

MODIS Vegetation Indices *166*

MODIS Vegetation Production and Net Primary Production *170*

MOPITT (on Terra)

MOPITT Geolocated Radiances *74*

MOPITT CO Profile and CO Column, and CH_4 Column Data *146*

PR (on TRMM)

PR Radar Total Power, Noise, and Reflectivity *51*

PR Rain Occurrence and Rain Type and Bright Band *80*

PR Surface Cross-Section as Function of Scan Angle *79*

PR Range Profiles of Rain and Water Content *81*

PR Monthly Accumulated Rainfall & Vertical Structure, Monthly Combined Accumulated Surface Rainfall *82*

TMI (on TRMM)

TMI Calibrated Brightness Temperatures *51*

TMI Surface Rainfall and Vertical Structure *83*

TMI Monthly Surface Rainfall *84*

TRMM

TRMM Instantaneous Radar Site Rain Map *89*

TRMM Instantaneous Radar Site Convective/ Stratiform Map *90*

TRMM Instantaneous Radar Site 3-D Reflectivities *91*

TRMM Combined Surface Rainfall Rate and Vertical Structure *85*

TRMM Monthly Combined Accumulated Rainfall and Vertical Structure *86*

TRMM 1° Daily Combined Rainfall and Monthly Combined Instrument Rainfall *88*

TRMM 5-Day Site Rain Map *92*

TRMM 30-Day Site Rain Map *93*

TRMM Monthly 3-D Structure *93*

VIRS (on TRMM)

VIRS Calibrated Radiances *52*